Minoru Fujimoto

Thermodynamics of Crystalline States

Springer

Thermodynamics of Crystalline States

Minoru Fujimoto

Thermodynamics of Crystalline States

Springer

Minoru Fujimoto
Department of Physics
University of Guelph
Guelph, ON N1G 2W1, Canada
minorufuji@rogers.com

ISBN 978-1-4419-6687-2 e-ISBN 978-1-4419-6688-9
DOI 10.1007/978-1-4419-6688-9
Springer New York Heidelberg Dordrecht London

Library of Congress Control Number: 2010935845

Preface

Originated from studies on steam engines, thermodynamics is formulated traditionally for homogeneous materials. Applying to condensed matters however, laws of thermodynamics have to be evaluated with respect to the structural detail. Following after Kirkwood's *chemical thermodynamics*, the author's attempt is to discuss lattice dynamics in crystalline states in light of the traditional laws. It is noted that lattice symmetry remains as implicit in crystalline states if assumed as homogeneous, whereas deformed crystals with disrupted symmetry are not necessarily stable and inhomogeneous, exhibiting *mesoscopic* properties. In this context, the lattice dynamics in uniform crystalline states should accordingly be revised. Although mostly presumptive in the literature, such attempts should be formulated with fundamental principles for modern thermodynamics. I have selected structural changes and superconducting transitions for this book to discuss as basic phenomena in crystals in thermal environment.

Born and Huang have laid ground for thermodynamics of crystalline states in their book *Dynamical Theory of Crystal Lattices*. They assumed, however, that order–disorder phenomena were independent from the lattice dynamics, and hence excluded from their book. On the other hand, new evidence indicates that the problem must be treated otherwise; the lattice does play a vital role in ordering processes. Accordingly, I was motivated to write about physics of crystal lattice in the light of Born–Huang's principles, which constitutes my primary objective in this book.

In modern experiments, mesoscopic objects in crystals can be investigated within timescale of observation, yielding results that appear somewhat unusual, if compared with macroscopic experiments. It is important that thermodynamic relations in mesoscopic states should be expressed with respect to the timescale of observation. Also significant is that mesoscopic quantities in crystals are driven by internal interactions of nonlinear character. In this book, I have therefore discussed thermodynamic quantities with respect to the timescale of observation, including elementary accounts of nonlinear physics to discuss long-range correlations, which I believe is the first attempt in a textbook of thermodynamics. For convenience of readers who are not particularly familiar with nonlinear physics, I have attached Appendix, listing some useful formula of elliptic functions.

I have written this book primarily for advanced students in physics and engineering, assuming their knowledge of traditional thermodynamics and quantum theories. Although written as a textbook, this book may not be suitable for use in a regular classroom. However, it is designed to serve as a useful reference for seminar discussions. It is my hope to see if this book is found as stimulating for advanced studies of condensed matter.

I should mention with my sincere appreciation that I have benefited for my writing from numerous discussions and comments with my colleagues and students. Finally, I thank my wife Haruko for her continuous support and encouragement.

November 2009 M. Fujimoto

Contents

Chapter 1
Introduction

The basic objective in this book is to determine the dynamical role of the lattice structure for structural changes. In this chapter, thermodynamic principles are reviewed for crystalline states, realizing that the concept of order variables should be redefined in relation to lattice excitations. Although implicit in thermodynamic functions, the lattice is dynamically essential for structural and superconducting transitions in crystals. It is also significant that order variables emerge in finite amplitude at a critical temperature as related with an *adiabatic potential* in a crystal. Here, we introduce necessary modifications of the traditional principles, serving as a preliminary account of thermodynamics of crystalline states.

1.1 Crystalline Phases

Originated from steam engines with compressed vapor, today's thermodynamics is a well-established discipline of physics for thermal properties of matter. If characterized by a uniform density, a crystal can be in a thermodynamic state expressed by functions of temperature and pressure of the surroundings. Specified by symmetry of the lattice structure, properties of a single crystal are essentially due to masses and other physical nature of constituents at lattice points, although geometrical symmetry per se cannot be responsible for physical properties. In thermodynamics of crystalline states, structural changes are still an outstanding problem, but cannot be properly solved with uniform state functions, unless the structural detail is taken into account. A structural transition is generally *discontinuous* at a specific temperature, below which even a chemically pure crystal becomes inhomogeneous and composed of substructures in smaller volume, for example, *domains*, in thermal equilibrium. Domains in finite volume are not uniform in principle, but a transformation from one kind to the other can be described with thermodynamic principles, if some realistic internal variables can be specified. In fact, among various types of crystals, there are some inhomogeneous crystals signified by distributed *sinusoidal* densities, which are regarded as *modulated* thermodynamic states. Consistent with

M. Fujimoto, *Thermodynamics of Crystalline States*,
DOI 10.1007/978-1-4419-6688-9_1, © Springer Science+Business Media, LLC 2010

Kirkwood's definition [1] in chemical thermodynamics, thermodynamic functions can be defined with continuous internal variables of space coordinates, in addition to temperature and pressure of the surroundings.

In *Dynamical Theory of Crystal Lattices*, Born and Huang [2] laid foundation of thermodynamics of crystalline states in 1954, but their general theory has not been fully substantiated by experimental results, perhaps supporting data were not properly analyzed at that time. In today's literature however, there are many results available for evaluating their theory, yet such a task has not been carried out properly.

Needless to say, a crystalline state is very different from a gaseous state of a large number of *free* constituent particles. A crystal packed with identical constituents is characterized by distinct symmetry, whereas fast molecular motion prevails in gaseous states. The *internal energy* of a gas is primarily kinetic energies of particles in free motion, whereas in a crystal it is essentially intermolecular potential energies. A structural change between different crystalline phases is a dynamic process across their boundaries. Also, it is significant that a gas is normally confined to a container in finite volume, whereas a crystal has its own volume under given conditions. Nevertheless, the surface boundaries are often neglected, or dealt with under a simplified mathematical conjecture, besides surfaces have only a little contribution to bulk properties of a crystal in large size.

In thermodynamics, a crystal must always be in *contact* with the surroundings in equilibrium. Assuming no chemical activity, surfaces provide a *physical contact*, where only *heat* can be exchanged with the surroundings. Joule demonstrated that heat is nothing but energy, although it is of a unique type of energy among others. Boltzmann interpreted that heat is originated from randomly distributed microscopic energies in the surroundings. Excitations in a crystal are basically due to the vibrating lattice at a given temperature, which are quantum mechanically a gas of *phonons* in random motion, as Planck postulated for thermal radiation. The phonon spectrum is virtually continuous; the *internal energy* is associated statistically with the average phonon energies. In this context, the lattice symmetry remains implicit in thermodynamic functions that are defined as uniform in a stable crystal at constant volume V.

Equilibrium between two bodies in thermal contact can be characterized by a common *temperature* T, indicating that there are no net flows of heat across the surfaces. For a combined system of a crystal and its surroundings, the total amount of fluctuating heat ΔQ is signified as negative, that is, $\Delta Q \leq 0$, implying that any thermal process should be fundamentally *irreversible* in nature, as stated by the *second law* of thermodynamics. Depending on the process, ΔQ cannot be *uniquely* specified as a function of temperature and pressure; hence, the *heat quantity* Q cannot be a state function. Instead, a function S defined by $\Delta Q/T = \Delta S$ is utilized as a state function, if the *integrating denominator* T can be found for ΔS to be a *total differential*, representing a reversible contact by another common quantity S between the crystal and surroundings. Clausius generalized this argument in an integral form $\oint_C \Delta Q/T \leq 0$ or $\oint_C \mathrm{d}S \leq 0$ along a closed curve C in a *phase diagram*, where the equality sign is assigned for a *reversible* process. Thermal

equilibrium can therefore be specified by a *maximum* of the state function S, called the *entropy*. Boltzmann interpreted the entropy S in terms of *thermodynamic probability* $g(T)$, representing the average of randomly distributed microscopic energies in the surrondings. He wrote the relation

$$S = k_{\mathrm{B}} \ln g(T), \tag{1.1}$$

where k_{B} is the Boltzmann constant. It is significant that such a probability is a valid concept for crystalline states to be in equilibrium at temperature T and pressure p; random phonon energies allow statistical description.

Physical properties of a crystal can be represented by the internal energy $U(p, T)$, which can be varied by not only heat Q but also external work W, as stated by *the first law of thermodynamics*, that is,

$$\Delta U = Q + W. \tag{1.2}$$

In a solid, mechanical work can change the volume, accompanying a structural modification, which can be performed by an external force, electric and magnetic fields, if constituent molecules consist of electric or magnetic moments. Denoting such elemental variables by σ_m located at lattice sites m, the work W performed by an external agent X can be expressed as $W = -\sum_m \sigma_m X$. These σ_m are generally called *order variables*.

It is realized that internal variables σ_m depend on their sites in the lattice, and generally *correlated* with each other. Internal correlations are primarily independent of temperature, hence occurring *adiabatically*, whereas the heat quantity Q depends on the temperature, flowing in and out of a crystal in *isothermal* conditions. Nevertheless, internal correlations in crystals may generally be observed as weakly temperature dependent.

Mutually correlated σ_m can be expressed in a propagating mode, if a crystal is in an excited condition, exhibiting modulated lattice translation. Owing to their nonlinear character, such correlations can be considered as driven by an *adiabatic potential* ΔU_m at the lattice point m, as will be discussed in Chap. 7. In this case, their propagation can be characterized by a modulated periodicity different from the original lattice, showing a periodically *ordered* structure. On the other hand, if correlations occur only in short distances between σ_m and σ_n, their energies can be expressed by $-J_{mn}\sigma_m\sigma_n$. In this case, by writing

$$-\sum_n J_{mn}\sigma_m\sigma_n = -\sigma_m X_m, \tag{1.3}$$

we can consider the internal field $X_m = \sum_n J_{mn}\sigma_n$. Taking the spatial average over all lattice sites, we can consider the *mean-field average* $\langle X_m \rangle$ instead of X_m. For nonvanishing $\langle \sigma_m \rangle \neq 0$, (1.3) can be interpreted as work performed by $\langle X_m \rangle$ on $\langle \sigma_m \rangle$, representing the correlation energy in mean-field accuracy. However, if expressing (1.3) as $-\langle \sigma_m \rangle X_{\mathrm{int}}$, the *internal field* X_{int} may be regarded in better

accuracy than $\langle X_m \rangle$. If the corresponding *adiabatic potential* ΔU_m can be specified, we have the relation $X_{\text{int}} = -\partial \Delta U_m / \partial x_m$, which gives an alternative expression for $\sum_n J_{mn}\sigma_n$.

In the presence of an external field X, the effective field can then be assumed as $X + X_{\text{int}} = X'$. Although X is an adiabatic variable, X_{int} can be a function of T and p, so that the effective field X' is generally temperature dependent, that is, $X' = X'(T)$ under a constant p. The macroscopic energy relation for a general process can then be expressed as

$$\Delta U \leq \Delta Q - \Delta(\sigma X') \quad \text{or} \quad \Delta U - T\Delta S + \Delta(\sigma X') \leq 0.$$

Defining the Gibbs potential $G = U - TS + \sigma X'$, we obtain the equilibrium condition

$$\Delta G \leq 0. \tag{1.4}$$

This indicates that a minimum of the Gibbs potential can determine equilibrium against any variation of thermodynamic variables.

In practice, it is important to identify order variables σ_m, against which the Gibbs function can be minimized for equilibrium under a fixed external condition. If a crystal is assumed as a continuous medium, distributed microscopic variables σ_m among lattice sites can be expressed by an averaged continuous variable σ, called the *order parameter* in the *mean-field approximation*. The Gibbs function can then be given as $G(p, T; \sigma)$, where σ is normally defined to take values restricted in the range $0<\sigma<1$. Noted that some crystals are ordered *spontaneously* with no external agent, for which the internal field X_{int} is considered as responsible. For a ferromagnetic crystal, Weiss (1907) postulated such a field X_{int} as proportional to σ, which is the magnetization in the mean-field approximation.

According to (1.4), under a constant T–p condition, thermal equilibrium can be determined by fluctuating σ at a minimum of the Gibbs function. Such fluctuations may occur in a crystal spontaneously, establishing equilibrium as determined by (1.4). As substantiated by observed anomalies, such spontaneous fluctuations are not hypothetical, as will be discussed in later chapters.

1.2 Structural Changes

In equilibrium conditions, crystalline states are stable, but transformable from one state to another by varying surroundings and external forces. We consider that the order variables σ_m in collective motion are responsible for such *phase transitions*. Although primarily independent of the hosting lattice, the correlated variables can modify the lattice translational symmetry, leading to another structure in different symmetry. In this case, due to Newton's action–reaction principle, correlated displacements $\boldsymbol{u}_m$ of lattice points can also be considered to counteract σ_m. Born and Huang [1] proposed that structural stability should be maintained with

minimum strains, which can be determined by minimizing the Gibbs potential modified for such a deformed crystal.

Considering a transition from a phase 1 to another phase 2 at critical conditions p_c and T_c, the Gibbs potential can be expressed as $G(p_c, T_c; \sigma_1, \sigma_2)$, where σ_1 and σ_2 are variables to represent two phases, signifying that the crystal is composed of mixed phases during the process. In fact, these σ_1 and σ_2 may be randomly distributed variables, so that the mixed composition considered here is not well defined. Nevertheless, we write the Gibbs potential in the presence of an applied field X at the critical temperature as

$$G_{\text{trans}} = G(p_c, T_c; \sigma_1, \sigma_2) - (\sigma_1 + \sigma_2)X.$$

On the other hand, the Gibbs potentials for coexisting phases 1 and 2 at p and T can be expressed as

$$G_1 = G(p, T) - \sigma_1 X \quad \text{and} \quad G_2 = G(p, T) - \sigma_2 X.$$

For a *binary transition* characterized by $\sigma_1 = -\sigma_2$, we can consider fluctuations $\Delta\sigma_1 = -\Delta\sigma_2$, for which the change in the Gibbs potential can be expanded as

$$\Delta G_{\text{trans}} = \frac{1}{2} \sum_{i,j=1,2} \left(\frac{\partial^2 G}{\partial \sigma_i \partial \sigma_j} \right)_{p,T} \Delta\sigma_i \Delta\sigma_j + \cdots. \tag{1.5}$$

Neglecting higher-order terms for small $\Delta\sigma_i$, a nonvanishing ΔG_{trans} gives a discontinuity at the transition. On the other hand, if the inversion does not exist, ΔG_{trans} is dominated by a finite first-order derivative of G; the phase transition signified by the first-order term is called the *first-order transition*. For a binary case as given by (1.5), ΔG_{trans} of the second-order terms are predominant, and the transition is called *second order*, according to the *Ehrenfest's classification*. It is noted from (1.5) that both the correlations $\Delta\sigma_i \Delta\sigma_j$ and the second-order derivatives of G should not vanish for second-order phase transitions. It is significant that the presence of internal correlations $\Delta\sigma_i \Delta\sigma_j$ is necessary for the transition to be second order, which is in fact substantiated by *transition anomalies*.

First-order transitions are characterized by $G_1 = G_2$, if $X = 0$; otherwise,

$$\Delta G_{1,2} = (\sigma_2 - \sigma_1)X. \tag{1.6}$$

The Gibbs potential and order parameter are referred to as *extensive variables*; by definition these are thermodynamic quantities proportional to the corresponding volumes. Denoting domain volumes by V_1 and V_2, the total volume is determined by $V_1 + V_2 = V$. Hence, (1.6) can be interpreted in terms of the volume ratio V_1/V_2, or by σ_1/σ_2 that can be varied with an applied X (see Chap. 4). Domain volumes are thus transformable by applying X, as $V_1 \leftrightarrows V_2$.

Figure 1.1 shows a phase diagram, where Gibbs functions of two phases G_1 and G_2 are schematically plotted in a p–T plane. The crossing point $P(p_o, T_o)$ indicates

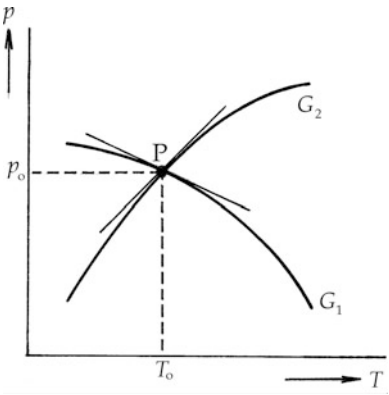

Fig. 1.1 Phase equilibrium in the p–T diagram. Two curves of Gibbs functions $G_1(p,T)$ and $G_2(p,T)$ cross at a point $P(p_o, T_o)$, representing thermal equilibrium between phases 1 and 2. If the transition is discontinuous, such Gibbs functions cannot specify the equilibrium sufficiently at P, requiring another variable, for example, σ.

the external condition for a transition between G_1 and G_2; however, the discontinuity ΔG is implicit in this diagram. Nevertheless, at P there is a discontinuous change of curvature as related to ΔG_{trans}. Figure 1.2a illustrates a continuous second-order transition $G_1 \rightarrow G_2$ at the critical temperature T_c. In the phase diagram σ–T shown in Fig. 1.2b however, a continuous transition is broadened by fluctuations in the vicinity of T_c. At noncritical temperatures below T_c the first-order transformation $\sigma_1 \leftrightarrow \sigma_2$ can be performed by applying a force X as described by (1.6).

1.3 Modulated Phases

Associated with lattice excitations, the order variable σ is primarily in propagation through the crystal space, but modulated in finite amplitude. Such a modulated wave is in *standing-wave* form in practical crystals in thermal equilibrium, thereby detectable during an ordering process, and in *sinusoidal phases* of some crystalline systems. Such standing waves can signify a thermodynamic crystalline state with modulated symmetry. In this sense, a modulated σ is essential, which may be called a *mesoscopic* variable. Following after Kirkwood's definition, we consider such phases specified by a continuous variable σ as thermodynamic phases.

In a practical observation, the Gibbs potential for a mesoscopic state should be expressed by a time average

$$(G)_{p,T} = \frac{1}{t_o}\int_0^{t_o} \mathrm{d}t \left(\frac{1}{V}\int_V g(\boldsymbol{r},t)\mathrm{d}^3\boldsymbol{r} \right),$$

where t_o is the timescale of observation, $g(\boldsymbol{r},t)$ is the density of the potential, and V is a sampling volume. Writing as

$$\frac{1}{t_o}\int_0^{t_o} g(\boldsymbol{r},t)\mathrm{d}t = \langle g(\boldsymbol{r})\rangle_t,$$

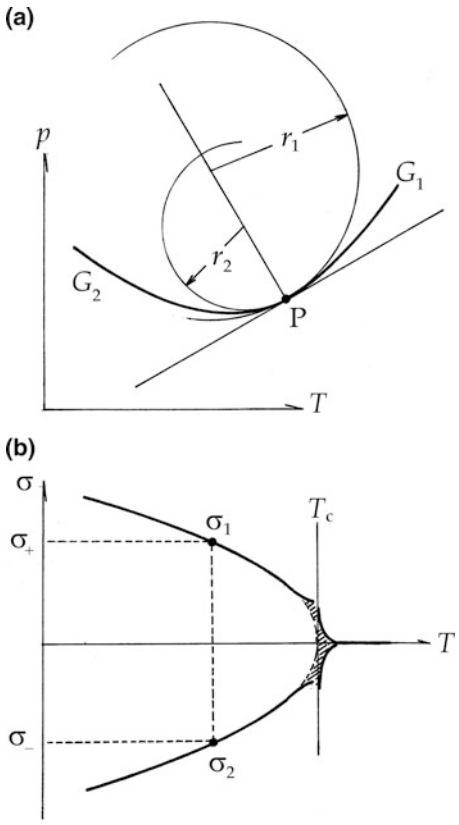

Fig. 1.2 (**a**) The second-order phase transition is characterized by two functions G_1 and G_2 that have a common tangent and different curvatures at P in the p–T diagram. (**b**) Equilibrium between binary domains specified by σ_1 and σ_2, which are separated phases at temperatures below the critical temperature T_c. Transition anomalies near T_c are shown schematically by the shaded area.

$(G)_{p,T}$ can be expressed as a spatial average

$$(G)_{p,T} = \frac{1}{V}\int_V \langle g(\boldsymbol{r})\rangle_t \mathrm{d}^3\boldsymbol{r} \tag{1.7}$$

over the volume V. The time-averaged density $\langle g(\boldsymbol{r})\rangle_t$ can be sampled in practical experiments. Although the simplest assumption is to consider (1.7) by the *mean-field average*, it is important that $\langle g(\boldsymbol{r})\rangle_t$ can be measured by sampling experiments, providing more accurate information than mean-field approximation. In practice, a mesoscopic variable $\sigma(\boldsymbol{r}, t)$ can thus be sampled as $\langle \sigma(\boldsymbol{r})\rangle_t$ that is informative for the spatial distribution. It is noted that the timescale t_o and sampling volume V are usually specified for sampling experiments.

Further, the dynamical variation of $g(\boldsymbol{r})$ is essentially *adiabatic*, but recognized actually as temperature dependent in crystals in thermodynamic environment. Such a variation may cause a volume change, although ignored in traditional arguments. In order for (1.7) to be a meaningful space–time average, the function $(G)_{p,T}$ should

be obtained after a thermal relaxation process in the modulated lattice, in order to represent the consequence of the Born–Huang principle [2].

1.4 Superconducting States in Metals

The superconducting transition in metals is interpreted as a condensation phenomenon in the reciprocal space. Although characterized by supercurrent and Meissner's magnetic effects, thermally superconducting phase transitions were recognized in specific heat measurements, which can be interpreted with the concept of *condensates*. Fröhlich's field-theoretical model of electron–phonon interaction has provided a clear image of condensates to initiate a phase transition, for which the theory of Bardeen, Cooper, and Schrieffer allows to define order variables. The last three chapters in this book are devoted to discussions of superconducting transitions in metals analogous to structural changes; both phase changes are signified by nonlinear adiabatic potentials that arise from the lattice.

Exercises 1

1. What is the mean-field average? If a physical event at each lattice point is random and independent in space, the average should always be zero, should it not? There must be some kind of correlations among them, in order to have a nonzero average. Discuss this issue.
2. Review Ehrenfest's classification of phase transitions from a standard book on thermodynamics. In his definition of second-order transitions, vanishing first-order derivatives and nonzero second-order derivatives of the Gibbs function are necessary. On the other hand, we noted that correlations $\Delta\sigma_i \Delta\sigma_j$ among internal variables are also required for the definition. Is this a conflict? If so, this problem should be discussed to clear the apparent conflict before proceeding to the following chapters.

Part I
Phonons and Order Variables

Chapter 2
Phonons

In this chapter, dynamics of an idealized lattice is discussed as an approximate model for practical crystals in complex structure. Lattice vibrations in propagating modes represent fundamental excitations in the periodic structure, being characterized by frequencies and wave vectors distributed in virtually continuous spectra. Quantum theoretically, the lattice dynamics is represented by a *phonon* gas, where phonon quanta behave like classical particles. On the other hand, lattice excitations at low frequencies can be responsible for the strained structure. For thermoelastic properties of crystals, such excitations play essential roles, depending on thermal and mechanical conditions of the surroundings.

2.1 Normal Modes in a Simple Crystal

For a cubic lattice of N-particles of identical mass, first we solve the *classical* equations of motion by taking nearest-neighbor interactions into account. Although the problem is essentially *quantum mechanical*, the classical results are also useful in the approximate approach. It is noted that lattice symmetry is invariant with nearest-neighbor interactions to retain the lattice stability. In harmonic approximation, the equations of motion are *linear*, and separable into $3N$ independent equations. Each one is a one-dimensional equation along symmetry axes, and the total number of particles in the crystal is $3N$. In such an idealized case, the classical equations of motion can be written as

$$\ddot{x}_n = \omega^2(x_{n+1} + x_{n-1} - 2x_n), \quad \ddot{y}_n = \omega^2(y_{n+1} + y_{n-1} - 2y_n), \quad \text{and}$$
$$\ddot{z}_n = \omega^2(z_{n+1} + z_{n-1} - 2z_n),$$

where the suffixes n indicate lattice sites and $\omega^2 = \kappa/m$, where κ and m denote the mass of a constituent particle and the force constant, respectively. Instead of

M. Fujimoto, *Thermodynamics of Crystalline States*,
DOI 10.1007/978-1-4419-6688-9_2, © Springer Science+Business Media, LLC 2010

rectangular coordinates x_n, y_n, and z_n, we can use the generalized coordinates q_n, with which the equations of motion can be written as

$$\ddot{q}_n = \omega^2(q_{n+1} + q_{n-1} - 2q_n). \tag{2.1}$$

Defining the conjugate momentum to q_n by $p_n = m\dot{q}_n$, the *Hamiltonian* of the vibrating lattice can be expressed as

$$\mathcal{H} = \sum_{n=0}^{N} \left\{ \frac{p_n^2}{2m} + \frac{m\omega^2}{2}(q_{n+1} - q_n)^2 + \frac{m\omega^2}{2}(q_n - q_{n-1})^2 \right\}. \tag{2.2}$$

In the summation, each expression for n represents one-dimensional chain of identical masses m, as illustrated in Fig. 2.1a.

Normal coordinates and *conjugate momenta*, Q_k and P_k, can be expressed by the Fourier expansions

$$q_n = \frac{1}{\sqrt{N}} \sum_{k=0}^{N} Q_k \exp \mathrm{i}kna \quad \text{and} \quad p_n = \frac{1}{\sqrt{N}} \sum_{k=0}^{N} P_k \exp \mathrm{i}kna, \tag{2.3}$$

where a is the *lattice constant*. For each normal mode, the amplitudes Q_k and P_k are related as

$$Q_{-k} = Q_k^*, \quad P_{-k} = P_k^*, \quad \text{and} \quad \sum_{n=0}^{N} \exp \mathrm{i}(k - k')na = N\delta_{kk'}, \tag{2.4}$$

where $\delta_{kk'}$ is *Kronecker's delta*, that is, $\delta_{kk'} = 1$ for $k = k'$, otherwise zero for $k = k'$.

Using normal coordinates, the Hamiltonian can be expressed as

$$\mathcal{H} = \frac{1}{2m} \sum_{k=0}^{2\pi/a} \left\{ P_k P_k^* + Q_k Q_k^* m^2 \omega^2 \left(\sin^2 \frac{ka}{2} \right) \right\}, \tag{2.5}$$

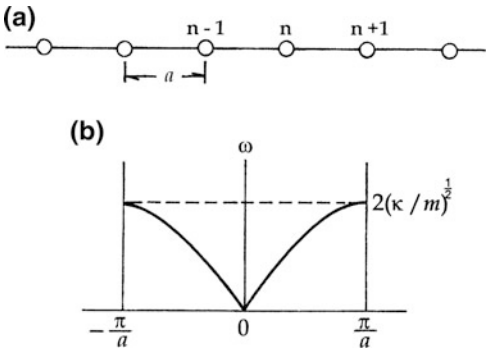

Fig. 2.1 (**a**) One-dimensional monatomic chain of the lattice constant a. (**b**) A dispersion curve ω versus k of the chain lattice.

where

$$\ddot{Q}_k = -m^2\omega^2 Q_k \tag{2.6}$$

and

$$\omega_k = 2\omega \sin\frac{ka}{2} = 2\sqrt{\frac{\kappa}{m}}\sin\frac{ka}{2}. \tag{2.7}$$

As indicated by (2.7), the lattice modes of coupled oscillators are *dispersive*, signified by ω_k that is not linearly related with k. From (2.5), $\mathcal{H}$ composed of N independent harmonic oscillators is expressed by the normal coordinates Q_k and conjugate momenta P_k, where $k = 2\pi n/Na$ and $n = 0, 1, 2, \ldots, N$. Figure 2.1b shows the dispersion relation (2.7) of the characteristic frequency ω_k.

Equation (2.6) can be solved with the initial conditions for Q_k and $\dot{Q}_k$ at $t = 0$, and the solution is expressed as

$$Q_k(t) = Q_k(0)\cos\omega_k t + \frac{\dot{Q}_k(0)}{\omega_k}\sin\omega_k t.$$

Accordingly, we have

$$q_n(t) = \frac{1}{\sqrt{N}}\sum_k \sum_{n'=n,n\pm1} \left[q_{n'}(0)\cos\{ka(n-n') - \omega_k t\} + \frac{\dot{q}_{n'}}{\omega_k}\sin\{ka(n-n') - \omega_k t\}\right], \tag{2.8}$$

where $a(n - n')$ represents distances between sites n and n'. Considering a cubic volume L^3 where $L = Na$, the whole crystal is packed by a large number of these unit volumes. Composed of such units, we can ignore surfaces from a large crystal, setting periodic boundary conditions $q_{n=0}(t) = q_{n=N}(t)$ for $L = Na$. Expressing the coordinates by $x = na$, (2.8) can be written as

$$q(x,t) = \sum_k [A_k \cos(\pm kx - \omega_k t) + B_k \sin(\pm kx - \omega_k t)],$$

where $A_k = q_k(0)/\sqrt{N}$ and $B_k = \dot{q}_k(0)/\omega_k\sqrt{N}$. The boundary conditions at $x = 0$ and $x = L$ can thus be specified by $kL = 2\pi n$ or $k = 2\pi n/L$, where $n = 0, 1, 2, \ldots, N$. Hence, for a large L, the position x can be assumed to be a continuous variable. Consisting of propagating waves in $\pm x$-directions, $q(x, t)$ can be conveniently written in complex exponential form, that is,

$$q(x,t) = \sum_k C_k \exp \mathrm{i}(\pm kx - \omega_k t + \varphi_k), \tag{2.9}$$

where $C_k^2 = A_k^2 + B_k^2$ and $\tan\varphi_k = B_k/A_k$. In three-dimensional crystals, these one-dimensional modes along x, y and z axes are independent of each other; there are in total $3N$ normal modes in the crystal.

2.2 Quantized Normal Modes

The Hamiltonian of a crystal lattice can be separated into $3N$ independent normal modes, expressing propagations along the symmetry axes, on each we have $k = 1, 2, \ldots, N$. In quantum theory, the normal coordinate Q_k and conjugate momentum $P_k = -\mathrm{i}\hbar(\partial/\partial Q_k)$ are *operators*, where $\hbar$ is the Planck constant h divided by 2π, obeying commutation relations

$$[Q_k, Q_{k'}] = 0, \quad [P_k, P_{k'}] = 0, \quad \text{and} \quad [P_k, Q_{k'}] = \mathrm{i}\hbar\delta_{kk'}. \tag{2.10}$$

We consider the Hamiltonian operator

$$\mathcal{H}_k = \frac{1}{2m}(P_k P_k^\dagger + m^2\omega_k^2 Q_k Q_k^\dagger) \tag{2.11a}$$

for the normal mode k, where $P_k^\dagger$ and $Q_k^\dagger$ are *transposed* matrix operators of the complex conjugates P_k^* and Q_k^*, respectively.

Denoting the eigenvalues of $\mathcal{H}_k$ by ε_k, we have the equation

$$\mathcal{H}_k\psi_k = \varepsilon_k\psi_k. \tag{2.11b}$$

For real ε_k, P_k and Q_k should be *Hermitian* operators, as characterized by $P_k^\dagger = P_{-k}$. Defining operators

$$b_k = \frac{m\omega_k Q_k + \mathrm{i}P_k^\dagger}{\sqrt{2m\varepsilon_k}} \quad \text{and} \quad b_k^\dagger = \frac{m\omega_k Q_k^\dagger - \mathrm{i}P_k}{\sqrt{2m\varepsilon_k}}, \tag{2.12}$$

we obtain the relation

$$\begin{aligned} b_k b_k^\dagger &= \frac{1}{2m\varepsilon_k}(m^2\omega_k^2 Q_k^\dagger Q_k + P_k^\dagger P_k) + \frac{\mathrm{i}\omega_k}{2\varepsilon_k}(Q_k^\dagger P_k^\dagger - P_k Q_k) \\ &= \frac{H_k}{\varepsilon_k} + \frac{\mathrm{i}\omega_k}{2\varepsilon_k}(Q_{-k}P_{-k} - P_k Q_k). \end{aligned}$$

From this, we can derive

$$\mathcal{H}_k = \hbar\omega_k\left(b_k^\dagger b_k + \frac{1}{2}\right), \quad \text{if } \varepsilon_k = \frac{1}{2}\hbar\omega_k. \tag{2.13}$$

Therefore, $\mathcal{H}_k$ are commutable with the operator $b_k^\dagger b_k$, that is,

$$[\mathcal{H}_k, b_k^\dagger b_k] = 0,$$

and from (2.12)

$$[b_{k'}, b_k^\dagger] = \delta_{k'k}, \quad [b_{k'}, b_k] = 0, \quad \text{and} \quad [b_{k'}^\dagger, b_k^\dagger] = 0.$$

Accordingly, we obtain

$$[\mathcal{H}_k, b_k^\dagger] = \hbar\omega_k b_k^\dagger \quad \text{and} \quad [b_k, \mathcal{H}_k] = \hbar\omega_k b_k.$$

Combining these with (2.11b), the relations

$$\mathcal{H}_k(b_k^\dagger \psi_k) = (\varepsilon_k + \hbar\omega_k)(b_k^\dagger \psi_k) \quad \text{and} \quad \mathcal{H}_k(b_k \psi_k) = (\varepsilon_k - \hbar\omega_k)(b_k \psi_k)$$

can be derived, which indicate that $b_k^\dagger \psi_k$ and $b_k \psi_k$ are eigenfunctions for the energies $\varepsilon_k + \hbar\omega_k$ and $\varepsilon_k - \hbar\omega_k$, respectively. In this context, $b_k^\dagger$ and b_k are referred to as *creation* and *annihilation* operators for the energy quantum $\hbar\omega_k$, and we can write

$$b_k^\dagger b_k = 1. \tag{2.14}$$

Applying the creation operator $b_k^\dagger$ on the ground-state function ψ_k n_k-times, the eigenvalue of the wave function $(b_k^\dagger)^{n_k}\psi_k$ can be expressed as $[n_k + (1/2)]\hbar\omega_k$, indicating that this state consists of n_k quanta plus the ground-state energy $(1/2)\hbar\omega_k$. Considering $\hbar\omega_k$ like a particle, called a *phonon*, such an exited state with n_k identical phonons is multiply degenerated by *permutation* $n_k!$. Hence, the normalized wave function of a phonon can be expressed by $(1/\sqrt{n_k!})(b_k^\dagger)^{n_k}\psi_k$. The total lattice energy in an excited state, which consists of $n_1, n_2, \ldots$ phonons in the normal modes $1, 2, \ldots$, can then be expressed by

$$U(n_1, n_2, \ldots) = U_\mathrm{o} + \sum_k n_k \hbar\omega_k, \tag{2.15a}$$

where $U_\mathrm{o} = \sum_k \hbar\omega_k/2$ is the total zero-point energy. The corresponding wave function can be written as

$$\Psi(n_1, n_2, \ldots) = \frac{(b_1^\dagger)^{n_1}(b_2^\dagger)^{n_2}\cdots}{\sqrt{n_1! n_2! \cdots}}(\psi_1\psi_2\cdots), \tag{2.15b}$$

describing a system of $n_1, n_2, \ldots$ phonons of energies $n_1\hbar\omega_{k_1}, n_2\hbar\omega_{k_2}, \ldots$, leaving the total number $n_1 + n_2 + \cdots$ as undetermined.

2.3 Phonon Momentum

In the foregoing, we discussed a one-dimensional chain of mass particles as a model for a real crystal in three dimensions. This model is valid in harmonic accuracy; however, it is not sufficient for real crystals. In general, the lattice vibration propagating in arbitrary direction can be regarded as the *vibrating field*, which is more appropriate concept than the classical theory of normal modes. Considering sound waves in anisotropic media, such a field is a more realistic concept, where quantized phonons behave like free particles.

Setting rectangular coordinates x, y, z along the symmetry axes in an orthorhombic crystal, lattice vibrations can be described in classical theory by a set of equations

$$\begin{aligned}
\frac{p_{x,n_1}^2}{2m} + \frac{\kappa}{2}\left\{(q_{x,n_1} - q_{x,n_1+1})^2 + (q_{x,n_1} - q_{x,n_1-1})^2\right\} &= \varepsilon_{x,n_1}, \\
\frac{p_{y,n_2}^2}{2m} + \frac{\kappa}{2}\left\{(q_{y,n_2} - q_{y,n_2+1})^2 + (q_{y,n_2} - q_{y,n_2-1})^2\right\} &= \varepsilon_{y,n_2}, \\
\frac{p_{z,n_3}^2}{2m} + \frac{\kappa}{2}\left\{(q_{z,n_3} - q_{z,n_3+1})^2 + (q_{z,n_3} - q_{z,n_3-1})^2\right\} &= \varepsilon_{z,n_3},
\end{aligned} \tag{2.16}$$

where $\varepsilon_{x,n_1} + \varepsilon_{y,n_2} + \varepsilon_{z,n_3} = \varepsilon_{n_1 n_2 n_3}$ is the vibration energy at a lattice site specified by indexes (n_1, n_2, n_3), and κ is the force constant.

The variables $q_{x,n_1}, q_{y,n_2}, q_{z,n_3}$ in (2.16) are three components of a classical vector $\boldsymbol{q}$, which can be interpreted as *probability amplitudes* of the harmonic displacement in the vibration field. In this assumption, we can define a wave function for the *displacement field* $\Psi(n_1, n_2, n_3) = q_{x,n_1} q_{y,n_2} q_{z,n_3}$, for which these components can be written as

$$q(x,t) = \sum_{k_x} C_{k,x} \exp \mathrm{i}\left(\pm k_x x - \omega_{k_x} t + \varphi_{k_x}\right),$$

$$q(y,t) = \sum_{k_y} C_{k_y} \exp \mathrm{i}\left(\pm k_y y - \omega_{k_y} t + \varphi_{k_y}\right),$$

$$q(z,t) = \sum_{k_z} C_{k_y} \exp \mathrm{i}\left(\pm k_z z - \omega_{k_z} t + \varphi_{k_z}\right),$$

and hence

$$\Psi(n_1, n_2, n_3) = \sum_k \mathcal{A}_k \exp \mathrm{i}\left(\pm \boldsymbol{k} \cdot \boldsymbol{r} - \frac{n_1 \varepsilon_{x,n_1} + n_2 \varepsilon_{y,n_2} + n_3 \varepsilon_{z,n_3}}{\hbar} t + \varphi_k\right).$$

Here, $\mathcal{A}_k = C_{k_x} C_{k_y} C_{k_z}$, $\varphi_k = \varphi_{k_x} + \varphi_{k_y} + \varphi_{k_z}$, and $\boldsymbol{k} = (k_x, k_y, k_z)$ are the amplitude, arbitrary phase constant, and wave vector, respectively. Further writing

$$\frac{n_1 \varepsilon_{x,n_1} + n_2 \varepsilon_{y,n_2} + n_3 \varepsilon_{z,n_3}}{\hbar} = \omega_k, \tag{2.17a}$$

the field propagation along the direction of a vector $\boldsymbol{k}$ can be expressed as

$$\Psi(\boldsymbol{k}, \omega_k) = \mathcal{A}_k \exp \mathrm{i}(\pm \boldsymbol{k} \cdot \boldsymbol{r} - \omega_k t + \varphi_k), \tag{2.17b}$$

describing a phonon of energy $\hbar\omega_k$ and momentum $\pm \hbar \boldsymbol{k}$. For a small value of $|\boldsymbol{k}|$, the propagation in a cubic lattice can be characterized by a constant speed v of propagation determined by $\omega_k = v|\boldsymbol{k}|$, for which we have no *dispersion* in this approximation.

The phonon propagation can be described in the space of k_x, k_y, k_z called a *reciprocal lattice* space, as illustrated in two dimensions in Fig. 2.2. We have the relations

$$k_x = \frac{2\pi n_1}{L}, \quad k_y = \frac{2\pi n_2}{L}, \quad \text{and} \quad k_z = \frac{2\pi n_3}{L}$$

in a cubic crystal. A discrete set of integers (n_1, n_2, n_3) determines a momentum of a phonon propagating in the direction of $\boldsymbol{k}$, where $|\boldsymbol{k}| = \frac{2\pi}{L}\sqrt{n_x^2 + n_y^2 + n_z^2}$. All points on a spherical surface of radius $|\boldsymbol{k}|$ correspond to the same $\hbar\omega_k$, which are almost continuously distributed on the sphere of a sufficiently large radius.

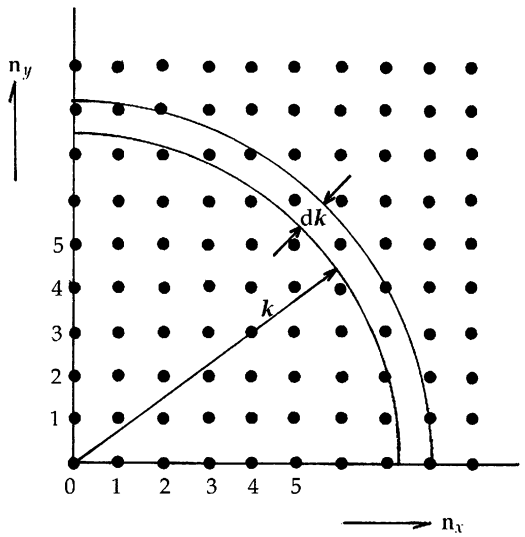

Fig. 2.2 Two-dimensional reciprocal lattice. A lattice point is indicated by (k_x, k_y). Two-quarter circles of radii k and $k + \mathrm{d}k$ show surfaces of constant ε_k and $\varepsilon_{k+\mathrm{d}k}$ for small $|\boldsymbol{k}|$ in $k_x k_y$-plane.

2.4 Thermal Equilibrium

In thermodynamics, a crystal must always be in *thermal contact* with the surroundings. The quantized vibration field should therefore be in equilibrium with the heat reservoir. A large number of phonons are in free motion, traveling randomly in all directions through the lattice, reflecting from surfaces, where their energy and momentum are exchanged with the surroundings. In thermal equilibrium, the phonon distribution can therefore be described statistically with the concept of probability.

For such a crystal in thermal equilibrium with the heat reservoir, the total internal energy should be written as $U + U_\mathrm{s}$, where U_s is a contribution from the heat reservoir. The total $U + U_\mathrm{s}$ should take a stationary value against any variations of the other variables to specify equilibrium. Signified by random phonons, the internal energy of a crystal can be calculated with statistical probabilities w and w_s for deviations from equilibrium. In this case, the product probability ww_s can be considered to be maximum for $U + U_\mathrm{s}$ to be constant. Accordingly, we set up a variation problem as

$$\delta(ww_\mathrm{s}) = 0 \quad \text{and} \quad \delta(U + U_\mathrm{s}) = 0.$$

Therefore, for arbitrary variations we can write

$$w_\mathrm{s}\delta w + w\delta w_\mathrm{s} = 0 \quad \text{and} \quad \delta U + \delta U_\mathrm{s} = 0,$$

and we can derive the relation

$$\frac{\delta(\ln w)}{\delta U} = \frac{\delta(\ln w_\mathrm{s})}{\delta U_\mathrm{s}}.$$

The quantity in common between U and U_s can be defined as the equilibrium temperature. Therefore, writing it as $\beta = 1/k_\mathrm{B}T$, we obtain the relation

$$\frac{\delta(\ln w)}{\delta U} = \beta = \frac{1}{k_\mathrm{B}T} \quad \text{or} \quad w = w_\mathrm{o}\exp\left(-\frac{U}{k_\mathrm{B}T}\right), \tag{2.18}$$

where w_o is the integration constant to be determined with the quantum nature of absolute zero $T = 0\,\mathrm{K}$, and k_B is the Boltzmann constant. This allows defining absolute zero temperature by $U = 0$; however, due to uncertainty $T = 0$ cannot be reached quantum theoretically. The ground-state energy $U_\mathrm{o} = (1/2)N\hbar\omega_\mathrm{o}$ is referred to as the *zero-point energy*.

Although only vibrating lattice was considered so far, properties of a crystal can also be contributed by additional variables located at lattice points or *interstitial* sites in a crystal. These variables are primarily independent of lattice vibrations, but

can interact with the lattice in some crystals. Nevertheless, denoting such microscopic energies and their probabilities by ε_i and w_i, we can write

$$U = \sum_i \varepsilon_i \quad \text{and} \quad w = \prod_i w_i,$$

where

$$w_i = w_o \exp\left(-\frac{\varepsilon_i}{k_B T}\right), \tag{2.19}$$

which is known as the *Boltzmann probability*. The probabilities w_i must satisfy the relation $\sum_i w_i = 1$, regarding these *exclusive* events; and $w_o = 1/Z$, where $Z = \sum_i \exp(-\varepsilon_i/k_B T)$ is the *partition function*. Constituting a *microcanonical ensemble*, thermal properties of a crystal due to these microscopic variables can be calculated with the partition function Z.

2.5 Specific Heat

Thermal properties of a crystal can be represented by a specific heat C_V at constant volume V, which is defined as $C_V = (\partial U/\partial T)_V$. The internal energy U is given by the sum of normal mode energies $\varepsilon_k = (n_k + (1/2))\hbar\omega_k$ for the wave vector $\boldsymbol{k}$ in virtually any direction in the reciprocal lattice. Denoting the number of phonons of energies ε_k by $g(k)$, we can write the partition function as

$$Z_k = g(k) \exp\left(-\frac{\varepsilon_k}{k_B T}\right) = g(k) \exp\left(-\frac{\hbar\omega_k}{2k_B T}\right) \sum_{n_k=0}^{\infty} \exp\left(-\frac{n_k \hbar\omega_k}{k_B T}\right),$$

where the summation is an infinite series, if $\hbar\omega_k/k_B T < 1$. In fact, this condition is met in a crystal at a given temperatures, so that Z can be calculated as

$$Z_k = g(k) \frac{\exp(-\hbar\omega_k/2k_B T)}{1 - \exp(-\hbar\omega_k/k_B T)}.$$

For the whole system, the partition function can be calculated as $Z = \prod_k Z_k$ and hence $\ln Z = \sum_k \ln Z_k$, from which the free energy can be expressed as $F = k_B T \sum_k \ln Z_k$, and we have

$$\ln Z_k = -\frac{\hbar\omega_k}{2} + k_B T \ln g(k) - k_B T \ln\left\{1 - \exp\left(-\frac{\hbar\omega_k}{k_B T}\right)\right\}.$$

Using the relation $F = U - TS = U + T(\partial F/\partial T)_V$, we obtain

$$U = -T^2(\partial/\partial T)\ (F/T)$$

Therefore

$$U = U_o + \sum_k \frac{\hbar\omega_k}{\exp(\hbar\omega_k/k_B T) - 1} \quad \text{and} \quad U_o = \frac{1}{2}\sum_k \hbar\omega_k. \tag{2.20}$$

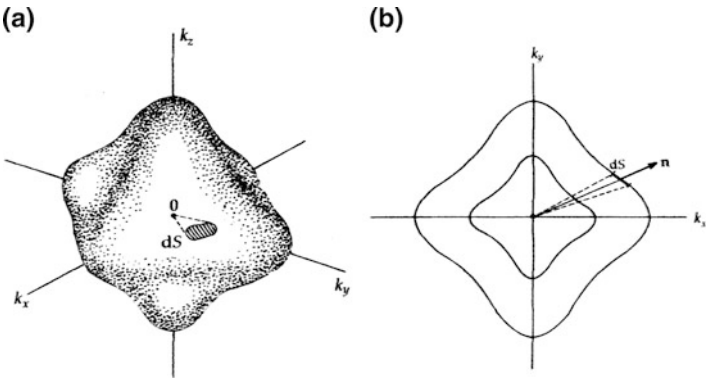

Fig. 2.3 (**a**) A typical constant-energy surface in three-dimensional reciprocal space, where dS is a differential area on the surface. (**b**) The two-dimensional view in the k_xk_y-plane.

The specific heat at constant volume can then be expressed as

$$C_V = \left(\frac{\partial U}{\partial T}\right)_V = k_\mathrm{B} \sum_k \frac{(\hbar\omega_k/k_\mathrm{B}T)^2 \exp(\hbar\omega_k/k_\mathrm{B}T)}{(\exp(\hbar\omega_k/k_\mathrm{B}T) - 1)^2}. \tag{2.21}$$

To calculate C_V with (2.21), we need to evaluate the summation for the number of phonon states on an energy surface $\varepsilon_k = \hbar(\omega_k + 1/2) =$ constant in the reciprocal space. For an anisotropic crystal, such a surface is not spherical, but complex as shown in Fig. 2.3a. The summation in (2.21) can therefore be re-expressed by a volume integration in the $\boldsymbol{k}$-space, where the volume element is given by $\mathrm{d}^3\boldsymbol{k} = \mathrm{d}\boldsymbol{k} \cdot \mathrm{d}\boldsymbol{S} = \mathrm{d}k_\perp |d\boldsymbol{S}|$. Here, $\mathrm{d}k_\perp$ is the component of d$\boldsymbol{k}$ perpendicular to the surface element $|\mathrm{d}\boldsymbol{S}| = \mathrm{d}S$, as illustrated two dimensionally in Fig. 2.3b. By definition, we can write $\mathrm{d}\omega_k = \mathrm{d}\varepsilon_k/\hbar = (1/\hbar)|\mathrm{grad}_k\varepsilon(\boldsymbol{k})|\mathrm{d}k_\perp$, where $(1/\hbar)|\nabla_k\varepsilon(\boldsymbol{k})| = v_\mathrm{g}$ is the *group velocity* for dispersive propagation, and hence $\mathrm{d}k_\perp = \mathrm{d}\omega_k/v_\mathrm{g}$. Using these notations, (2.21) can be expressed as

$$C_V = k_\mathrm{B} \int_{\omega_k} \frac{(\hbar\omega_k/k_\mathrm{B}T)^2 \exp(\hbar\omega_k/k_\mathrm{B}T)}{(\exp(\hbar\omega_k/k_\mathrm{B}T) - 1)^2} \mathcal{D}(\omega_k)\mathrm{d}\omega_k, \tag{2.22a}$$

where

$$\mathcal{D}(\omega_k) = \left(\frac{L}{2\pi}\right)^3 \oint_S \frac{\mathrm{d}S}{v_\mathrm{g}} \tag{2.22b}$$

is the density of phonon states on the surface S.

Tedious numerical calculations were carried out in early studies on representative crystals; the result obtained from a diamond lattice is shown in Fig. 2.4a, comparing with calculated dispersion relations for longitudinal and transversal modes in the vibration field, which are characterized by zero and nonzero frequencies at $k = 0$, respectively. Due to these characters, the frequency distribution is

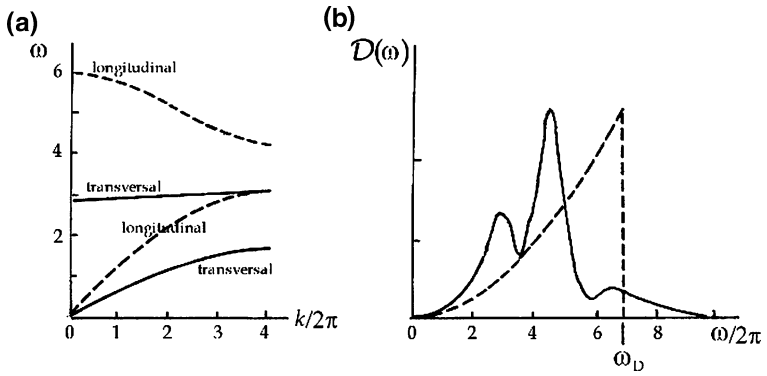

Fig. 2.4 (**a**) Examples of practical dispersion curves. Longitudinal and transverse dispersions are shown by solid and broken curves, respectively. (**b**) The solid curve shows an example of an observed density function, being compared with the broken curve of Debye's model.

complicated as shown in the figure. On the other hand, Einstein and Debye proposed simplified formula for densities $\mathcal{D}(\omega_k)$, which are approximate but useful for evaluating thermal properties of crystals.

2.6 Approximate Models

2.6.1 Einstein's Model

At elevated temperatures T, we can assume that properties of a crystal are dominated by a phonon energy $\hbar\omega_o$. Einstein proposed to consider a single mode frequency ω_o, disregarding all others in the vibration spectrum. In this model, (2.22b) can be simplified as $\mathcal{D}(\omega_o) = 1$, and hence the specific heat (2.22a) and the internal energy can be expressed as

$$C_V = 3Nk_B \frac{\xi^2 \exp\xi}{(\exp\xi - 1)^2} \quad \text{and} \quad U = 3Nk_B\left(\frac{1}{2}\xi + \frac{\xi}{\exp\xi - 1}\right), \tag{2.23}$$

respectively, where $\xi = \Theta_E/T$; the parameter $\Theta_E = \hbar\omega_o/k_B$ is known as the *Einstein temperature*. It is noted that in the limit $\xi \to 0$, we obtain $C_V \to 3Nk_B$.

At high temperatures, U can be attributed to independent constituent masses vibrating in *degrees of freedom* 2; hence, the corresponding thermal energy is $2 \times \frac{1}{2}k_BT$, and

$$U = 3Nk_BT \quad \text{and} \quad C_V = 3Nk_B. \tag{2.24}$$

This is known as the *Dulong-Petit law*.

2.6.2 Debye's Model

At low temperatures, longitudinal vibrations at low frequencies are dominant modes, which are characterized by nondispersive relation $\omega = v_g k$. The speed v_g is nearly constant because of a nearly spherical surface for constant energy in the $\boldsymbol{k}$-space. Letting $v_g = v$ for brevity, (2.22b) can be expressed as

$$\mathcal{D}(\omega) = \left(\frac{L}{2\pi}\right)^3 \frac{4\pi\omega^2}{v^3}. \tag{2.25}$$

Debye assumed that with increasing frequency, the density $\mathcal{D}(\omega)$ should be terminated at a frequency $\omega = \omega_D$, called Debye's *cutoff frequency*, as shown by the broken curve in Fig. 2.4b. In this case, the density function $\mathcal{D}(\omega) \propto \omega^2$ should be normalized as $\int_0^{\omega_D} \mathcal{D}(\omega)\mathrm{d}\omega = 3N$, so that (2.25) can be replaced by

$$\mathcal{D}(\omega) = \frac{9N}{\omega_D^3}\omega^2. \tag{2.26}$$

Therefore, in the Debye's model, we have

$$U = 3Nk_B T \int_0^{\omega_D} \left(\frac{\hbar\omega}{2} + \frac{\hbar\omega}{\exp(\hbar\omega/k_B T) - 1}\right) \frac{3\omega^2 \mathrm{d}\omega}{\omega_D^3}$$

and

$$C_V = 3Nk_B \int_0^{\omega_D} \frac{\exp(\hbar\omega/k_B T)}{(\exp(\hbar\omega/k_B T) - 1)^2} \left(\frac{\hbar\omega}{k_B T}\right)^2 \frac{3\omega^2 \mathrm{d}\omega}{\omega_D^3}.$$

Defining parameters $\hbar\omega_D/k_B T = \Theta_D$ and $\hbar\omega/k_B T = \xi$, similar to Einstein's model, these expressions can be written as

$$U = \frac{9}{8}Nk_B\Theta_D + 9Nk_B T\left(\frac{T}{\Theta_D}\right)^3 \int_0^{\Theta_D/T} \frac{\xi^3}{\exp\xi - 1}\mathrm{d}\xi$$

and

$$C_V = 9Nk_B\left(\frac{T}{\Theta_D}\right)^3 \int_0^{\Theta_D/T} \frac{\xi^4 \exp\xi}{(\exp\xi - 1)^2}\mathrm{d}\xi.$$

Introducing the function defined by

$$\eta\left(\frac{\Theta_D}{T}\right) = 3\left(\frac{T}{\Theta_D}\right)^3 \int_0^{\Theta_D/T} \frac{\xi^3 \mathrm{d}\xi}{\exp\xi - 1}, \tag{2.27}$$

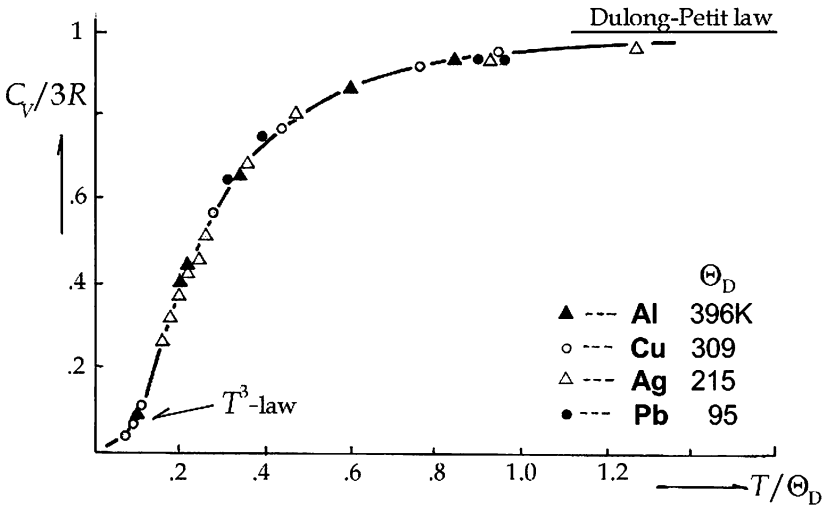

Fig. 2.5 Observed specific heat $C_V/3R$ against T/Θ_D for representative metals. R is the molar gas constant. In the bottom-right corner, shown are values of Θ_D for these metals. The T^3 law and Dulong–Petit limits are indicated to compare with experimental results.

known as the *Debye function*. The expression $C_V = 3Nk_B\eta(\Theta_D/T)$ describes temperature-dependent C_V for $T<\Theta_D$. In the limit of $\Theta_D/T \to \infty$ however, these U and C_V are dominated by the integral

$$\int_0^\infty \frac{\xi^3 d\xi}{\exp\xi - 1} = \frac{\pi^4}{15},$$

and hence the formula

$$\begin{aligned} U &= \frac{9}{8}Nk_B\Theta_D + 9Nk_BT\left(\frac{T}{\Theta_D}\right)^3\frac{\pi^4}{15}, \\ C_V &= 9Nk_B\left(\frac{T}{\Theta_D}\right)^3\frac{\pi^4}{15}. \end{aligned} \tag{2.28}$$

can be used for lower temperatures than Θ_D. In the Debye's model, we have thus the approximate relation $C_V \propto T^3$ for $T<\Theta_D$, which is known as *Debye's T^3-law*.

Figure 2.5 shows a comparison of observed values of C_V from representative monatomic crystals with the Debye and Dulong–Petit laws, valid at low and high temperatures, respectively, showing reasonable agreements.

2.7 Phonon Statistics 1

We discussed that the lattice vibration field can be considered as a gas of phonon particles $(\hbar\omega_k, \hbar k)$. However, a phonon is a quantum-mechanical particle that cannot be considered as a classical particle. It is noted that a large number of phonons can exist in a lattice in excited states and that phonons are independent

each other, but fundamentally *unidentifiable* particles. Therefore, they do not obey Boltzmann statistics for classical particles. Besides, the *total* number of phonons is left undetermined; the boundaries between the crystal and heat reservoir should be *open* to exchange phonons and heat. In this case, the Gibbs potential of the crystal should be expressed as $G(p,T,n)$, where n represents the average number of phonons in a given crystal.

Restricting to a constant p condition, the equilibrium between the crystal and reservoir can be obtained by minimizing the total Gibbs function, $G = G_1(T,n_1) + G_2(T,n_2)$, under the condition $n_1 + n_2 =$ constant. Here, the indexes 1 and 2 are assigned for the crystal and the surroundings, respectively. Using variation principles for a small arbitrary change $\delta n_2 = n_1 - n_2$, we obtain

$$\delta G = \left(\frac{\partial G_1}{\partial n_1}\right)_{p,T} \delta n_1 + \left(\frac{\partial G_2}{\partial n_2}\right)_{p,T} \delta n_2 = 0 \quad \text{and} \quad \delta n_1 + \delta n_2 = 0,$$

therefore

$$\left(\frac{\partial G_1}{\partial n_1}\right)_{p,T} = \left(\frac{\partial G_2}{\partial n_2}\right)_{p,T}.$$

This is a quantity, known as the *chemical potential* μ, between the crystal and the reservoir; namely for particle transfer we have $\mu_1 = \mu_2$ in equilibrium. Using a chemical potential, a variation of the Gibbs potential for an open crystal can be expressed as

$$\mathrm{d}G = \mathrm{d}U - T\mathrm{d}S + p\mathrm{d}V - \mu\mathrm{d}N, \tag{2.29}$$

where $N = n_1 + n_2$ is a constant.

For a thermodynamic state characterized by the internal energy U_o and phonon number N_o, we consider probabilities in statistical mechanics for the states determined by $(U_\mathrm{o}, N_\mathrm{o})$ and $(U_\mathrm{o} - \varepsilon, N_\mathrm{o} - n)$. Such probabilities are related to the entropy as given by the Boltzmann formula, that is,

$$g_\mathrm{o} = \exp\frac{S(U_\mathrm{o}, N_\mathrm{o})}{k_\mathrm{B}} \quad \text{and} \quad g = \exp\frac{S(U_\mathrm{o} - \varepsilon, N_\mathrm{o} - n)}{k_\mathrm{B}}.$$

Hence, we have

$$\frac{g}{g_\mathrm{o}} = \frac{\exp\{S(U_\mathrm{o} - \varepsilon, N_\mathrm{o} - n)/k_\mathrm{B}\}}{\exp\{S(U_\mathrm{o}, N_\mathrm{o})/k_\mathrm{B}\}} = \exp\frac{\Delta S}{k_\mathrm{B}},$$

where

$$\Delta S = S(U_\mathrm{o} - \varepsilon, N_\mathrm{o} - n) - S(U_\mathrm{o}, N_\mathrm{o}) = -\left(\frac{\partial S}{\partial U_\mathrm{o}}\right)_{N_\mathrm{o}} \varepsilon - \left(\frac{\partial S}{\partial N_\mathrm{o}}\right)_{U_\mathrm{o}} n.$$

Using (2.29), we can derive the relations

$$\left(\frac{\partial S}{\partial U_\mathrm{o}}\right)_{N_\mathrm{o}} = \frac{1}{T} \quad \text{and} \quad \left(\frac{\partial S}{\partial N_\mathrm{o}}\right)_{U_\mathrm{o}} = -\frac{\mu}{T},$$

so that

$$g = g_{\mathrm{o}} \exp \frac{\mu n - \varepsilon}{k_{\mathrm{B}} T}. \tag{2.30}$$

For a phonon system, the energy ε can be determined by any wave vector $\boldsymbol{k}$, where $|\boldsymbol{k}| = 1, 2, \ldots, 3N$, and N can take any number of $0, 1, \ldots, \infty$, and (2.30) is called the *Gibbs factor*, instead of the Boltzmann factor for a closed system. Depending on the type of application, it is handy to define the notation $\lambda = \exp(\mu / k_{\mathrm{B}} T)$, and write $g = g_{\mathrm{o}} \lambda^n \exp(-\varepsilon / k_{\mathrm{B}} T)$. Here, the parameter λ represents a probability for the energy level ε to accommodate one phonon, whereas the Boltzmann factor expresses *isothermal* probability.

For a phonon system, the energy levels are given by $\varepsilon_n = n\hbar\omega$; therefore using the Gibbs factor for $\varepsilon = \hbar\omega$, the partition function for an open phonon system can be expressed as

$$Z = \sum_{n=0}^{N} \lambda^n \exp\left(-\frac{n\varepsilon}{k_{\mathrm{B}} T}\right) = \sum_{n=0}^{N} \left\{ \lambda \exp\left(-\frac{\varepsilon}{k_{\mathrm{B}} T}\right) \right\}^n.$$

Considering that $\lambda \exp(-\varepsilon / k_{\mathrm{B}} T) < 1$, this can be evaluated as

$$Z = \frac{1}{1 - \lambda \exp(-\varepsilon / k_{\mathrm{B}} T)}.$$

Using this, so-called the *grand partition function*, the average number of phonons can be calculated as

$$\langle n \rangle = \lambda \frac{\partial}{\partial \lambda} \ln Z = \frac{1}{\frac{1}{\lambda} \exp\left(-\frac{\varepsilon}{k_{\mathrm{B}} T}\right) - 1} = \frac{1}{\exp \frac{\varepsilon - \mu}{k_{\mathrm{B}} T} - 1}, \tag{2.31}$$

which is known as the *Bose–Einstein distribution*. So far, phonon gas was discussed specifically, but the Bose–Einstein statistics (2.31) can be used for all identical particles that are characterized by plus parity. Phonons are examples of particles called *Bosons*. Those particles of minus parity will be discussed in Chap. 11 for electrons as an example.

2.8 Compressibility of a Crystal

In the foregoing, we considered a crystal under a constant volume condition. On the other hand, under constant temperature, the Helmholtz free energy can vary with a volume change ΔV, as expressed by

$$\Delta F = \left(\frac{\partial F}{\partial V}\right)_T \Delta V,$$

where $p = -(\partial F/\partial V)_T$ may be considered for the *pressure* on the phonon gas in a crystal. At a given temperature, such a volume change is offset by the external pressure p, and hence the quantity $-p\Delta V$ is regarded as an *adiabatic work* on the crystal.

It is realized that volume-dependent energies need to be included in the free energy of a crystal, in order to deal with the pressure from outside. Considering such an additional energy $U_o = U_o(V)$, the free energy can be expressed as

$$F = U_o + 9Nk_BT\left(\frac{T}{\Theta_D}\right)^3 \int_0^{\Theta_D/T} \left[\frac{\xi}{2} + \ln\{1-\exp(-\xi)\}\right] \xi^2 d\xi = U_o + 3Nk_BT\eta\left(\frac{\Theta_D}{T}\right), \tag{2.32}$$

where $\eta(\Theta_D/T)$ is the Debye function defined in (2.27), for which we have the relation

$$\left(\frac{\partial \eta}{\partial \ln \Theta_D}\right)_T = -\left(\frac{\partial \eta}{\partial \ln T}\right)_V = -\frac{T}{\Theta_D}\frac{\partial \eta}{\partial T}. \tag{2.33}$$

Writing $\zeta = \zeta(T,V) = T\eta(\Theta_D/T)$ for convenience, we obtain

$$\left(\frac{\partial \zeta}{\partial V}\right)_T = -\frac{\gamma}{V}\left(\frac{\partial \zeta}{\partial \ln \Theta_D}\right)_T = \frac{\gamma T}{V}\left(\frac{\partial \eta}{\partial \ln T}\right)_V,$$

where the factor

$$\gamma = -\frac{d\ln \Theta}{d\ln V}$$

is known as *Grüneisen's constant*. Using (2.30), the above relation can be re-expressed as

$$\left(\frac{\partial \zeta}{\partial V}\right)_T = \frac{\gamma}{V}\left\{T\left(\frac{\partial \zeta}{\partial T}\right)_V - \zeta\right\}.$$

From (2.29), we have $3Nk_B\zeta(T,V) = F - U_o$; therefore, this can be written as

$$\left\{\frac{\partial (F-U_o)}{\partial V}\right\}_T = \frac{\gamma}{V}\left\{T\left(\frac{\partial (F-U_o)}{\partial T}\right)_V - F + U_o\right\}. \tag{2.34}$$

Noted $U_o = U_o(V)$, the derivative in the first term of the right-hand side is equal to $T(\partial F/\partial T)_V = -TS$; hence, the quantity in the curly brackets becomes $-U + U_o = U_{vib}$ that represents the energy of lattice vibration. From (2.31), we can derive the expression for pressure in a crystal, that is,

$$p = -\frac{dU_o}{dV} + \frac{\gamma U_{vib}}{V}, \tag{2.35}$$

which is known as *Mie–Grüneisen's equation of state*.

The compressibility is defined as

$$\kappa = -\frac{1}{V}\left(\frac{\partial V}{\partial p}\right)_T, \tag{2.36}$$

which can be obtained for a crystal by using (2.32). Writing (2.32) as $pV = -V(\mathrm{d}U_\mathrm{o}/\mathrm{d}V) + \gamma U_\mathrm{vib}$, and differentiating it, we can derive

$$p + V\left(\frac{\partial p}{\partial V}\right)_T = -\frac{\mathrm{d}U_\mathrm{o}}{\mathrm{d}V} - V\frac{\mathrm{d}^2U_\mathrm{o}}{\mathrm{d}V^2} + \gamma\left(\frac{\partial U_\mathrm{vib}}{\partial V}\right)_T.$$

Since the atmospheric pressure is negligible compared with those in a crystal, we may omit p, and also from (2.31)

$$\left(\frac{\partial U_\mathrm{vib}}{\partial V}\right)_T = \frac{\gamma}{V}\left\{T\left(\frac{\partial U_\mathrm{vib}}{\partial T}\right)_V - U_\mathrm{vib}\right\}$$

in the above expression. Thus, the compressibility can be obtained from

$$\frac{1}{\kappa} = -V\left(\frac{\partial p}{\partial V}\right)_T = \frac{\mathrm{d}U_\mathrm{o}}{\mathrm{d}V} + V\frac{\mathrm{d}^2U_\mathrm{o}}{\mathrm{d}V^2} - \frac{\gamma^2}{V}(TC_V - U_\mathrm{o}), \tag{2.37}$$

where $C_V = (\partial U_\mathrm{vib}/\partial T)_V$ is the specific heat of lattice vibrations.

If $p = 0$, the volume of a crystal is constant, that is, $V = V_\mathrm{o}$ and $\mathrm{d}U_\mathrm{o}/\mathrm{d}V = 0$, besides $U_\mathrm{vib} =$ constant of V. Therefore, we can write $1/\kappa_\mathrm{o} = V_\mathrm{o}(\mathrm{d}^2U_\mathrm{o}/\mathrm{d}V^2)_{V=V_\mathrm{o}}$, meaning a hypothetical compressibility κ_o in equilibrium at $p = 0$. Then with (2.34), the *volume expansion* can be defined as

$$\beta = \frac{V - V_\mathrm{o}}{V_\mathrm{o}} = \frac{\kappa_\mathrm{o}\gamma U_\mathrm{vib}}{V}. \tag{2.38}$$

Further, using (2.32),

$$\left(\frac{\partial p}{\partial T}\right)_V = \frac{\gamma}{V}\left(\frac{\partial U_\mathrm{vib}}{\partial T}\right)_V = \frac{\gamma C_V}{V},$$

which can also be written as

$$\left(\frac{\partial p}{\partial T}\right)_V = \frac{\dfrac{1}{V}\left(\dfrac{\partial V}{\partial T}\right)_p}{-\dfrac{1}{V}\left(\dfrac{\partial V}{\partial p}\right)_T},$$

and hence we have the relation among γ, κ, and β, that is, $\gamma = -(V/C_V)(\beta/\kappa)$.

Table 2.1 Debye's temperatures Θ_D determined by thermal and elastic experiments.

	Fe	Al	Cu	Pb	Ag
Thermal	453	398	315	88	215
Elastic[a]	461	402	332	73	214

Data from Becker [3]
[a]Calculated with elastic data at room temperature.

Such constants as Θ, κ, β, and γ are related with each other, and significant parameters to characterize the nature of crystals. Table 2.1 shows measured values of Θ_D by thermal and elastic experiments on some representative monatomic crystals.

Exercises 2

1. It is significant that the number of phonons in a crystals is left as arbitrary, which is characteristic for Boson particles. Sound wave propagation at low values of $\boldsymbol{k}$ and ω can be interpreted as transporting phonons, which is a typical example of low-level excitations, regardless of temperature. Discuss why the undetermined number of particles is significant in Boson statistics? Is there any other Boson systems where the number of particles is a fixed constant?
2. Einstein's model for the specific heat is consistent with assuming crystals as a uniform medium. Is it an adequate assumption that elastic properties are attributed to each unit cell, if the crystal is not uniform? At sufficiently high temperatures, a crystal can be considered as uniform. Why? Discuss the validity of Einstein's model at high temperatures.
3. Compare the average number of phonons $\langle n \rangle$ calculated from (2.26) with that expressed by (2.31). Notice that the difference between them depends on the chemical potential: $\mu = 0$ or $\mu \neq 0$. Discuss the role of a chemical potential in making these two cases different.
4. The wave function of a phonon is expressed by (2.17b). Therefore in a system of many phonons, phonon wave functions are substantially overlapped in the crystal space. This is the fundamental reason why phonons are unidentifiable particles; hence, phonon gas may be regarded as condensed liquid. For Boson particles ^{4}He, discuss if helium-4 gas can be condensed to a liquid phase at 4.2 K.
5. Are the hydrostatic pressure p and compressibility discussed in Sect. 2.8 adequate for anisotropic crystals? Comment on these thermodynamic theories applied to anisotropic crystals.

Chapter 3
Order Variables and Adiabatic Potentials

Thermal properties of a crystal are primarily due to the vibrating lattice, while dielectric, magnetic, and mechanical properties can be determined from measured response functions of a crystal to an applied field or force. Such an external action X on *internal variables* σ is primarily an *adiabatic variable* independent of temperature. As in a compressed gas, the external work on a crystal is expressed by $-\sigma X$, and hence the Gibbs potential can be defined by $G = U - TS + \sigma X$. On the other hand, internal variables σ at lattice sites can be independent of each other in some cases, but correlated in other conditions. In the latter, the effect of X is expressed effectively as $-\sigma(X + X_{\text{int}})$, where X_{int} is an *internal field* that was originally proposed by P. Weiss for a ferromagnet. In this chapter, these internal variables σ and X_{int} are discussed in terms of correlations in a crystal, leading to Weiss' concept to be included in the Gibbs function.

3.1 One-Dimensional Ionic Chains

The lattice excitation in an ionic chain crystal at a low energy is characterized by a wave vector $\boldsymbol{k}$ and frequency ω, propagating in the direction of $\boldsymbol{k}$. We consider here one-dimensional chain of ions in an ionic crystal, which is perturbed with surrounding chains.

In this section, following Born and von Kárman, we consider a one-dimensional chain of positive and negative ions arranged alternately, as illustrated in Fig. 3.1. Coulomb interactions between ionic charges are cancelled out, so that we assume ionic charges as insignificant for the dynamics of ions, if there is no electric field applied externally. With this assumption, the interionic potential is essentially elastic one between ions in the nearest distance. Denoting such a short-range potential by $\phi(r - r_{\text{o}})$, where r_{o} is the ionic distance in the static chain, we can write the equations of motion for ionic masses m_+ and m_- as

M. Fujimoto, *Thermodynamics of Crystalline States*,
DOI 10.1007/978-1-4419-6688-9_3,

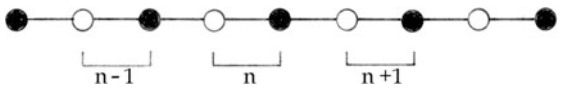

Fig. 3.1 Dipolar chain lattice in one dimension. Plus and minus ions are located in pair at each lattice sites $\ldots, n-1, n, n+1, \ldots$.

$$m_+\ddot{u}_n^+ = -\phi'(r_\mathrm{o} + u_n^- - u_n^+) + \phi'(r_\mathrm{o} + u_n^+ - u_{n-1}^-) = \phi''(r_\mathrm{o})(u_n^- + u_{n-1}^- - 2u_n^+)$$

and

$$m_-\ddot{u}_n^- = -\phi'(r_\mathrm{o} + u_{n+1}^+ - u_n^-) + \phi'(r_\mathrm{o} + u_n^- - u_n^+) = \phi''(r_\mathrm{o})(u_{n+1}^+ + u_n^+ - 2u_n^-),$$

where the suffix n indicates lattice sites for a pair of $\pm$ ions as shown in Fig. 3.1. By letting $u_n^\pm = u_\mathrm{o}^\pm \exp \mathrm{i}(kx_n - \omega t)$ and $|x_{n+1} - x_n| = r_\mathrm{o}$ in the above, we can derive time-independent equations:

$$\begin{aligned} \{m_+\omega^2 - 2\phi''(r_\mathrm{o})\}u_\mathrm{o}^+ + \phi''(r_\mathrm{o})\{1 + \exp(-\mathrm{i}kr_\mathrm{o})\}u_\mathrm{o}^- = 0, \\ \phi(r_\mathrm{o})\{1 + \exp(\mathrm{i}kr_\mathrm{o})\}u_\mathrm{o}^+ + \{m_-\omega^2 - 2\phi''(r_\mathrm{o})\}u_\mathrm{o}^- = 0. \end{aligned} \tag{i}$$

If the determinant of these coefficients in (i) can be equal to zero, the equations are soluble for u_o^+ and u_o^- for secular oscillations, that is,

$$\begin{vmatrix} m_+\omega^2 - 2\phi''(r_\mathrm{o}) & \phi''(r_\mathrm{o})\{1 + \exp(-\mathrm{i}kr_\mathrm{o})\} \\ \phi''(r_\mathrm{o})\{1 - \exp(\mathrm{i}kr_\mathrm{o})\} & m_-\omega^2 - 2\phi''(r_\mathrm{o}) \end{vmatrix} = 0.$$

Therefore, for a given value of k, ω^2 can be determined as

$$\omega^2 = \frac{\phi''(r_\mathrm{o})}{m_+m_-}\left\{(m_+ + m_-) \pm \sqrt{(m_+ + m_-)^2 - 4m_+m_-\sin^2\frac{kr_\mathrm{o}}{2}}\right\}. \tag{ii}$$

And from (i), the amplitude ratio is

$$\frac{u_\mathrm{o}^+}{u_\mathrm{o}^-} = \frac{-m_-\{1 + \exp(-\mathrm{i}kr_\mathrm{o})\}}{(m_+ - m_-) \pm \sqrt{(m_+ + m_-)^2 - 4m_+m_-\sin^2\frac{kr_\mathrm{o}}{2}}}. \tag{iii}$$

It is noted from (ii) that the solution for the $+$ sign is characterized with $\omega^2 \neq 0$ at $k = 0$, whereas for the $-$ sign, the solution can be signified by $\omega^2 = 0$ at $k = 0$; the general relation between ω and k derived from (ii) is the *dispersion relation* along the ionic chain. In the latter case of $-$ sign, at small values of k we have

$$\omega \approx k\sqrt{\frac{\phi''(r_o)}{2(m_+ + m_-)}}.$$

For such a vibration, called an *acoustic mode*, the speed of propagation is approximately given by $v = \omega/k$, where $v = \sqrt{\phi''(r_o)/2(m_+ + m_-)}$, depending on the mass $m_+ + m_-$. On the other hand, for the former mode of + sign, called the *optic mode*, we have

$$\omega = \sqrt{\frac{2(m_+ + m_-)\phi''(r_o)}{m_+ m_-}} \neq 0 \quad \text{at } k = 0,$$

and its propagation is signified by the *reduced mass* $\mu = m_+ m_-/(m_+ + m_-)$, and characterized by nonzero frequency at $k = 0$. For an optic mode at $k = 0$, from (iii) we obtain the relation

$$\frac{u_o^+}{u_o^-} = -\frac{m_-}{m_+} \quad \text{or} \quad m_+ u_o^+ + m_- u_o^- = 0. \tag{iv}$$

This indicates that the center of mass of ± ions is unchanged. In contrast, an acoustic mode represents the center-of-mass motion that can be described by

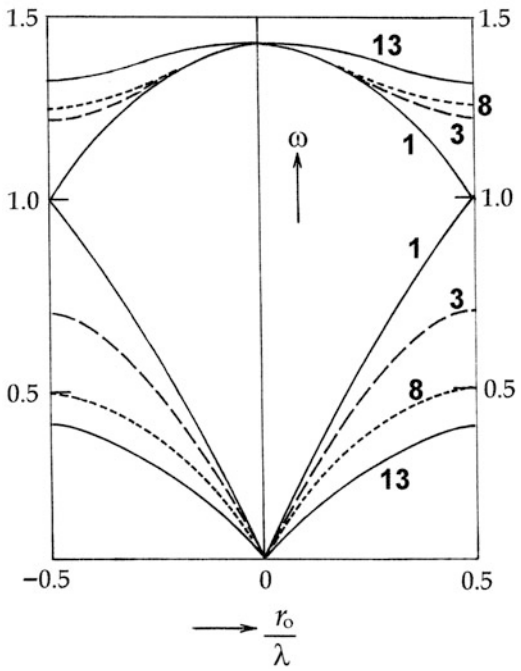

Fig. 3.2 Dispersion curves in one-dimensional dipolar lattice. *Thick numbers* indicate mass ratios m_-/m_+. Frequency gaps between acoustic and optic modes, except for $m_-/m_+ = 1$.

the center-of-mass coordinate $u_o^{cm} = (m_+ u_o^+ + m_- u_o^-)/(m_+ + m_-)$, varying as $u_n^{cm} = u_o^{cm} \exp i(kx - \omega t)$.

The dispersion relations (ii) are sketched numerically in Fig. 3.2, where ω is plotted as a function of r_o/λ, where λ is the wavelength related as $k = 2\pi/\lambda$, for various numerical values of mass ratio m_-/m_+ as indicated in the figure. It is noted that except for $m_-/m_+ = 1$, there is a frequency gap between optic and acoustic modes.

In the foregoing theory, ionic charges were disregarded for the dynamics of the chain. However, in optic modes the electric dipole moment p_n is explicit in the ionic displacement at each site n, that is,

$$p_n = e(u_+ - u_-) = eu(u_o^+ - u_o^-) \exp i(kx_n - \omega t). \tag{v}$$

It is noted, however, that these charges arise normally from loosely bound electrons in ions, instead of whole ions. Although implicit in the foregoing theory, such a dipole moment p_n depends on the mass of displaced charges, making the dynamics substantially different from the ionic displacements; the motion of p_n is actually signified by the reduced mass. Nevertheless, in the presence of an applied electric field E, the significant interaction is $-p_n E$, regardless of the origin of charges.

3.2 Order Variables

Microscopic dipole moments associated with optic modes act as order variables in the dielectric crystal. They are identical at all lattice sites, and regarded primarily as independent from each other; otherwise correlated in collective motion, depending on thermodynamic conditions. Such variables are magnetic moments in a magnetic crystal, where displaced spins of constituent molecules are responsible for magnetic properties in strained structure. Order variables are not always identifiable from crystallographic data, but their activity is recognizable from dielectric and magnetic evidence, and considered as responsible for changing lattice symmetry. Associated with electronic *displacements* from their original sites, correlated order variables can be regarded as *classical vectors* in the timescale of observation. If occurring in *finite magnitudes*, the space symmetry is disrupted, resulting in a structural change of a crystal.

Realized from the above example of a dipolar chain, electric dipole moments in optic modes are characterized by the reduced mass, instead of heavier ionic masses. The charge displacements arise from displacing electrons, so that p_n in motion is distinctively different from an acoustic excitation characterized by the ionic mass. In Sect. 3.3, we will discuss the general theory of displacements of small masses in a crystal with Born–Oppenheimer's approximation, where the mass ratio between the charge carrier and the rest of the ion yields a significant criterion for dynamics

of order variables. Meanwhile, examples of order variables are shown in the following for representative structural changes, where such variables can be visualized from crystallographic data at least qualitatively.

3.2.1 Perovskite Crystals

In crystals of perovskites with chemical formula ABO_3, an octahedral $(BO)_6^{2-}$ ion is surrounded by eight A^{2+} ions at the corners of a cubic cell as illustrated by Fig. 3.3. Typically, the negative ionic group in *bipyramidal* shape has an additional degree of freedom, in which the central ion B^{4+} can be displaced between two positions marked by 1 and 1′ in Fig. 3.3a, or the group as a whole is rotated in either direction 1 or 1′ as shown in Fig. 3.3b. Related by *inversion* with respect to the center, such linear or angular displacements between 1 and 1′ are considered as responsible for a *binary transition* between macroscopic phases that are also related by inversion, as indicated for $BaTiO_3$ and $SrTiO_3$ crystals, respectively. In the former case, the center of the group shifts either toward the $+x$ or $-x$ direction, generating an electric dipole moment along the x-axis, whereas in the latter the center of the ion remains unchanged but the structure may be strained around the x-axis. In both cases, the order variable is defined as a vector component σ_x varying as a function of time t. In practice, the

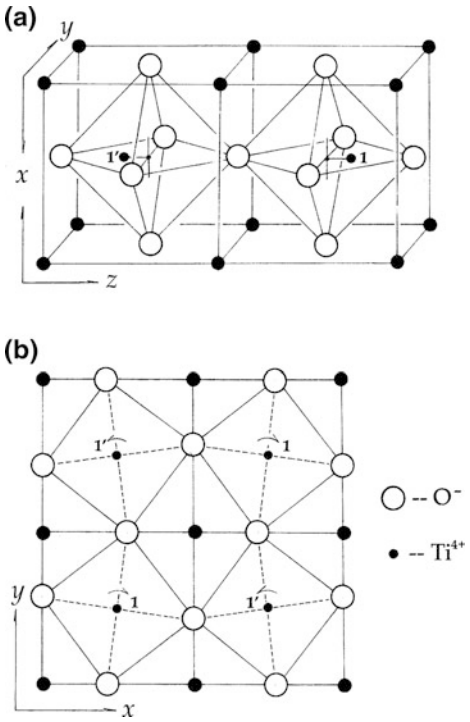

Fig. 3.3 Structure of a perovskite crystal: (**a**) $BaTiO_3$ type and (**b**) $SrTiO_3$ type. An Ti^{4+} ion in the bipyramidal TiO_6^{2-} complex is in motion between 1 and 1′ related by inversion.

timescale of inversion, as compared with that of observation, is a significant factor for such moving σ_x to be detectable. Assuming that such displacements occur randomly at lattice sites, we may consider their statistical average determined by the probability difference between 1 and 1′ states, that is, $\langle \sigma_x \rangle = p_1 - p_{1'}$.

3.2.2 *Tris-Sarcosine Calcium Chloride*

Sarcosine is an organic amino acid, $H_3C-NH_2-CH_2-CO_2H$, crystallizing with inorganic $CaCl_2$ molecules in *quasi-orthorhombic* structure at room temperatures, when prepared from aqueous solutions. The crystal is *twinned* in quasi-hexagonal form and spontaneously strained, consisting of slightly monoclinic *ferroelastic* domains along the *a*-axis; a single-domain sample can be cut out for experiments. A *tris*-sarcosine calcium chloride (TSCC) crystal exhibits a *ferroelectric* phase transition at 120 K under atmospheric pressure. Figure 3.4a shows the result of X-ray crystallographic studies by Kakudo and his collaborators [4], in which a quasihexagonal molecular arrangement is evident in the *bc*-plane. Figure 3.4b illustrates the $Ca^{2+}O_6^-$ complex, where the central Ca^{2+} ion is symmetrically surrounded by six sarcosine molecules. In paramagnetic resonance experiments with *transition ions*, for example, Mn^{2+}, substituting for the Ca^{2+} ion, the order variable can be identified as associated with the $Ca^{2+}O_6^-$ complex.

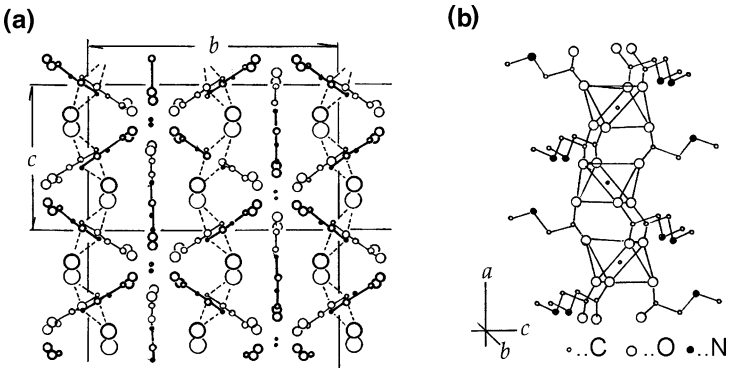

Fig. 3.4 Molecular arrangement in a TSCC crystal: (**a**) a view in the *bc*-plane and (**b**) structure around a Ca^{2+} ion surrounded by six O^- of sarcosine molecules. The order variable σ is associated with such bipyramidal CaO_6 complexes, executing binary fluctuations.

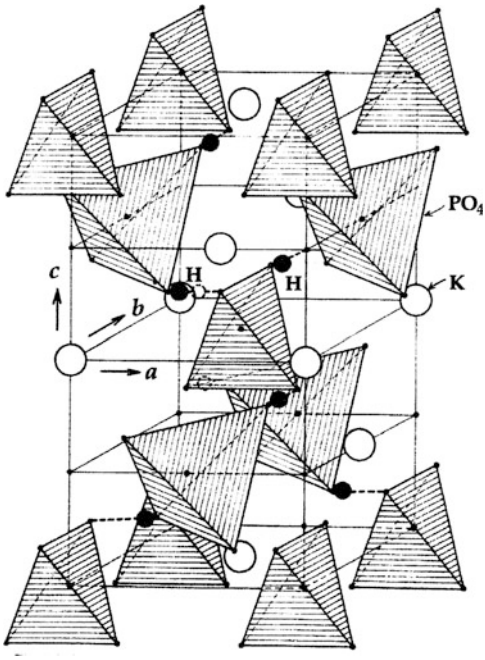

Fig. 3.5 Structure of a KDP crystal. The order variable can be associated with a pyramidal PO_4 ion with four surrounding protons; two protons at closer and two others at distant positions to PO_4.

3.2.3 Potassium Dihydrogen Phosphate

Figure 3.5 shows the molecular arrangement in orthorhombic crystals of potassium dihydrogen phosphate (KDP), KH_2PO_4. In this structure, *tetrahedral* phosphate ions PO_4^{3-} are linked with each other via four hydrogen bonds, as illustrated in the figure. Along each bond direction, a proton oscillates between two positions, and each PO_4^{3-} tetrahedron is consequently distorted or disoriented, depending on the proton configuration in the four hydrogen bonds. Therefore, the order variable should be associated with the complex structure of PO_4^{3-} with four attached protons. In this model, a vector variable of the proton group may be coupled with the orientation of PO_4^{3-}, but the order variable has not been identified exactly yet, which can be studied by experiments with more-than-one paramagnetic probes.

3.3 Born–Oppenheimer's Approximation

Born and Huang [2] discussed a dynamic displacement of an electron from the constituent ion at a lattice site in Born–Oppenheimer's approximation. Although unspecified in their theory, there should be a conceivable origin for separating them,

as in Newton's classical action–reaction principle. Signified by the reduced mass, such a relative displacement can be significantly affected by the corresponding ionic displacement. In so-called *adiabatic approximation*, these authors showed the presence of a potential responsible for the displacement, which we shall call an *adiabatic potential*.

We consider in the following an electron of mass m that belongs to an ion of mass M at a site n. Because of $m \ll M$, the reduced mass is nearly the same as m, and the mass of the remaining ion is almost identical to M; that is, $\mu \approx m$ and $M - m \approx M$. To simplify the argument, we denote displacements of these particles from static positions by x_n and X_n, respectively, in one dimension. For the mass m, we have the Hamiltonian

$$\mathcal{H}_{\mathrm{o}} = -\sum_n \frac{\hbar^2}{2m}\frac{\partial^2}{\partial x_n^2} + U, \tag{3.1}$$

where $U = \sum_n U_n$ is the potential energy that is perturbed as

$$\mathcal{H} = \mathcal{H}_{\mathrm{o}} - \sum_n \frac{\hbar^2}{2M}\frac{\partial^2}{\partial X_n^2}.$$

Defining a parameter κ by $\kappa^4 = m/M$, the perturbing term can be expressed as $\kappa^4\mathcal{H}_1$, where

$$\mathcal{H}_1 = -\sum_n \frac{\hbar^2}{2m}\frac{\partial^2}{\partial X_n^2}, \tag{3.2}$$

and hence the perturbed Hamiltonian can be expressed by

$$\mathcal{H} = \mathcal{H}_{\mathrm{o}} + \kappa^4\mathcal{H}_1. \tag{3.3}$$

Omitting the index n for brevity, we write the unperturbed and perturbed wave equations as

$$\mathcal{H}_{\mathrm{o}}\phi_i(x,X) = \varepsilon_i(X)\phi_i(x,X) \tag{3.4a}$$

and

$$\mathcal{H}\psi_i(x,X) = E_i\psi_i(x,X), \tag{3.4b}$$

where the eigenvalues ε_i and E_i are indexed by i for the unperturbed and perturbed equations (3.4a) and (3.4b), respectively. Assuming that the lattice displacement is restricted in the vicinity of $X = X_{\mathrm{o}}$, so that we set the origin at $x = 0$ for $X = X_{\mathrm{o}}$. A small ionic displacement u can then be represented by

$$X - X_{\mathrm{o}} = \kappa u. \tag{3.5}$$

First, we expand unperturbed functions in (3.4a) with respect to κu, and write them in power series of κ, that is,

$$\varepsilon_i(X) = \varepsilon_i(X_\mathrm{o} + \kappa u) = \varepsilon_i^{(0)} + \kappa\varepsilon_i^{(1)} + \kappa^2\varepsilon_i^{(2)} + \cdots,$$

$$\phi_i(x, X_\mathrm{o} + \kappa u) = \phi_i^{(0)} + \kappa\phi_i^{(1)} + \kappa^2\phi_i^{(2)} + \cdots,$$

$$\mathcal{H}_o\left(x, \frac{\partial}{\partial x}, X_\mathrm{o} + \kappa u\right) = \mathcal{H}_\mathrm{o}^{(0)} + \kappa\mathcal{H}_\mathrm{o}^{(1)} + \kappa^2\mathcal{H}_\mathrm{o}^{(2)} + \cdots,$$

where $\phi_i^{(0)}, \phi_i^{(1)}, \phi_i^{(2)}, \ldots$ are mutually orthogonal functions. Using these expansions in (3.4a), and setting all coefficients of terms $\kappa^0, \kappa, \kappa^2, \ldots$ equal to zero, we have

$$(\mathcal{H}_\mathrm{o}^{(0)} - \varepsilon_i^{(0)})\phi_\mathrm{o}^{(0)} = 0, \tag{ia}$$

$$(\mathcal{H}_\mathrm{o}^{(0)} - \varepsilon_i^{(0)})\phi_i^{(1)} = -(\mathcal{H}_\mathrm{o}^{(1)} - \varepsilon_i^{(1)})\phi_i^{(0)}, \tag{iia}$$

$$(\mathcal{H}_\mathrm{o}^{(0)} - \varepsilon_i^{(0)})\phi_i^{(2)} = -(\mathcal{H}_\mathrm{o}^{(1)} - \varepsilon_i^{(1)})\phi_i^{(1)} - (\mathcal{H}_\mathrm{o}^{(2)} - \varepsilon_i^{(2)})\phi_i^{(0)}, \tag{iiia}$$

$$\cdots\cdots\cdots$$

The perturbed Hamiltonian can then be written as

$$\mathcal{H} = \mathcal{H}_\mathrm{o}^{(0)} + \kappa\mathcal{H}_\mathrm{o}^{(1)} + \kappa^2(\mathcal{H}_\mathrm{o}^{(2)} + \mathcal{H}_1^{(2)}) + \kappa^3\mathcal{H}_\mathrm{o}^{(3)} + \cdots,$$

in which the term $\kappa^4\mathcal{H}_1$ was replaced for convenience by

$$\kappa^4\mathcal{H}_1 = \kappa^2\mathcal{H}_1^{(2)} \quad \text{and} \quad \mathcal{H}_1^{(2)} = -\sum \frac{\hbar^2}{2m}\frac{\partial^2}{\partial u^2}.$$

For the perturbed equation (3.4b), eigenvalues and eigenfunctions are expanded in similar manner as above, that is,

$$E_i = E_i^{(0)} + \kappa E_i^{(1)} + \kappa^2 E_i^{(2)} + \cdots$$

and

$$\psi_i = \psi_i^{(0)} + \kappa\psi_i^{(1)} + \kappa^2\psi_i^{(2)} + \cdots.$$

Noting $E_i^{(0)} = \varepsilon_i^{(0)}$, we obtain the following relations:

$$(\mathcal{H}_\mathrm{o}^{(0)} - \varepsilon_i^{(0)})\psi_i^{(0)} = 0, \tag{ib}$$

$$(\mathcal{H}_{\mathrm{o}}^{(0)} - \varepsilon_i^{(0)})\psi_i^{(1)} = -(\mathcal{H}_{\mathrm{o}}^{(1)} - E_i^{(1)})\psi_i^{(0)}, \tag{iib}$$

$$(\mathcal{H}_{\mathrm{o}}^{(0)} - \varepsilon_i^{(0)})\psi_i^{(2)} = -(\mathcal{H}_{\mathrm{o}}^{(1)} - E_i^{(1)})\psi_i^{(1)} - (\mathcal{H}_{\mathrm{o}}^{(2)} + \mathcal{H}_1^{(2)} - E_i^{(2)})\psi_i^{(0)}, \tag{iiib}$$

.....

First, from (ia) and (ib), we see that $\psi_i^{(0)}(x) = \phi_i^{(0)}(x, X_{\mathrm{o}})$ is a solution that represents the approximation at $u = 0$. Therefore, for a nonzero u we write

$$\psi_i^{(0)}(x, u) = \chi^{(0)}(u)\phi_i^{(0)}(x), \tag{iv}$$

where $\chi^{(0)}(u)$ is an arbitrary function of u. Using (iv), the inhomogeneous equation (iib) can be solved, if

$$\int \phi_i^{(0)}(\mathcal{H}_{\mathrm{o}}^{(1)} - E_i^{(1)})\psi_i^{(0)}\mathrm{d}x = \chi^{(0)}(u)\int \phi_i^{(0)}(\mathcal{H}_{\mathrm{o}}^{(1)} - E_i^{(1)})\phi_i^{(0)}\mathrm{d}x = 0.$$

On the other hand, from (iia) we have

$$\int \phi_i^{(0)}(\mathcal{H}_{\mathrm{o}}^{(0)} - \varepsilon_i^{(0)})\phi_i^{(1)}\mathrm{d}x = -\int \phi_{\mathrm{o}}^{(0)}(\mathcal{H}_o^{(1)} - \varepsilon_o^{(1)})\phi_{\mathrm{o}}^{(0)}\mathrm{d}x = 0,$$

because $\phi_i^{(0)}$ and $\phi_i^{(1)}$ are independent and orthogonal functions. Comparing these results, we obtain $E_i^{(1)} = \varepsilon_i^{(1)}$. It is noted at this point that $\varepsilon_i^{(1)}$ is the coefficient of κu_i in the expansion, so we can write $\kappa\varepsilon_i^{(1)} = (\partial\varepsilon_i/\partial X_i)_{X_i = X_{\mathrm{o}}}\kappa u_i$, which is zero at $u_i = 0$. On the other hand, $E_i^{(1)}$ is also a similar coefficient in the expansion series, and hence independent of u_i. In this way, we have the relation

$$E_i^{(1)} = \varepsilon_1^{(1)} = 0.$$

Also $\mathcal{H}_{\mathrm{o}}^{(1)} = 0$ in this case, and we see that $\phi_i^{(1)}$ is a solution of (iib). Thus, we can write a linear combination

$$\psi_i^{(1)} = \chi^{(0)}(u)\phi_i^{(1)}(x) + \chi^{(1)}(u)\phi_i^{(0)}(x) \tag{v}$$

for the perturbed state in accuracy of κ, where $\chi^{(0)}(u)$ and $\chi^{(1)}(u)$ are arbitrary functions of u.

Using (v) and $E_i^{(1)} = 0$ in (iiib), we obtain

$$\begin{aligned}(\mathcal{H}_{\mathrm{o}}^{(0)} - \varepsilon_i^{(0)})\psi_i^{(2)} = &-\mathcal{H}_{\mathrm{o}}^{(1)}\chi^{(0)}\phi_i^{(1)} - (\mathcal{H}_{\mathrm{o}}^{(2)} + \mathcal{H}_1^{(2)} - E_i^{(2)})\chi^{(0)}\phi_i^{(0)} \\ &- \mathcal{H}_{\mathrm{o}}^{(1)}\chi^{(1)}\phi_i^{(0)}.\end{aligned} \tag{vi}$$

Subtracting $\chi^{(1)} \times$ (iia) and $\chi^{(0)} \times$ (iiia) from this expression, we can derive

$$(\mathcal{H}_{\mathrm{o}}^{(0)} - \varepsilon_i^{(0)})(\psi_i^{(2)} - \chi^{(0)}\phi_i^{(2)} - \chi^{(1)}\phi_i^{(1)}) = -(\mathcal{H}_1^{(2)} + \varepsilon_i^{(2)} - E_i^{(2)})\chi^{(0)}\phi_i^{(0)},$$

which is soluble if

$$\int \phi_i^{(0)}(\mathcal{H}_i^{(2)} + \varepsilon_i^{(2)} - E_i^{(2)})\chi^{(0)}\phi_i^{(0)}\mathrm{d}x = 0.$$

Noted that $(\mathcal{H}_1^{(2)} + \varepsilon_i^{(2)} - E_i^{(2)})\chi^{(0)}$ in the integrand is independent of x, this condition is met if

$$(\mathcal{H}_1^{(2)} + \varepsilon_i^{(2)} - E_i^{(2)})\chi^{(0)}(u) = 0. \tag{vii}$$

Equation (vii) implies that motion of mass M perturbed by the displacement u is harmonic and independent of x. In this approximation, the lattice structure remains therefore unmodified, when the approximate wave function is $\psi_i(x,u) = \psi_i^{(0)} + \kappa\psi_i^{(1)}$ in the first order of κ, which is called *harmonic approximation*.

In the second order of κ^2, we have

$$\psi_i(x,u) = \psi_i^{(0)} + \kappa\psi_i^{(1)} + \kappa^2\psi_i^{(2)}, \tag{viii}$$

for which $\psi_i^{(2)}$ can be obtained as follows. Owing to (vii), (vi) can be expressed as

$$(\mathcal{H}_{\mathrm{o}}^{(2)} - \varepsilon_i^{(0)})(\psi_i^{(2)} - \chi^{(0)}\phi_i^{(2)} - \chi^{(1)}\phi_i^{(1)}) = 0,$$

which should be consistent with (ia) and (ib), that is, $(\mathcal{H}_{\mathrm{o}}^{(0)} - \varepsilon_i^{(0)})\psi_i^{(2)} = 0$. The solution can be written as $\chi^{(2)}\phi_i^{(0)}$, where $\chi^{(2)}$ is another arbitrary function of u. Therefore, we have the relation

$$\chi^{(2)}\phi_i^{(0)} = \psi_i^{(2)} - \chi^{(0)}\phi_i^{(2)} - \chi^{(1)}\phi_i^{(1)}.$$

Accordingly,

$$\psi_i^{(2)}(x,u) = \chi^{(0)}(u)\phi_i^{(2)}(x,u) + \chi^{(1)}(u)\phi_i^{(1)}(x,u) + \chi^{(2)}(u)\phi_i^{(0)}(x). \tag{ix}$$

Using (iv), (v), and (ix) in (viii), we can write

$$\begin{aligned}\Psi_i(x,u) &= \chi^{(0)}(u)\{\phi_i^{(0)}(x) + \kappa\phi_i^{(1)}(x,u) + \kappa^2\phi_i^{(2)}(x,u)\} \\ &\quad + \kappa\chi^{(1)}\{\phi_i^{(0)}(x) + \kappa\phi_i^{(1)}(x,u)\} + \kappa^2\chi^{(2)}(u)\phi_i^{(0)}(x) \\ &= \{\chi^{(0)}(u) + \kappa\chi^{(1)}(u) + \kappa^2\chi^{(2)}(u)\}\phi_i^{(0)} + \{\chi^{(0)}(u) \\ &\quad + \kappa\chi^{(1)}(u)\}\kappa\phi_i^{(1)} + \chi^{(0)}(u)\kappa^2\phi_i^{(2)}.\end{aligned}$$

This can be re-expressed approximately as

$$\approx \{\chi^{(0)}(u) + \kappa\chi^{(1)}(u) + \kappa^2\chi^{(2)}(u)\}\{\phi_i^{(0)}(x) + \kappa\phi_i^{(1)}(x,u) + \kappa^2\phi_i^{(2)}(x,u)\},$$

if adding higher-order terms $\kappa^3\chi^{(2)}\phi_i^{(1)}$ and $\kappa^3\chi^{(1)}\phi_i^{(2)} + \kappa^4\chi^{(2)}\phi_i^{(2)}$. This result indicates that in accuracy of κ^2, the motion of m can be considered as almost independent of M. In this accuracy, the motion should be determined thermodynamically by an adiabatic force; hence, we call it *adiabatic approximation*.

In adiabatic approximation, modified lattice motion is independent of order variables. This is an important feature for the adiabatic process in thermodynamics, because all thermal effects in crystals come through the lattice. Although the origin for displacements is unspecified, the presence of an internal potential ΔU is clear in Born–Huang's theory, as it is explicit in the adiabatic approximation. The modified Hamiltonian in adiabatic approximation can be written as

$$\mathcal{H} = \mathcal{H}_{\mathrm{o}}^{(0)} + \kappa^2\mathcal{H}_1^{(2)} + \Delta U, \tag{3.6a}$$

where

$$\Delta U = \kappa^2\varepsilon_i^{(1)}(u) + \kappa^3\varepsilon_i^{(3)}(u) + \kappa^4\{\varepsilon_i^{(4)}(u) + C\} \tag{3.6b}$$

and C is a constant related with $\partial^2\varepsilon_i^{(2)}/\partial u^2$ as verified in [2], where further detailed calculations to higher order are discussed. This ΔU is an *adiabatic potential* responsible for the displacement of an electron, as described by (3.6a).

With respect to the center of mass of a constituent ion, the force $\partial\Delta U/\partial x$ is counteracted by $-\partial\Delta U/\partial x$, and hence ΔU is implicit for the order variable. In contrast, it is explicit in the relative coordinate system. Further, for a real system, the adiabatic potential should be expressed in three-dimensional crystal space. As $\varepsilon_i^{(1)}, \varepsilon_i^{(3)}, \varepsilon_i^{(4)}, \ldots$ in (3.6b) represents $u_i, u_i^3, u_i^4, \ldots$ times corresponding derivatives, the adiabatic potentials can be expressed by these power terms of mixed components, for example, $V_\alpha u_{i\alpha}, V_{\alpha\beta\gamma}u_{i\alpha}u_{i\beta}u_{i\gamma}, V_{\alpha\beta\gamma\delta}u_{i\alpha}u_{i\beta}u_{i\gamma}u_{i\delta}, \ldots$, pending values of coefficients $V_{\ldots}$, and $\alpha, \beta, \ldots$ represent x, y, and z. Each of these potentials can play specific roles, as will be discussed later.

3.4 Lattice Periodicity and the Bloch Theorem

3.4.1 The Reciprocal Lattice

In Sect. 3.3, we discussed a displaced electron from a constituent ion. At the transition threshold, such a displacement cannot be *simultaneous* at all sites quantum mechanically. It is a classical postulate to assume identical displacements at all lattice sites. Nevertheless, the lattice symmetry can be disrupted by

an adiabatic potential ΔU that is related with heavy mass M of the constituent ions. On the other hand, if randomly moving from original sites, each displacement occurs in arbitrary phase, which should be synchronized to attain minimum strains in the new structure. We can consider such a phasing process for *transition anomalies*. Despite of the uncertain phase, it is a valid assumption that the displacement u_i can be described by a *classical vector* in finite amplitude. After such phasing, both u_i and $\Delta U(u_i)$ emerge simultaneously at a critical temperature.

In stable crystals, all physical events at lattice sites are assumed as identical, except for surfaces and defects. Therefore, any function at a lattice site i, for example, $u(r_i, t)$, must be invariant by space translations at arbitrary time t. The translation can be specified by a vector

$$\boldsymbol{R} = n_1\boldsymbol{a}_1 + n_2\boldsymbol{a}_2 + n_3\boldsymbol{a}_3, \tag{3.7}$$

where $\boldsymbol{a}_1, \boldsymbol{a}_2, \boldsymbol{a}_3$ are basic unit translations in the lattice and n_1, n_2, n_3 are integers. Therefore, the space invariance can be expressed at time t by

$$u(\boldsymbol{r}_i, t) = u(\boldsymbol{r}_i + \boldsymbol{R}, t). \tag{3.8}$$

Such a function can be expressed by a linear combination of exponential functions, that is,

$$u(\boldsymbol{r}_i, t) = \sum_G u_G \exp \mathrm{i}(\boldsymbol{G}\cdot\boldsymbol{r}_i - \omega t), \tag{3.9}$$

for which the vector $\boldsymbol{G}$ is determined by the periodicity condition (3.8). We can then obtain the relation $\exp \mathrm{i}\boldsymbol{G}\cdot\boldsymbol{R} = 1$, that is, $\boldsymbol{G}\cdot\boldsymbol{R} = 2\pi \times (0 \text{ or integer})$, from which we obtain $\boldsymbol{G} \parallel \boldsymbol{R}$ and $|\boldsymbol{G}| = (2\pi \times \text{integer})/|\boldsymbol{R}|$. Corresponding to basic translations $\boldsymbol{a}_1$, $\boldsymbol{a}_2$, and $\boldsymbol{a}_3$, we define the reciprocal vectors

$$\boldsymbol{a}_1^* = \frac{2\pi}{\Omega}(\boldsymbol{a}_2 \times \boldsymbol{a}_3), \quad \boldsymbol{a}_2^* = \frac{2\pi}{\Omega}(\boldsymbol{a}_3 \times \boldsymbol{a}_1), \quad \text{and} \quad \boldsymbol{a}_3^* = \frac{2\pi}{\Omega}(\boldsymbol{a}_1 \times \boldsymbol{a}_2), \tag{3.10}$$

where $\Omega = (\boldsymbol{a}_1\boldsymbol{a}_2\boldsymbol{a}_3)$ is the volume of the primitive cell of the *reciprocal lattice*. Writing

$$\boldsymbol{G} = h\boldsymbol{a}_1^* + k\boldsymbol{a}_2^* + l\boldsymbol{a}_3^*, \tag{3.11a}$$

we obtain the relation

$$hn_1 + kn_2 + \ln_3 = 2\pi \times \text{integer}, \tag{3.11b}$$

where h, k, and l are integers; hence, $(h\boldsymbol{a}_1^*, k\boldsymbol{a}_2^*, l\boldsymbol{a}_3^*)$ gives a basic translation in the reciprocal lattice. Applying periodic boundary conditions to a crystal in large cubic volume $V = L_1L_2L_3$, we have the relation $\boldsymbol{G}\cdot\boldsymbol{R} = 2\pi \times \text{integer}$ for $|\boldsymbol{R}| = L_1, L_2, L_3$;

therefore, $G_1 = (2\pi/L_1)n_1$, $G_2 = (2\pi/L_2)n_2$, and $G_3 = (2\pi/L_3)n_3$. The vectors $\boldsymbol{a}_1^*$, $\boldsymbol{a}_2^*$, and $\boldsymbol{a}_3^*$ constitute *orthonormal* relations in the *crystal space* of basic vectors $\boldsymbol{a}_1$, $\boldsymbol{a}_2$, and $\boldsymbol{a}_3$; namely, $\boldsymbol{a}_1^* \cdot \boldsymbol{a}_1 = 2\pi$, $\boldsymbol{a}_1^* \cdot \boldsymbol{a}_2 = 0$, etc. Mutually independent displacement modes in crystal space can be specified by wave vectors $\boldsymbol{G}$.

Equation (3.9) implies that any function $f(\boldsymbol{r}_i, t)$ defined at lattice site i of a crystal represents propagation with a kinetic energy proportional to $\boldsymbol{G}^2$. The displacement u_i and its conjugate momentum can be expressed by a point in the dual crystal and reciprocal space; the latter is equivalent to the momentum space in analytical mechanics. In crystals, such a variable as in (3.9) can be activated thermally as well as adiabatically by internal and external fields. With inversion symmetry, the propagation in crystals is signified by wave vectors $\pm 2G$, but a frequency ω is positive because time is a positive variable. The displacement u_i in a crystal can therefore be written as

$$u_i = u_G \exp \mathrm{i}(\pm \boldsymbol{G} \cdot \boldsymbol{r}_i - \omega t) \quad \text{or} \quad u_G = u_i \exp i(\mp \boldsymbol{G} \cdot \boldsymbol{r}_i + \omega t), \tag{3.12}$$

representing waves propagating in opposite directions.

Dynamically an adiabatic potential $\Delta U(u_i)$ is responsible for u_i in classical description; both are *in phase*, propagating in an arbitrary direction $\boldsymbol{R}(n_1, n_2, n_3)$, signified by the phase $\phi_i = \boldsymbol{G} \cdot \boldsymbol{r}_i - \omega t + (\text{arbitrary angle})$. The phase ϕ_i is an internal variable whose values can be restricted effectively to $0 \leq \phi_i \leq 2\pi$. Nonetheless, since ϕ_i is almost continuous in the range of 2π, we can define a continuous *phase variable* $\phi = \boldsymbol{G} \cdot \boldsymbol{r} - \omega t$ in the same range, that is, $0 \leq \phi \leq 2\pi$, which is adequate for a crystal in sufficiently large size. Although such a conversion as $\phi_i \to \phi$ is just a matter of convenience, physically a phasing process is involved in minimizing structural strains. Referring to an arbitrary coordinates $(\boldsymbol{r}, t)$, such a continuous phase variable ϕ is necessary to specify a *mesoscopic* state of a crystal.

Including such a mesoscopic mode (3.12), for a crystalline state we have to consider a periodic lattice potential for the translation (3.7). It is significant that the mode u_G and ΔU_G are in phase at a wave vector $\boldsymbol{G}$, whose spatial periodicity is determined by the wavelength $\lambda = 2\pi/|\boldsymbol{G}|$.

3.4.2 The Bloch Theorem

An excitation in a crystal is given as a propagation mode through the periodic structure along the direction of a reciprocal vector $\boldsymbol{G}$ given by (3.11a). If the displacement u_i is considered as in Sect. 3.4.1, at the critical temperature we expect anomalies as related to space–time uncertainties of u_i. However disregarding anomalies in this section, we discuss ionic excitations in a crystal, which can be expressed by the wave function $\psi(\boldsymbol{r})$, where $\boldsymbol{r}$ is an arbitrary position in the range $0 \leq r \leq \lambda$.

For the wave function $\psi(\boldsymbol{r})$, we write the Hamiltonian equation

$$\mathcal{H}\psi(\boldsymbol{r}) = \left\{\frac{p^2}{2m} + V(\boldsymbol{r})\right\}\psi(\boldsymbol{r}) = E\psi(\boldsymbol{r}), \tag{3.13}$$

where $V(\boldsymbol{r})$ is the adiabatic potential that satisfies the periodic condition

$$V(\boldsymbol{r}) = V(\boldsymbol{r} + \boldsymbol{R}).$$

We can similarly assume

$$\psi(\boldsymbol{r}) = \psi(\boldsymbol{r} + \boldsymbol{R}), \tag{3.14}$$

implying that $V(\boldsymbol{r})$ and $\psi(\boldsymbol{r})$ can both be in phase.

For one-dimensional chain, we can write $\boldsymbol{R} = n\boldsymbol{a}$, where the vector $\boldsymbol{a}$ is the translation unit, and $n = 1, 2, \ldots, N$, where N is the total number of lattice sites on the line. From (3.14), the functions at all n are equal to $\psi(r)$, therefore

$$\psi(\boldsymbol{r} + n\boldsymbol{a}) = c^n\psi(\boldsymbol{r}),$$

so that $c^n = 1$ or $c = \exp(2\pi n\mathrm{i})$, which is satisfied by $L = na$ and $2\pi n/L = |\boldsymbol{G}|$. Therefore, we can write

$$\psi(\boldsymbol{r} + n\boldsymbol{a}) = \{\exp \mathrm{i}\boldsymbol{G} \cdot (n\boldsymbol{a})\}\psi(\boldsymbol{r}).$$

Combining this with the Fourier expansion $\psi(\boldsymbol{r}) = \sum_G \varphi_G \exp \mathrm{i}\boldsymbol{G} \cdot \boldsymbol{r}$, translational symmetry can be expressed by

$$\psi(\boldsymbol{r} + \boldsymbol{R}) = \sum_G \varphi_G(\boldsymbol{r}) \exp \mathrm{i}\boldsymbol{G} \cdot (\boldsymbol{r} + \boldsymbol{R}), \tag{3.15a}$$

where $\boldsymbol{R}$ is an arbitrary lattice point given by (3.7) and $\varphi_G(r)$ is the amplitude of the wave propagating along the direction of $\boldsymbol{G}$. Equation (3.15a) is generally called the *Bloch theorem*.

The above argument applies generally to *tight-bound electrons* in crystals. In this model, electrons are in orbits around ions, but not necessarily transportable for electric conduction through the lattice. On the other hand, for a *loosely bound electron* in typical metals, the Bloch theorem can also be employed, constituting the basic model for metallic conduction. In this case, we consider the wave function

$$\psi(\boldsymbol{r}) = \sum_k \varphi_k(\boldsymbol{r}) \exp \mathrm{i}\boldsymbol{k} \cdot \boldsymbol{r}. \tag{3.15b}$$

Written similar to (3.15a), this wave function describes a nearly free electron propagating with a wave vector $\boldsymbol{k}$.

The momentum is expressed by a differential operator $\boldsymbol{p} = -\mathrm{i}\hbar\nabla$ in quantum theory. Operating $\boldsymbol{p}$ on $\psi(\boldsymbol{r})$, we have

$$\boldsymbol{p}\psi_k(\boldsymbol{r}) = \exp \mathrm{i}\boldsymbol{k}\cdot\boldsymbol{r}(\hbar\boldsymbol{k}+\boldsymbol{p})\varphi_k(\boldsymbol{r}),$$

and hence

$$\boldsymbol{p}^2\psi_k(\boldsymbol{r}) = \exp \mathrm{i}\boldsymbol{k}\cdot\boldsymbol{r}(\hbar\boldsymbol{k}+\boldsymbol{p})^2\varphi_k(\boldsymbol{r}).$$

Accordingly, Equation (3.13) can be expressed as

$$\left\{\frac{1}{2m}(\boldsymbol{p}+\hbar\boldsymbol{k})^2 + V(\boldsymbol{r})\right\}\varphi_k(\boldsymbol{r}) = \varepsilon_k\varphi_k(\boldsymbol{r}) \tag{3.16a}$$

or

$$\left\{-\frac{\hbar^2}{2m}(\boldsymbol{\nabla}^2 + 2\mathrm{i}\boldsymbol{k}\cdot\boldsymbol{\nabla}) + V(\boldsymbol{r})\right\}\varphi_k(\boldsymbol{r}) = \left(\varepsilon_k - \frac{\hbar^2k^2}{2m}\right)\varphi_k(\boldsymbol{r}). \tag{3.16b}$$

Applying (3.8) to each k of (3.15b),

$$\psi_k(\boldsymbol{r}) = \sum_G \varphi_{k+G}(\boldsymbol{r})\exp \mathrm{i}(\boldsymbol{k}+\boldsymbol{G})\cdot\boldsymbol{r},$$

where for the amplitudes we have a periodicity relation

$$\varphi_k(\boldsymbol{r}) = \varphi_{k+G}(\boldsymbol{r})$$

at all the reciprocal lattice points in the direction of $\boldsymbol{k}$. Eigenvalues ε_k of (3.15a) are also characterized by a periodic relation

$$\varepsilon_k = \varepsilon_{k+G}. \tag{3.17}$$

Accordingly, constant-energy surfaces in polyhedral shape can be determined by $|\boldsymbol{G}|$, which can be constructed in the reciprocal space.

3.4.3 *Lattice Symmetry*

In the foregoing, a weak ionic excitation in a noncritical region of a crystal was discussed with the Bloch theorem, referring to an arbitrary lattice point $\boldsymbol{r}$. Such excitations considered as propagating waves should be standing waves in crystals, in order for them to be sampled with appropriate probes. Characterized by the wave vector $\boldsymbol{k}$ and energy ε_k, the Bloch excitation is caused in phase with an adiabatic lattice potential. As discussed in Sect. 3.4.1, such excitations occur in random phase ϕ_i in the range $0 \le \phi_i \le 2\pi$ in repetition; hence, ϕ_i can be replaced by a single

continuous phase variable ϕ in the range $0 < \phi < 2\pi$. Translational lattice symmetry can therefore be expressed by an *operator* T as

$$T\varphi_k(\boldsymbol{r}) = \varphi_k(\boldsymbol{r} + \boldsymbol{R}) = (\exp \mathrm{i}\boldsymbol{k} \cdot \boldsymbol{R})\varphi_k(\boldsymbol{r}), \tag{3.18}$$

which is equal to $\varphi_k(\boldsymbol{r})$, if $\boldsymbol{k} = \boldsymbol{G}$; a group of these operators T constitutes the *space group* of a crystal.

In addition to space symmetry, the *primitive cell* needs to be specified by a *point group*, consisting of *rotation*, *reflection*, etc., for complete characterization of the lattice structure. Elements of the point group constitute an orthogonal set of invariant coordinate transformations. Signifying a point operation by S, we have the relation

$$S\varphi_k(\boldsymbol{r}) = \varphi_k(S^{-1}\boldsymbol{r}). \tag{3.19}$$

In a crystal in thermal and adiabatic equilibrium, the function $\varphi_k(\boldsymbol{r})$ must be invariant under the operations T and S, as we set $\boldsymbol{k} = \boldsymbol{G}$ in (3.18). We can also verify that the wave equation (3.16a) or (3.16b) is invariant under S, where the eigenvalue ε_k is degenerate s-fold, if s is the number of symmetry elements of the point group. Further, we should consider an additional *space inversion* $\boldsymbol{r} \to -\boldsymbol{r}$, signifying a phase reversal $\phi \to -\phi$ at any time, which is a requirement for unpolarized states. For the group theory of crystalline lattices, interested readers are referred to Tinkham [5].

3.4.4 The Brillouin Zone

Crystal symmetry characterizes the geometrical structure of a lattice, whereas the corresponding reciprocal lattice exhibits symmetry of excitations within the structure. Physically, such excitations arise from lattice vibrations that are signified by $\boldsymbol{k}$ and ε_k. Equations (3.16a) and (3.16b) are written for excitations in the reciprocal lattice, in which the vectors $\boldsymbol{k}$ and $\boldsymbol{k} + \boldsymbol{G}$ specify dynamically identical states. Owing to the identity relation in repetition, the reciprocal lattice can be reduced to a zone specified by values of $\boldsymbol{G}$, which is called the *Brillouin zone*.

Figure 3.6a shows an example of a Brillouin zone in one dimension, where the zone center is at $G = 0$, and the zone boundaries are between the first and the next ones as determined by $k = \pm G/2 = \pm\pi/a$. These boundaries are signified by reflections, where the wave functions $\psi_k(\boldsymbol{r})$ of (3.15b) on both sides are connected as

$$\psi_k\left(\frac{\pi}{a}\right) = \psi_k\left(-\frac{\pi}{a}\right) \quad \text{for} \quad k = \pm\frac{\pi}{a}.$$

Therefore, $\psi_k(\boldsymbol{r})$ are in standing waves in the form

$$\psi_{k=\pi/a}(x) = \sin\frac{\pi x}{a}\ \varphi_{k=\pi/a}(x) \quad \text{or} \quad \psi_{k=\pi/a}(x) = \cos\frac{\pi x}{a}\ \varphi_{k=\pi/a}(x).$$

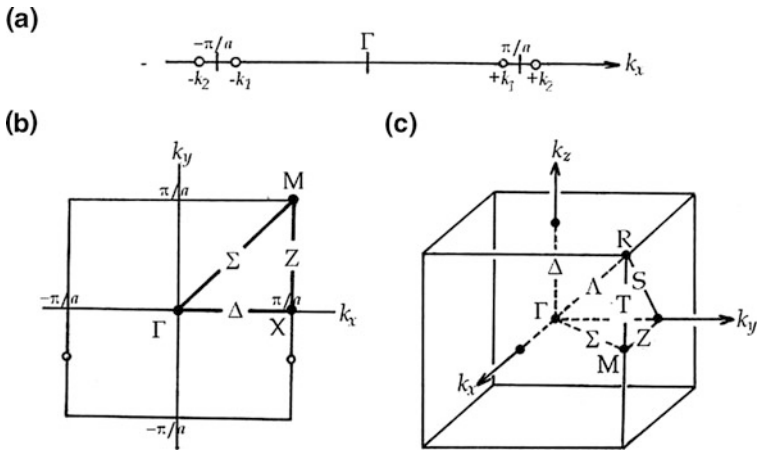

Fig. 3.6 (**a**) Brillouin zone in one dimension, $-\pi/a<k_x<\pi/a$; the zone center is Γ. (**b**) Two-dimensional Brillouin zone in the k_xk_y-plane. (**c**) Brillouin zone in a cubic lattice.

Also notable is that the eigenvalue ε_k is a continuous function of $\boldsymbol{k}$, for which we have a relation

$$\nabla_k \varepsilon_k = 0 \quad \text{at} \quad k = \pm\frac{\pi}{a}. \tag{3.20}$$

Figure 3.6b illustrates the Brillouin zone of a square lattice. Symmetry of the point group is expressed as $4mm$; a fourfold axis of two sets of mirror planes m_x, m_y, and two diagonal planes $m_d, m_{d'}$. Specific points Γ, M, X and specific lines Δ, Z, Σ are significant, as indicated in the figure. The point Γ is at the origin $\boldsymbol{k} = 0$, transforming into itself under all operations in the point group. The point M transforms into itself or into the opposite corner of the square under the same operations; these corners are related with each other by the same reciprocal vector, and hence the four corners are equivalent. The point X is invariant under the operations 2_z, m_x, m_y, where a reflection m_x and a rotation 2_z in succession carried a point $(\frac{\pi}{a}, 0)$ into the identical point $(-\frac{\pi}{a}, 0)$.

Particular lines $\Delta, \Sigma, \mathrm{Z}$ are invariant under mirror reflections m_x, m_d, m_y, respectively. It is noted that by m_x, an arbitrary point $A(\frac{\pi}{a}, -k_y)$ on the line Z can be carried to the identical point $B(-\frac{\pi}{a}, -k_y)$ that differs by the vector $G = (\frac{2\pi}{a}, 0, 0)$, implying that (3.20) can be applied to all points on the zone boundaries.

For a simple cubic lattice, such specific points and lines as in the square lattice are shown in Fig. 3.6c, where the basic feature of the Brillouin zone can be confirmed by using the point group operations of $\frac{4}{m}, \bar{3}, \frac{2}{m}$. There are four special points R, M, X, Γ and five specific lines, $\Delta, S, T, \Sigma, Z, \Lambda$, indicated in the figure, representing invariant points and lines under the point group operations similar to those in the two-dimensional square lattice. We shall not discuss on crystal symmetry any further, leaving the detail to a standard reference book on group theory [5].

3.5 Phonon Scatterings

For an adiabatic excitation in a crystal, the wave function is normally in standing waves, being characterized by an invariant eigenvalue ε_k by a translation $\boldsymbol{k} \rightarrow \boldsymbol{k} + \boldsymbol{G}$ in the reciprocal space. Using the Bloch theory, this feature is immediately clear from the relations $\psi_{k+G}(\boldsymbol{r}) = \psi_k(\boldsymbol{r})$ and $\varepsilon_{k+G} = \varepsilon_k$, as can be verified in the first Brillouin zone.

Considering that the order variable $\sigma_k(\phi)$ in a crystal can be described by the wave function $\psi_k(\boldsymbol{r}, t) = \psi_k(\phi)$, $\sigma_k(\phi)$ is associated with the density $\psi_k(\phi)^* \psi_k(\phi)$, which is determined by the wave equation

$$\frac{\partial^2 \boldsymbol{\sigma}_k}{\partial t^2} - \frac{1}{v_k^2} \boldsymbol{\Delta} \boldsymbol{\sigma}_\kappa = -\frac{\partial \Delta U}{\partial \phi_k}, \tag{3.21}$$

where $\boldsymbol{\Delta} \equiv \boldsymbol{\nabla}^2$ is the Laplacian operator. The function $\boldsymbol{\sigma}_k(\phi_k)$ represents free propagation along the direction of $\boldsymbol{k}$, if ΔU is constant or in quadratic for free propagation. Otherwise (3.21) is an inhomogeneous differential equation, whose nonlinear solutions will be discussed later in Chap. 7. In thermodynamics, order variables are temperature-dependent variables and subjected to a practical observation within a given timescale. In addition, depending on the condition of a crystal, collective $\boldsymbol{\sigma}_k$ and $\boldsymbol{\sigma}_{k'}$ can be correlated, as indicated by nonzero ΔU.

In harmonic approximation, the potential ΔU can be quadratic, making the structure stable, where $\boldsymbol{\sigma}_k$ are in free propagation. The corresponding $\boldsymbol{\sigma}_i$ is therefore distributed among lattice points, with probabilities determined by the mean-field approximation. In contrast, in an anharmonic potential ΔU, the correlated $\boldsymbol{\sigma}_k$ is expressed by a classical vector in finite amplitude. A symmetry change between different phases is associated with a change in ΔU that occurs at the critical temperature.

It is important to realize that order variables $\boldsymbol{\sigma}_i$ emerge as related to spontaneous displacements $\boldsymbol{u}_k$ in the lattice, playing together a significant role in a modulated state of a crystal. We shall call such coupled variables $(\boldsymbol{\sigma}_k, \boldsymbol{u}_k)$ a *condensate* by analogy of a condensing liquid. In crystals, condensates are formed to stabilize modulated structure, as postulated by Born and Huang. Representing a modulated state, condensates are said to be *mesoscopic*, as characterized by distributed densities. In this book, we restrict the use of the word *macroscopic* only to uniform crystals. The mesoscopic state is signified by finite displacements $\boldsymbol{u}_k$ that scatter phonons inelastically, and hence the condensate $(\boldsymbol{\sigma}_k, \boldsymbol{u}_k)$ exhibits usually temperature dependence.

The potential ΔU can be expressed in series expansion with respect to the components u_x, u_y, u_z of $\boldsymbol{u}_k$, that is,

$$\Delta U = \sum_\alpha V_\alpha^{(1)} u_\alpha + \sum_{\alpha\beta} V_{\alpha\beta}^{(2)} u_\alpha u_\beta + \sum_{\alpha\beta\gamma} V_{\alpha\beta\gamma}^{(3)} u_\alpha u_\beta u_\gamma + \cdots, \tag{3.22}$$

where the indexes $\alpha, \beta, \gamma, \ldots$ stand for coordinates x, y, z. We can write these displacement components in (3.22) as $u_\alpha = u_{\alpha o} \exp \mathrm{i}(\boldsymbol{k}_\alpha \cdot \boldsymbol{r} - \omega_\alpha t)$. Denoting

scattering phonons by two sets of wave vectors and frequencies $(\boldsymbol{K}_1, \Omega_1)$ and $(\boldsymbol{K}_2, \Omega_2)$, the first term in the series of (3.22) can give rise to an off-diagonal element, for example,

$$u_{\alpha o}^2 V_{\alpha o}^{(1)} \{\exp \mathrm{i}(\boldsymbol{K}_1 + \boldsymbol{k}_\alpha - \boldsymbol{K}_2) \cdot \boldsymbol{r}\} \frac{1}{2t_o} \int_{-t_o}^{+t_o} \exp \mathrm{i}(-\Omega_1 - \omega_\alpha + \Omega_2) t \, \mathrm{d}t,$$

which is equal to $u_{\alpha o}^2 V_\alpha^{(1)}$, if $\boldsymbol{K}_2 - \boldsymbol{K}_1 = 2k_\alpha$ and $\Omega_2 - \Omega_1 = \omega_\alpha$, giving a probability for the phonon state to change from $(\boldsymbol{K}_1, \Omega_1)$ to $(\boldsymbol{K}_1 + 2k_\alpha, \Omega_1 + \omega_\alpha)$. In the above expression, t_o is the *timescale* of observation and therefore the time-related integral on the right-hand side can be calculated as

$$\frac{1}{2t_o} \int_{-t_o}^{+t_o} \exp \mathrm{i}(\Delta\Omega - \omega_\alpha) t \, \mathrm{d}t = \frac{\sin(\Delta\Omega - \omega_\alpha) t_o}{(\Delta\Omega - \omega_\alpha) t_o},$$

which is equal to 1, if $\Delta\Omega = \omega_\alpha$. Owing to a variety of $\Delta\Omega$ for inelastic scatterings, such a time-dependent ΔU can be significant only if $(\Delta\Omega - \omega_\alpha) t_o \sim 1$ at normal temperatures, causing a thermal transition. Such scatterings can also take place with to odd terms in (3.22), that is, $V_\alpha^{(1)}$, $V_{\alpha\beta\gamma}^{(3)}$, etc., which are observable within the timescale t_o, if $(\Delta\Omega - \omega_\alpha) t_o \leq 1$. In these cases, the scattered phonon transfers its energy to the surroundings; the process is normally called *thermal relaxation*.

Further noted is that even terms in (3.22) give rise to secular potentials. For example, the *quartic* term of $V_{\alpha\beta\gamma\delta}^{(4)}$ can be time independent with a four-phonon scattering as specified by

$$\boldsymbol{K}_\alpha - \boldsymbol{K}_\beta = \boldsymbol{K}_\delta - \boldsymbol{K}_\gamma + \boldsymbol{G} \quad \text{and} \quad \omega_\beta - \omega_\alpha = \omega_\gamma - \omega_\delta. \tag{3.23}$$

Owing to such time-independent components, $\Delta U(\phi)$ can be with a propagation mode, moving with $\boldsymbol{\sigma}(\phi)$, as described by the nonlinear equation (3.21), yielding solutions that are significantly different from free propagation.

Exercises 3

1. Discuss the phasing process of distributed $\boldsymbol{\sigma}_i$, referring to Born–Huang's postulate.
2. Although unspecified in Sect. 3.3, it is important to realize that the displacements $\boldsymbol{u}_i$ have a directional character with respect to the symmetry axes of a crystal. Accordingly, order variables $\boldsymbol{\sigma}_i$ coupled with $\boldsymbol{u}_i$ can violate space symmetry, if they are in finite magnitude. We can expect that mutual correlations and modified potentials ΔU_i are responsible for finite magnitudes of $\boldsymbol{\sigma}_i$ and $\boldsymbol{u}_i$. Discuss this problem in qualitative manner.
3. With lattice dynamics alone, we cannot deal with thermodynamic problems. In Sect. 3.5, we discussed phonon scatterings by $\boldsymbol{u}_i$ in general. Realize that no transfer of thermal energy occurs if $\boldsymbol{u}_i$ is in harmonic motion. Why?

Chapter 4
Statistical Theories of Binary Ordering

Order–disorder phenomena in alloys and magnetic crystals can be analyzed by statistical theories, assuming that the lattice structure plays no significant role. Lattice vibrations and symmetry are therefore implicit in thermodynamic functions in these theories. Restricted in mean-field accuracy, the statistical theory has only limited access to experimental details, for which a different approach is needed beyond the probability concept. In ordering processes, the lattice stability is an important issue, but statistical theories cannot deal with symmetry changes. Nevertheless, in this chapter, we review existing theories because the probability concept is still useful for simplifying the problem. Characterized by a random process, statistical theories are valid in some aspects of ordering processes, leaving symmetry-related problems to different studies.

4.1 Probabilities in Binary Alloys

Properties of binary alloys, such as β-brass CuZn, are well documented, exhibiting order–disorder transitions at specific temperatures T_c. In their statistical theory, Bragg and Williams [6] considered *probabilities* for pairs of *like-atoms* A–A and B–B, and for *unlike-atoms* A–B or B–A to be at nearest-neighbor lattice sites, thereby introducing the concept of *short-* and *long-range order*. Judging from observed T_c of the order of 450°C, the lattice in β-brass is not so rigid because of the constituents in diffusive motion; nonetheless, such probabilities in the lattice can be defined by the Boltzmann statistics, as verified in later discussions.

We define probabilities $p_n(\mathrm{A})$ and $p_n(\mathrm{B})$ for a lattice site n to be occupied by an atom A and an atom B, respectively. For such exclusive events, we have the relation

$$p_n(\mathrm{A}) + p_n(\mathrm{B}) = 1 \tag{4.1a}$$

M. Fujimoto, *Thermodynamics of Crystalline States*,
DOI 10.1007/978-1-4419-6688-9_4,

and define the order variable as

$$\sigma_n = p_n(\mathrm{A}) - p_n(\mathrm{B}). \tag{4.1b}$$

Here, by definition, we have $0 \leq p_n(\mathrm{A}), p_n(\mathrm{B}) \leq 1$, and hence the variable σ_n is in the range $-1 \leq \sigma_n \leq 1$. The *disordered state* characterized by $p_n(\mathrm{A}) = p_n(\mathrm{B}) = 1/2$ can therefore be expressed by $\sigma_n = 0$, whereas the state where all sites are occupied either by A or B, called *complete order*, can be signified by $\sigma_n = \pm 1$, indicating that the crystal is composed of ordered A-domain and B-domain in equal volumes; otherwise, the whole crystal should consist of intermingled sublattices of A and B, representing *alloy*. However, it is an empirical matter, if we have domains in two volumes or alloy in the whole volume; these two cases remain as theoretically undetermined, as will be discussed in the next section. In partially ordered states in a mixed atomic arrangement, the variables σ_n are distributed among lattice sites. Assuming a random arrangement of σ_n, it is logical to consider the average $\langle \sigma_n \rangle = \frac{1}{N} \sum_n \sigma_n$ over N lattice sites to express the macroscopic degree of order; we can thereby define the *order parameter* by $\eta = \langle \sigma_n \rangle$. This is known as the *mean-field average*. In practice, it is a useful approximation; however, its validity should be justified experimentally.

However, for a system characterized by randomness, it is a common practice to use the *correlation function* defined by

$$\Gamma = \langle (\sigma_m - \eta)(\sigma_n - \eta) \rangle = \langle \sigma_m \sigma_n - \eta^2 \rangle, \tag{4.2}$$

after taking the relations $\langle \sigma_m \rangle = \langle \sigma_n \rangle = \eta$ into account.

It is significant to assume that each σ_n at lattice site n is correlated only with the nearest neighbors σ_m by an amount of energy ε_{mn}, composing the short-range interaction energy E_n with all σ_m at the surrounding sites m. Restricting to nearest neighbors only, E_n can be expressed as

$$E_n = \sum_m \{\varepsilon_{mn}^{\mathrm{AA}} p_m(\mathrm{A}) p_n(\mathrm{A}) + \varepsilon_{mn}^{\mathrm{BB}} p_m(\mathrm{B}) p_n(\mathrm{B}) + \varepsilon_{mn}^{\mathrm{AB}} p_m(\mathrm{A}) p_n(\mathrm{B}) + \varepsilon_{mn}^{\mathrm{BA}} p_m(\mathrm{B}) p_n(\mathrm{A})\}.$$

Using (4.1a) and (4.1b), we have

$$p_n(\mathrm{A}) = \frac{1}{2}(1 + \sigma_n) \quad \text{and} \quad p_n(\mathrm{B}) = \frac{1}{2}(1 - \sigma_n),$$

and similar expressions for $p_m(\mathrm{A})$ and $p_m(\mathrm{B})$ at a site m. Substituting these for probabilities in the above expression, the short-range energy E_n can be expressed in terms of σ_n and σ_m as

$$E_n = \sum_m E_{mn},$$

where

$$E_{mn} = \frac{1}{2}(2\varepsilon_{mn}^{\mathrm{AB}} + \varepsilon_{mn}^{\mathrm{AA}} + \varepsilon_{mn}^{\mathrm{BB}}) + \frac{1}{4}(\varepsilon_{mn}^{\mathrm{AA}} - \varepsilon_{mn}^{\mathrm{BB}})(\sigma_m + \sigma_n) + \frac{1}{4}(2\varepsilon_{mn}^{\mathrm{AB}} - \varepsilon_{mn}^{\mathrm{AA}} - \varepsilon_{mn}^{\mathrm{BB}})\sigma_m\sigma_n.$$

Abbreviating $K_{mn} = \frac{1}{4}(\varepsilon_{mn}^{\mathrm{BB}} - \varepsilon_{mn}^{\mathrm{AA}})$ and $J_{mn} = \frac{1}{4}(\varepsilon_{mn}^{\mathrm{AA}} + \varepsilon_{mn}^{\mathrm{BB}} - 2\varepsilon_{mn}^{\mathrm{AB}})$, E_{mn} can be written as

$$E_{mn} = \text{constant} - K_{mn}(\sigma_m + \sigma_n) - J_{mn}\sigma_m\sigma_n.$$

Since $\varepsilon_{mn}^{\mathrm{AA}} \approx \varepsilon_{mn}^{\mathrm{BB}}$ for like-atoms in alloys, we can assume $K_{mn} \approx 0$. Disregarding the constant term, the short-range interaction energy is therefore dominated by the term of J_{mn}, that is,

$$E_{mn} = -J_{mn}\sigma_m\sigma_n. \tag{4.3}$$

Although the factor J_{mn} is not known from the first principle, the product $\sigma_m\sigma_n$ in (4.3) represents the correlation energy between neighboring order variables. We may therefore consider that the mean-field average $\langle E_{mn}\rangle$ is proportional to $\langle\sigma_m\sigma_n\rangle$ for $m \neq n$. In any case, (4.3) is a general form of correlation energy, for which J_{mn} indicates the strength of correlation.

4.2 The Bragg–Williams Theory

Bragg and Williams considered that the number of unlike pairs A–B is essential for expressing the degree of disorder, which can be evaluated by mean-field averages of probabilities

$$\langle p_n(\mathrm{A})\rangle = \langle p_m(\mathrm{A})\rangle = \frac{1}{2}(1+\eta) \quad \text{and} \quad \langle p_n(\mathrm{B})\rangle = \langle p_m(\mathrm{B})\rangle = \frac{1}{2}(1-\eta).$$

In a crystal of N lattice sites in total, we consider that each lattice point has z nearest sites. In this case, the number of unlike pairs can be expressed by

$$N_{\mathrm{AB}} = 2Nz\langle p_n(\mathrm{A})\rangle\langle p_m(\mathrm{B})\rangle = \frac{1}{2}Nz(1-\eta^2).$$

This indicates that $N_{\mathrm{AB}} = \frac{1}{2}Nz$ in the disordered state for $\eta = 0$, but $N_{\mathrm{AB}} = 0$ in the completely ordered states for $\eta = \pm 1$. Therefore in the former case, the short-range energy $E(\eta)$ is given as $E(0) = 0$. On the other hand, in complete ordered case, it is expressed by $E(\pm 1) = -\frac{1}{2}NJz$. For a partially ordered state for $0<|\eta|<1$, the short-range energy is given by

$$E(\eta) = -\frac{1}{2}NJz\eta^2, \tag{4.4}$$

where $J = \langle J_{mn} \rangle$ is the mean-field average. We consider that (4.4) represents the energy for *long-range interactions*, because $\langle J_{mn} \rangle$ is averaged over the whole crystal.

The macroscopic ordering energy $E(\eta)$ can be statistically calculated with a probability $g(\eta)$ for N_{AB} unlike pairs to be found at a given temperature T, which can be given by the number of combined A and B atoms to be placed independently among N sites. That is,

$$g(\eta) = \binom{N}{N\langle p_n(\mathrm{A}) \rangle} \binom{N}{N\langle p_n(\mathrm{B}) \rangle} = N^2 \binom{1}{\frac{1+\eta}{2}} \binom{1}{\frac{1-\eta}{2}}.$$

In this case, using (2.19), the macroscopic properties can be determined by maximum of the probability

$$W = w_{\mathrm{L}} w(\eta) = w_{\mathrm{L}} g(\eta) \exp\left\{ -\frac{E(\eta)}{k_{\mathrm{B}} T} \right\},$$

where the lattice contribution, if any, can be included in w_{L}, which however is a trivial factor under a constant volume condition. The thermodynamic equilibrium can then be obtained for minimizing Helmholtz' free energy $F = -k_{\mathrm{B}} T \ln W$. Solving the equation $(\partial F / \partial \eta)_V = 0$, we have

$$\frac{\partial}{\partial \eta} \left\{ \ln w_{\mathrm{L}} + \ln g(\eta) + \frac{N z J \eta^2}{2 k_{\mathrm{B}} T} \right\} = 0.$$

For a large N, the second term can be evaluated by using Stirling's formula, that is,

$$\frac{\partial \ln g(\eta)}{\partial \eta} = -\frac{N}{2} \ln \frac{1+\eta}{1-\eta} \quad \text{and} \quad \frac{z J \eta}{k_{\mathrm{B}} T} = \ln \frac{1+\eta}{1-\eta},$$

from which we obtain

$$\eta = \tanh \frac{z J \eta}{2 k_{\mathrm{B}} T}. \tag{4.5}$$

Equation (4.5) can be solved graphically for η, as shown in Fig. 4.1, where the straight line $\eta = (2k_{\mathrm{B}} T / zJ) y$ and the curve $\eta = \tanh y$ cross at a point P to determine the value of the order parameter η at a given temperature T. It is noted that the origin $\eta = 0$ is the only crossing point if $\eta = y$, where the straight line is tangential to the curve, determining the transition temperature $T_{\mathrm{c}} = zJ / 2k_{\mathrm{B}}$. Also noted is that there is one crossing point at all temperatures below T_{c}, while no solution is found at temperatures above T_{c}.

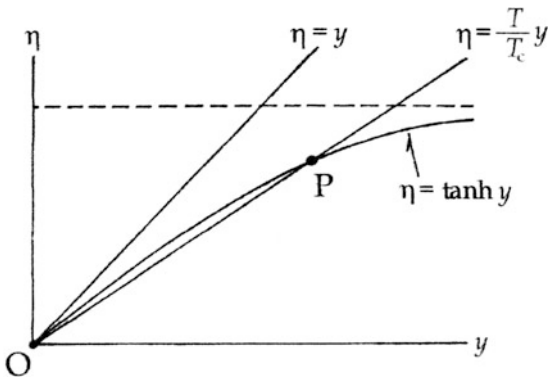

Fig. 4.1 Graphic solution of (4.5). Crossing points P between the straight line $\eta = y$ and the curve $\eta = \tanh y$. At $T = T_c$, the crossing point $\eta = 0$ is at O. For $T<T_c$, there is one crossing point P. No solution for $T>T_c$.

Writing $y = (T_c/T)\eta$ for convenience, the function $\tanh y$ can be expanded into a series, which may be truncated at low power if the temperature is close to T_c, that is,

$$y^2 = 3\left(\frac{T}{T_c}\right)^2\left(\frac{T_c}{T} - 1\right),$$

and hence

$$\eta^2 = \frac{3(T_c - T)}{T_c}.$$

Therefore η is characterized by parabolic temperature dependence, that is, $\eta \propto \sqrt{T_c - T}$ for $T \leq T_c$, as illustrated in Fig. 4.2a. In this analysis, the specific heat C_V is discontinuous at $T = T_c$; because $E = 0$ for $\eta = 0$ for $T > T_c$, whereas by differentiating (4.4) we obtain

$$\left(\frac{\partial E}{\partial T}\right)_V = -\frac{1}{2}NzJ\frac{\mathrm{d}\eta^2}{\mathrm{d}T} = \frac{3}{2}Nk_B \quad \text{for} \quad T < T_c.$$

Accordingly, the discontinuity of C_V at $T = T_c$ is given by

$$\Delta C_V = \frac{3}{2}Nk_B. \tag{4.6}$$

Figure 4.2b shows the specific curve in the vicinity of T_c sketched against temperature. However, as compared with the experimental curve of Cu–Zn alloy, there is a considerable discrepancy from the mean-field theory.

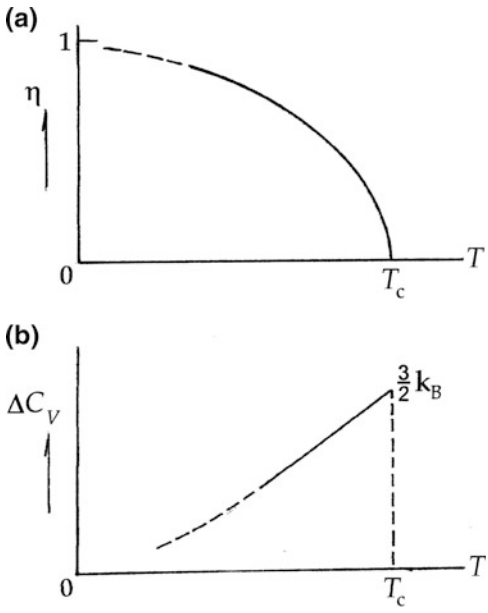

Fig. 4.2 Mean-field approximation. (**a**) Order parameter $\eta = \eta(T)$. (**b**) Specific heat discontinuity at T_c.

4.3 Becker's Interpretation

In the Bragg–Williams theory, an alloy can be segregated into two-component parts below T_c. Although signified by $\pm\eta$, these parts cannot be specified by their volumes. In fact, a segregated alloy exhibits two domains of different volumes with lowering temperature. Domains are characterized by their volumes V_A and V_B in practice; the numbers N_A and N_B in the theory must therefore be associated with the corresponding volumes by the relation $V_A + V_B = V$, where V is the volume of the whole alloy. Following Becker's book [3], domain volumes are discussed here, giving a practical interpretation of segregated or mixed states.

Writing $N_A = \gamma N$, we have $N_B = (1-\gamma)N$, where γ is a continuous parameter, $0 \le \gamma \le 1$. A constant parameter γ can be used like another order parameter without referring to the lattice structure. We can assume that in a fixed structure $\gamma = V_A/V$ and $1-\gamma = V_B/V$ because of the relations $N_A \propto V_A$ and $N_B \propto V_B$. In this case, the ordering energy (4.4) can be written as

$$E(\gamma) = -\frac{1}{2}NJz\gamma(1-\gamma).$$

In the whole crystal, this energy state can be weighted by the probability

$$w(\gamma) = \binom{N}{N\gamma}\binom{N}{N(1-\gamma)}.$$

Therefore, the free energy is calculated as

$$F = Nk_{\mathrm{B}}Tf(\gamma),$$

where

$$f(\gamma) = \gamma \ln \gamma + (1-\gamma)\ln(1-\gamma) + \frac{Jz}{k_{\mathrm{B}}T}\gamma(1-\gamma).$$

In equilibrium, two domains can be distinguished by different sets of parameters (N_1, γ_1) and (N_2, γ_2), with which the free energy of a whole alloy can be expressed as

$$F = k_{\mathrm{B}}T\{N_1 f(\gamma_1) + N_2 f(\gamma_2)\},$$

where

$$N_1 + N_2 = N \quad \text{and} \quad N_1\gamma_1 + N_2\gamma_2 = N\gamma.$$

For thermal equilibrium between two domains, F can be minimized against any variations δN_1 and δN_2 with Lagrange's method of multipliers λ and μ. Namely, from $\delta F = 0$, we obtain

$$f(\gamma_1) + \lambda + \mu\gamma_1 = 0 \quad \text{and} \quad f(\gamma_2) + \lambda + \mu\gamma_2 = 0,$$

and write

$$f'(\gamma_1) + \mu = 0 \quad \text{and} \quad f'(\gamma_2) + \mu = 0$$

to assure the minimum against variations $\delta\gamma_1$ and $\delta\gamma_2$. Eliminating λ and μ from these relations, we can derive

$$f'(\gamma_1) = f'(\gamma_2) \quad \text{and} \quad f(\gamma_1) - f(\gamma_2) = f'(\gamma)(\gamma_1 - \gamma_2).$$

Figure 4.3a shows Becker's numerical analysis for the function $f(\gamma)$, where considering $s = zJ/k_{\mathrm{B}}T$ as an adjustable parameter, curves are drawn for $s = 0$, 2, 3 and 6. For $s = 2$, that is, $T = zJ/2k_{\mathrm{B}} = T_{\mathrm{c}}$, the curve shows a single minimum at $\gamma_1 = \gamma_2 = \gamma/2$. On the other hand, for $s = 3$, two different minima at $\gamma_1 \neq \gamma_2$ are found with $f'(\gamma_1) = f'(\gamma_2)$ symmetrically as illustrated; one close to $\gamma = 0$ and the other close to $\gamma = 1$. For a larger value of s, for example, $s = 6$, these are very close to 0 and 1, respectively. Figure 4.3b is the plot for T verses γ or η, where the left and right branches below T_{c} are for the domains A and B; the volume ratios V_{A}/V and V_{B}/V are related as $V_{\mathrm{A}} + V_{\mathrm{B}} = V$.

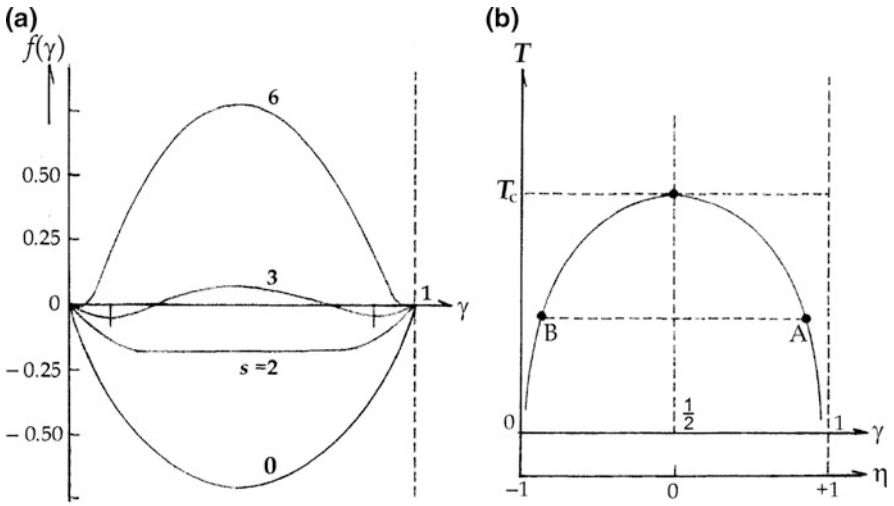

Fig. 4.3 Becker's graphic solutions. (**a**) $f(\gamma)$ verses γ. (**b**) T verses γ and η.

We realize that Becker's interpretation is an addendum to Bragg–Williams' theory; we consider that each constituent atom occupies a finite volume in a rigid crystal. In this context, Becker's theory disregards the lattice structure entirely.

4.4 Ferromagnetic Order

Heisenberg (1929) postulated that electron exchange between magnetic ions is responsible for spin ordering in a ferromagnetic crystal, which is expressed by a Hamiltonian

$$\mathcal{H}_{n,n+1} = -\frac{1}{2}\mathcal{J}\boldsymbol{s}_n \cdot 2\boldsymbol{s}_{n+1}, \tag{4.7}$$

where $\mathcal{J}$ is the *exchange integral* between valence electrons of neighboring ions at n and $n + 1$ sites. $\mathcal{H}_{n,n+1}$ in (4.7) is expressed as a correlation $\boldsymbol{s}_n \cdot \boldsymbol{s}_{n+1}$ between neighboring spins. Instead of spin $\boldsymbol{s}_n$, order vectors defined as $\boldsymbol{\sigma}_n = \gamma \boldsymbol{s}_n$ with the gyromagnetic ratio γ can be used for (4.7) to express the correlation energy between ions at these sites. Writing therefore $J_{nm} = \frac{1}{2}\mathcal{J}_{nm}$, we have

$$\mathcal{H}_{nm} = -J_{nm}\boldsymbol{\sigma}_n \cdot \boldsymbol{\sigma}_m$$

for a magnetic system, where $\boldsymbol{\sigma}_n \cdot \boldsymbol{\sigma}_m$ is the scalar product of vectors.

In an uniform magnetic field $\boldsymbol{B}$ applied externally, the energy of $\boldsymbol{\sigma}_n$ can be written as

$$\mathcal{H}_n = -\boldsymbol{\sigma}_n \cdot \boldsymbol{B} + \sum_m J_{nm} \boldsymbol{\sigma}_n \cdot \boldsymbol{\sigma}_m,$$

where the summation includes all $\boldsymbol{\sigma}_m$ that interact with $\boldsymbol{\sigma}_n$. Therefore, we can assume that $\boldsymbol{\sigma}_n$ is exposed to the effective magnetic field $\boldsymbol{B} + \boldsymbol{B}_n$, where $\boldsymbol{B}_n = \left\langle \sum_m J_{nm} \boldsymbol{\sigma}_m \right\rangle$ is the mean-field average. Such an internal field as $\boldsymbol{B}_n$ was first postulated by Weiss, who assumed that $\boldsymbol{B}_n$ is proportional to $\langle \sigma_n \rangle$; $\boldsymbol{B}_n = \lambda \langle \sigma_n \rangle$ was called the *molecular field*. This concept can be used for long-range spin correlations in the mean-field accuracy. In this book, we shall refer to it as the *Weiss field*. In a magnetic crystal, $\langle \sigma_n \rangle$ is the magnetization $\boldsymbol{M}$ and the effective magnetic field $\boldsymbol{B} + \lambda \boldsymbol{M}$ can be assumed to act on uncorrelated $\langle \boldsymbol{\sigma}_n \rangle$. In this case, we can write

$$\boldsymbol{M} = \chi_{\mathrm{o}} (\boldsymbol{B} + \lambda \boldsymbol{M}), \tag{4.8a}$$

where χ_{o} is a paramagnetic susceptibility, for which we can use Curie's law $\chi_{\mathrm{o}} = C/T$ with the Curie's constant C. From (4.8a), we can obtain the ferromagnetic susceptibility

$$\chi = \frac{M}{B} = \frac{C}{T - C\lambda} = \frac{C}{T - T_{\mathrm{c}}}. \tag{4.8b}$$

This is known as the *Curie–Weiss law*, where $T_{\mathrm{c}} = C\lambda$ indicates the transition temperature that is related to the long-range parameter λ. Equation (4.8b) is applicable to temperatures close to T_{c}, considering magnetic correlations as weak perturbations. In the mean-field approximation, the ferromagnetic phase transition is characterized by singular behavior of χ at $T = T_{\mathrm{c}}$.

The Weiss field has a significant implication for an ordering process in the mean-field approximation. The ordering energy $E = -\frac{1}{2} NzJ\eta^2$ in (4.4) for a binary state can be expressed as $E = -\eta X_{\mathrm{int}}$, where $X_{\mathrm{int}} = \frac{1}{2} zJ\eta$. By writing $\frac{1}{2} zJ = \lambda$, such an expression is found analogous to the magnetization energy $-\boldsymbol{M} \cdot \boldsymbol{B}_n = -\lambda \boldsymbol{M}^2$.

Rewriting (4.5) as

$$\eta = \tanh \frac{X_{\mathrm{int}}}{k_{\mathrm{B}} T} = \frac{\exp\left(-\dfrac{(-1) X_{\mathrm{int}}}{k_{\mathrm{B}} T} \right) - \exp\left(-\dfrac{(+1) X_{\mathrm{int}}}{k_{\mathrm{B}} T} \right)}{\exp\left(-\dfrac{(-1) X_{\mathrm{int}}}{k_{\mathrm{B}} T} \right) + \exp\left(-\dfrac{(+1) X_{\mathrm{int}}}{k_{\mathrm{B}} T} \right)},$$

this expression can be interpreted as

$$\eta = \langle \sigma_n \rangle = \langle p_n(\mathrm{A}) \rangle - \langle p_n(\mathrm{B}) \rangle, \tag{4.9}$$

where

$$\langle p_n(\mathrm{A})\rangle = \frac{1}{Z}\exp\left(-\frac{(-1)X_{\mathrm{int}}}{k_{\mathrm{B}}T}\right), \quad \langle p_n(\mathrm{B})\rangle = \frac{1}{Z}\exp\left(-\frac{(+1)X_{\mathrm{int}}}{k_{\mathrm{B}}T}\right),$$

and

$$Z = \exp\left(-\frac{(-1)X_{\mathrm{int}}}{k_{\mathrm{B}}T}\right) + \exp\left(-\frac{(+1)X_{\mathrm{int}}}{k_{\mathrm{B}}T}\right).$$

Equation (4.9) indicates that an order parameter is defined by the difference of Boltzmann probabilities between two inversion states ± 1 separated by the Weiss field X_{int}. Accordingly, Bragg–Williams' probabilities for binary states at a given temperature can be determined by the Weiss field that represents distant correlations. Discussing on the statistical distribution of X_{int} at a given temperature, the ordering in Bragg–Williams' theory is clearly an isothermal process.

4.5 Ferromagnetic Transitions in Applied Magnetic Fields

Binary ferromagnetic spin order can be modified by an externally applied field B. According to Weiss, we can consider that magnetic spins s_n are in the effective magnetic field $B + B_n$, and the magnetic ordering energy can be expressed by

$$E_{\pm} = \lambda M^2 \pm MB = -M(B_{\mathrm{int}} \mp B).$$

Denoting the numbers of + spins and − spins in unit volume of the crystal by N_+ and N_-, the order parameter can be expressed by

$$\eta = \frac{N_+ - N_-}{N_+ + N_-},$$

where $N_+ + N_- = N$ is the total number of spins. Following Becker's argument in Sect. 4.3, for the order parameter, we can use domain volumes V_+ and V_-, instead of N_+ and N_-, if the crystal volume is unchanged.

Writing that $N_{\pm} = \frac{N}{2}(1 \pm \eta)$, we can express

$$M = N\gamma\eta \quad \text{and} \quad E(\pm\eta) = -\frac{1}{2}NJz\eta^2 \mp N\gamma\eta B.$$

And, the thermal properties can be determined by the free energy $F = -k_{\mathrm{B}}T\ln Z$, where the function $Z = Z(\eta)$ is given by

$$Z = Z(+\eta)Z(-\eta) = \binom{N}{N_+}\binom{N}{N_-}\exp\left(-\frac{E(+\eta)+E(-\eta)}{k_{\mathrm{B}}T}\right).$$

The most probable values of N_+ and N_- can be determined in such a way that $\ln Z(+\eta)$ and $\ln Z(-\eta)$ are maximized, respectively. Using the relation $\mathrm{d}N_+ = -\mathrm{d}N_-$ from a constant N, we therefore have

$$\frac{\mathrm{d}}{\mathrm{d}N_+}\ln\binom{N}{N_+} = \frac{\mathrm{d}}{\mathrm{d}N_+}(-N_+\ln N_+ + N_-\ln N_-) = \frac{1}{k_\mathrm{B}T}\frac{\mathrm{d}E(+\eta)}{\mathrm{d}N_+}$$

and

$$\frac{\mathrm{d}}{\mathrm{d}N_+}\ln\binom{N}{N_-} = -\frac{\mathrm{d}}{\mathrm{d}N_-}\ln\binom{N}{N_-} = -\frac{1}{k_\mathrm{B}T}\frac{\mathrm{d}E(-\eta)}{\mathrm{d}N_-}.$$

From these, we obtain

$$\ln\frac{N_-}{N_+} = \frac{2}{Nk_\mathrm{B}T}\frac{\mathrm{d}E(\pm\eta)}{\mathrm{d}\eta},$$

and hence

$$\ln\frac{1-\eta}{1+\eta} = -\frac{2}{k_\mathrm{B}T}\left(\frac{1}{2}Jz\eta \pm \gamma B\right),$$

which can be solved for η, obtaining

$$\eta = \tanh\left(\frac{Jz\eta}{2k_\mathrm{B}T} \pm \frac{\gamma B}{k_\mathrm{B}T}\right). \tag{4.10}$$

This is identical to (4.5) if $B = 0$, therefore (4.10) can also be solved graphically. Namely, writing $y = (Jz/2k_\mathrm{B}T)\eta + (\gamma B/k_\mathrm{B}T)$, (4.10) is expressed as $\eta = \tanh y$; the value of η can be determined in the η–y plane from the crossing point between the straight line and the tanh curve, as illustrated in Fig. 4.4. Although we can define

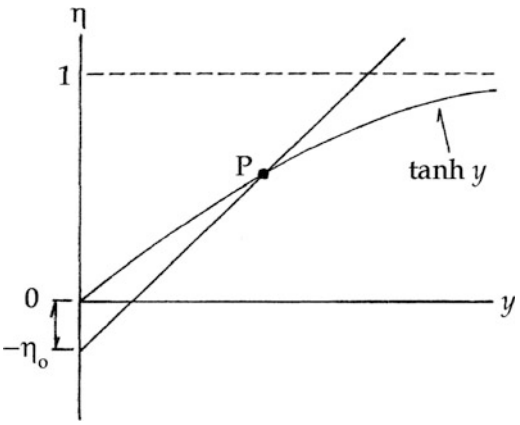

Fig. 4.4 Graphic solution of (4.10). $\eta = -\eta_\mathrm{o}$ at T_c, and one crossing point for $T<T_\mathrm{c}$.

$T_c = Jz/2k_B$ for $B = 0$, the crossing point does not correspond to $\eta = 0$ if $B \neq 0$, in which case T_c does not signify a transition. However, the intercept $\gamma B/k_B T$ on the η-axis is small and insignificant in a practical magnetic field, where the transition temperature T_c can be determined as permitted within accuracy of $\gamma B/k_B T \approx 0$.

Exercises 4

1. In this chapter, order variables σ_n and their short-range correlations (4.5) are all defined statistically. In contrast, Heisenberg's spin–spin interactions were derived quantum mechanically, which is interpreted as adiabatic in thermodynamics. Despite of different approaches, we have a consistent result expressed by (4.5). However, extending (4.5) for long-range correlations is hardly acceptable, because of lacking randomness in the system. Discuss in detail on this issue.
2. Can the mean-field average be consistent with the Boltzmann statistics? If Weiss molecular field is interpreted as the mean-field average $\lambda\langle\sigma_n\rangle$, $\langle\sigma_n\rangle$ is the mean-field average. Therefore, it appears to be incorrect to assume that $\langle\sigma_n\rangle = \eta$, as the order parameter can be determined statistically. How do you resolve this conceptual conflict?

Part II
Structural Phase Changes

Chapter 5
Pseudospin Clusters and Short-Range Correlations

Structural phase transformations constitute a major subject of investigation in thermodynamics of crystalline states. A partial displacement in the constituent molecule represented by an order variable is essential for describing structural changes. Although considered as primarily independent of the lattice structure, such an order variable in finite magnitude disrupts local symmetry in a crystal. Correlations of these variables between adjacent sites are responsible for their clustering, leading to a macroscopic symmetry change. Following Born and Huang, we consider clustered order variables in a short range to form *condensates* for minimal structural strains in the lattice. Consequently, a condensate is characterized by a specific wave vector for propagation in the lattice. In this chapter, we define *pseudospins* for binary order variables and discuss the nature of their correlations in short range.

5.1 Pseudospins for Binary Displacements

The lattice structure is characterized by the *space group*, where all lattice sites are identical, and constituent molecules are configured by the *point group*. Dynamically, masses of constituents are in vibrating motion of harmonic modes, forming a stable structure at their average positions. On the other hand, restricted by the point group, a specific part of the constituent can be in motion independent of lattice vibrations. Exemplified in perovskite crystals, such parts defined as *order variables* can be in collective motion under thermal conditions, which are evidenced by *diffuse* X-ray diffraction patterns. Figure 5.1 is an X-ray photograph obtained from a perovskite crystal of $NiNbO_3$ at 700°C, showing a diffuse pattern due to a slow movement of constituent ions.

Among such displacive phase transitions in perovskite crystals, $SrTiO_3$ and $BaTiO_3$ show typical structural changes that are illustrated schematically in Fig. 3.3a, b. Here, we consider that the Ti^{4+} ion in Fig. 3.3a can fluctuate at a fast rate between two positions 1 and 1′ in the octahedral SiO_6^{2-} group along the

M. Fujimoto, *Thermodynamics of Crystalline States*,
DOI 10.1007/978-1-4419-6688-9_5, © Springer Science+Business Media, LLC 2010

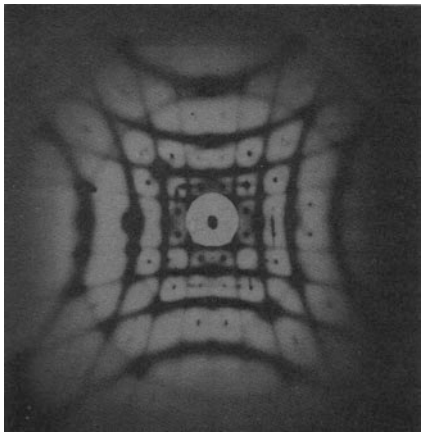

Fig. 5.1 A diffuse X-ray diffraction photograph from $NiNbO_3$ at 700°C (from [12]).

z-direction with an equal probability, where the point symmetry remains invariant under fast inversion. In Fig. 3.3b shown is similar inversion that arises from fast rotation of TiO_6^{2-} by small positive and negative angles around the z-axis. In these cases, a vector variable $\boldsymbol{\sigma}_n$ parallel to the z-axis represents such inversion symmetry at a site n.

In a packed structure of perovskite, a variable $\boldsymbol{\sigma}_n$ inverting 1 and $1'$ can be regarded primarily as independent from $\boldsymbol{\sigma}_m$ at other sites $(m \neq n)$, but these can be correlated with each other, depending on the thermal condition. The correlations are considered to be caused by an *adiabatic potential* originated from the lattice. Expressing by a Hamiltonian $\mathcal{H}$, we can write the equation of motion as

$$\mathrm{i}\hbar \frac{\partial \boldsymbol{\sigma}_n}{\partial t} = [\mathcal{H}, \boldsymbol{\sigma}_n]. \tag{5.1}$$

To consider $\boldsymbol{\sigma}_n$ in classical motion, it is necessary to take a timescale of observation t_o into account; thereby, the time derivative in (5.1) can be replaced by the average

$$\left\langle \frac{\partial \boldsymbol{\sigma}_n}{\partial t} \right\rangle_t = \frac{1}{t_\mathrm{o}} \int_0^{t_\mathrm{o}} \left(\frac{\partial \boldsymbol{\sigma}_n}{\partial t} \right) \mathrm{d}t.$$

This should vanish however, if $t_\mathrm{o} \to \infty$, as is normally assumed in statistical mechanics of equilibrium states. In this case, (5.1) should be written as

$$[\mathcal{H}, \langle \boldsymbol{\sigma}_n \rangle_t] = 0, \tag{5.2}$$

indicating that the observed $\langle \boldsymbol{\sigma}_n \rangle_t$ is commutable with $\mathcal{H}$. In contrast, if t_o is finite, a relaxation formula

$$\left\langle \frac{\partial \boldsymbol{\sigma}_n}{\partial t} \right\rangle_t = -\frac{\langle \boldsymbol{\sigma}_n \rangle_t}{\tau} \tag{5.3}$$

should be utilized in (5.1), where τ is a relaxation time under isothermal conditions. Therefore, we have

$$\frac{\mathrm{i}\hbar \langle \boldsymbol{\sigma}_n \rangle_t}{\tau} = [\mathcal{H}, \langle \boldsymbol{\sigma}_n \rangle_t].$$

Landau [6] assumed that the commutator on the left-hand side can be replaced by a product of uncertainties $-\mathrm{i}\Delta\varepsilon\Delta\langle \boldsymbol{\sigma}_n \rangle_t$ originating from distributed eigenvalues ε and $\langle \boldsymbol{\sigma}_n \rangle_t$. Specified by τ, the interacting lattice is clearly responsible for these uncertainties. We can then write the uncertainty relation

$$\Delta\varepsilon \cdot \frac{\Delta\langle \boldsymbol{\sigma}_n \rangle_t}{\langle \boldsymbol{\sigma}_n \rangle_t} \approx \frac{\hbar}{\tau}. \tag{5.4}$$

If (5.2) is valid, we have $\Delta\varepsilon = 0$ and $\mathcal{H} = 0$. Otherwise, (5.3) due to nonzero $\mathcal{H}$ signifies the outset of a transition, for which Landau proposed that (5.4) determines the character of order variables $\langle \boldsymbol{\sigma}_n \rangle_t$ at the threshold.

If $\Delta\langle \boldsymbol{\sigma}_n \rangle_t > \langle \boldsymbol{\sigma}_n \rangle_t$, $\langle \boldsymbol{\sigma}_n \rangle_t$ is quantum mechanical because of the uncertainty $\Delta\langle \boldsymbol{\sigma}_n \rangle_t$ dominating over $\langle \boldsymbol{\sigma}_n \rangle$; if on the other hand $\Delta\langle \boldsymbol{\sigma}_n \rangle_t < \langle \boldsymbol{\sigma}_n \rangle_t$, $\langle \boldsymbol{\sigma}_n \rangle_t$ can be a classical vector because of a negligible $\Delta\langle \boldsymbol{\sigma}_n \rangle_t$. Setting the relation $\Delta\varepsilon \approx k_\mathrm{B} T_\mathrm{c}$, (5.4) provides a criterion for the character of $\langle \boldsymbol{\sigma}_n \rangle_t$ to be justified with respect to the critical temperature T_c, that is,

$$\tau T_\mathrm{c} \gg \frac{\hbar}{k_\mathrm{B}} \sim 10^{-11}\,\mathrm{s\,K}. \tag{5.5}$$

In perovskites, phase transitions are called *displacive* in the range $100\,\mathrm{K} < T_\mathrm{c} < 200\,\mathrm{K}$, and estimated relaxation time is about 0.5×10^{-13} s. Therefore, the value of τT_c is roughly 500 times larger than the Landau's limit 10^{-11} given by (5.5), confirming that $\langle \boldsymbol{\sigma}_n \rangle_t$ represents a classical displacement at and below T_c. On the other hand, in crystals of hydrogen-bonding KDP, we have $T_\mathrm{c} \approx 1{,}000\,\mathrm{K}$ and $\tau \approx 10^{-13}$ s, so that $\tau T_\mathrm{c} \approx 10^{-11}$, indicating that $\langle \boldsymbol{\sigma}_n \rangle_t$ is barely in quantum character. In KDP, the order variable is rated as quantum mechanical, although not precisely identified as in perovskites.

Characterized by inversion, $\langle \boldsymbol{\sigma}_n \rangle_t$ shows similar behavior to a conventional spin variable of $\pm\frac{1}{2}$, in which sense it is called a *pseudospin*. For $\Delta\varepsilon \neq 0$, inversion of a pseudospin can be analyzed in slow tunneling motion, so that the phase transition cannot be continuous, accompanying fluctuations of the order of $\Delta\varepsilon$. In this case, the order variable behaves almost like a classical vector in the lattice, for which we can consider statistical correlations between adjacent sites.

5.2 A Tunneling Model

The pseudospin inversion is essentially a quantum-mechanical tunneling through a potential $U(z_n)$ corresponding to $\Delta\varepsilon$, where z_n is the position of the pseudospin on the direction of fluctuation. In this section, we discuss such a model of inversion in one dimension, following Blinc and Zeks [7].

Omitting the suffix n for simplicity, we assume that the unperturbed state can be determined by the wave equation

$$\mathcal{H}_{\rm o}\varphi_{\rm o} = \varepsilon_{\rm o}\varphi_{\rm o},$$

where the eigenvalue is positive, that is, $\varepsilon_{\rm o} > 0$, representing the kinetic energy of fluctuations. For such a particle we consider an effective potential of so-called a *double well*, where the central hump represents the perturbing potential $U(z)$. The ground energy $\varepsilon_{\rm o}$ is therefore doubly degenerate because of the symmetry. The wave functions in the right and left wells are denoted by $\varphi_{\rm o}(+z)$ and $\varphi_{\rm o}(-z)$, respectively. By the perturbing potential $U(z)$, the degenerate level $\varepsilon_{\rm o}$ is split into two energies, corresponding to symmetric and antisymmetric combinations of these wave functions. Namely, marked by suffixes $+$ and $-$, we have

$$\psi_+ = \frac{\varphi_{\rm o}(+z) + \varphi_{\rm o}(-z)}{\sqrt{2}} \quad \text{and} \quad \psi_- = \frac{\varphi_{\rm o}(+z) - \varphi_{\rm o}(-z)}{\sqrt{2}},$$

which are normalized as

$$\psi_+^*\psi_+ + \psi_-^*\psi_- = \varphi_{\rm o}^*(+z)\varphi_{\rm o}(+z) + \varphi_0^*(-z)\varphi_{\rm o}(-z) = 1.$$

Here, the terms $\varphi_{\rm o}^*(+z)\varphi_{\rm o}(+z)$ and $\varphi_{\rm o}^*(-z)\varphi_{\rm o}(-z)$ represent the probabilities $p_n(+z)$ and $p_n(-z)$ for the particle to be at $+z$ and $-z$, respectively, so that $p_n(+z) + p_n(-z) = 1$.

The perturbed Hamiltonian can then be expressed by

$$\mathcal{H} = \varepsilon_+\psi_+^*\psi_+ + \varepsilon_-\psi_-^*\psi_- = \varepsilon_{\rm o}(\psi_+^*\psi_+ + \psi_-^*\psi_-) - \frac{U(0)}{2}(\psi_+^*\psi_+ - \psi_-^*\psi_-),$$

hence $\varepsilon_\pm = \varepsilon_{\rm o} \pm U(0)/2$ and $\varepsilon_+ - \varepsilon_- = U(0)$. Therefore, we can define

$$\sigma_z = \psi_+^*\psi_+ - \psi_-^*\psi_- = p_n(+z) - p_n(-z), \tag{5.6a}$$

to express the z-component of a vector $\boldsymbol{\sigma}_n$. For the transverse components of $\boldsymbol{\sigma}_n$, we consider

$$\sigma_x = \varphi_{\rm o}^*(+z)\varphi_{\rm o}(-z) + \varphi_{\rm o}^*(-z)\varphi_{\rm o}(+z) \tag{5.6b}$$

and

$$\sigma_y = \varphi_o^*(+z)\varphi_o(-z) - \varphi_o^*(-z)\varphi_o(+z), \tag{5.6c}$$

then we can show the commutation relations

$$[\sigma_x, \sigma_y] = i\sigma_z, \quad [\sigma_y, \sigma_z] = i\sigma_x, \quad \text{and} \quad [\sigma_z, \sigma_x] = i\sigma_y. \tag{5.6d}$$

These are required relations for $(\sigma_x, \sigma_y, \sigma_z)$ to constitute a quantum-mechanical vector $\boldsymbol{\sigma}_n$.

5.3 Pseudospin Correlations

Correlations between pseudospins in a crystal are signified by the distance between right and left wells, or left and right, of adjacent pseudospins. Considering two pseudospins at adjacent sites n and $n+1$, the correlation energy can be written as

$$\mathcal{H}_{n,n+1} = \sum_{\alpha\beta;\gamma\delta} (\psi^*_{n,\alpha}\psi_{n,\beta} V_{\alpha\beta;\gamma\delta} \psi^*_{n+1,\gamma}\psi_{n+1,\delta}), \tag{5.7}$$

where $V_{\alpha\beta;\gamma\delta}$ are interaction tensor elements between the density matrices $(\psi^*_{n\alpha}\psi_{n\beta})$ and $(\psi^*_{n+1,\alpha}\psi_{n+1,\beta})$. The indexes α, β, γ, and δ represent either $+$ or $-$ at each of the sites n and $n+1$ in the chain. The interaction elements $V_{\alpha\beta;\gamma\delta}$ can be signified by symmetry as

$$V_{++--} = V_{--++},\ V_{+-+-} = V_{-+-+} = V_{-++-},\ \text{etc.}$$

for which the density elements can be expressed explicitly as

$$\begin{aligned}\psi^*_{n+}\psi_{n+} = \tfrac{1}{2}\{&\varphi_o^*(+z)\varphi_o(+z) + \varphi_o^*(-z)\varphi_o(-z) + \varphi_o^*(+z)\varphi_o(-z)\\ &+\varphi_o^*(-z)\varphi_o(+z)\} = \tfrac{1}{2}(1+\sigma_{nz}),\end{aligned}$$

$$\begin{aligned}\psi^*_{n+}\psi_{n-} = \tfrac{1}{2}\{&\varphi_o^*(+z)\varphi_o(+z) - \varphi_o^*(-z)\varphi_o(-z) - \varphi_o^*(+z)\varphi_o(-z)\\ &+\varphi_o^*(-z)\varphi_o(+z)\} = \tfrac{1}{2}(\sigma_{nx} - \sigma_{ny}),\end{aligned}$$

etc., and also similar expressions for $\psi^*_{n+1,+}\psi_{n+1,+}$, $\psi^*_{n+1,+}\psi_{n+1,-}$, etc.

Therefore $\mathcal{H}_{n,n+1}$ can be written in terms of components of pseudospins $\boldsymbol{\sigma}_n$ and $\boldsymbol{\sigma}_{n+1}$ as

$$\mathcal{H}_{n,n+1} = -J_{n,n+1}\sigma_{n,z}\sigma_{n+1,z} - K_{n,n+1}\sigma_{n,x}\sigma_{n+1,x}, \tag{5.8}$$

where

$$J_{n,n+1} = 2V_{+-+-} \text{ and } K_{n.n+1} = 2V_{+-+-} - V_{++++} - V_{----}$$

The total Hamiltonian of two adjacent pseudospins can then be expressed as

$$\begin{aligned}\mathcal{H} &= \mathcal{H}_n + \mathcal{H}_{n+1} + \mathcal{H}_{n,n+1} \\ &= \varepsilon_o - \frac{U}{2}(\sigma_{n,z} + \sigma_{n+1,z}) - J_{n,n+1}\sigma_{n,z}\sigma_{n+1,z} - K_{n,n+1}\sigma_{n,x}\sigma_{n+1,x}.\end{aligned} \tag{5.9}$$

The second term on the right-hand side is the average energy of pseudospins, as if the potential U were applied externally; the interaction energy between $\boldsymbol{\sigma}_n$ and $\boldsymbol{\sigma}_{n+1}$ is described by the parameters $J_{n,n+1}$ and $K_{n,n+1}$ in the third and fourth terms, respectively. Equation (5.9) is analogous to the classical correlations discussed in Sect. 4.1.

Nevertheless, for small ε_o and U at the threshold of a structural change, $\boldsymbol{\sigma}_n$ and $\boldsymbol{\sigma}_{n+1}$ are considered as classical vectors, as justified for perovkites in Sect. 5.1. In this case, we can assume that $V_{++++} = V_{----}$ by symmetry and obtain $J_{n,n+1} = K_{n,n+1}$. Therefore, the interaction terms in (5.9) can be given essentially in scalar product form as

$$\mathcal{H}_{n,n+1} = -J_{n,n+1}\boldsymbol{\sigma}_n \cdot \boldsymbol{\sigma}_{n+1}, \tag{5.10}$$

for correlation energies between classical vectors $\boldsymbol{\sigma}_n$ and $\boldsymbol{\sigma}_{n+1}$.

In a binary crystal for $T > T_c$, pseudospins are in harmonic motion in the lattice because $U = 0$, and hence we can assume $\langle p_n(+)\rangle_t = \langle p_n(-)\rangle_t$, the equal probability for $\pm\frac{1}{2}$ in random motion. On the other hand, if electrically dipolar pseudospins are in an applied field $\boldsymbol{E}$, we have to consider the potential $U = -e\langle\boldsymbol{\sigma}_n\rangle_t \cdot \mathbf{E}$. In this case, the thermal averages of $\langle p_n(\pm)\rangle_t$ at a temperature T are unequal and proportional to the Boltzmann factor $\exp\left(-\frac{\pm U}{k_B T}\right)$, and the order parameter is given by

$$\eta = \langle\sigma_{n,z}\rangle_t = \langle p_n(+z)\rangle_t - \langle p_n(-z)\rangle_t. \tag{5.11}$$

Nevertheless, signified by a change in lattice symmetry, the structural change can be attributed to *displacive* vectors in finite magnitude, as exemplified by typical structural changes in perovskites. We consider that a center potential $U(z_n)$ emerges at the critical temperature T_c from the deformed structure, as discussed in Chap. 3 with the Born–Huang principle.

5.4 Condensates

Order variables $\boldsymbol{\sigma}_n$ for a spontaneous structural change are classical vectors, for which an adiabatic potential U_n is responsible. Consequently, the lattice points should be displaced by $\boldsymbol{u}_n$ from original sites by the force $-\boldsymbol{\nabla}U_n$, counteracting against the force $\boldsymbol{\nabla}U_n$ on $\boldsymbol{\sigma}_n$ in the center-of-mass coordinate system, as implied by

Newton's action–reaction principle. Thus, classical displacements $(\boldsymbol{\sigma}_n, \boldsymbol{u}_n)$ should always take place together during a structural change, for which a periodic potential $\sum_n U_n$ is responsible. Such a pair of displacements shall be called the *condensate* hereafter by analogy with a condensing gas.

These $\boldsymbol{\sigma}_n$ and $\boldsymbol{u}_n$ should be in phase, as expanded in Fourier series. Therefore, the former can be expressed as

$$\boldsymbol{\sigma}_n = \sum_n \boldsymbol{\sigma}_k \exp \mathrm{i}(\boldsymbol{k} \cdot \boldsymbol{r}_n - \omega t_n), \tag{5.12}$$

representing a wave packet defined by the summation over possible values of $\boldsymbol{k}$. By virtue of space-reversal symmetry, (5.12) should be invariant for inversion $\boldsymbol{r}_n \to -\boldsymbol{r}_n$; hence, we can consider $\boldsymbol{\sigma}_k$ is invariant for $\boldsymbol{k} \to -\boldsymbol{k}$ equivalently. On the other hand, time-reversal symmetry must be omitted in all thermal applications. For the summation in (5.12), we can therefore consider only $\pm\,\boldsymbol{k}$ and $t_n > 0$. In a crystal in finite size, these waves should therefore be observed as standing, which are expressed by their phases $\phi_\pm = \pm\boldsymbol{k} \cdot \boldsymbol{r}_n - \omega t_n$ that is *pinned* as $\phi_\pm(\boldsymbol{r}_n) = 0$ at $(\boldsymbol{r}_n, 0)$. We can therefore deal with pseudospin waves that are always pinned at $\phi = 0$, regardless of the position and time. Thus, we obtain the relation

$$\boldsymbol{\sigma}_k = -\boldsymbol{\sigma}_{-k}.$$

In this context, (5.12) can be written as

$$\boldsymbol{\sigma}_n = \boldsymbol{\sigma}_{+k} \exp \mathrm{i}(\boldsymbol{k} \cdot \boldsymbol{r}_n - \omega t_n) + \sigma_{-k} \exp \mathrm{i}(-\boldsymbol{k} \cdot \boldsymbol{r}_n + \omega t_n), \tag{5.13a}$$

where

$$\boldsymbol{\sigma}_{\pm k} = \sum_n \boldsymbol{\sigma}_n \exp \mathrm{i}(\mp\boldsymbol{k} \cdot \boldsymbol{r}_n \pm \omega t_n). \tag{5.13b}$$

It is noted that the phase variable $\phi_n = \boldsymbol{k} \cdot \boldsymbol{r}_n - \omega t_n$ at arbitrary $(\boldsymbol{r}_n, t_n)$ is essential for $\boldsymbol{\sigma}_n$, which is invariant in phase reversal $\phi_n \to -\phi_n$.

Physically, it is significant that the lattice is strained by the displacements $\boldsymbol{\sigma}_n$ and the corresponding $\boldsymbol{u}_n$. For strained crystals, Born and Huang [2] have proposed that the strain energy should be minimized for stability. Hereafter, this proposal is called the *Born–Huang principle*. Although difficult to express it explicitly, we may assume that the combined local displacement as $a\boldsymbol{\sigma}_n + b\boldsymbol{u}_n$, with constants a and b, is responsible for strained structure of a crystal. The strain energy can then be expressed as proportional to

$$\begin{aligned} &\sum_{n,n'} (a\boldsymbol{\sigma}_n + b\boldsymbol{u}_n)^* (a\boldsymbol{\sigma}_{n'} + b\boldsymbol{u}_{n'}) \\ &\quad = \sum_{n,n'} aa^* \boldsymbol{\sigma}_n \cdot \boldsymbol{\sigma}^*_{n'} + \sum_{n,n'} bb^* \boldsymbol{u}_n \cdot \boldsymbol{u}^*_{n'} + \sum_{n,n'} (a_n b^*_{n'} \boldsymbol{\sigma}_n \cdot \boldsymbol{u}^*_{n'} + b_n a_{n'} \boldsymbol{u}_n \cdot \boldsymbol{\sigma}^*_{n'}). \end{aligned} \tag{5.14}$$

This can be minimized for strain-free equilibrium, for which all variables at sites n and n' in these products are necessarily *in phase*.

Noted that these variables characterized by phases $\phi_n = \boldsymbol{k} \cdot \boldsymbol{r}_n - \omega t_n$ are generally *incoherent*, for which the Born-Huang principle suggests that a *thermal phasing process* forced by the periodic potential $\sum_n U_n$ can take place to make them *coherent* for minimal strains. Namely, we can write

$$\frac{\mathrm{d}}{\mathrm{d}t}(\boldsymbol{\sigma}_n - \boldsymbol{\sigma}_\mathrm{o}) = -\frac{\boldsymbol{\sigma}_n - \boldsymbol{\sigma}_\mathrm{o}}{\tau}, \tag{5.15}$$

where τ is a time constant. By this process, random phases of $\boldsymbol{\sigma}_n$ become in phase, as expressed by $\boldsymbol{\sigma}_\mathrm{o}$, thereby making the crystal strain-free. While consistent with Born–Huang's proposal, such a phasing process is postulated for a condensate to stabilize the lattice.

Further, we postulate that these $\boldsymbol{\sigma}_n$ at nearest-neighbor sites n and n' become coherent, forming *clustered* pseudospins in phase. Such a cluster can be considered as a *seed* for the condensate to grow larger with increasing range of correlations. It is considered that the strain energy can be lowered by clustering, where the discontinuity in the corresponding internal energy is responsible for a sharp rise in the specific heat $C_p - T$ curve at T_c, as shown in Fig. 5.2. In contrast, a gradual tale in the curve between T_c^* and T_c can be attributed to another phasing process, which together can be considered as a precursor of the transition.

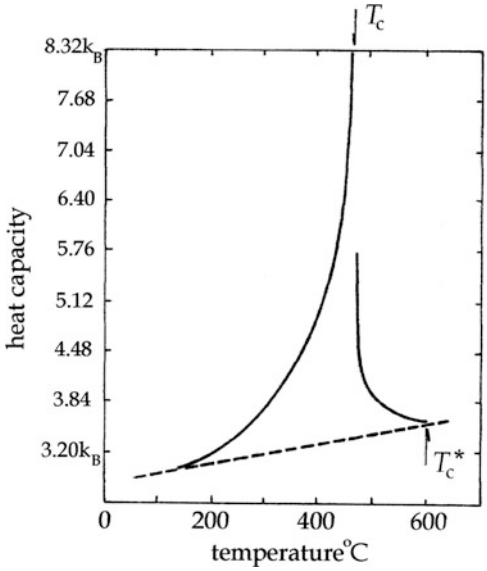

Fig. 5.2 An example of a transition anomaly from β-brass, which are characterized by a sharp rise at T_c, a narrow starting range from the threshold T_c^* and a gradual tail after the transition (from [13]).

Following (5.10), for classical pseudospins, the correlation energy is expressed as

$$\mathcal{H}_n = -\sum_m J_{mn}\boldsymbol{\sigma}_m \cdot \boldsymbol{\sigma}_n, \tag{5.16}$$

where the index m refers generally to interacting sites with $\boldsymbol{\sigma}_n$. In (5.16), the distance of correlations is unspecified, but normally limited to the nearest and next-nearest neighbors.

Setting fluctuations aside, we assume that pseudospins in a cluster become all in phase at temperatures below T_c. For clustered pseudospins, we write $\boldsymbol{\sigma}_m = \sigma_o \boldsymbol{e}_m$ and $\boldsymbol{\sigma}_n = \sigma_o \boldsymbol{e}_n$, where σ_o is the amplitude, and $\boldsymbol{e}_m$ and $\boldsymbol{e}_n$ are unit vectors. Figure 5.3 sketches clustered pseudospins in a perovskite crystal. With respect to the center of TiO_6^{2-} ion, the short-range correlations with the nearest and next-nearest neighbors are indicated by J and J', respectively, in the bc-plane. Assuming that σ_o is constant, these unit vectors can be expressed as

$$\boldsymbol{e}_m = \boldsymbol{e}_{+q} \exp \mathrm{i}(\boldsymbol{q} \cdot \boldsymbol{r}_m - \omega t_m) + \boldsymbol{e}_{-q} \exp \mathrm{i}(-\boldsymbol{q} \cdot \boldsymbol{r}_m + \omega t_m)$$

and

$$\boldsymbol{e}_n = \boldsymbol{e}_{+q} \exp \mathrm{i}(\boldsymbol{q} \cdot \boldsymbol{r}_n - \omega t_n) + \boldsymbol{e}_{-q} \exp \mathrm{i}(-\boldsymbol{q} \cdot \boldsymbol{r}_n + \omega t_n).$$

The short-range correlation energy (5.16) can then be expressed as

$$\mathcal{H}_n = -\sum_m 2\sigma_o^2 \boldsymbol{e}_{+q} \cdot \boldsymbol{e}_{-q} \exp \mathrm{i}q \cdot (\boldsymbol{r}_m - \boldsymbol{r}_n) \exp \mathrm{i}\omega(t_n - t_m).$$

In practice, the time average $\langle \mathcal{H}_n \rangle_t = \frac{1}{2t_o} \int_{-t_o}^{+t_o} \mathcal{H}_n \mathrm{d}(t_n - t_m)$ over the timescale of observation t_o is a measurable quantity, which can be written as

$$\langle \mathcal{H}_n \rangle_t = -\sigma_o^2 \Gamma_t \boldsymbol{e}_{+q} \cdot \boldsymbol{e}_{-q} \sum_{m,n} J_{mn} \exp \mathrm{i}\boldsymbol{q} \cdot (\boldsymbol{r}_m - \boldsymbol{r}_n), \tag{5.17}$$

where

$$\Gamma_t = \frac{1}{2t_o} \int_{-t_o}^{+t_o} \exp\{-\mathrm{i}(t_m - t_n)\} \mathrm{d}(t_m - t_n) = \frac{\sin \omega t_o}{\omega t_o}$$

is the time correlation function with a value close to 1, if $\omega t_o < 1$. Equation (5.17) can be re-expressed as

$$\langle \mathcal{H}_n \rangle_t = -\sigma_o^2 \Gamma_t \boldsymbol{e}_{+q} \cdot \boldsymbol{e}_{-q} J_n(\boldsymbol{q}), \tag{5.18a}$$

where

$$J_n(\boldsymbol{q}) = \sum_m J_{mn} \exp \mathrm{i}\boldsymbol{q} \cdot (\boldsymbol{r}_m - \boldsymbol{r}_n). \tag{5.18b}$$

$\langle \mathcal{H}_n \rangle_t$ in (5.18a) can be minimized, if a specific wave vector $\boldsymbol{q} = \boldsymbol{k}$ can be found to satisfy the equation:

$$\boldsymbol{\nabla}_q J_n(\boldsymbol{q}) = 0. \tag{5.18c}$$

Depending on the values of J_{mn}, such a wave vector $\boldsymbol{k}$ can specify the direction for the cluster to grow, as will be shown by the examples in the next section.

Although expressed in complex form for mathematical convenience, $\boldsymbol{\sigma}_n$ is in fact real, so that the Fourier transform should have a relation $\boldsymbol{\sigma}^*_{+q} = \boldsymbol{\sigma}_{-q}$, and hence for unit vectors

$$\boldsymbol{e}^*_{+q} = \boldsymbol{e}_{-q}. \tag{i}$$

Accordingly, the normalization condition in the reciprocal space can be written as

$$N = \boldsymbol{e}^*_{+q} \cdot \boldsymbol{e}_{+q} + \boldsymbol{e}^*_{-q} \cdot \boldsymbol{e}_{-q} = 2\boldsymbol{e}_{+q} \cdot \boldsymbol{e}_{-q}. \tag{ii}$$

On the other hand, the vectors $\boldsymbol{e}_n$ are also normalized in the crystal space; we have another equation for normalization, that is,

$$N = \sum_n \boldsymbol{e}^*_n \cdot \boldsymbol{e}_n = 2\boldsymbol{e}_{+q} \cdot \boldsymbol{e}_{-q} + \boldsymbol{e}^2_{+q} \exp(2\mathrm{i}\boldsymbol{q} \cdot \boldsymbol{r}_n) + \boldsymbol{e}^2_{-q} \exp(-2\mathrm{i}\boldsymbol{q} \cdot \boldsymbol{r}_n). \tag{ii'}$$

Equations (ii) and (ii′) should be identical regardless of n, for which either

$$\exp(2\mathrm{i}\boldsymbol{q} \cdot \boldsymbol{r}_n) = \exp(-2\mathrm{i}\boldsymbol{q} \cdot \boldsymbol{r}_n) = 0 \tag{iii}$$

or

$$\boldsymbol{e}^2_{+q} = \boldsymbol{e}^2_{-q} = 0 \tag{iv}$$

need to be satisfied. If (iii) is independent of n, we have either $\boldsymbol{q} = 0$ or $\boldsymbol{G}/2$, corresponding to *ferrodistortive* or *antiferrodistortive* arrangements of $\boldsymbol{\sigma}_n$ along these directions of $\boldsymbol{k}$, whereas (iv) indicates that $(e_q)^2_x + (e_q)^2_y + (e_q)^2_z = 0$, for which values of the vector $\boldsymbol{q}$ can be arbitrary, independent of the lattice periodicity. If taking $\left(e_{q_x}\right)^2 = 1$, for example, we have $\left(e_{q_y}\right)^2 + \left(e_{q_z}\right)^2 = -1$, and hence $e_{q_x} = \exp \mathrm{i}\varphi$ and $e_{q_y} \pm \mathrm{i}e_{q_z} = \mathrm{i} \exp \mathrm{i}\varphi$, where $\varphi = qx + \text{constant}$ can be obtained for an arbitrary angle φ. Such arrangements of classical pseudospins $\boldsymbol{\sigma}_n$ along the specific $\boldsymbol{k}$ are called *incommensurate* with respect to the periodic lattice. In these

cases, the discrete phase $\phi_n = \boldsymbol{q} \cdot \boldsymbol{r}_n - \omega t_n$ is practically a continuous angle in the region $0 \leq \phi_n \leq 2\pi$; hence, these discrete angles ϕ_n can be replaced by a continuous angle ϕ in the same region $0 \leq \phi \leq 2\pi$.

5.5 Examples of Pseudospin Clusters

Calculating short-range correlations by (5.18a)–(5.18c) is a familiar method for magnetic crystals, resulting in magnetic spin arrangements of various types [8]. Using (5.18a)–(5.18c), symmetry changes in structural transformations can be interpreted similarly. In this section, examples are shown for some representative systems.

5.5.1 Cubic-to-Tetragonal Transition in $SrTiO_3$

Figure 5.3 shows a structural view of a $SrTiO_3$ crystal, illustrating short-range correlations in the vicinity of TiO_6^{2-} at the center. In the cubic phase, three lattice constants along the symmetry axes are denoted by a, b, and c for mathematical convenience, and correlation strengths J_{mn} with the nearest and next-nearest neighbors expressed by J and J', respectively. In this model of a pseudospin cluster, the correlation energy can be calculated by (5.18a), where the parameter $J_n(\boldsymbol{q})$ determined by (5.18b) is expressed as

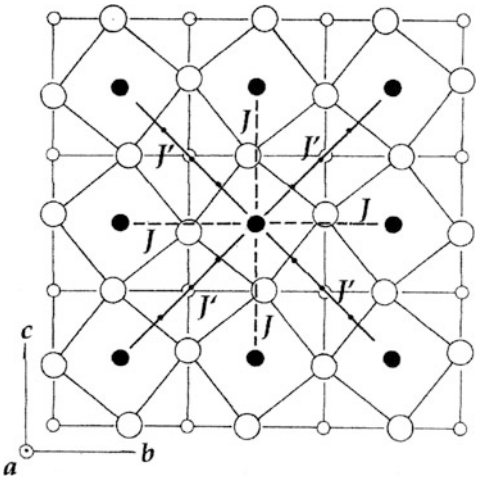

Fig. 5.3 Model of the short-range cluster in perovskites. Interactions J and J' are assigned for 6 nearest and 12 next-nearest neighbors, respectively.

$$J(\boldsymbol{q}) = 2J\{\cos(q_a a) + \cos(q_b b) + \cos(q_c c)\} + 4J'\{\cos(q_b b)\cos(q_c c) + \cos(q_c c)\cos(q_a a) + \cos(q_a a)\cos(q_b b)\},$$

where the index n is omitted. Using this expression in (5.18c), we can obtain the specific wave vector $\boldsymbol{q} = \boldsymbol{k}$ by solving the equations

$$\begin{aligned} &\sin(k_a a)\{J + 2J'\cos(k_b b) + 2J'\cos(k_c c)\} = 0, \\ &\sin(k_b b)\{J + 2J'\cos(k_c c) + 2J'\cos(k_a a)\} = 0, \\ &\sin(k_c c)\{J + 2J'\cos(k_a a) + 2J'\cos(k_b b)\} = 0, \end{aligned} \tag{i}$$

for $\boldsymbol{k} = (k_a, k_b, k_c)$.

It is found that either one of the following wave vectors can satisfy (i). Namely: $\boldsymbol{k}_1 = (k_{1a}, k_{1b}, k_{1c})$ for

$$\sin(k_{1a}a) = \sin(k_{1b}b) = \sin(k_{1c}c) = 0. \tag{ii}$$

$\boldsymbol{k}_2 = (k_{2a}, k_{2b}, k_{2c})$ for

$$\begin{aligned} &\sin(k_{2a}a) = 0, \quad \cos(k_{2b}b) = \cos(k_{2c}c) = -1 + \tfrac{J}{2J'}; \\ &\sin(k_{2b}b) = 0, \quad \cos(k_{2c}c) = \cos(k_{2a}a) = -1 + \tfrac{J}{2J'}; \\ &\sin(k_{2c}c) = 0, \quad \cos(k_{2a}a) = \cos(k_{2b}b) = -1 + \tfrac{J}{2J'}. \end{aligned} \tag{iii}$$

And, $\boldsymbol{k}_3 = (k_{3a}, k_{3b}, k_{3c})$ for

$$\begin{aligned} &\cos(k_{3a}a) = 0, \quad \cos(k_{3b}b) = \cos(k_{3c}c) = -\tfrac{J}{2J'}; \\ &\cos(k_{3b}b) = 0, \quad \cos(k_{3c}c) = \cos(k_{3a}a) = -\tfrac{J}{2J'}; \\ &\cos(k_{3c}c) = 0, \quad \cos(k_{3a}a) = \cos(k_{3b}b) = -\tfrac{J}{2J'}. \end{aligned} \tag{iv}$$

Solution (ii) gives a wave vector $\boldsymbol{k}_1 = \left(\frac{\pi l}{a}, \frac{\pi m}{b}, \frac{\pi n}{c}\right)$, where l, m, and n are 0 or $\pm$ integers, which gives commensurate arrangements with $J(\boldsymbol{k}_1) = 6J + 12J'$ due to 6 nearest and 12 next-nearest neighbors in the cluster. On the other hand, for $\boldsymbol{k}_2$, a component k_{2a} is commensurate along the a-axis, whereas the other k_{2b} and k_{2c} are incommensurate along the b and c axes in two dimensions, provided that $|1 - (J/2J')| \leq 1$. Solution (iii) shows a similar two-dimensional incommensurability in the ca- and ab-planes.

Solution (iv) provides a similar result to (iii); the first set gives an incommensurate arrangement in the bc-plane, if $|J/2J'| \leq 1$, and commensurate along the a-axis, and so on.

Applying these results to $SrTiO_3$, it is clear that a tetragonal phase below T_c occurs at a Brillouin zone-boundary incommensurate in two dimensions, which is actually confirmed by the neutron inelastic scattering experiments, showing a dip in the phonon energy at about $T_c \approx 130\,\mathrm{K}$. As shown in Fig. 5.4, the lowest dip appeared at $q/b^* = \frac{1}{2} + \delta_b$, where the shift δ_b was attributed to a perturbation at

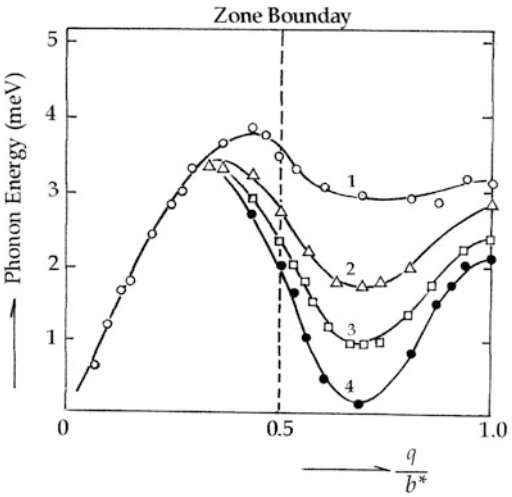

Fig. 5.4 Phonon dispersion curves in K_2SeO_4 near the Brillouin zone boundary obtained by neutron inelastic scatterings. Curves 1, 2, 3, and 4 were determined at 250, 175, 145, and 130 K, respectively (from [14]).

the zone boundary. However, in the magnetic resonance experiment by Müller et al. [9], the incommensurate wave vector can be expressed as

$$k_a = l\left(\frac{1}{2} - \delta_a\right)a^* \quad \text{and} \quad k_c = n\left(\frac{1}{2} - \delta_c\right)c^*,$$

in the *ac*-plane, where a^* and c^* are reciprocal lattice constants. Small shifts δ_a, δ_b, and δ_c are *incommensurate parameters*, arising from perturbations at the zone boundary. It is noted that the foregoing argument is only mathematical, due to unknown J and J'. However, the calculation predicts at least the symmetry properties of condensates in perovskites.

5.5.2 *Monoclinic Crystals of Tris-Sarcosine Calcium Chloride*

Tris-sarcosine calcium chloride (TSCC), where *sarcosine* is an *amino acid* $H_3C - NH_2 - CO_2H$, can crystallize in *twin* from aqueous solutions at room temperature. A single-domain crystal is optically uniform, and obtained by cutting a naturally grown crystal, which is spontaneously strained along the *a*-axis and slightly monoclinic along the *b*-direction. The molecular arrangement is sketched in Fig. 3.4a. We already discussed the pseudospin model with Fig. 3.4b, where a Ca^{2+} ion is surrounded octahedrally by six O^- of carboxyl ions $-CO_2H$ of sarcosine molecules. In Fig. 5.5a shown is a model for a pseudospin cluster in TSCC, which is composed of pseudospins in nearest-neighbor distances on the *a*, *b*, and *c* axes as well as in the diagonal directions in the *bc*-plane.

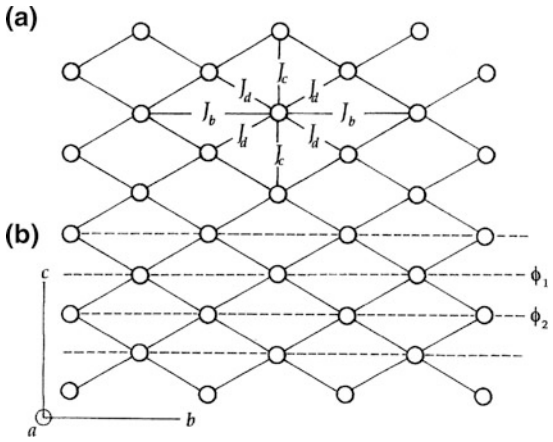

Fig. 5.5 Pseudospin lattice in a crystal of TSCC. (**a**) A pseudospin cluster in the *bc*-plane. (**b**) Parallel pseudospin chains shown by *broken lines*. The adjacent chains are characterized by different phases $0<\phi_1, \phi_2<2\pi$.

Denoting these correlation parameters by J_a, J_b, J_c, and J_d, (5.18b) can be written as

$$J(\boldsymbol{q}) = 2J_a(q_a a) + 2J_b\cos(q_b b) + 2J_c\cos(q_c c) + 4J_d\cos\frac{q_b b}{2}\cos\frac{q_c c}{2}.$$

From (5.18c) applied to this $J(\boldsymbol{q})$, we can determine the wave vector $\boldsymbol{k}$ for minimal strains. By similar calculation to perovskites in Sect. 5.5.1, the following specific $\boldsymbol{k}$-vectors can be considered for cluster energies. That is,

$$\boldsymbol{k}_1 = \left(\frac{\pi l}{a}, \frac{\pi m}{b}, \frac{\pi n}{c}\right);$$

and

$$\boldsymbol{k}_2 = \left(\frac{\pi l}{a}, k_{2b}, \frac{\pi n}{c}\right) \quad \text{where} \quad \cos\frac{k_{2b}b}{2} = -\frac{J_d}{2J_b};$$

$$\boldsymbol{k}_3 = \left(\frac{\pi l}{a}, \frac{\pi m}{b}, k_{3c}\right) \quad \text{where} \quad \cos\frac{k_{3c}c}{2} = -\frac{J_d}{2J_c}.$$

Here, l, m, and n are zero or integers. Among these, $\boldsymbol{k}_1$ is a commensurate vector with the lattice, for which we have $J(\boldsymbol{k}_1) = 2J_a + 2J_b + 2J_c$.

In contrast, $\boldsymbol{k}_2$ and $\boldsymbol{k}_3$ are incommensurate vectors on the b and c axes, provided that $|J_d/2J_b| \leq 1$ and $|J_d/2J_c| \leq 1$, respectively. The thermodynamic phase of a TSCC crystal below 120 K is known as ferroelectric and characterized by spontaneous polarization along the b-axis, for which the vector $\boldsymbol{k}_2$ is therefore considered as responsible. For $\boldsymbol{q} = \boldsymbol{k}_2$, we have

$$J(\boldsymbol{k}_2) = 2J_a + 2J_b + 2J_c - \frac{2J_d^2}{J_b} = 2J_a + 2J_c + 2J_b\left(1 - \frac{J_d^2}{J_b^2}\right);$$

this should be positive for stable arrangement. If $J_d = 0$, we have $J(\boldsymbol{k}_2) = \quad J(\boldsymbol{k}_1)$. On the other hand, for $J_d = -2J_b$, we have $J(\boldsymbol{k}_2) = 2J_a - 6J_b + 2J_c < J(\boldsymbol{k}_1)$, which gives a lower correlation energy than the commensurate phase of $\boldsymbol{k}_1$. Writing $\varphi = k_b b/2$ in $\cos\frac{k_b b}{2} = -J_d/2J_b$, the above $J(\boldsymbol{k}_2)$ can be re-expressed as

$$J(\boldsymbol{k}_2) = 2J_a + 2J_c + 2J_b \cos 2\varphi + 4J_d \cos\varphi. \tag{5.19}$$

This is a well-known formula in the theory of magnetism for a spiral arrangement of spins in one dimension [10].

In TSCC crystals, interactions between adjacent pseudospin chains are significant for longitudinal propagation along the b-axis, as shown in Fig. 5.5b, whereas the correlations between chains 1 and 2 appear to be responsible for transverse motion. For a similar situation in charge–density–wave systems, Rice [11] suggested such an interchain potential as $J_d \propto \cos(\phi_1 - \phi_2)$, where two chains are signified by phases ϕ_1 and ϕ_2, as illustrated in Fig. 5.5b, c. In this model, $J_d \to 0$, if assuming $\Delta\phi = \phi_1 - \phi_2 \to 0$; such a phasing mechanism leads all chains in parallel to the b-axis to a domain wall on the ac-plane.

Exercises 5

1. Order variables $\boldsymbol{\sigma}_n$ located at lattice sites n are subjects of practical observation such as X-ray diffraction. Collisions between $\boldsymbol{\sigma}_n$ and X-ray photons occur at space–time coordinates (x_n, t_n), which are distributed in the target area of a collimated X-ray beam. Therefore, we have randomly distributed phases in the diffracted beam, which can be recognized as uncertainties. Landau's criterion (5.5) is clearly concerned about such uncertainties. Review his argument, referring to the quantum-mechanical uncertainty principle. Also, why the energy uncertainty can be justified with the equipartition theorem of statistical mechanics?

2. Why should we consider a group of ordered pseudospins as the cluster at the threshold of a structural change? Is it consistent with the Born–Huang principle? Discuss this question in qualitative manner.

3. Clustering with short-range correlations discussed in Sect. 5.4 can be characterized as phasing of pseudospins for collective motion. Justify this phasing process in terms of the Born–Huang principle. Can the process be considered as isothermal in thermodynamic environment? *Hint*: See if phonon scatterings can be inelastic, when two phonons are considered as interacting with correlated pseudospins as $\boldsymbol{\sigma}_n \cdot \boldsymbol{\sigma}_{n'}$.

4. In a perovskite crystal, either of conditions (iii) and (iv) in Sect. 5.5.1 was considered for two-dimensional order, which was actually substantiated experimentally. Discuss the theoretical reason for supporting two-dimensional order.

Chapter 6
Critical Fluctuations

Landau (1937) showed a simplified approach to the order–disorder problem. While the underlying assumptions need to be revised for dynamical aspects of ordering, adiabatic fluctuations arising from correlations cannot be discussed with his abstract theory. If incorporated with the condensate model however, the theory becomes acceptable beyond mean-field accuracy. In this chapter, considering Landau's argument as prerequisite to refined theories, critical fluctuations in correlated pseudospins are discussed for binary systems. Also here, *pinning* of collective pseudospin modes is discussed, which is normally *extrinsic* in character, but can be *intrinsic* as well, considering pseudospin correlations. In a pinning potential field, the pseudospin mode is in standing waves in the crystal space, which are detectable in practical experiments.

6.1 The Landau Theory of Binary Transitions

For a crystal exhibiting binary order, Landau [6] proposed a theory of a second-order phase transition, using the Gibbs potential defined as a function of the order parameter η. The parameter η varies between 0 and 1, representing disordered and ordered states, respectively. Landau's order parameter is a continuous function of temperature under a constant p, signifying the mean-field average of distributed variables σ_n over the entire lattice sites n; hence, his theory is valid in the mean-field accuracy. We note that the transition temperature T_o in this approximation is always higher than the observed temperature T_c, indicating a significant discrepancy from the mean-field theory.

The Gibbs potential below T_o is assumed to be given by a power expansion of η, that is,

$$G(\eta) = G(0) + \frac{1}{2}A\eta^2 + \frac{1}{4}B\eta^4 + \frac{1}{6}C\eta^6 + \ldots, \tag{6.1}$$

M. Fujimoto, *Thermodynamics of Crystalline States*,
DOI 10.1007/978-1-4419-6688-9_6,

where $G(0)$ represents the value for $\eta = 0$. Higher-order terms in (6.1) imply the significance of η in finite magnitude. Terms of higher-than-second power in this expansion are responsible for nonlinear ordering, modulating the lattice as anharmonic; however, the lattice is disregarded in Landau's theory. In (6.1), odd-power terms are excluded for a binary system that is characterized by *inversion symmetry*, $\eta \leftrightarrow -\eta$. Therefore, we have the relation

$$G(\eta) = G(-\eta). \tag{6.2}$$

This hypothesis is also essential for order variables to be a displacement vector in the lattice structure. Although Landau considered η as a scalar quantity, η can generally be a vector.

In equilibrium, the function $G(\eta)$ should take a minimal value at $\eta = \eta_o$, around which an arbitrary variation $\Delta\eta = \eta - \eta_o$ may be considered mathematically. We can therefore assume a change

$$\Delta G = G(\eta) - G(\eta_o) \geq 0.$$

The value of η_o can therefore be determined from $(\partial \Delta G/\partial \eta)_{p.T} = 0$. For a small $|\eta|$ in the vicinity of T_o, (6.1) can be *truncated* at the fourth-order term η^4 in sufficient accuracy, that is,

$$\Delta G(\eta) = \frac{1}{2}A\eta^2 + \frac{1}{4}B\eta^4.$$

Differentiating this with respect to η, we obtain the equation $A\eta_o + B\eta_o^3 = 0$. Therefore, the equilibrium can be determined by either

$$\eta_o = 0 \quad \text{or} \quad \eta_o^2 = -\frac{A}{B}. \tag{6.3a}$$

In the former, $\eta_o = 0$ represents the disordered state. For the latter, Landau postulated that the factor A is temperature dependent and expressed as

$$A = A'(T - T_o) \quad \text{for} \quad T > T_o \tag{6.4a}$$

and

$$A = A'(T_o - T) \quad \text{for} \quad T > T_o, \tag{6.4b}$$

where A' is a positive constant; B is assumed as a positive temperature-independent constant. Using (6.4b), the second solution $\eta_o^2 = -A/B$ in (6.3a) can be written as

$$\eta_o^2 = \frac{A'}{B}(T_o - T) \quad \text{for} \quad T < T_o. \tag{6.3b}$$

In Landau's theory, the transition can be determined by the factor A reversing sign at $T = T_o$ and by a positive B that emerges at T_o, thereby shifting equilibrium from $\eta_o = 0$ to $\pm\eta_o = \pm\sqrt{A'/B(T_o - T)}$ with decreasing temperature. Thermal equilibrium is determined by

$$G(0) \quad \text{at} \quad \eta_o = 0 \quad \text{for} \quad T \geq T_o,$$

and

$$G(\eta_o) = G(0) - \frac{3A'^2}{4B} \quad \text{at} \quad \eta_o = \pm\sqrt{\frac{A'}{B}} \quad \text{for} \quad T < T_o.$$

Figure 6.1 shows schematically a change of the Gibbs potential with varying temperature. For $T > T_o$, $\eta_o = 0$ for equilibrium at all temperatures as shown by Fig. 6.1a. For $T < T_o$, $\eta_o = \pm\sqrt{A'/B(T_o - T)}$ from (6.3b), shifting equilibrium with a *parabolic* temperature dependence, and lowering the minimum by $-3A'^2/4B$, as illustrated in Figs. 6.1b, c. As illustrated in this figure, ordering starts at $T = T_o$ with lowering temperature; signs $\pm$ indicate two opposite domains.

So far, we discussed Landau's theory in the framework of equilibrium thermodynamics. The *variation* principle can be applied to minimize $G(\eta)$; however, the variation can physically arise from real fluctuations, which were not considered in the traditional thermodynamics. At the minimum of the Gibbs potential in Landau'

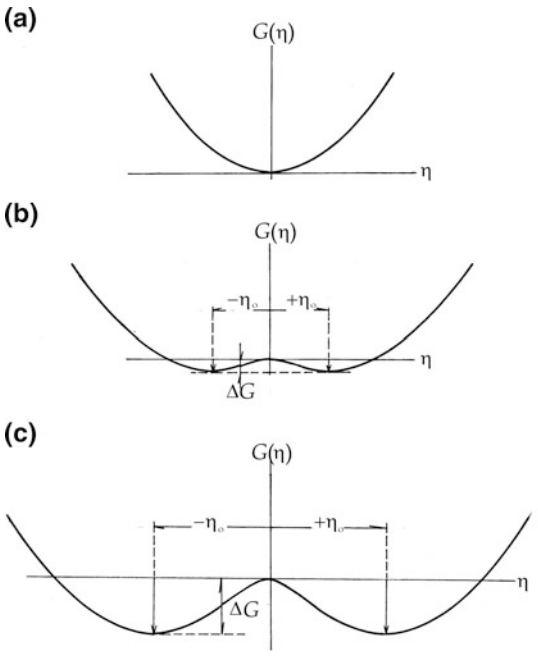

Fig. 6.1 Landau's quartic potentials. (**a**) $T = T_o$; (**b**) and (**c**) for $T < T_o$. Binary equilibrium is indicated by two-way shifts and increasing depths of minima with decreasing temperature.

theory, the variation $\eta - \eta_o$ at a constant p and T condition should be originated from an internal mechanism that may be expressed by expansion terms in (6.1). In the condensate model on the other hand, we consider adiabatic potentials ΔU_n at the lattice sites as related with η. In this context, Landau's expansion terms can be interpreted as

$$\Delta G = \frac{A}{2}\eta^2 + \frac{B}{4}\eta^4 + \ldots = \langle \Delta U_n \rangle = -\eta X_{\text{int}}, \tag{6.5}$$

where $X_{\text{int}} = -\partial\langle \Delta U_n \rangle / \partial\eta$ represents the internal field in the mean-field approximation. Such an internal field X_{int} is an adiabatic variable that can be considered as if applied externally, similar to Weiss' molecular field in magnetic crystals. As related in (6.5), these ΔG and $\Delta\eta$ can be regarded as internal fluctuations of G and η.

In dielectric or magnetic crystals, the order parameter η is associated with microscopic dipole or magnetic moments, respectively. Therefore, such η can respond to applied electric or magnetic fields. Denoting an external field as X, we can include an additional term $-\eta X$ in the Gibbs function. Assuming a small variation of η in the vicinity of T_o, we can write

$$\Delta G_> = \Delta G(\eta) - \eta X = \frac{1}{2}A\eta^2 - \eta X$$

for $T > T_o$, where the equilibrium can be determined from $(\partial G_> / \partial \eta)_{p,T} = 0$, that is, $A\eta - X = 0$, from which the *susceptibility* is expressed by

$$\chi_{T>T_o} = \frac{\eta_o}{X} = \frac{1}{A} = \frac{1}{A'(T - T_o)}, \tag{6.6a}$$

where $\eta_o = 0$ in equilibrium, and $A = A'(T - T_o)$ from (6.4a). The susceptibility (6.6a) indicates that the system can be ordered by X to such an extent as determined by the term of A in the Gibbs potential, even at temperatures above T_o.

For $T < T_o$, on the other hand, since $\Delta G(\eta)$ is contributed by $1/4B\eta^4$ as well, the equilibrium is determined by minimizing

$$\Delta G_< = \frac{1}{2}A\eta^2 + \frac{1}{4}B\eta^4 - \eta X,$$

and hence $A\eta_o + B\eta_o^3 - X = 0$, in which $\eta_o^2 = -A/B$ gives equilibrium at $T < T_o$. Accordingly, we have

$$\chi_{T<T_o} = \frac{\eta_o}{2A} = \frac{1}{2A'(T_o - T)}, \tag{6.6b}$$

where $A = A'(T_o - T)$ as assumed in (6.4b).

Both (6.6a) and (6.6b) are generally called Curie–Weiss' laws, indicating a singularity at T_o, where the approaching is characterized by constants $1/A'$ or

$1/2A'$ for $T > T_o$ or $T < T_o$, respectively. Of course, these expressions are meaningful only if the strength of an applied X is regarded as negligible.

6.2 Adiabatic Fluctuations

We assume that the Gibbs potential fluctuates with the order parameter under the critical condition, varying with an internal mechanism. With fluctuations of the order parameter, the volume of a crystal may not be constant, but change adiabatically under constant T. In a condensate, fluctuations are in *sinusoidal excitations* in random phase, hence diminishing in a *phasing* process. Therefore, such fluctuations in a crystal are quite different in character from thermal fluctuations in random type.

Corresponding to $\Delta G = (A'/2)(T_o - T)\eta^2 + (B/4)\eta^4$ for $T<T_o$, we can consider a change of the adiabatic potential in similar type, that is, $\Delta U_n=(1/2)a\boldsymbol{\sigma}_n^2+(1/4)b\boldsymbol{\sigma}_n^4$, at a temperature T_c^* close to T_c, representing the outset of phase fluctuations. Below T_c^*, we consider $a < 0$ and $b > 0$, indicating that the pseudospin vector $\boldsymbol{\sigma}_n$ behaves like a classical displacement, as discussed in Chap. 5. Due to the positive quartic term $(1/4)b\boldsymbol{\sigma}_n^4$, the equilibrium position of $\boldsymbol{\sigma}_n$ shifts closer to the neighboring pseudospin $\boldsymbol{\sigma}_m (m \neq n)$, so that their mutual correlations between them become appreciable. In this context, the potential ΔU_n is responsible for correlations at temperatures close to T_c^*. Therefore, it is reasonable to consider ΔU_n for the motion of $\boldsymbol{\sigma}_n$.

In the condensate model, the order variable $\boldsymbol{\sigma}_n$ can be expressed primarily as $\boldsymbol{\sigma}_n = \sum_k \boldsymbol{\sigma}_k \exp \mathrm{i}(\boldsymbol{k} \cdot \boldsymbol{r}_n - \omega t_n)$, where $\boldsymbol{k}$ and ω are distributed, representing a displacement at a site n. In the Fourier transform $\boldsymbol{\sigma}_k = \sum_n \boldsymbol{\sigma}_n \exp(-\mathrm{i}(\boldsymbol{k} \cdot \boldsymbol{r}_n - \omega t_n))$, the amplitude $\boldsymbol{\sigma}_n$ is finite, but the phase $\phi_n = \boldsymbol{k} \cdot \boldsymbol{r}_n - \omega t_n$ is distributed in the range $0 \leq \phi_n \leq 2\pi$ in repetition. In the critical region however, such a phase ϕ_n is uncertain by an amount $\Delta\phi_n$ as related to uncertain $\Delta\boldsymbol{k}$ and $\Delta\omega$. The critical region is therefore dominated by distributed phases $\phi_n + \Delta\phi_n$, which we call hereafter *phase fluctuations* or simply *fluctuations*.

In a continuum lattice, distributed phases ϕ_n can be replaced by a single continuous phase $\phi = \boldsymbol{k} \cdot \boldsymbol{r} - \omega t$ in the range $0 \leq \phi \leq 2\pi$, but accompanying uncertainty $\Delta\phi$, omitting the index n. We can therefore write $\boldsymbol{\sigma}_k = \boldsymbol{\sigma}_o \exp\{-\mathrm{i}(\phi + \Delta\phi)\}$ to represent correlated pseudospins, where $|\boldsymbol{k}|^{-1}$ determines an effective measure of the correlation distance in the moving frame of condensates. Further notable is that $\boldsymbol{\sigma}_k$ is no longer sinusoidal in the presence of a quartic potential, as verified theoretically by Krumshansl et al. [15]. As will be discussed later, $\boldsymbol{\sigma}_k$ can generally be described by an elliptic function, showing *nonlinear* character of distant correlations. Writing $\boldsymbol{\sigma}_k = \boldsymbol{\sigma}_o f(\phi + \Delta\phi)$, the finite amplitude $\boldsymbol{\sigma}_o$ is related with the velocity of propagation, which is typical for nonlinear propagation, and $f(\phi + \Delta\phi)$ is a function of a fluctuation phase.

With Born–Huang's principle, we assume that distributed phases ϕ_n in the critical region can become *in phase* with the lattice excitation. The process for $\Delta\phi \to 0$ is primarily adiabatic as forced by the lattice excitation. The nonlinear $\boldsymbol{\sigma}_k$

and the corresponding adiabatic potential ΔU_k become in phase after $\Delta\phi \to 0$ in the propagating reference frame. Considering the space inversion $\boldsymbol{r} \to -\boldsymbol{r}$ in a binary crystal, two phase variables $\phi = \pm\boldsymbol{k}\cdot\boldsymbol{r} - \omega t$ are significant for fluctuations. For such a variable $\boldsymbol{\sigma}_k = \boldsymbol{\sigma}_0 f(\phi)$ after thermal phasing, we have the relation

$$\boldsymbol{\sigma}_{-k} = \boldsymbol{\sigma}_k^*, \tag{6.7}$$

with respect to the inversion center $\phi = 0$. In practice, there should be a potential in a crystal, providing $\boldsymbol{\sigma}_{\pm k}$ with respect to the inversion center, which is called a *pinning potential*. Thus, these two waves $\boldsymbol{\sigma}_{\pm k}$ are pinned in equilibrium crystals.

Although attributed to Born–Huang's principle, it is significant to realize that such a phasing as assumed in the foregoing should take place thermally by exchanging energy with the heat reservoir at the boundaries. In this context, the phasing can be observed as thermal relaxation of mesoscopic variables to a stable lattice structure, which is not describable by the dynamical theory alone.

6.3 Critical Anomalies

At the threshold of the transition, we consider that collective modes $\boldsymbol{\sigma}_{\pm k} = \boldsymbol{\sigma}_0 \exp \mathrm{i}(\pm\boldsymbol{k}\cdot\boldsymbol{r} - \omega t)$ are pinned by the potential $\Delta U_k = (a/2)\boldsymbol{\sigma}_k^2 + (b/4)\boldsymbol{\sigma}_k^4$ at $\phi = 0$, where both $\boldsymbol{\sigma}_k$ and ΔU_k become stationary in the moving coordinate system at $\boldsymbol{k}$.

The Gibbs function can fluctuate between $G(\boldsymbol{\sigma}_{+k})$ and $G(\boldsymbol{\sigma}_{-k})$ with the corresponding collective modes $\boldsymbol{\sigma}_{+k} = \boldsymbol{\sigma}_0 \exp \mathrm{i}\phi$ and $\boldsymbol{\sigma}_{-k} = \boldsymbol{\sigma}_0 \exp(-\mathrm{i}\phi)$, where $\phi = \boldsymbol{k}\cdot\boldsymbol{r} - \omega t$, across a positive potential barrier ΔU at $\phi = 0$ at a temperature close to T_c^*. The potential ΔU is a symmetrical function with respect to $\phi = 0$, which can be considered as proportional to $\cos(2\phi)$, because of the quadratic term dominant at temperatures close to T_c. Assuming the amplitude $\boldsymbol{\sigma}_0$ as constant, the Gibbs function is a function of ϕ, which fluctuates between $\phi_+ = +\boldsymbol{k}\cdot\boldsymbol{r} - \omega t$ and

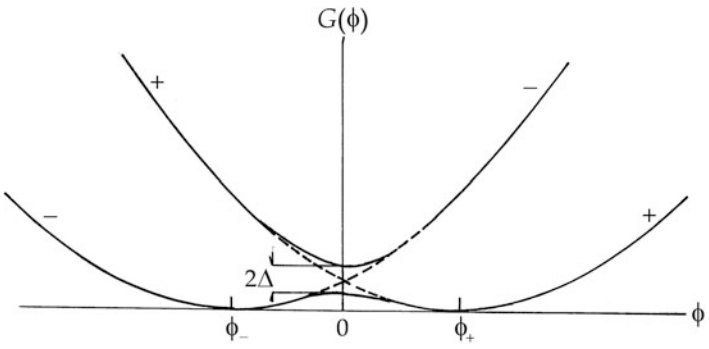

Fig. 6.2 Phase fluctuations of the Gibbs potential at the critical condition.

$\phi_- = -\boldsymbol{k}\cdot\boldsymbol{r} - \omega t$, as illustrated in Fig. 6.2. For two parabolic curves for $G(\pm\phi)$, their minimum positions are indicated by ϕ_+ and ϕ_-, respectively, where phase fluctuations occur in the range $\phi_- < \phi < \phi_+$ through the potential $\Delta U = V\cos 2\phi$, where $V > 0$. As a simple *level-crossing* in quantum mechanics, we solve the problem by considering $\boldsymbol{\sigma}_{\pm k}$ as the wavefunctions of the equation $\mathcal{H}\boldsymbol{\sigma}_{\pm k} = \varepsilon_\pm \boldsymbol{\sigma}_{\pm k}$. The degenerate eigenvalues, $\varepsilon_+ = \varepsilon_-$, represent kinetic energies of phase fluctuations, which are perturbed by the potential ΔU.

In this case, the perturbed function can be expressed as a linear combination of $\boldsymbol{\sigma}_+$ and $\boldsymbol{\sigma}_-$, and so we write

$$\boldsymbol{\sigma} = c_+\boldsymbol{\sigma}_+ + c_-\boldsymbol{\sigma}_- \quad \text{and} \quad c_+^2 + c_-^2 = 1, \tag{6.8}$$

where c_+ and c_- are normalizing coefficients, for the perturbed equation $(\mathcal{H} + V\cos 2\phi)\boldsymbol{\sigma} = \varepsilon\boldsymbol{\sigma}$. These coefficients c_+ and c_- can be determined, if

$$\begin{vmatrix} \varepsilon_+ - \varepsilon & \Delta \\ \Delta & \varepsilon_- - \varepsilon \end{vmatrix} = 0, \tag{6.9}$$

where

$$\Delta = \frac{\int_0^{2\pi} \boldsymbol{\sigma}_+^*(V\cos 2\phi)\boldsymbol{\sigma}_- \mathrm{d}\phi}{\int_0^{2\pi} \mathrm{d}\phi = \frac{V\boldsymbol{\sigma}_\mathrm{o}^2}{2\pi}\int_0^{2\pi} \exp(-2\mathrm{i}\phi)\cos 2\phi \mathrm{d}\phi} = \frac{V\boldsymbol{\sigma}_\mathrm{o}^2}{\pi}\int_0^{\pi} \cos^2(2\phi)\mathrm{d}\phi$$
$$= \frac{V\boldsymbol{\sigma}_\mathrm{o}^2}{2\pi}. \tag{6.10}$$

Solving (6.9) for the perturbed energy ε, we obtain

$$\varepsilon = \frac{\varepsilon_+ + \varepsilon_-}{2} \pm \sqrt{\left(\frac{\varepsilon_+ - \varepsilon_-}{2}\right)^2 - \Delta^2},$$

which can be simplified as $\varepsilon = \varepsilon_\mathrm{o} \pm \Delta$, if writing the unperturbed energies as $\varepsilon_+ = \varepsilon_- = \varepsilon_\mathrm{o}$. Thus the degeneracy of the fluctuation energy is lifted, resulting in a gap 2Δ, as indicated in Fig. 6.2.

In this case, the coefficients c_+ and c_- should satisfy the relations $c_+^2 = c_-^2 = 1/2$, because of the normalization (6.8); hence, we obtain symmetrical and antisymmetrical functions:

$$\boldsymbol{\sigma}_A = \frac{\boldsymbol{\sigma}_+ + \boldsymbol{\sigma}_-}{\sqrt{2}} \quad \text{and} \quad \boldsymbol{\sigma}_P = \frac{\boldsymbol{\sigma}_+ - \boldsymbol{\sigma}_-}{\sqrt{2}}, \tag{6.11a}$$

which can be assigned to $\varepsilon_\mathrm{o} + \Delta$ and $\varepsilon_\mathrm{o} - \Delta$, respectively. The perturbed states are therefore characterized by $\boldsymbol{\sigma}_A = \sqrt{2}\boldsymbol{\sigma}_\mathrm{o}\cos\phi$ and $\boldsymbol{\sigma}_P = \sqrt{2}\mathrm{i}\boldsymbol{\sigma}_\mathrm{o}\sin\phi$, which are called the *amplitude* and *phase modes*, respectively, giving two separate modes of fluctuations. The critical region signified by these two modes (6.11a) was actually observed in neutron inelastic scattering and magnetic resonance experiments, as described in Chap. 10.

In the thermodynamic environment, the fluctuations are observed as the energy loss via thermal relaxations with varying temperature. Actually, with decreasing temperature, the amplitude mode was found to fade away thermally faster than the phase mode. It is noted that the Gibbs potential for the stable phase mode is expressed by quadratic and quartic potentials, shifting equilibrium from $\phi = 0$ to $\phi = \phi_{\pm}$ with decreasing temperature, representing separated domains in a crystal.

6.4 Observing Anomalies

In the transition region, the fluctuations are spread anomalously in a form different from random fluctuations, which we call *critical anomalies*. In fact, due to symmetrical and asymmetrical modes

$$\boldsymbol{\sigma}_A = \sqrt{2}\boldsymbol{\sigma}_{\mathrm{o}} \cos\phi \quad \text{and} \quad \boldsymbol{\sigma}_P = \sqrt{2}\mathrm{i}\boldsymbol{\sigma}_{\mathrm{o}} \sin\phi, \tag{6.11b}$$

the anomalies are signified by distributed phases ϕ in the range $0 \le \phi \le 2\pi$ in repetition, In practical experiments, such fluctuations can be detected, if the timescale of observation t_{o} is sufficiently shorter than the repeat time $2\pi/\omega$; otherwise, they are averaged out. Accordingly, observed results can be analyzed by means of these time averages $\langle \boldsymbol{\sigma}_A \rangle_t$ and $\langle \boldsymbol{\sigma}_P \rangle_t$. Assuming that $\boldsymbol{\sigma}_{\mathrm{o}}$ is constant, we have

$$\langle \boldsymbol{\sigma}_A \rangle_t = \sqrt{2}\boldsymbol{\sigma}_{\mathrm{o}} \frac{1}{t_{\mathrm{o}}} \int_0^{t_{\mathrm{o}}} \cos(\boldsymbol{k}\cdot\boldsymbol{r} - \omega t)\mathrm{d}t = 2\sqrt{2}\boldsymbol{\sigma}_{\mathrm{o}} \frac{\sin\omega t_{\mathrm{o}}}{\omega t_{\mathrm{o}}} \cos\boldsymbol{k}\cdot\boldsymbol{r}$$

and

$$\langle \boldsymbol{\sigma}_P \rangle_t = 2\mathrm{i}\sqrt{2}\boldsymbol{\sigma}_{\mathrm{o}} \frac{1}{t_{\mathrm{o}}} \int_0^{t_{\mathrm{o}}} \sin(\boldsymbol{k}\cdot\boldsymbol{r} - \omega t)\mathrm{d}t = 2\sqrt{2}\mathrm{i}\boldsymbol{\sigma}_{\mathrm{o}} \frac{\sin\omega t_{\mathrm{o}}}{\omega t_{\mathrm{o}}} \sin\boldsymbol{k}\cdot\boldsymbol{r}.$$

Amplitudes of these modes are reduced by the factor $\Gamma = \sin\omega t_{\mathrm{o}}/\omega t_{\mathrm{o}}$ that determines the width of fluctuations depending on t_{o}; namely, $\Gamma \to 1$ if $\omega t_{\mathrm{o}} \to 0$. Further $\boldsymbol{k}\cdot\boldsymbol{r}$ represents the *spatial phase* ϕ_{s} to determine the observed width, which can be measured with the effective amplitude $\Gamma|\boldsymbol{\sigma}_{\mathrm{o}}|$ in a specified timescale t_{o}.

Owing to the classical character, these $\langle \boldsymbol{\sigma}_A \rangle_t$ and $\langle \boldsymbol{\sigma}_P \rangle_t$ may be considered as longitudinal and transverse components of a complex pseudospin $\sigma = \sigma_A + \mathrm{i}\sigma_P$, where

$$\sigma_A = \sigma_{\mathrm{o}} \cos\phi_s, \quad \sigma_P = \sigma_{\mathrm{o}} \sin\phi_s \quad \text{and} \quad \sigma_{\mathrm{o}} = 2\sqrt{2}|\boldsymbol{\sigma}_{\mathrm{o}}|\Gamma. \tag{6.12}$$

In practice, these components are measured from a sample crystal oriented in the laboratory reference. Therefore, the quantities proportional to $\sigma_{A,P}$ can be expressed as $\int_0^{2\pi} f_{A,P}(\phi_s)\sigma_{A,P}\mathrm{d}\phi_s$, where $f_{A,P}(\phi_s)$ are densities of fluctuations distributed

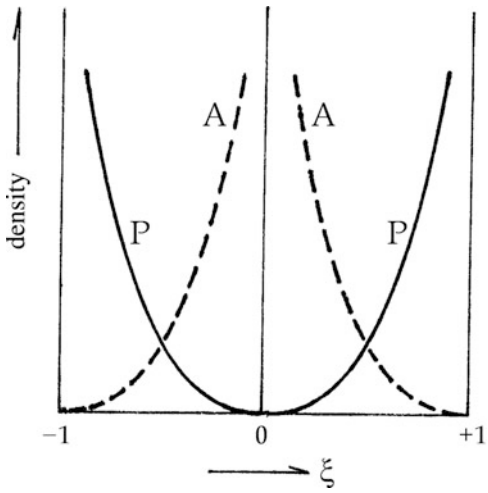

Fig. 6.3 Intensity distributions of the amplitude mode (A) and phase mode (P).

between ϕ_s and $\phi_s + \mathrm{d}\phi_s$. In practice, a linear variable ξ, defined by $\xi = \cos\phi_s$, and hence $\pm\sqrt{1-\xi^2} = \sin\phi_s$, is more convenient than the angular variable ϕ_s. So converting variables from ϕ_s to ξ, we obtain the following quantities

$$\int_{-1}^{+1} f_A(\xi)\frac{\sigma_\mathrm{o}}{\xi}\mathrm{d}\xi \quad \text{and} \quad \int_{-1}^{+1} f_P(\xi)\frac{\sigma_\mathrm{o}}{\sqrt{1-\xi^2}}\mathrm{d}\xi,$$

for σ_A and σ_P modes, respectively. Figure 6.3 shows curves of these density functions, where A and P modes exhibit clearly distinctive shapes. The latter is distributed between $+\sigma_\mathrm{o}$ and $-\sigma_\mathrm{o}$ with the width $2\sigma_\mathrm{o} \propto \Gamma$, whereas the former is a single line at the center $\phi = 0$. Practical examples of observed anomalies are shown in Chap. 10.

6.5 Extrinsic Pinning

An ideal crystal is characterized by translational symmetry of a periodic structure. In contrast, practical crystals are by no means perfect because of the presence of many types of imperfections such as lattice defects, dislocations, impurities, and surfaces. Apart from surfaces that determine thermal properties of crystals, the other imperfections can usually be reduced by careful preparation; thereby, a crystal can be assumed to be nearly perfect. If this is the case, most significant are *point defects* that disrupt translational lattice symmetry. However, if a crystal contains such defects that are arranged in a manner different from the lattice periodicity, we say that is *pseudosymmetry*. Order variables may be pinned by pseudosymmetric potentials, causing a transition in different type.

6.5.1 Pinning by Point Defects

A practical crystal contains some unavoidable imperfections that are mostly missing constituents or impurity ions at lattice sites. Translational space symmetry is disrupted by such *point defects*, by which collective pseudospin modes can be pinned, exhibiting standing waves in a crystal.

A point defect can be represented by a potential as a function of distance $\boldsymbol{r} - \boldsymbol{r}_i$ from a defective lattice site $\boldsymbol{r}_i$. Such a defect potential is not harmonic in a crystal, but we assume that it is confined symmetrically to the vicinity of the defect site. Nevertheless, in a crystalline phase in low defect density, propagation of pseudospin modes $\boldsymbol{\sigma}_\mathrm{o} \exp(\pm \mathrm{i}\phi_i)$ is perturbed by a defect potential at site i; mathematically, the problem is the same as in Sect. 6.3.

At such *extrinsic* defects in a crystal, fluctuations can be either symmetric or antisymmetric with respect to the defect center; the former is for defects at a regular lattice site, whereas the latter can represent surface sites. Considering the symmetric combination, $(\boldsymbol{\sigma}_{+,i} + \boldsymbol{\sigma}_{-,i})/\sqrt{2} = \sqrt{2}\boldsymbol{\sigma}_\mathrm{o} \cos\phi_i$, we express the pinning potential as

$$V(\phi) = -V_\mathrm{o} \cos\phi, \tag{6.13}$$

where ϕ is the phase variable in the range $0 \le \phi \le 2\pi$; the minimum is located at $\phi = 0$. Here, the magnitude is expressed as V_o in (6.10) applied to this case. Needless to say, (6.13) is a meaningful potential, provided that ϕ_i are continuous distributed.

Considering surfaces as imperfections, we take antisymmetric function $(\boldsymbol{\sigma}_{+,i} - \boldsymbol{\sigma}_{-,i})/\sqrt{2}$ to express the pinning potential as $-V_\mathrm{o} \sin\phi$, which however does not give minimum at $\phi = 0$. Therefore, we may consider that the pinning occurs at $\phi = \pi/2$, for which the pinning potential is defined by the same expression as (6.13), considering that ϕ is an angular deviation from $\pi/2$. Point defects, including surfaces, can therefore be considered as extrinsic perturbations; thereby, a pseudospin mode can be pinned at the threshold of transition, exhibiting phase fluctuations as described by (6.13).

6.5.2 Pinning by an Electric Field

If the order variables are electrically dipolar, the arrangement of $\boldsymbol{\sigma}_n$ can be perturbed by an electric field $\boldsymbol{E}$ applied externally. In this case the crystal is stabilized with an additional potential energy $-\left(\sum_n \boldsymbol{\sigma}_n\right) \cdot \boldsymbol{E}$. Here, the field $\boldsymbol{E}$, if uniform, is *asymmetrical* at all sites n, hence, those $\boldsymbol{\sigma}_n$ mode interacting with the field is expressed by an asymmetric combination $(\boldsymbol{\sigma}_{n,+k} - \boldsymbol{\sigma}_{n,-k})/\sqrt{2}$ that is proportional to $\sin\phi_{n,k}$. In this case, the pinning potential can be expressed as

$$V_E(\phi) = -\sigma_\mathrm{o} E \sin\phi. \tag{6.14a}$$

However, $V_E(0) = 0$ at the pinning center is $\phi = 0$. This can be lowered if the phase ϕ shifts by $\pi/2$, namely,

$$V_E\left(\phi+\frac{\pi}{2}\right)=-\sigma_{\mathrm{o}}E\sin\left(\phi+\frac{\pi}{2}\right)=-\sigma_{\mathrm{o}}E\cos\phi, \tag{6.14b}$$

which gives minimum at $\phi=\pi/2$.

In magnetic resonance studies on the ferroelectric phase transition of TSCC crystals, two fluctuation modes σ_A and σ_P were identified. In the presence of a weak electric field, it was observed that the spectrum of σ_A split into two lines with increasing E at a temperature below T_{c}, which was interpreted by a change of the pinning potential from (6.14a) to (6.14b) with shifting ϕ by $\pi/2$ in a thermal relaxation.

6.5.3 *Surface Pinning*

Surfaces are not defects, but a pseudospin mode $\boldsymbol{\sigma}_s$ can be interacted with an antisymmetric field A similar to an electric field in character, assuming that surface point behaves like a reflecting wall. Considering perfect reflection, the mode should be a standing wave $(\boldsymbol{\sigma}_{-s,k}-\boldsymbol{\sigma}_{-s,-k})/\sqrt{2}$ inside a crystal, whereas $\boldsymbol{\sigma}_{+s}=0$ outside, respectively, where the indexes $-s$ and $+s$ signify inside and outside. Therefore, we can write the pinning potential as

$$V_S=-\sigma_{\mathrm{o}}A\sin\phi \quad \text{for} \quad -\pi<\phi\le 0. \tag{6.15}$$

Thermodynamically, heat exchange with the surroundings can be considered for V_S to associate with a lattice mode. The corresponding lattice displacement $\boldsymbol{u}$ at $\phi=0$ is responsible for the heat transfer as perturbed by phonon scatterings.

Exercises 6

1. In the Landau theory, the order parameter was considered as a scalar quantity. Considering the theory for a vector variable $\boldsymbol{\sigma}=\boldsymbol{\sigma}_{\mathrm{o}}\exp \mathrm{i}\phi$, (6.1) is a function of the magnitude square $\boldsymbol{\sigma}_{\mathrm{o}}^2$. In this case, the theory disregards the phase ϕ and all space–time uncertainties. Is this consistent with the mean-field approximation?
2. Critical fluctuations are observed in two modes, $\boldsymbol{\sigma}_A$ and $\boldsymbol{\sigma}_P$. Experimentally, we know that $\boldsymbol{\sigma}_A$-mode is temperature dependent, decreasing below T_{c}, whereas $\boldsymbol{\sigma}_P$ is stable. What is the reason for that? Explain on the basis of the condensate model.
3. Usually, critical fluctuations can be observed in two modes, $\boldsymbol{\sigma}_A$ and $\boldsymbol{\sigma}_P$ of clustered pseudospins pinned by the adiabatic potential. Extrinsically pinned pseudospins $\boldsymbol{\sigma}$ are either symmetric or antisymmetric, but the former is not distinguishable from $\boldsymbol{\sigma}_A$. Further, $\boldsymbol{\sigma}_P$ are characterized by phase shifting on lowering temperature, while $\boldsymbol{\sigma}_A$ and defect-pinned $\boldsymbol{\sigma}$ remains unchanged with temperature. Discuss these features of pinned pseudospins in terms of pinning potentials.

Chapter 7
Pseudospin Correlations

Landau's expansion (6.1) can be interpreted as an adiabatic potential for pseudospin correlations in a mesoscopic state. By virtue of Born–Huang's principle, a change of the Gibbs potential ΔG due to an adiabatic potential ΔU represents changing correlations with temperature below T_c. Analyzed with a truncated ΔU in one dimension, however, the dynamics of σ should reflect lattice symmetry in a crystal. Using ΔU defined as consistent with lattice symmetry, the propagating vector $\boldsymbol{\sigma}$ can be described in three-dimensional crystal space. Signified by the transverse component, the variable $\boldsymbol{\sigma}$ is found to be incommensurate with the lattice periodicity. In this chapter, the nature of a propagating $\boldsymbol{\sigma}$ is discussed for their correlations with pinning potentials in crystals.

7.1 Propagation of a Collective Pseudospin Mode

Pseudospins $\boldsymbol{\sigma}_n$ and their Fourier transform $\boldsymbol{\sigma}_k$ in a periodic lattice constitute a *vector field*, which is a convenient concept to describe propagation along the direction of $\boldsymbol{k}$. This is a useful approach to a continuum field at a small $|k|$, similar to the phonon field representing lattice vibrations. It is the *Helmholtz theorem* in classical field theory that such a pseudospin field consists of two independent subfields that are *longitudinal* and *transverse* to the direction of $\boldsymbol{k}$. We consider that such $\boldsymbol{\sigma}_k$ as expressed by classical vectors are in free propagation in the absence of an external field; otherwise, the collective motion is restricted by an adiabatic potential:

$$\Delta U(\boldsymbol{\sigma}_k) = \frac{1}{2} a \boldsymbol{\sigma}_k^2 + \frac{1}{4} b \boldsymbol{\sigma}_k^4.$$

We first consider longitudinal propagation along $\boldsymbol{k}$, writing $\boldsymbol{\sigma}_k$ as a function of space–time coordinates x and t. Although signified by two components σ_k and $\sigma_{\perp k}$,

M. Fujimoto, *Thermodynamics of Crystalline States*,
DOI 10.1007/978-1-4419-6688-9_7, © Springer Science+Business Media, LLC 2010

we set the transverse component $\sigma_{\perp k}$ aside and write the wave equation for the longitudinal component σ_k as

$$m\left(\frac{\partial^2}{\partial t^2} - v_o^2 \frac{\partial^2}{\partial x^2}\right)\sigma_k(x,t) = -\frac{\partial \Delta U}{\partial x} = -\sigma_{ko} k\left(a\sigma_k + b\sigma_k^3\right), \tag{7.1a}$$

where $\sigma_k(x,t) = \sigma(kx - \omega t)$, $v_o = \omega/k$ is the speed of propagation in the crystal space, and the amplitude σ_{ko} can be infinitesimal for a small k, if ignoring ΔU as constant. In the presence of ΔU, Krumshansl et al. [15] solved (7.1a) by re-expressing it in a simplified form

$$\frac{d^2 Y}{d\phi^2} + Y - Y^3 = 0, \tag{7.1b}$$

using rescaled variables

$$Y = \frac{\sigma_k}{\sigma_{ko}} \quad \text{and} \quad \phi = k(x - vt), \tag{7.1c}$$

where

$$\sigma_{ko} = \sqrt{\frac{|a|}{b}}, \quad k^2 = \frac{|a|}{m\left(v_o^2 - v^2\right)} = \frac{k_o^2}{1 - \frac{v^2}{v_o^2}} \quad \text{and} \quad k_o^2 = \frac{|a|}{m v_o^2}.$$

The corresponding frequency can be obtained by the relation $\omega = v_o k$, as expressed by

$$\omega^2 = v_o^2\left(k^2 - k_o^2\right), \tag{7.2}$$

indicating that the propagation is *dispersive*. It is noted from (7.2) that $\omega = 0$ if $k = k_o$, but for a finite ω we should have $v < v_o$ and $k > k_o$. The former case can then be assigned to the critical temperature $T = T_c^*$, and the latter to $T < T_c^*$, respectively. The dispersion (7.2) is originated from the nonlinear character of (7.1a).

For a small σ_k, the term Y^3 in (7.1b) can be ignored, in which case (7.1b) is a linear equation, whose solution is sinusoidal, that is, $Y = Y_o \sin(\phi + \phi_o)$. Here Y_o is infinitesimal and $\phi_o = 0$ can be chosen as the reference point. Nevertheless, the nonlinear equation (7.1b) can be solved analytically as shown below.

Integrating (7.1b) once, we obtain

$$2\left(\frac{dY}{d\phi}\right)^2 = \left(\lambda^2 - Y^2\right)\left(\mu^2 - Y^2\right), \tag{7.3}$$

where

$$\lambda^2 = 1 - \sqrt{1 - \alpha^2} \quad \text{and} \quad \mu^2 = 1 + \sqrt{1 - \alpha^2},$$

where $\alpha = (\mathrm{d}Y/\mathrm{d}\phi)_{\phi=0}$ is a constant of integration. Writing $\xi = Y/\lambda$ for convenience, (7.3) can be re-expressed in integral form as

$$\frac{\phi_1}{\sqrt{2}\kappa} = \int_0^{\xi_1} \frac{\mathrm{d}\xi}{\sqrt{(1-\xi^2)(1-\kappa^2\xi^2)}}, \tag{7.4a}$$

where ξ_1 is the upper limit of the variable ξ, and the corresponding phase ϕ is specified as ϕ_1. Here, the ratio $\kappa = \lambda/\mu$ is called the *modulus* of the *elliptic integral of the first kind* (7.4a). It is noted that the constants λ and μ can be written in terms of the modulus κ, that is,

$$\lambda = \frac{\sqrt{2}\kappa}{\sqrt{1+\kappa^2}} \quad \text{and} \quad \mu = \frac{\sqrt{2}}{\sqrt{1+\kappa^2}}.$$

The inverse function of the integral (7.4a) can be written as

$$\xi_1 = \mathrm{sn}\,\frac{\phi_1}{\sqrt{2}\kappa}, \tag{7.4b}$$

which is known as *Jacobi's elliptic sn-funcion*. Using previous notations, the nonlinear mode σ_1 can be expressed as

$$\sigma_1 = \lambda\sigma_\mathrm{o}\mathrm{sn}\,\frac{\phi_1}{\sqrt{2}\kappa}, \tag{7.5}$$

showing an elliptical wave that is modified from a sinusoidal wave by λ, μ, κ and α. Also significant is that the amplitude of σ_1 and phase ϕ_1 are both determined by the integral in (7.4a) that is typical for nonlinear waves.

Using an angular variable Θ defined by $\xi = \sin\Theta$, (7.4a) is expressed as

$$\frac{\phi_1}{\sqrt{2}\kappa} = \int_0^{\Theta_1} \frac{\mathrm{d}\Theta}{\sqrt{1-\kappa^2\sin^2\Theta}}, \tag{7.6a}$$

where Θ_1 represents an *effective sinusoidal phase* of ξ_1, which is useful to express the propagation as a sinusoidal function, that is,

$$\mathrm{sn}\,\frac{\phi_1}{\sqrt{2}\kappa} = \sin\Theta_1. \tag{7.6b}$$

In this way, σ_1 can be regarded as the longitudinal component of a classical vector, that is, $\sigma_1 = \lambda\sigma_\mathrm{o}\sin\Theta_1$ with effective amplitude $\lambda\sigma_\mathrm{o}$. In fact, Jacobi named Θ_1 as the *amplitude function* and wrote

$$\Theta_1 = \mathrm{am}\left(\int_0^{\Theta_1} \frac{\mathrm{d}\Theta}{\sqrt{1-\kappa^2\sin^2\Theta}}\right).$$

Nevertheless, we stay on the definition of *effective phase angle*. Figure 7.1 shows the relation between the elliptic integral

$$u(\kappa) = \int_0^{\Theta_1} \frac{\mathrm{d}\Theta}{\sqrt{1 - \kappa^2 \sin^2\Theta}}$$

and Jacobi's $\Theta_1 = \mathrm{am}\, u$, plotted for $\kappa = 0.5$ and 0.9.

Except for $\kappa = 1$, the sn-function (7.6b) is periodic, whose periodicity is expressed by the repetitive unit determined by the difference between $\Theta_1 = 0$ and $\Theta_1 = 2\pi$. That is, the period of the sn-function is given as

$$K(\kappa) = \int_0^{\frac{\pi}{2}} \frac{\mathrm{d}\Theta}{\sqrt{1 - \kappa^2 \sin^2\Theta}}, \tag{7.7}$$

and this is called the *complete elliptic integral*. We consider that long-range correlations are included in (7.5) for $0 < \kappa < 1$. The range of $0 < \Theta = \pi$ is equal to the period of sn-function $4K(\kappa)$.

For $\kappa = 1$ or $\lambda = \mu = 1$ by definition, (7.6a) can specifically be integrated as

$$\sigma_1 = \sigma_o \tanh \frac{\phi_1}{\sqrt{2}}, \tag{7.8}$$

showing $\sigma_1 \to \sigma_o$ in the limit of $\phi_1 \to \infty$. Figure 7.2 illustrates curves of (7.5) and (7.8) for representative values of the modulus κ.

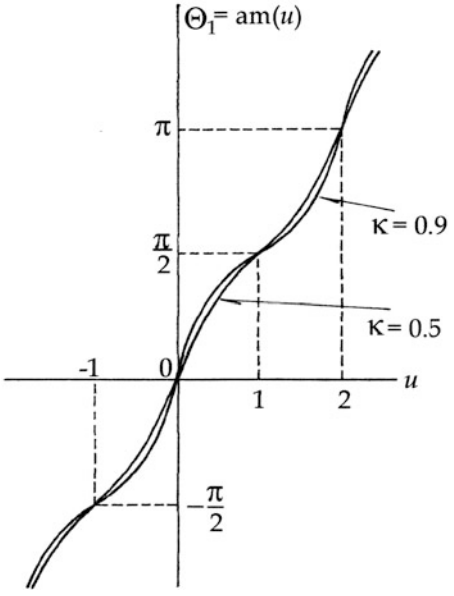

Fig. 7.1 Effective phase $\Theta_1(u)$ and (Jacobi's amplitude function) vs. u.

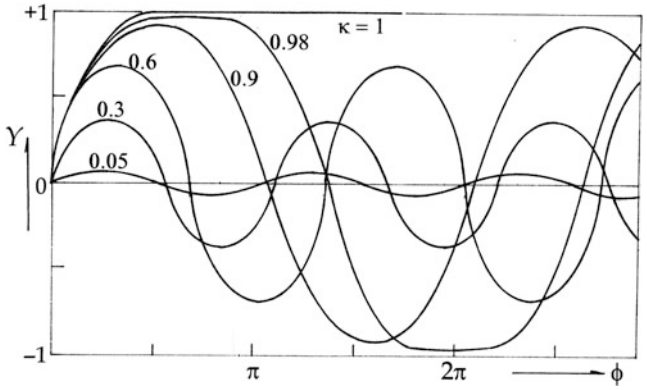

Fig. 7.2 Elliptic functions $\mathrm{sn}\left(\phi/\sqrt{2}\kappa\right)$ plotted against ϕ for various values of the modulus κ.

7.2 Transverse Components and the Cnoidal Potential

In the above dynamical theory, the amplitude σ_o is left undetermined, which should however take a finite value originated from thermal interactions with the surroundings at a given temperature. Leaving the temperature dependence to later discussions, for the periodic solution (7.5) for $0 < \kappa < 1$, we have $\sigma_1 = \lambda\sigma_o \sin\Theta_1$ that represents the longitudinal component of a vector $\lambda\boldsymbol{\sigma}_o$. We can therefore consider the transverse component $\sigma_{1\perp}$ that can be written as

$$\sigma_{1\perp} = \lambda\sigma_o \cos\Theta_1 = \lambda\sigma_o \mathrm{cn}\frac{\phi_1}{\sqrt{2}\kappa} \quad \text{for} \quad 0 < \kappa < 1, \tag{7.9a}$$

using elliptic cn-function, so that we have the relation $\sigma_1^2 + \sigma_{1\perp}^2 = \lambda^2\sigma_o^2$.

From (7.8) for $\kappa = 1$, the transverse component can be expressed as

$$\sigma_{1\perp} = \sigma_o \mathrm{sech}\frac{\phi_1}{\sqrt{2}} \quad \text{for} \quad \kappa = 1, \tag{7.9b}$$

and we have $\sigma_1^2 + \sigma_{1\perp}^2 = \sigma_o^2$.

In the presence of the transverse component of a longitudinally correlated pseudospin, we can consider an adiabatic potential $\Delta U(\sigma_{1\perp}) = 1/2a\sigma_{1\perp}^2$, assuming that there is no *cross correlations* with adjacent parallel chains in a crystal. On the other hand, it is noted that the pseudospin direction is reversed across $\phi_1 = 0$ and $n\pi$ of the periodic sn-function, for which a work by a force $F = -\partial U/\partial x = -k\partial U/\partial\phi_1$ is required, which can be calculated as $W = -\int_{-\delta}^{+\delta} \sigma_1 \frac{\partial U}{\partial\phi_1} \mathrm{d}\phi_1$ over the phase reversing region of width 2δ. Here, the potential U can be expressed as proportional to $\sigma_{1\perp}^2$, if there are no transverse correlations. In fact, in the vicinity

of $\phi_1 = 0$, we consider $\sigma_1(\phi_1) = \sigma_{1\perp}(\phi_1 + \pi/2) \approx \lambda\sigma_o$ and $\partial U/\partial\phi_1 \propto \mathrm{d}/\mathrm{d}\phi_1$ $\mathrm{cn}^2\phi_1/\sqrt{2}\kappa$, so that

$$\frac{\mathrm{d}W}{\mathrm{d}\phi_1} = -2\lambda^2\sigma_o^2\left(\mathrm{cn}\frac{\phi_1}{\sqrt{2}\kappa}\right)\frac{\mathrm{d}}{\mathrm{d}\phi_1}\left(\mathrm{cn}\frac{\phi_1}{\sqrt{2}\kappa}\right).$$

In the theory of elliptic functions, the differentiation can be performed with another elliptic function defined by $\mathrm{dn}^2u = 1 - \kappa^2\mathrm{sn}^2u$. With a dn-function for a general variable u, we have formula

$$(\mathrm{sn}u)' = \mathrm{cn}u\ \mathrm{dn}u, \quad (\mathrm{cn}u)' = -\mathrm{sn}u\ \mathrm{dn}u \quad \text{and} \quad (\mathrm{dn}u)' = -\kappa^2\mathrm{sn}u\ \mathrm{cn}u,$$

as listed in Appendix. Letting $u = \phi_1/\sqrt{2}\kappa$, with these formula, the above $\mathrm{d}W$ can be written as

$$\frac{\mathrm{d}W}{\mathrm{d}\phi_1} = \frac{1}{\sqrt{2}\kappa}\frac{\mathrm{d}W}{\mathrm{d}u} = \frac{2\lambda^2\sigma_o^2}{\sqrt{2}\kappa}\mathrm{cn}u\ \mathrm{sn}u\ \mathrm{dn}u = -\frac{2\lambda^2\sigma_o^2}{\sqrt{2}\kappa^3}(\mathrm{dn}u)(\mathrm{dn}u)'$$
$$= -\frac{\lambda^2\sigma_o^2}{\kappa^2}\frac{\mathrm{d}}{\mathrm{d}\phi_1}\mathrm{dn}^2\frac{\phi_1}{\sqrt{2}\kappa}.$$

Expressing W for the adiabatic potential, we have

$$\Delta U(\kappa) = \mu^2\sigma_o^2\mathrm{dn}^2\frac{\phi_1}{\sqrt{2}\kappa} \quad \text{for} \quad 0 < \kappa < 1. \tag{7.10a}$$

A potential proportional dn^2u shows the same wave form as sn^2u and cn^2u, so that (7.10a) is generally referred to as a *cnoidal potential*. On the other hand, for $\kappa = 1$, $\mathrm{dn}u = \mathrm{sech}u$

$$\Delta U(\kappa = 1) = \sigma_o^2\mathrm{sech}^2\frac{\phi_1}{\sqrt{2}} \quad \text{for} \quad \kappa = 1. \tag{7.10b}$$

In this case, $\sigma_{1\perp}$ approaches $\pm\ \sigma_o \times \infty$ in the limit of $\phi_1 \to \infty$, which can be assigned to a *domain boundary* where the pseudospin direction is reversed. These boundaries at $\phi_1 = 0$ and ∞ are identical, as indicated by inversion symmetry. Figure 7.3a, b and c, the curves of $\boldsymbol{\sigma}_1$, σ_1, and $\sigma_{1\perp}$ near the boundary, is plotted, respectively, against ϕ to illustrate their behaviors.

7.3 The Lifshitz' Condition for Incommensurability

We notice that the elliptic function for $0 < \kappa < 1$ is periodic, but its period is not necessarily the same as lattice periodicity. In such a case, the pseudospin mode is called *incommensurate*; however, it can be *commensurate* if one of these phases matches the other. Adiabatic fluctuations are generally incommensurate, but may

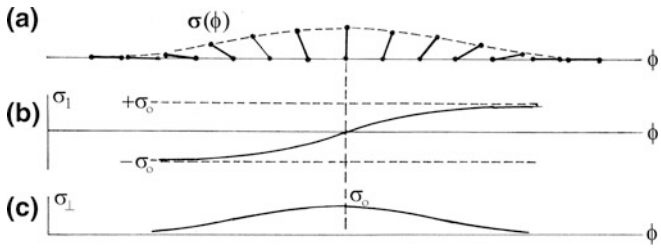

Fig. 7.3 A pseudospin mode along x direction for $\kappa = 1$. (**a**) Distributed mode vectors in the xz plane. (**b**) The longitudinal component $\sigma_1(\phi)$. (**c**) The transverse component $\sigma_{1\perp}(\phi)$.

become commensurate if pinned by a potential with the lattice symmetry. Lifshitz derived the statistical condition for incommensurability, which is a significant criterion for fluctuations in crystalline states.

For practical analysis of experimental results, mesoscopic pseudospin modes of elliptic and hyperbolic functions can conveniently be expressed as

$$\sigma_1 = \sigma_o \sin\Theta_1 \quad \text{and} \quad \sigma_\perp = \sigma_o \cos\Theta_1$$

that are components of a classical vector $\boldsymbol{\sigma} = (\sigma_1,\ \sigma_\perp)$, where σ_o and $\Theta_1(x,t)$ are the amplitude and phase, respectively. In the condensate model, these dynamical variables are temperature dependent, because the corresponding lattice displacements $(u_1,\ u_\perp)$ can scatter phonons inelastically. It is noted that the phase variable $\Theta_1(x,\ t)$ is spatially periodic with the period $4K(\kappa)$ that is not necessarily in phase with the lattice translation. In any case, the observed pseudospins can be expressed with temperature-dependent amplitude and phase. The Gibbs potential can therefore be specified by such a mesoscopic variable $\boldsymbol{\sigma}$, or by σ_o and Θ; $G(p,T;\boldsymbol{\sigma})$ takes a minimum value in equilibrium. For small but finite amplitude σ_o, the extent of pseudospin correlations can be specified by the phase function Θ.

Lifshitz considered statistically such correlation energies as determined by $J_{ij}\boldsymbol{\sigma}_i \cdot \boldsymbol{\sigma}_j$, and derived the thermodynamic condition for incommensurability. In practice, such time-dependent quantities in thermodynamic argument should be averaged over the timescale of observation, that is, $\langle \ldots \rangle_t$. Further, we assume that the correlated pseudospin $\boldsymbol{\sigma}_k$ is a function of x in the longitudinal variation, and that fluctuations between x_i and x_j can be signified by $\delta x = x_i - x_j$ and $x = 1/2(x_i + x_j)$. The correlation function can therefore be written as proportional to

$$\begin{aligned}\left\langle \sigma^*(x_i)\sigma(x_j) + \sigma(x_i)\sigma^*(x_j)\right\rangle_t &= 2\langle \sigma^*(x)\sigma(x)\rangle_t + \left\langle \sigma^*(x)\frac{\partial\sigma(x)}{\partial x} - \sigma(x)\frac{\partial\sigma^*(x)}{\partial x}\right\rangle_t \delta x \\ &+ \left\langle \sigma^*(x)\frac{\partial\sigma(x)}{\partial x} + \sigma(x)\frac{\partial\sigma^*(x)}{\partial x}\right\rangle_t (\delta x)^2 \\ &+ \left\langle \frac{\partial\sigma^*(x)}{\partial x}\frac{\partial^2\sigma(x)}{\partial x^2} - \frac{\partial\sigma(x)}{\partial x}\frac{\partial^2\sigma^*(x)}{\partial x^2}\right\rangle_t (\delta x)^3 \\ &+ \ldots\ldots\end{aligned}$$

Lifshitz considered that the Gibbs potential is contributed significantly by such correlation terms as related to δx, that is,

$$G_{\mathrm{L}} = \frac{iD}{2}\int_0^L \left\langle \sigma^* \frac{\partial \sigma}{\partial x} - \sigma \frac{\partial \sigma^*}{\partial x} \right\rangle_{\mathrm{t}} \frac{\mathrm{d}x}{L} + \frac{iD}{2}\int_0^L \left\langle \frac{\partial \sigma^* 0}{\partial x}\frac{\partial^2 \sigma}{\partial x^2} - \frac{\partial \sigma}{\partial x}\frac{\partial^2 \sigma^*}{\partial x^2} \right\rangle_t (\delta x)^2 \frac{\mathrm{d}x}{L} + \ldots, \tag{7.11}$$

where $iD/2$ is defined for convenience as a constant proportional to δx. The Gibbs potential can then be written as

$$G(\sigma) = G(0) + \int_0^L \left\langle \frac{mv_{\mathrm{o}}^2}{2}\left|\frac{\partial \sigma}{\partial x}\right|^2 + \frac{a}{2}|\sigma|^2 + \frac{b}{4}|\sigma|^4 \right\rangle_t \frac{\mathrm{d}x}{L} + G_{\mathrm{L}}, \tag{7.12}$$

where the upper limit L represents a sampling length of the mesoscopic σ in practical experiments. Writing $\sigma = \sigma_{\mathrm{o}} \exp \mathrm{i}\phi$, $G(\sigma)$ is a function of σ_{o} and ϕ, we have (7.12) re-expressed as

$$G(\sigma_{\mathrm{o}}, \phi) = G(0) + \int_0^L \left\langle \frac{a\sigma_{\mathrm{o}}^2}{2} + \frac{b\sigma_{\mathrm{o}}^4}{4} + \frac{mv_{\mathrm{o}}^2}{2}\left(\frac{\mathrm{d}\sigma_o}{\mathrm{d}x}\right)^2 + \frac{mv_{\mathrm{o}}^2\sigma_{\mathrm{o}}^2}{2}\left(\frac{\mathrm{d}\phi}{\mathrm{d}x}\right)^2 + D\sigma_{\mathrm{o}}^2\frac{\mathrm{d}\phi}{\mathrm{d}x}\left(1 + \delta x^2 \frac{\mathrm{d}^2\phi}{\mathrm{d}x^2}\right) \right\rangle_t \frac{\mathrm{d}x}{L},$$

which is minimized for equilibrium by setting $\partial G/\partial \sigma_{\mathrm{o}} = 0$ and $\partial G/\partial \phi = 0$ simultaneously. Carrying out these partial differentiations of $G(\sigma_{\mathrm{o}}, \phi)$, we obtain the equations

$$a\sigma_{\mathrm{o}} + b\sigma_{\mathrm{o}}^3 + mv_{\mathrm{o}}^2\frac{\mathrm{d}^2\sigma_{\mathrm{o}}}{\mathrm{d}x^2} + mv_{\mathrm{o}}^2\left(\frac{\mathrm{d}\sigma_{\mathrm{o}}}{\mathrm{d}x}\right)^2 + 2D\sigma_{\mathrm{o}}\frac{\mathrm{d}\phi}{\mathrm{d}x}\left(1 + \delta x^2\frac{\mathrm{d}^2\phi}{\mathrm{d}x^2}\right) = 0$$

and

$$\left(mv_{\mathrm{o}}^2\frac{\mathrm{d}\phi}{\mathrm{d}x} + D\sigma_{\mathrm{o}}^2\right)\frac{\mathrm{d}}{\mathrm{d}\phi}\left\{\frac{\mathrm{d}\phi}{\mathrm{d}x}\left(1 + \delta x^2\frac{\mathrm{d}^2\phi}{\mathrm{d}x^2}\right)\right\} = 0.$$

From the second equation, we see immediately that

$$\frac{\mathrm{d}\phi}{\mathrm{d}x} = -\frac{D}{mv_{\mathrm{o}}^2} = q, \tag{7.13}$$

which is the wave number independent of the lattice periodicity, since D and mv_{o}^2 are both constants that are unrelated with the lattice; q is therefore incommensurate

with the lattice. Also, assuming that σ_o is primarily independent of x in the first relation, we can solve the first relation for σ_o^2, that is,

$$\sigma_\mathrm{o}^2 = -\frac{a - \left(D/mv_\mathrm{o}^2\right)}{b}.$$

Thus, the wave $\sigma_\mathrm{o} \exp \mathrm{i}qx$ is incommensurate if $D \neq 0$, which is known as the Lifshitz' theorem. Literally, incommensurability originates from a nonvanishing displacement $\langle \delta x \rangle_t$ of lattice points, for which Lifshitz' expression $D \neq 0$ is an obvious requirement.

7.4 Pseudopotentials

The space group may be modified with additional translational symmetry called *pseudosymmetry*, signifying a periodic rotation of local structure, for instance m times over a multiple lattice spacing. On a so-called *screw axis* of m-fold rotation, we can consider a commensurate potential V_m^L, where correlated pseudospins $\sigma(\phi)$ can be pinned, if the spatial phase of ϕ matches such lattice spacing. Assuming that a lattice with pseudosymmetry is signified by transversal displacements of lattice points

$$u = u_\mathrm{o} \exp\left(\pm i\theta_p\right), \quad \text{where } \theta_p = \frac{2\pi}{m}p \quad \text{and } p = 0, 1, 2, \ldots, m-1, \tag{7.14}$$

along the m-fold screw axis, we can consider the potential

$$\begin{aligned} V_m^\mathrm{L}(\theta_\mathrm{o}, \theta_1, \ldots, \theta_{m-1}) &\propto \sum\nolimits_p u_p \\ &= u_\mathrm{o} \sum\nolimits_p \left\{\exp \mathrm{i}\theta_p + \exp\left(-\mathrm{i}\theta_p\right)\right\} = 2u_\mathrm{o} \sum\nolimits_p \cos\theta_p. \end{aligned}$$

Here, these angles θ_p can be re-expressed by the lattice coordinates $x_p = pa_\mathrm{o}$ combined with (7.14); $\theta_p = (2\pi/m)(x_p/a_\mathrm{o}) = G_m x_p$, where $G_m = 2\pi/ma_\mathrm{o}$, and therefore we have $V_m^\mathrm{L} \propto \sum_p \cos\left(G_m x_p\right)$. Consider that a mesoscopic pseudospin mode $\sigma = \sigma_\mathrm{o} \exp \mathrm{i}\phi$ is pinned by the adiabatic potential $V_m(\phi)$ corresponding to V_m^L, we should have a phase matching $G_m x_p = m\phi$, so that

$$\cos(m\phi) = \frac{1}{2}\{\exp(\mathrm{i}m\phi) + \exp(-\mathrm{i}m\phi)\} = \frac{1}{2\sigma_\mathrm{o}^m}(\sigma^m + \sigma^{-m}).$$

Therefore, the potential $V_m(\phi)$ is characteristically a function of $\sigma(\phi)$ and expressed as

$$V_m(\phi) = \frac{2\rho}{m}(\sigma^m + \sigma^{-m}) = \frac{2\rho\sigma_\mathrm{o}^m}{m}\cos(m\phi), \tag{7.15}$$

where ρ is the proportionality constant.

The Gibbs function can then be written as

$$G(\sigma) = \int_0^L \left\{ \frac{a\sigma^*\sigma}{2} + \frac{b(\sigma^*\sigma)^2}{4} + \frac{mv_o^2}{2}\frac{\partial\sigma^*}{\partial x}\frac{\partial\sigma}{\partial x} + V_m(\phi) \right\} \frac{\mathrm{d}x}{L}.$$

Considering the time average of the integrand $\langle \ldots \rangle_t$ for practical measurements,

$$G(\sigma_o, \phi) = \int_0^L \left\langle \frac{a\sigma_o^2}{2} + \frac{b\sigma_o^4}{4} + \frac{mv_o^2}{2}\left(\frac{\partial\sigma_o}{\partial x}\right)^2 + \frac{mv_o^2\sigma_o^2}{2}\left(\frac{\partial\phi}{\partial x}\right)^2 + \frac{2\rho\sigma_o^m}{m}\cos(m\phi) \right\rangle_t \frac{\mathrm{d}x}{L}.$$

Setting $\partial G(\sigma_o, \phi)/\partial\sigma_o = 0$ and $\partial G(\sigma_o, \phi)/\partial\phi = 0$ for minimum of $G(\sigma_o, \phi)$, we obtain

$$a\sigma_o + b\sigma_o^3 + 2\rho\sigma_o^{m-1}\cos(m\phi) + mv_o^2\left\{ \sigma_o\left(\frac{\mathrm{d}\phi}{\mathrm{d}x}\right)^2 + \frac{\mathrm{d}^2\sigma_o}{\mathrm{d}x^2} \right\} = 0 \qquad \text{(i)}$$

and

$$mv_o^2\sigma_o^2\frac{\mathrm{d}^2\phi}{\mathrm{d}x^2} - 2\rho\sigma_o^m\sin(m\phi) = 0. \qquad \text{(ii)}$$

Integrating the second equation, (ii) can be modified as

$$\frac{1}{2}mv_o^2\sigma_o^2\left(\frac{\mathrm{d}\phi}{\mathrm{d}x}\right)^2 + V_m(\phi) = \text{constant},$$

expressing a conservation law that is analogous to a simple pendulum with a finite amplitude. Using abbreviations $\psi = m\phi$ and $\zeta = 2m\rho\sigma_o^{m-2}/mv_o^2$, (ii) be simplified as

$$\frac{\mathrm{d}^2\psi}{\mathrm{d}x^2} - \zeta\sin\psi = 0. \qquad (7.15a)$$

This is a standard form of the *sine-Gordon equation*. For the conservation law, (7.15a) can be integrated as

$$\frac{1}{2}\left(\frac{\mathrm{d}\psi}{\mathrm{d}x}\right)^2 - \zeta\cos\psi = E, \qquad (7.15b)$$

where the constant E represents the energy of an equivalent pendulum. On the other hand, (i) determines the amplitude σ_o, which is not constant as in a simple pendulum, depending on the phase ψ. Such a phase-related amplitude is typical for a nonlinear oscillation.

Equation (7.15b) can be written in an integrated form

$$x - x_o = \int_0^{\psi_1} \frac{d\psi}{\sqrt{2(E + \zeta \cos\psi)}},$$

where the upper and lower limit ψ_1 and 0 correspond to coordinates x and x_o. This integral can be expressed by the elliptic integral of the first kind, if the modulus κ is defined by $\kappa^2 = 2\zeta/E + \zeta$, that is, if $\kappa^2 < 1$

$$x - x_o = \frac{\kappa}{\sqrt{\zeta}} \int_0^{\Theta_1} \frac{d\Theta}{\sqrt{1 - \kappa^2 \sin^2\Theta}},$$

where $\Theta = \frac{\psi}{2}$. Therefore,

$$\sin\Theta_1 = \mathrm{sn}\frac{\sqrt{\zeta}(x - x_o)}{\kappa} \quad \text{for} \quad 0 < \kappa < 1,$$

and

$$\sin\Theta_1 = \tanh\sqrt{\zeta}(x - x_o) \quad \text{for} \quad \kappa = 1.$$

To discuss the phase matching condition, it is convenient to define $x - x_o = \Lambda(\kappa)$ corresponding to the phase difference between $\Theta_1 = 0$ and $\Theta_1 = \pi$, that is,

$$\Lambda(\kappa) = \frac{\kappa}{\sqrt{\zeta}} \int_0^{\pi} \frac{d\Theta}{\sqrt{1 - \kappa^2 \sin^2\Theta}} = \frac{2\kappa K(\kappa)}{\sqrt{\zeta}}, \tag{7.16}$$

where $K(\kappa)$ is the complete elliptic integral of the first kind as defined in (7.7). Phase matching with the pseudopotential $V_m^{\mathrm{L}} = V_o \sum_p \cos(G_m x_p)$ may be stated by $G_m x_p = \Theta_p = 2\pi p/m$, assuming that the pseudospin wave reflects perfectly from the potential barrier V_o. However, depending on the structural detail, V_o is considered as an *inductive* reflector, accompanying a phase shift on reflection. Therefore, the pseudopotential is normally expressed as

$$V_m^{\mathrm{L}} = -V_o \sum_p \cos\{\Theta_p(1 - \delta_p)\}, \tag{7.17}$$

where δ_p is called the *incommensurate parameter*, since the phase matching is not always perfect.

Figure 7.4 illustrates the behavior of Θ_p, as described by $\sin(2\pi p/m) = \mathrm{sn}\sqrt{\zeta}(x - x_o)/\kappa$, against $x - x_o$, showing characteristic lengths $\Lambda(\kappa)$ that determined by (7.16). In the above, we assumed that $\kappa^2 < 1$, which means $E < -\zeta$ by definition. On the other hand, if $E > -\zeta$ we have a case for $\kappa^2 > 1$. If ζ can be ignored, the sine-Gordon equation can be reduced to an equation for free motion; no

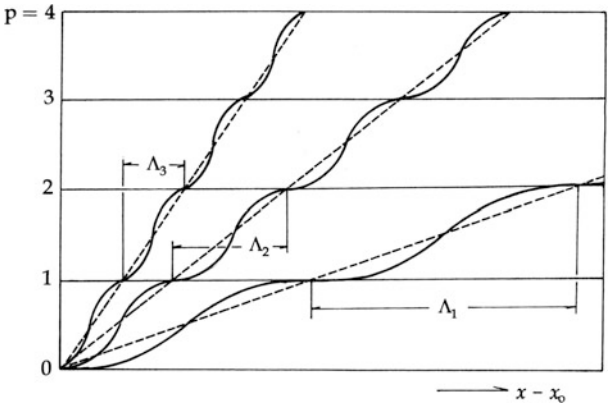

Fig. 7.4 Phase variables of a collective mode pinned by a pseudopotential $V_m(\phi)$.

pinning occurs if $V_m(\phi)$ is disregarded. In this context, the change from $\kappa > 1$ to $\kappa < 1$ with lowering temperature signifies a transition to a mesoscopic phase in commensurate structure.

Although one-dimensional correlations are a valid assumption for anisotropic crystals, experimentally such a model should be evaluated on sample crystals of high quality characterized by a small defect density. For such phase-locking phase transitions in K_2ZnCl_4 and Rb_2ZnCl_4 crystals, Pan and Unruh [16] reported laminar patterns of such *discommensurattion* lines perpendicular to the x-direction after transitions recorded by transmission electron microscopy (TEM). Although there were additional "splittings" and "vortex-like" patterns, the dominant laminar structure in the dark fields is deniable evidence for pseudopotential as discussed in the above.

Exercises 7

1. Derive (7.1b) from the wave equation

$$m\left(\frac{\partial^2}{\partial t^2} - v_o^2 \frac{\partial^2}{\partial x^2}\right)\sigma_k(x,t) = -k\left(a\sigma_k + b\sigma_k^3\right),$$

   using rescaled variables (7.1c).

2. The Lifshitz' theory is based on statistical correlations whose energy is minimized by the variation principle. Although mathematical, the arbitrary variations can be considered as related to thermal fluctuations. If Lifshitz' calculation is performed with this interpretation, the incommensurability should be consistent with observed results obtained with varying temperature. Discuss the validity of Lifshitz' theory for thermal fluctuations.

Chapter 8
The Soliton Theory

The adiabatic potential was discussed in the foregoing for pseudospin correlations in crystalline states. In this chapter, we learn that some aspects of the problem can be analyzed by the soliton theory in better accuracy. Mathematically, solutions of the *Korteweg–deVries equation* are expressed by elliptic functions of the propagating phase. The traditional concept of long-range order in crystalline states can be revised with soliton solutions, which however need to be subjected to phonon scatterings for thermodynamic descriptions. While collective pseudospins are not fully describable in one dimension, the soliton theory can explain the nonlinear propagation in sufficient accuracy.

8.1 A Longitudinal Dispersive Mode of Collective Pseudospins

In the expression $\boldsymbol{\sigma} = \boldsymbol{\sigma}_{\mathrm{o}} \exp \mathrm{i}\phi$ for a collective pseudospin mode, the phase ϕ is independent of the amplitude $\boldsymbol{\sigma}_{\mathrm{o}}$, only if considered as infinitesimal. For a finite $\boldsymbol{\sigma}_{\mathrm{o}}$, on the other hand, the propagation is *dispersive*, for which the speed v is not constant. Physically, there should be an internal force in the crystal; thereby, the transversal component $\boldsymbol{\sigma}_{\perp}$ plays a significant role.

Such a mesoscopic variable $\boldsymbol{\sigma}$ can be considered to represent a classical *vector field* in crystal space, where the propagation at long wavelengths is described by analogy of a continuous fluid. We consider that the pseudospin density ρ and its *conjugate* current density $j = \rho v$ represent a continuous flow at a constant speed v under a constant pressure p. On the other hand, if there is a pressure gradient $-\partial p/\partial x$ along the direction x of propagation, the speed v cannot be constant, resulting in speed-dependent amplitude. In a condensate, the gradient $-\partial p/\partial x$ can be considered to arise from the force $-\partial \Delta U/\partial x$. For a change of the speed v, we can write the equation

$$\frac{\partial v}{\partial t} + v\frac{\partial v}{\partial x} = -\frac{1}{\rho_{\mathrm{o}}}\frac{\partial p}{\partial x}, \tag{i}$$

M. Fujimoto, *Thermodynamics of Crystalline States*,
DOI 10.1007/978-1-4419-6688-9_8, © Springer Science+Business Media, LLC 2010

where $\rho_o = \boldsymbol{\sigma}_o^2$ is a constant density if the nonlinear term $v(\partial v/\partial x)$ can be ignored. However, actually the density ρ is not confined to the x-axis and transversally spread; hence, we can write $\rho_o = \rho_x + \rho_z$ assuming ρ_o as a function of x and z, for which the y-direction is ignored for simplicity. Then, the equations of continuity can be written as

$$\frac{\partial \rho_x}{\partial t} + \rho_o \frac{\partial v}{\partial x} = 0 \quad \text{and} \quad \frac{\partial \rho_z}{\partial t} = 0. \tag{ii}$$

The density ρ_x flows on the x-axis but ρ_z does not propagate along the z-direction, remaining in the vicinity of the axis. We assume that ρ_z satisfy the equation

$$\frac{\partial^2 \rho_z}{\partial t^2} + \alpha(\rho_z - \rho_o) = p, \tag{iii}$$

where α is a restoring force constant.

Equation (i) is nonlinear because of the term $v(\partial v/\partial x)$, whereas (ii) and (iii) are linear equations. We consider $v(\partial v/\partial x)$ as a perturbation, which can be ignored, if (i) is linearized. Both density components ρ_x andρ_z are functions of x and z, but we assume the same amplitude, that is, $|\rho_x| = |\rho_z| = \rho_o$. By introducing a set of reduced variables $x' = \sqrt{\alpha}x, t' = \sqrt{\alpha}t$, and $\rho' = (\rho - \rho_o)/\rho_o$, equations (i), (ii) and (iii) can be linearized as

$$\frac{\partial v}{\partial t'} + \frac{\partial p'}{\partial x'} = 0, \quad \frac{\partial \rho'}{\partial t'} - \frac{\partial v}{\partial x'} = 0, \quad \text{and} \quad \frac{\partial^2 \rho'}{\partial t^2} + \rho' = p', \tag{iv}$$

where $p' = p/\rho_o$ for simplicity. For these linearized equations (iv), the variables, ρ', v, p', an all be proportional to $\exp i(kx' - \omega t')$, where $\omega = vk$. Therefore the dispersion relation

$$\omega^2 = \frac{k^2}{1 + k^2}, \quad \text{or} \quad \omega \approx k - \frac{1}{2}k^3$$

can be obtained for a small k, but the speed v is not a constant. In the expression $\exp i(kx' - \omega t') = \exp i\{k(x' - t') - (1/2)k^3 t'\}$, we write $k(x' - t') = \xi$ and $(1/2)k^3 t' = \tau$, performing a coordinate transformation from (x', t') to (ξ, τ) by differential relations

$$\frac{\partial}{\partial x'} = k\frac{\partial}{\partial \xi} \quad \text{and} \quad \frac{\partial}{\partial t'} = -k\frac{\partial}{\partial \xi} + \frac{1}{2}k^3\frac{\partial}{\partial \tau}. \tag{v}$$

First expressing (i) and (ii) in terms of $x', t'$and p', we obtain

$$\frac{\partial v}{\partial t'} + v\frac{\partial v}{\partial x'} + \frac{\partial p'}{\partial x'} = 0 \quad \text{and} \quad \frac{\partial \rho'}{\partial t'} + \frac{\partial v}{\partial x'} + \frac{\partial(\rho' v)}{\partial x'} = 0.$$

These equations, combined with the last one in (iv), can be transformed by (v) to express them with coordinates ξ and τ. That is

$$\begin{aligned} &-\frac{\partial v}{\partial \xi}+\frac{1}{2}k^2\frac{\partial v}{\partial \tau}+v\frac{\partial v}{\partial \xi}+\frac{\partial p'}{\partial \xi}=0,\\ &-\frac{\partial \rho'}{\partial \xi}+\frac{1}{2}k^2\frac{\partial \rho'}{\partial \tau}+\frac{\partial v}{\partial \xi}+\frac{\partial(\rho' v)}{\partial \xi}=0,\\ &p'=\rho'+k^2\frac{\partial^2\rho'}{\partial \xi^2}-k^4\frac{\partial^2\rho'}{\partial \xi\partial \tau}+\frac{1}{4}k^6\frac{\partial^2\rho'}{\partial \tau^2}. \end{aligned} \tag{vi}$$

Here, quantities ρ', p', and $v - v_o$ that emerge at T_c can be expressed in power series with respect to small k^2, which are written in asymptotic form

$$\rho' = k^2{\rho_1}' + k^4{\rho_2}' + \cdots,$$

$$p' = k^2{p_1}' + k^4{p_2}' + \cdots,$$

and

$$v - v_o = k^2 v_1 + k^4 v_2 + \cdots.$$

Substituting these expansions for ρ', p', and v' in (vi), we compare coefficients of terms k^2, k^4,... separately.

From the factors proportional to k^2, we obtain

$$-\frac{\partial {\rho_1}'}{\partial \xi}+\frac{\partial v_1}{\partial \xi}=0, \quad -\frac{\partial v_1}{\partial \xi}+\frac{\partial {p_1}'}{\partial \xi}=0, \quad \text{and} \quad {p_1}' = {\rho_1}'.$$

After combining the first two relations, the third one can be expressed as

$${p_1}' = {\rho_1}' = v_1 + \varphi(\tau), \tag{vii}$$

where $\varphi(\tau)$ is an arbitrary function of τ.

Next, comparing coefficients in the k^4 terms, we obtain

$$-\frac{\partial {\rho_2}'}{\partial \xi}+\frac{1}{2}\frac{\partial {\rho_1}'}{\partial \tau}+\frac{\partial v_2}{\partial \xi}+\frac{\partial({\rho_1}' v_1)}{\partial \xi}=0,$$

$$-\frac{\partial v_2}{\partial \xi}+\frac{1}{2}\frac{\partial v_1}{\partial \tau}+v_1\frac{\partial v_1}{\partial \xi}+\frac{\partial {p_2}'}{\partial \xi}=0,$$

and

$${p_2}' = {\rho_2}' + \frac{\partial^2 {\rho_1}'}{\partial \xi^2}.$$

Eliminating ρ_2', v_2, and p_2' from these equations, we arrive at the relations for ρ_1', v_1, and p_1', that is,

$$\frac{\partial v_1}{\partial \tau} + 3v_1 \frac{\partial v_1}{\partial \xi} + \frac{\partial^3 v_1}{\partial \xi^3} + \varphi \frac{\partial v_1}{\partial \xi} + \frac{\partial \varphi}{\partial \tau} = 0,$$

and

$$\frac{\partial \rho_1'}{\partial \tau} + 3\rho_1' \frac{\partial \rho_1'}{\partial \xi} + \frac{\partial^3 \rho_1'}{\partial \xi^3} - \varphi \frac{\partial \rho_1'}{\partial \xi} - \frac{\partial \varphi}{\partial \tau} = 0.$$

Note that these equations for $v_1$and ρ_1' become identical, if the function $\varphi(\tau)$ is chosen to satisfy the relation

$$\varphi \frac{\partial(\rho_1', v_1)}{\partial \xi} + \frac{\partial \varphi}{\partial \tau} = 0.$$

Due to (vii), we notice that p_1' also satisfies this equation for v_1 or ρ_1'. We can therefore write the equation

$$\frac{\partial V_1}{\partial \tau} + 3V_1 \frac{\partial V_1}{\partial \xi} + \frac{\partial^3 V_1}{\partial \xi^3} = 0, \tag{8.1}$$

where V_1 represents v_1', ρ_1', and p_1' that are functions of ξ and τ. This equation is known as the Korteweg–deVries equation. By definition, ξ is a modified phase of propagation, whereas τ signifies evolving nonlinearity. It is noted that τ is not necessarily the *real time*, but representing any parameter for evolving the nonlinear process such as temperature if considering thermodynamic environment. The quantity $k^2 V_1$ is called a *soliton* because it exhibits a particle-like behavior, as will be explained later. In this approximation, it is significant that the mesoscopic pseudospin mode is driven in phase by an adiabatic force with increasing nonlinearity.

In the above, we discussed a one-dimensional chain of classical pseudospins by analogy of fluid, for which a pressure gradient $-\partial p/\partial x$ can be interpreted as related with $\partial p'/\partial \xi = k^2(\partial^3 \rho_1'/\partial \xi^3)$ in the accuracy of k^4. In this hydrodynamic approach, the pressure p can be considered as a force related to "viscous correlations" among pseudospins.

8.2 The Korteweg–deVries Equation

In this section, we continue to discuss the function $\boldsymbol{\sigma}(\phi)$ in one dimension, taking only a longitudinal component for simplicity. We can disregard the time t in $\boldsymbol{\sigma}(x, t)$ to write it simply as $\boldsymbol{\sigma}(x)$, which is legitimate because the coordinate

transformation $x - v_o t \to x$ makes the coordinate system stationary with respect to x. In such a moving frame of reference $\boldsymbol{\sigma}(x)$ represents a mesoscopic pseudospin $\boldsymbol{\sigma}(x)$, for which we have the differential equation

$$\mathcal{D}^2\boldsymbol{\sigma}(x) = \varepsilon_o\boldsymbol{\sigma}(x), \tag{8.2}$$

where $\mathcal{D} = \partial/\partial x$ is a *differential operator*, and the eigenvalue ε_o representing the kinetic energy of propagation.

We consider a problem of finding such a potential $V(x)$ that makes the eigenvalue ε_o unchanged. In the presence of $V(x)$, (8.2) should be modified as

$$\mathcal{L}\boldsymbol{\sigma} = (\mathcal{D}^2 + V)\boldsymbol{\sigma} = \varepsilon\boldsymbol{\sigma}, \tag{8.3}$$

on which we impose the condition $\varepsilon = \varepsilon_o$, that is, $\mathrm{d}\varepsilon/\mathrm{d}\tau = 0$ with respect to the variable τ.

On the other hand, the nonlinearity of $\boldsymbol{\sigma}$ may evolve as described by the equation

$$\frac{\partial}{\partial\tau}\boldsymbol{\sigma}(x,\tau) = \mathcal{B}\boldsymbol{\sigma}(x,\tau), \tag{8.4}$$

where $\mathcal{B}$ is an operator function of $\mathcal{D}$, and τ is the variable for changing state of $\boldsymbol{\sigma}(x,\tau)$.

Suppose $\mathcal{B}$ is given in a simple form $\mathcal{B}_1 = c\mathcal{D}$, we obtain $\boldsymbol{\sigma}_\tau = c\boldsymbol{\sigma}_x$ from (8.3), signifying that σ is simply a function of $x - c\tau$. The $\mathcal{D}^2$ operator satisfies (8.2) where the eigenvalue ε_o is invariant, so that it is not considered for developing the nonlinearity. In contrast, if $\mathcal{B}$ is involved as proportional to $\mathcal{B}^3$, we can verify that a significant potential $V(x,\tau)$ may emerge from (8.3).

The wave equation can be expressed as

$$\mathcal{L}\boldsymbol{\sigma}(x,\tau) = \big\{\mathcal{D}^2 + V(x,\tau)\big\}\boldsymbol{\sigma}(x,\tau) = \varepsilon\boldsymbol{\sigma}(x,\tau) = \varepsilon_o\boldsymbol{\sigma}(x,\tau), \tag{8.5}$$

For convenience, differentiations are shorthanded by such suffixes as $\partial V/\partial x = V_x$, $\partial^2 V/\partial x^2 = V_{xx}$, etc. in the following arguments. Differentiating (8.4) with respect to τ, we have

$$\frac{\partial}{\partial\tau}(\mathcal{L}\boldsymbol{\sigma}) = \mathcal{L}_\tau\boldsymbol{\sigma} + \mathcal{L}\boldsymbol{\sigma}_\tau = -V_\tau\boldsymbol{\sigma} + \mathcal{L}B\boldsymbol{\sigma},$$

and

$$\frac{\partial}{\partial\tau}(\varepsilon\boldsymbol{\sigma}) = \varepsilon_\tau\boldsymbol{\sigma} + \varepsilon\boldsymbol{\sigma}_\tau = \varepsilon_\tau\boldsymbol{\sigma} + \varepsilon(\mathcal{B}\boldsymbol{\sigma}) = \varepsilon_\tau\boldsymbol{\sigma} + \mathcal{B}\mathcal{L}\boldsymbol{\sigma}.$$

Therefore

$$(-V_\tau + [\mathcal{L}, \mathcal{B}])\boldsymbol{\sigma} = \varepsilon_\tau \boldsymbol{\sigma}, \quad \text{where} \quad [\mathcal{L}, \mathcal{B}] = \mathcal{L}\mathcal{B} - \mathcal{B}\mathcal{L}$$

.

If the condition $\varepsilon_\tau = 0$ is fulfilled, the equation to be solved for V is given by

$$(-V_\tau + [\mathcal{L}, \mathcal{B}])\boldsymbol{\sigma}(x, \tau) = 0. \tag{8.6}$$

Assuming $\mathcal{B} = \mathcal{B}_3 = a\mathcal{D}^3 + c\mathcal{D} + b$ with a constant a, and variable coefficients b and c that are functions of x and τ, we have

$$[\mathcal{L}, \mathcal{B}_3]\boldsymbol{\sigma} = (2c_x + 3aV_x)\mathcal{D}^2\boldsymbol{\sigma} + (c_{xx} + 2b_x + 3aV_{xx})\mathcal{D}\boldsymbol{\sigma} + (b_{xx} + aV_{xxx} + cV_x)\boldsymbol{\sigma}.$$

To obtain a differential equation for $V(x - c\tau)$ from (8.5), the coefficients of $\mathcal{D}^2\boldsymbol{\sigma}$ and $\mathcal{D}\boldsymbol{\sigma}$ should vanish, so that we have

$$2c_x + 3aV_x = 0 \quad \text{and} \quad c_{xx} + 2b_x + 3aV_{xx} = 0.$$

Integrating these expressions, the coefficients $c$and b can be determined as

$$c = -\frac{3}{2}aV + C \quad \text{and} \quad b = -\frac{3}{4}aV_x + B,$$

where C and B are constants of integration.

Consequently, $[\mathcal{L}, \mathcal{B}_3]\boldsymbol{\sigma} = \{(a/4)(V_{xxx} - 6VV_x) + CV_x\}\boldsymbol{\sigma}$, and (8.6) can be expressed as

$$\frac{a}{4}(V_{xxx} - 6VV_x)\boldsymbol{\sigma} + (CV_x - V_\tau)\boldsymbol{\sigma} = 0.$$

Transforming variables (x, τ) back to $(x - c\tau, \tau)$, and setting $C = 0$ and $a = -4$, this equation can be expressed as

$$V_\tau - 6VV_x + V_{xxx} = 0. \tag{8.7}$$

This is the standard form of the Korteweg–deVries equation for the potential $V(x, \tau)$. As mentioned earlier, the corresponding pseudospin variable is in phase with $V(x, \tau)$, sharing a common equation of propagation with the same eigenvalue ε_o. Noting that the evolving equation is $\boldsymbol{\sigma}_\tau = (-4\mathcal{D}^3 + 6V\mathcal{D} + 3V_x + B)\boldsymbol{\sigma}$, where the phase can be expressed by $x - \alpha\tau$ with an arbitrary constant α· Interpreting it for a thermodynamic application, the constant α is the speed for the dispersive propagation and the variable τ can represent an energy transfer rate to the heat reservoir.

8.3 Solutions of the Korteweg–deVries Equation

Equation (8.7) can be analytically solved for the potential $V(x-\alpha\tau)$. Since such a potential is stationary in the frame of reference at a constant phase, we require the condition $\partial V/\partial(x-\alpha\tau)=0$, and hence $V_\tau=\alpha V_x$. Therefore, (8.7) can be written as $\alpha V_x-6VV_x+V_{xxx}=0$, that is,

$$\alpha V_x-3\frac{\mathrm{d}V^2}{\mathrm{d}x}+\frac{\mathrm{d}V_{xx}}{\mathrm{d}x}=0.$$

This can be integrated as

$$V_{xx}=3V^2-\alpha V+a,$$

where a is a constant of integration. Multiplying by V_x, this equation can be integrated once more, resulting in

$$V_x^2=2V^3-\alpha V^2+2aV+b,$$

where b is another constant. The right-hand side is algebraically an expression of third order with respect to V, and hence we can write it as

$$V_x^2=-2(V-V_1)(V-V_2)(V-V_3).$$

Here, V_1, V_2, and V_3 are three roots of the third-order equation $V_x^2(V)=0$. Illustrated in Fig. 8.1 are curves of the equation $-V_x^2=0$ plotted against V, which can cross the horizontal axis at three points V_1, V_2, and V_3, if they are all real (case A); otherwise at two real roots (case B) or only at one point (not shown). Since our

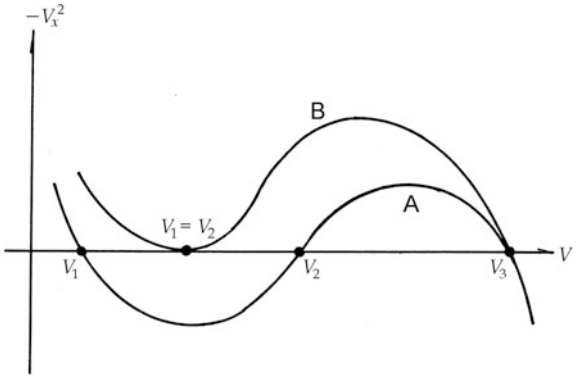

Fig. 8.1 Solving the Korteweg–deVries equation. Oscillatory and solitary solutions are represented by the curves A and B, respectively.

interest is only in a real V_x, we take the region $V_2<V<V_3$ of a curve A as a significant part for our purpose, which is characterized by $-V_x^2 > 0$.

We redefine the variable V by setting $V - V_3 = -g$ for the above third-order equation, which can then be expressed as

$$g_x^2 = 2g(V_3 - V_1 - g)(V_3 - V_2 - g).$$

Further, introducing another variable ξ by $g = (V_3 - V_2)\xi^2$, we obtain

$$\xi_x^2 = \frac{1}{2}(V_3 - V_1)(1 - \xi^2)(1 - \kappa^2\xi^2) \quad \text{where} \quad \kappa^2 = \frac{V_3 - V_2}{V_3 - V_1}.$$

By using a phase variable defined by $\phi = \sqrt{V_3 - V_1}x$, this can be modified as

$$2\xi_\phi^2 = (1 - \xi^2)(1 - \kappa^2\xi^2).$$

This can be written as a function in integral form

$$\frac{\phi_1}{\sqrt{2}} = \int_0^{\xi_1} \frac{d\xi}{\sqrt{(1 - \xi^2)(1 - \kappa^2\xi^2)}}, \tag{8.8a}$$

where the phase ϕ_1 is determined by the upper limit ξ_1 of this integral. Or in the reverse form, Jacobi's sn-function can be defined from (8.8a), that is,

$$\xi_1 = \mathrm{sn}\left(\frac{\phi_1}{\sqrt{2}}; \kappa\right). \tag{8.8b}$$

In previous notations, the soliton potential is expressed by

$$V(\phi) = V_3 - (V_3 - V_2)\mathrm{sn}^2(\sqrt{V_3 - V_1}\phi; \kappa) \quad \text{for} \quad 0 < \kappa < 1, \tag{8.9a}$$

where the sn^2-function is periodic with the period defined

$$2K(\kappa) = 2\int_0^1 \frac{d\xi}{\sqrt{(1 - \xi^2)(1 - \kappa^2\xi^2)}}.$$

On the other hand, the potential $V(\phi)$ in (8.9a) has an oscillating interval of $2K(\kappa)/\sqrt{V_3 - V_2}$, corresponding a finite amplitude $V_3 - V_2$. If $V_2 \to V_1$, we have the curve B in Fig. 8.1, for which $\kappa \to 1$ and $K(1) = \infty$. In this case, the potential is

$$V(\phi) = V_3 + (V_3 - V_2)\,\mathrm{sech}^2(\sqrt{V_3 - V_1}\phi). \tag{8.9b}$$

This shows a pulse-shaped potential with a height $V_3 - V_2$, propagating with effective phase $\sqrt{V_3 - V_1}\phi$. Specifically if $V_3 - V_2$ is infinitesimal, the modulus κ is almost zero; (8.9a) exhibits a sinusoidal variation

$$V(\phi) = V_3 + (V_3 - V_2)\sin^2(\sqrt{V_3 - V_1}\phi).$$

It is noted that the coefficients in (8.9a) and (8.9b) are related with the modulus κ. By definition $V_3 - V_2 = \kappa^2(V_3 - V_1)$, and hence the amplitude $V_3 - V_2$ is proportional to κ^2. Adjusting values of $V_1, V_2,$ and V_3, the potential $V(\phi)$ can be made as consistent with adiabatic potentials derived in Chap. 7.

Thus, solutions of the Korteweg–deVries equation are expressed by elliptic functions of a propagating phase, either oscillatory or in a pulse shape, depending on the modulus κ. Particularly, a solitary potential of (8.9b) is known as the *Eckart potential*. Such potentials behave like independent particles in a system of many solitons, which can be proven in more rigorous manner. Nevertheless, we are not going into the mathematical detail in this book, accepting the results.

Physically, the transverse density component ρ_z can be responsible for dispersive longitudinal $\boldsymbol{\sigma}_1$ mode; mathematically the relation between $\rho_z(\phi)$ and the soliton potential $V(\phi)$ was confirmed from the Korteweg–deVries equation. Further, in the above theory we consider $V(\phi)$ only as a scalar, but it should reflect symmetry of the adiabatic potential. In fact, in Sect. 8.1 we assumed $|\rho_x(\phi)| = |\rho_z(\phi')|$, ignoring the phase difference between ϕ and ϕ' of $\boldsymbol{\sigma}_x$ and $\boldsymbol{\sigma}_z$ components, respectively. However, taking (8.9a) for the potential for the longitudinal density $\rho_x(\phi)$, the potential

$$V(\phi') = V_2 + (V_3 - V_2)\mathrm{cn}^2(\sqrt{V_3 - V_1}\phi';\ \kappa'), \tag{8.10}$$

can be considered for the transversal density $\rho_z(\phi')$. In the above, the direction z is set arbitrarily perpendicular to x, however the choice should be decided according to the lattice symmetry in a given crystal. Also, owing to anisotropic correlations, the modulus κ' in (8.10) is not necessarily the same as κ for (8.9a). In order for the potentials (8.9a) and (8.10) to constitute the net potential for the vector $\boldsymbol{\sigma}$, the phase difference must be determined by $\phi - \phi' = K$, so that the adiabatic potential for $\boldsymbol{\sigma}$ should be given by

$$\Delta U(\boldsymbol{\sigma}) = V(\phi) + V_\perp(\phi - K), \tag{8.11}$$

where $V_\perp$ is for (8.10) acting on the transversal density.

Actually, Jacobi's elliptic functions can be expanded into power series as in Landau's expansion that can be truncated at a quartic term $\boldsymbol{\sigma}^4$ (see Appendix). It is therefore logical to consider for the Landau theory that the soliton potential is given by (8.11). The truncated potential can be expressed as $\Delta U = (a/2)\sigma^2 + (b/4)\sigma^4$ in the adiabatic approximation. Such a soliton interpretation of Landau's expansion owes the operator $\mathcal{B}_3$ that signifies the dispersive nature of the evolving equation

(8.4). At any rate, either elliptic or quartic potential is useful for practical analysis of mesoscopic variables.

It is notable that the soliton potential (8.9b) can be used for describing a domain wall, at which the component $\boldsymbol{\sigma}_1(\phi)$ for $\kappa = 1$ becomes singular at $\phi = 0$, where the direction is reversed with an energy proportional to $\boldsymbol{\sigma}_\perp^2$. In this interpretation, the adiabatic potential $\Delta U(\boldsymbol{\sigma}_\perp)$ in 7.9b represents the domain-wall energy in the limit of $\kappa \to 1$.

8.4 Cnoidal Theorem and the Eckart Potential

It is significant that adiabatic potentials obtained from the Korteweg–deVries equation are *conformable* with the order variable density; both are signified by the propagating phase $\phi = x - \alpha\tau$. Furthermore, by the coordinate transformation $x - \alpha\tau \to x'$, the potential $V(x')$ becomes always in phase with the order density $\boldsymbol{\sigma}(x')^2$ in the system of x'. Therefore omitting τ, we can express these as $V(x, \kappa)$ and $\boldsymbol{\sigma}(x, \kappa)^2$ for mathematical convenience.

The Eckart's potential (8.8b) characterized by a solitary peak can be written as

$$V(x) = -V_o \mathrm{sech}^2\left(\frac{x}{d}\right) \quad \text{for} \quad \kappa = 1. \tag{8.12}$$

excluding the constant term, where d is introduced to indicate the width $2d$ of the symmetric peak around $x = 0$, as shown in Fig. 8.2a. It is noted that (8.12) is related to 7.8b, whose transverse character is explicit in both; hence, the corresponding pseudospin component can be written as $\boldsymbol{\sigma}_\perp(x/d)$.

In contrast, the oscillatory potential (8.9a) is periodic in space. Although expressed as sn^2 for $0 < \kappa < 1$, such a potential is essentially the same as cn^2-function, because of the relation $\mathrm{sn}^2 + \mathrm{cn}^2 = 1$. In Chap. 7 we have shown that the transverse component $\boldsymbol{\sigma}_\perp(x, \kappa)$ is in motion with an adiabatic cnoidal potential:

$$V(x, \kappa) = -V_o \mathrm{dn}^2 u(x, \kappa), \tag{8.13a}$$

where V_o is a proportionalty constant. Because of the relation $\mathrm{dn}^2 u = 1 - \kappa^2 \mathrm{sn}^2 u$, (8.13a) gives an identical potential

$$V(x, \kappa) = -V_o \kappa^2 \mathrm{sn}^2 u(x, \kappa), \tag{8.13b}$$

ignoring the additive constant. In any case, all of these squared elliptic functions represent the periodic curve, called a *cnoidal* curve as sketched in Fig. 8.2b. For a physical application, the additive constant remains trivial, and hence the adiabatic potential $\Delta U(\boldsymbol{\sigma})$ is expressed by (8.13a) or (8.13b).

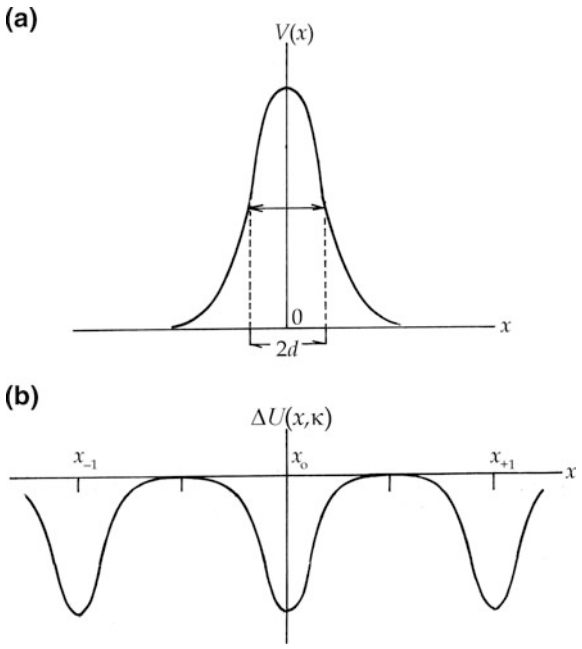

Fig. 8.2 (**a**) Eckart's potential of the half-width $2d$. (**b**) A sketch of a cnoidal potential $\mathrm{cn}^2(\phi/\sqrt{2}\kappa)$ with periodic peaks.

At this point, we introduce a mathematical theorem for a sn^2 function, stating that each peak of cnoidal expansion can be replaced by a $\mathrm{sec\,h}^2$ potential. The rigorous proof is too complex at the present level of mathematical theory; we only quote the resulting formula for the present discussions. The theorem states that

$$2\kappa^2 \mathrm{sn}^2 x = -2a \sum_{m=-\infty}^{m=+\infty} \mathrm{sech}^2(\sqrt{a}x - cm) + \text{constant}, \tag{8.14}$$

where

$$a = \frac{\pi^2}{4K'(\kappa)^2}, \quad c = \frac{\pi K(\kappa)}{K'(\kappa)}, \quad \text{and} \quad K'(\kappa) = K(\sqrt{1-\kappa^2}).$$

Here, m specifies the peak positions x_m along the x-axis for $-\infty < m < +\infty$; $K(\kappa)$ is the complete elliptic integral (7.7). Readers interested in the derivation of (8.12) should be directed to consult a standard textbook on elliptic functions. Owing to (8.14), the cnoidal potential can be replaced by a periodic array of Eckart's potentials that are located at $x = (c/\sqrt{a})\mathrm{m}$.

By virtue of this theorem, problems related to the oscillatory potential can be reduced to Eckart's potential as discussed in the next section.

8.5 Condensate Pinning by the Eckart Potentials

In this section, we discuss the eigenvalue problem of $\boldsymbol{\sigma}(x,\kappa)$ in the Eckart's potential field $V(x,\kappa)$. Denoting the eigenvalue by ε, the perturbed wave equation can be written as

$$\frac{\mathrm{d}^2\boldsymbol{\sigma}(x)}{\mathrm{d}x^2}+\left(\varepsilon+V_{\mathrm{o}}\mathrm{sech}^2\frac{x}{d}\right)\boldsymbol{\sigma}(x)=0.$$

For a stable pinning, the eigenvalue should be negative, so that we write $\varepsilon=-\mu^2\cdot$ Replacing x/d by x, and setting $V_{\mathrm{o}}d^2=v_{\mathrm{o}}$ and $\mu^2\mathrm{d}^2=\beta^2$, this equation can be expressed as

$$\frac{\mathrm{d}^2\boldsymbol{\sigma}(x)}{\mathrm{d}x^2}+(-\beta^2+\mathrm{v_o}\mathrm{sech}^2x)\boldsymbol{\sigma}(x)=0. \tag{8.15}$$

This is a familiar differential equation in Mathematical Physics, whose solution is expressed by *hypergeometric series*. Following Morse and Feshbach [17], we transform (8.15) to the hypergeometric equation in standard form.

By defining the relation $\boldsymbol{\sigma}(x)=Af(x)\mathrm{sech}^{\beta}x$, the differential equation for the function $f(x)$ can be obtained as

$$\frac{\mathrm{d}^2f}{\mathrm{d}x^2}-2\beta(\tanh x)\frac{\mathrm{d}f}{\mathrm{d}x}+(v_o-\beta^2-\beta)(\mathrm{sech}^2x)f(x)=0.$$

This can further be re-expressed in terms of another variable $\zeta=(1/2)(1-\tanh x)$ as

$$\zeta(1-\zeta)\frac{\mathrm{d}^2f}{\mathrm{d}\zeta^2}+(1+\beta)(1-2\zeta)\frac{\mathrm{d}f}{\mathrm{d}\zeta}+(v_{\mathrm{o}}-\beta^2-\beta)f(x)=0.$$

Then, we define such parameters **a**, **b**, and **c** that satisfy the relations

$$\mathbf{a}+\mathbf{b}=2\mathbf{c}-1,$$

where

$$\mathbf{c}=1+\beta\quad\text{and}\quad\mathbf{ab}=-v_{\mathrm{o}}+\beta^2-\beta;$$

that is,

$$\mathbf{a},\mathbf{b}=\frac{1}{2}+\beta\pm\sqrt{v_{\mathrm{o}}+\frac{1}{4}}.$$

Using **a**, **b**, and **c**, we obtain the hypergeometric equation expressed in standard form, that is,

$$\zeta(1-\zeta)\frac{\mathrm{d}^2 f}{\mathrm{d}\zeta^2}+\{c-(\mathbf{a}+\mathbf{b}+1)\zeta\}\frac{\mathrm{d}f}{\mathrm{d}\zeta}-\mathbf{ab}f=0. \tag{8.16}$$

Expressing as $f(\zeta)=F(\mathbf{a},\mathbf{b},\mathbf{c};\zeta)$, the solution of (8.16) is called a *hypergeometric function*.

The mesoscopic pseudospin variable $\boldsymbol{\sigma}(x,\kappa)$ can then be expressed as

$$\boldsymbol{\sigma}(x)=A\mathrm{sech}^{\beta}(x)F(\mathbf{a},\mathbf{b},\mathbf{c};\zeta). \tag{8.17}$$

However, we are only interested in extreme cases that can be specified by $\zeta\to 0$ and $\zeta\to 1$, in order to interpret them physically at far distances, for which we use the expansion formula:

$$F(\mathbf{a},\mathbf{b},\mathbf{c};\zeta)=1+\frac{\mathbf{ab}}{1!\mathbf{c}}\zeta+\frac{\mathbf{a}(\mathbf{a}+1)\mathbf{b}(\mathbf{b}+1)}{2!\mathbf{c}(\mathbf{c}+1)}\zeta^2+\cdots. \tag{8.18}$$

In the former case, we consider $x\to\infty$ corresponding to $\zeta\to 0$, and hence

$$\boldsymbol{\sigma}(x)_{x\to+\infty}\to A\,2^{\beta}\exp(-\beta x).$$

In the latter case of $\zeta\to 1$, we consider $x\to-\infty$

For calculating $\boldsymbol{\sigma}(x)$ in these cases, it is convenient to use the following formula [18]:

$$\begin{aligned}F(\mathbf{a},\mathbf{b},\mathbf{c};\zeta)=&\frac{\Gamma(\mathbf{c})\Gamma(\mathbf{c}-\mathbf{a}-\mathbf{b})}{\Gamma(\mathbf{c}-\mathbf{a})\Gamma(\mathbf{c}-\mathbf{b})}F(\mathbf{a},\mathbf{b},\mathbf{a}+\mathbf{b}-\mathbf{c}+1;\zeta)\\ +(1-\zeta)^{c-a-b}&\frac{\Gamma(\mathbf{c})\Gamma(\mathbf{a}+\mathbf{b}-\mathbf{c})}{\Gamma(\mathbf{a})\Gamma(\mathbf{b})}F(\mathbf{c}-\mathbf{a},\mathbf{c}-\mathbf{b},\mathbf{c}-\mathbf{a}-\mathbf{b}+1;1-\zeta),\end{aligned}$$

where $\Gamma(\cdots)$ are *gamma functions*. It is noted from (8.15) that the first term dominates $F(\mathbf{a},\mathbf{b},\mathbf{c};\zeta)$, if $\zeta\to 0$. On the other hand, if $\zeta\to 1$ we have $(1-\zeta)^{c-a-b}\approx 2^{\beta}\exp(-\beta x)$ and $F(\cdots;1-\zeta)\to 1$ in the second term, which dominates $F(\mathbf{a},\mathbf{b},\mathbf{c};\zeta)$. Considering a small value of β, we approximate that $\mathrm{sech}^{\beta}x\approx 2^{\beta}\exp(+\beta x)$ and $F(\mathbf{a},\mathbf{b},1+\beta;\zeta)\to 1$ in the first term. In this case, by using $\beta=-ik$ to express propagating waves we can write that

$$\begin{aligned}\boldsymbol{\sigma}(x)_{x\to+\infty}\propto&\frac{\Gamma(\mathbf{c})\Gamma(\mathbf{a}+\mathbf{b}-\mathbf{c})}{\Gamma(\mathbf{a})\Gamma(\mathbf{b})}\exp(+\mathrm{i}kx)+\frac{\Gamma(\mathbf{c})\Gamma(\mathbf{c}-\mathbf{a}-\mathbf{b})}{\Gamma(\mathbf{c}-\mathbf{a})\Gamma(\mathbf{c}-\mathbf{b})}\\ &\times\exp(-\mathrm{i}kx).\end{aligned} \tag{8.19}$$

Using expressions for **a**, **b**, and **c**, we notice that the numerators of these coefficients are $\Gamma(1+\beta)\Gamma(-\beta)$ and $\Gamma(1+\beta)\Gamma(\beta)$, respectively, whereas the denominators have singularities, depending on the value of v_o. In Fig. 8.3 shown is the curve of a gamma function $\Gamma(z)$ plotted against the variable z, where there are a number of poles at $z = 0, -1, -2, \ldots$. Hence, the first coefficient has singularities at

$$\mathbf{a}, \mathbf{b} = \frac{1}{2} + \beta \pm \sqrt{v_o + \frac{1}{4}} = -m, \quad m = 0, -1, -2, \ldots, \tag{i}$$

whereas the second coefficient can be specified by singularities for the denominator to become infinity, that is,

$$\Gamma(\mathbf{c}-\mathbf{a})\Gamma(\mathbf{c}-\mathbf{b}) = \Gamma\left(\frac{1}{2} + \sqrt{v_o + \frac{1}{4}}\right)\Gamma\left(\frac{1}{2} - \sqrt{v_o + \frac{1}{4}}\right) = \frac{\pi}{\cos\left(\pi\sqrt{v_o + \frac{1}{4}}\right)}$$

$$= \infty,$$

hence

$$\sqrt{v_o + \frac{1}{4}} = n + \frac{1}{2} \quad \text{or} \quad v_o = n(n+1), \tag{ii}$$

where n can be any integer. Combining (i) and (ii), we obtain

$$\beta = \left(n + \frac{1}{2}\right) - m - \frac{1}{2} = n - m, \tag{iii}$$

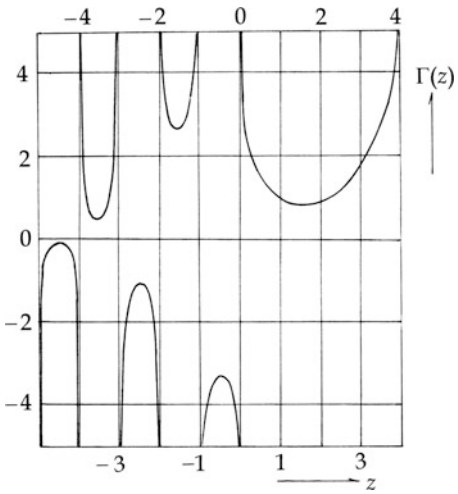

Fig. 8.3 Gamma function $\Gamma(z)$.

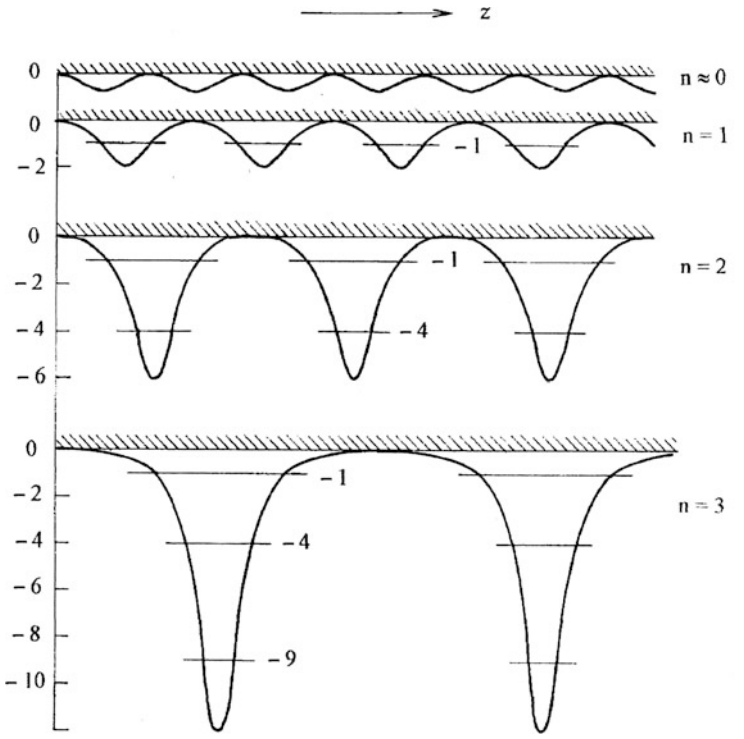

Fig. 8.4 Soliton levels in cnoidal potentials.

where $m = 0, 1, 2, \ldots, n-1$. Therefore the eigenvalues for $\beta > 0$ can be represented as $\beta_p = p = n, n-1, n-2, \ldots, 1$.

Imposing conditions for no transmission and reflection on (8.19), the pseudospin wave $\boldsymbol{\sigma}(x)$ can be in phase with the soliton potential, if $\rho(x)$ and $V(x)$ are conformal with integers specified by (i) and (ii). Therefore, by expressing the potential by eigenvalues p, the steady-state equation (8.15) for longitudinal wave functions $\boldsymbol{\sigma}_p(x)$ can be written as

$$\frac{\mathrm{d}^2\boldsymbol{\sigma}_p(x)}{\mathrm{d}x^2} + \left\{-\beta_p^2 + p(p+1)\mathrm{sech}^2 x\right\}\boldsymbol{\sigma}_p(x) = 0, \tag{iv}$$

where discrete eigenvalues $\varepsilon_p = -\beta_p^2$ can be determined by $\beta_p^2 = p^2$ that are indexed by $p = n, n-1, n-2, \ldots, 2, 1$. Writing the equation (iv) for two adjacent levels at n and $n-1$, we have

$$\frac{\mathrm{d}^2\boldsymbol{\sigma}_p}{\mathrm{d}x^2} + \left\{-p^2 + p(p+1)\mathrm{sech}^2 x\right\}\boldsymbol{\sigma}_p = 0$$

and

$$\frac{\mathrm{d}^2\boldsymbol{\sigma}_{p-1}}{\mathrm{d}x^2} + \left\{-(p-1)^2 + (p-1)p\mathrm{sech}^2 x\right\}\boldsymbol{\sigma}_{p-1} = 0.$$

Hence, for a change $\boldsymbol{\sigma}_{p-1} \rightarrow \boldsymbol{\sigma}_p$ the potential value decreases by $\Delta V_{p-1,p} = -2p\mathrm{sech}^2 x$. We consider that such transitions can take place as a thermal relaxation process with varying temperature. Dynamically inaccessible though, such transitions can be observed thermodynamically through interactions with the lattice. Corresponding lattice displacements u_p are subjected to phonon scatterings, resulting in relaxation processes between strained energies related to u_p^2 and u_{p-1}^2 that are proportional to T_p and T_{p-1}, respectively, using the equipartition theorem.

In Fig. 8.4, we show a change of the periodic potential (8.13b) with lowering temperature, where eigenvalues of the pseudospin density are indicated in each of periodic Eckart's potentials. Although not indicated in the figure, the density levels are actually in band structure whose widths are significantly broader at smaller n. In this context, it is reasonable to say that thermal relaxation processes are responsible for these transitions toward the lowest level determined by n^2 in each potential well.

8.6 Remarks on the Soliton Potential

In the foregoing theory, the soliton potential is derived mathematically for invariant eigenvalues of propagating pseudospins. Physically, it is clear that such a potential for the phase variable represents the correlation energy of pseudospins in the whole crystal, although we may write it as $\Delta U = -\sum_{i \neq j} J_{ij}\boldsymbol{\sigma}_i.\boldsymbol{\sigma}_j$. Formally, such a correlation energy as expressed by $\Delta U(\boldsymbol{\sigma}_1, \boldsymbol{\sigma}_2, ..., \boldsymbol{\sigma}_N)$ can be introduced by a canonical transformation from the Hamiltonian of independent $\boldsymbol{\sigma}_i$ and their conjugate momenta at sufficiently low temperatures; however, it is considered as sufficient for the present discussion that ΔU is so identified physically, being responsible for a modified lattice structure.

Exercises 8

1. Consider a one-dimensional oscillator, where the spring force F is given in a nonharmonic relation with the displacement x. Assuming $F = -ax - bx^3$, the equation of motion can be expressed as $m\ddot{x} = -ax - bx^3$. Replacing $\sqrt{a/m}t$ and $\sqrt{b/a}x$ by t and x, respectively, we write the equation as

$$\frac{\mathrm{d}^2 x}{\mathrm{d}t^2} = -x - x^3.$$

Integrating this equation, we obtain

$$\frac{1}{2}\left(\frac{\mathrm{d}x}{\mathrm{d}t}\right)^2 = E - \frac{x^2}{2} - \frac{x^4}{4},$$

where E is the integration constant. In this case, if $U = (x^2/2) + (x^4/4)$ is the potential energy, we have the energy conservation law $E =$ constant. Show the solution of the above non-linear equation is given by an elliptic function.
Answer. Solving the above for $\dot{x}$, we can write

$$t = \pm \int_0^x \frac{\mathrm{d}x}{\sqrt{2E - x^2 - (1/2)x^4}}.$$

Noting that the quantity inside the square root must be positive for a real solution, we assume that the motion is limited within a range $-a \le x \le +a$, where $E \le U$, as illustrated in Fig. 8.5a. Such limits $\pm a$ are determined by

$$a^4 + 2a^2 - 4E = 0 \quad \text{or} \quad a^2 = -1 + \sqrt{1 = 4E}.$$

Using a, we can write

$$2E - x^2 - \tfrac{1}{2}x^4 = \left(a^2 - x^2\right)\left(2 + a^2 + x^2\right).$$

Therefore, setting $x = a\cos\Theta$,

$$\mathrm{t}_1 = \pm \frac{1}{\sqrt{1 + a^2}} \int_0^{\Theta_1} \frac{\mathrm{d}\Theta}{\sqrt{1 - k^2 \sin^2\Theta}}, \quad \text{where} \quad k^2 = \frac{a^2}{2(1 + a^2)},$$

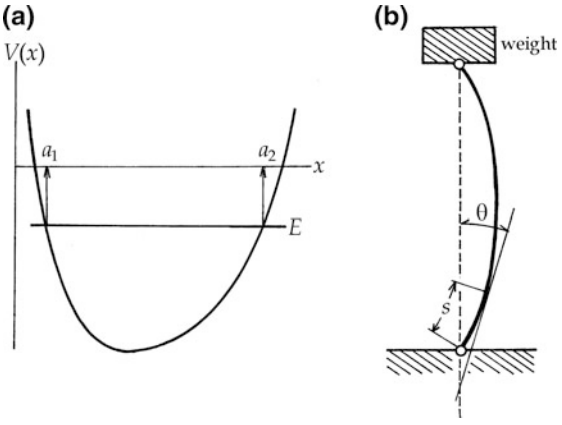

Fig. 8.5 (**a**) The oscillatory region $a_1 < x < a_2$ for $E \le V(x)$. (**b**) A model for buckling of an elastic rod.

and the period of oscillation is

$$T = \frac{4\sqrt{2}}{a} kK(k).$$

2. For the potential $U(x)$ in a more general form than in the problem (1), we can repeat the same argument. In a given $U(x)$, the motion is restricted in the range $a_1 \le x \le a_2$ in Fig. 8.5a. In this case, we can express that $2(E-U) = (x-a_1)(a_2-x)V(x)$. Converting x to an angular variable Θ by

$$x = \frac{a_1+a_2}{2} - \frac{a_1-a_2}{2}\cos\Theta$$

we can obtain

$$t_1 = \pm \int_0^{\Theta_1} \frac{\mathrm{d}\Theta}{\sqrt{V(\Theta)}}.$$

Using this result for the potential $U(x) = \frac{1}{2}ax^2 + \frac{1}{4}bx^4$ confirm the previous formula in the problem (1).

3. Anharmonic potentials as discussed in problems (1) and (2) represent the property of the spring force. On the other hand, we consider them as arising from condensates, which are temperature dependent in thermodynamic environment. The anharmonic part of the potential is considered as the adiabatic potential, although dynamically we cannot make it distinct from the spring force. While the crystal stability is attained by harmonic interaction, the anharmonicity arises from the lattice as an adiabatic potential. Discuss the physical origin of anharmonicity with respect to pseudospin–lattice interactions.

4. For stability of an elastic body, there is a nonlinear problem known as *buckling*, which is important for structural stability. Consider a uniform elastic rod. When compressed by external forces F and $-F$ applied at both ends, the rod stays straight until F reaches a critical strength, beyond which it is stable in bent shape, as illustrated in Fig. 8.5b.

The condition for elastic stability can be obtained with a simple analysis. Denoting the radius of curvature by R, mechanical equilibrium can be described as the torque $F \times y$proportional to R^{-1}, that is, $Fy = cR^{-1}$, where c is a constant. On the other hand, $1/R = (\mathrm{d}\theta/\mathrm{d}s)$, where θ and s are the angle and the length of the curved rod measured from one end, as indicated in the figure. Therefore, using the relation $\mathrm{d}y/\mathrm{d}s = \sin\theta$, we obtain

$$\frac{\mathrm{d}^2\theta}{\mathrm{d}s^2} - \zeta \sin\theta = 0, \quad \text{where} \quad \zeta = \frac{F}{c}.$$

This is a sine-Gordon equation, whose solution was discussed in Chap. 7. The problem can be concluded by stating that the longitudinal length of the bent rod l is given by

$$\Lambda(\kappa) = l$$

for which the value of κ can be determined numerically.

It is interesting that this classical buckling can be compared with an elliptic function for $\boldsymbol{\sigma}_1 = \lambda \boldsymbol{\sigma}_o \mathrm{sn}(\phi_1 / \sqrt{2}\kappa)$; in a continuous crystal, we have such a similarity to buckling.

Chapter 9
Soft Modes

Soft modes can be considered as direct evidence for structural changes in crystals because of their frequencies diminishing toward the critical temperature, destabilizing lattice structure. In dielectric crystals, soft modes are detected with time-dependent electric fields at low frequencies. In nondielectric crystals, neutron inelastic scatterings are the method for studying soft phonons. Although the spatial detail of condensates is implicit, the soft mode can be analyzed for symmetry changes at phase transitions, that is caused by an adiabatic potential. In this chapter, we discuss the relation between critical anomalies and soft modes observed in dielectric and neutron inelastic scattering experiments.

9.1 The Lyddane–Sachs–Teller Relation

In dielectric crystals, the polarization is associated with polar displacements that are related with lattice excitations. These displacements are represented by a polarization vector $\boldsymbol{P}(\boldsymbol{r}, t)$ that is a function of space–time in an externally applied electric field $\boldsymbol{E} = \boldsymbol{E}_{\mathrm{o}} \exp(-\mathrm{i}\omega t)$, where $\boldsymbol{E}_{\mathrm{o}}$ and ω are the amplitude and frequency, respectively. In ionic crystals, $\boldsymbol{P}(\boldsymbol{r}, t)$ is not only related to a mass displacement $\boldsymbol{u}(\boldsymbol{r}, t)$, but also contributed by the *ionic polarization* expressed by $\alpha \boldsymbol{E}$, where α is called the *ionic polarizability*. At low frequencies, it is significant that such functions $\boldsymbol{P}(\boldsymbol{r}, t)$ and $\boldsymbol{u}(\boldsymbol{r}, t)$ constitute *continuous fields*, just like the vibration field as discussed in Chap. 2. We can therefore write the equation

$$\boldsymbol{P} = a\boldsymbol{u} + b\boldsymbol{E}, \tag{9.1}$$

and for the polar lattice mode $\boldsymbol{u}$ we can assume an equation of motion

$$\frac{\partial^2 \boldsymbol{u}}{\partial \boldsymbol{t}^2} = a'\boldsymbol{u} + b'\boldsymbol{E}, \tag{9.2}$$

in a weak field $\boldsymbol{E}$, where a, b and a', b' are constants.

M. Fujimoto, *Thermodynamics of Crystalline States*,
DOI 10.1007/978-1-4419-6688-9_9, © Springer Science+Business Media, LLC 2010

Such mass displacements $\boldsymbol{u}(\boldsymbol{r},t)$ occur in a wave propagating along the direction of an applied field $\boldsymbol{E}(\boldsymbol{r},t)$, for which we can generally consider two independent modes of propagation characterized by $\operatorname{curl}\boldsymbol{u}=0$ and $\operatorname{div}\boldsymbol{u}=0$, which are known as *irrotational* and *solenoidal* component fields, respectively. Therefore, $\boldsymbol{u}$ is expressed as $\boldsymbol{u}=\boldsymbol{u}_{\mathrm{L}}+\boldsymbol{u}_{\mathrm{T}}$; $\boldsymbol{u}_{\mathrm{L}}$ is defined by $\operatorname{curl}\boldsymbol{u}_{\mathrm{L}}=0$ and $\operatorname{div}\boldsymbol{u}_{\mathrm{L}}\neq 0$, whereas $\boldsymbol{u}_{\mathrm{T}}$ is determined by $\operatorname{curl}\boldsymbol{u}_{\mathrm{T}}\neq 0$ and $\operatorname{div}\boldsymbol{u}_{\mathrm{T}}=0$. Here the indexes L and T indicate *longitudinal* and *transverse modes* with respect to the direction of $\boldsymbol{E}$.

Experimentally, if the external field is applied uniformly over the crystal, we write $\boldsymbol{E}=\boldsymbol{E}_{\mathrm{o}}\exp(-\mathrm{i}\omega t)$ with constant amplitude $\boldsymbol{E}_{\mathrm{o}}$. On the other hand, for $\boldsymbol{P}$ and $\boldsymbol{u}$ from internal origins, we can write $\boldsymbol{P}=\boldsymbol{P}_{\mathrm{o}}\exp(-\mathrm{i}\omega t)$ and $\boldsymbol{u}=\boldsymbol{u}_{\mathrm{o}}\exp(-\mathrm{i}\omega t)$ where their amplitudes $\boldsymbol{P}_{\mathrm{o}}$ and $\boldsymbol{u}_{\mathrm{o}}$ are proportional to $\exp\mathrm{i}\,\boldsymbol{k}\cdot\mathbf{r}$. From (9.1) and (9.2), we obtain the relations among these space-dependent amplitudes:

$$\boldsymbol{P}_{\mathrm{o}}=a\boldsymbol{u}_{\mathrm{o}}+b\boldsymbol{E}_{\mathrm{o}}\quad\text{and}\quad-\omega^2\boldsymbol{u}_{\mathrm{o}}=a'\boldsymbol{u}_{\mathrm{o}}+b'\boldsymbol{E}_{\mathrm{o}}.$$

Eliminating $\boldsymbol{u}_{\mathrm{o}}$, we obtain the relation

$$\boldsymbol{P}_{\mathrm{o}}=\left(b+\frac{ab'}{-a'-\omega^2}\right)\boldsymbol{E}_{\mathrm{o}}.$$

The dielectric function $\varepsilon(\omega)$ is defined by $\boldsymbol{D}_{\mathrm{o}}=\varepsilon(\omega)\boldsymbol{E}_{\mathrm{o}}=\varepsilon_{\mathrm{o}}\boldsymbol{E}_{\mathrm{o}}+\boldsymbol{P}_{\mathrm{o}}$, and the susceptibility χ by $\boldsymbol{P}_{\mathrm{o}}=\chi\varepsilon_{\mathrm{o}}\boldsymbol{E}_{\mathrm{o}}$; therefore, $\varepsilon(\omega)$ can be expressed as

$$\varepsilon(\omega)-\varepsilon_{\mathrm{o}}=b+\frac{ab'}{-a'-\omega^{2\prime}}$$

and hence

$$\varepsilon(\omega)=\varepsilon(\infty)+\frac{\varepsilon(0)-\varepsilon(\infty)}{1-(\omega^2/\omega_{\mathrm{o}}^2)},\tag{9.3}$$

where $b=\varepsilon(\infty)-\varepsilon_{\mathrm{o}}$ and $a'=-\omega_{\mathrm{o}}^2$, and hence $\frac{ab'}{\omega_{\mathrm{o}}^2}=\varepsilon(0)-\varepsilon(\infty)$. It is noted that (9.3) is a valid expression of the dielectric function at an arbitrary point $\boldsymbol{r}$ at a constant frequency ω_o, while the displacement $\boldsymbol{u}_{\mathrm{o}}$ at $\boldsymbol{r}$ depends on the strength of an applied field $\boldsymbol{E}_{\mathrm{o}}$.

In a continuum crystal, we decompose the displacement $\boldsymbol{u}(\boldsymbol{r},t)$ into solenoidal and irrotational components characterized by $\operatorname{div}\boldsymbol{u}_{\mathrm{T}}=0$ and $\operatorname{curl}\boldsymbol{u}_{\mathrm{L}}=0$, respectively. As these components $\boldsymbol{u}_{\mathrm{L}}$ and $\boldsymbol{u}_{\mathrm{T}}$ have amplitudes proportional to $\exp\mathrm{i}\,\boldsymbol{k}\cdot\mathbf{r}$, we can derive relations for these amplitudes $\boldsymbol{u}_{\mathrm{oL}}$ and $\boldsymbol{u}_{\mathrm{oT}}$, namely

$$\mathrm{i}\boldsymbol{k}\cdot\boldsymbol{u}_{\mathrm{oT}}=0\quad\text{or}\quad\boldsymbol{k}\perp\boldsymbol{u}_{\mathrm{oT}}$$

and

$$\mathrm{i}\boldsymbol{k}\times\boldsymbol{u}_{\mathrm{oL}}=0\quad\text{or}\quad\boldsymbol{k}\parallel\boldsymbol{u}_{\mathrm{oL}}.$$

Accordingly, by decomposing as $E = \boldsymbol{E}_{\mathrm{L}} + \boldsymbol{E}_{\mathrm{T}}$, where $\boldsymbol{E}_{\mathrm{T}} \perp \boldsymbol{u}_{\mathrm{L}}$ and $\boldsymbol{E}_{\mathrm{L}} \parallel \boldsymbol{u}_{\mathrm{L}}$, respectively, the dielectric response functions from $\boldsymbol{E}_{\mathrm{L}}$ and $\boldsymbol{E}_{\mathrm{T}}$ can be expressed separately.

At sufficiently low frequencies, the electric displacement $\boldsymbol{D}$ should satisfy the basic equation $\mathrm{div}\,\boldsymbol{D} = 0$, so that we have $\mathrm{div}\,\boldsymbol{P} = -\varepsilon_{\mathrm{o}}\mathrm{div}\,\boldsymbol{E}$. Hence, from (9.1), we obtain the relation $a\mathrm{div}\,u = -(\varepsilon_{\mathrm{o}} + b)\mathrm{div}\,E$. Thus, for a transverse mode, we obtain $\mathrm{div}\,\boldsymbol{u}_{\mathrm{T}} = 0$, and so $\mathrm{div}\,\boldsymbol{E}_{\mathrm{T}} = 0$. On the other hand, a longitudinal mode is characterized by $\mathrm{div}\,\boldsymbol{u}_{\mathrm{L}} \neq 0$, so that we have

$$\mathrm{div}\,\boldsymbol{E}_{\mathrm{L}} = -\frac{a}{\varepsilon_{\mathrm{o}} + b}\mathrm{div}\,\boldsymbol{u}_{\mathrm{L}} \quad \text{and} \quad -\omega_{\mathrm{L}}^2\boldsymbol{u}_{\mathrm{L}} = a'\boldsymbol{u}_{\mathrm{L}} + b'\boldsymbol{E}_{\mathrm{L}}.$$

Therefore, for $\boldsymbol{u}_{\mathrm{T}}$ and $\boldsymbol{u}_{\mathrm{L}}$ we have separate equations of propagation

$$\frac{\partial^2\boldsymbol{u}_{\mathrm{T}}}{\partial t^2} = a'\boldsymbol{u}_{\mathrm{T}} = -\omega_{\mathrm{o}}^2\boldsymbol{u}_{\mathrm{T}}$$

and

$$\frac{\partial^2\boldsymbol{u}_{\mathrm{L}}}{\partial t^2} = \left(a' + \frac{ab'}{\varepsilon_{\mathrm{o}} + b}\right)\boldsymbol{u}_{\mathrm{L}} = -\frac{\varepsilon(0)}{\varepsilon(\infty)}\omega_{\mathrm{o}}^2\boldsymbol{u}_{\mathrm{L}},$$

where

$$\omega_{\mathrm{oT}} = \omega_{\mathrm{o}} \quad \text{and} \quad \omega_{\mathrm{oL}} = \omega_{\mathrm{o}}\sqrt{\frac{\varepsilon(0)}{\varepsilon(\infty)}}$$

are characteristic frequencies of transverse and longitudinal modes, respectively. Accordingly, between these mode frequencies and dielectric constants, we find the relation

$$\frac{\omega_{\mathrm{oL}}^2}{\omega_{\mathrm{oT}}^2} = \frac{\varepsilon(0)}{\varepsilon(\infty)}. \tag{9.4}$$

This is known as the Lyddane–Sachs–Teller (LST) formula.

The dielectric function (9.3) plotted against ω exhibits a *forbidden gap* $\varepsilon(0) - \varepsilon(\infty)$, as shown in Fig. 9.1, where a singularity exists at $\omega = \omega_{\mathrm{oT}}$, and also $\varepsilon(\omega_{\mathrm{oL}}) = 0$ at $\omega = \omega_{\mathrm{oL}}$. The LST relation should be consistent with the Landau's theory in the mean-field approximation. For dielectric constants above and below T_{o}, dielectric constants can be written in terms of susceptibilities as

$$\varepsilon_{>}(0) = \varepsilon_{\mathrm{o}}(1 + \chi_{>}) \approx \varepsilon_o\chi_{>} \quad \text{and} \quad \varepsilon_{<}(0) = \varepsilon_{\mathrm{o}}(1 + \chi_{<}) \approx \varepsilon_{\mathrm{o}}\chi_{<}.$$

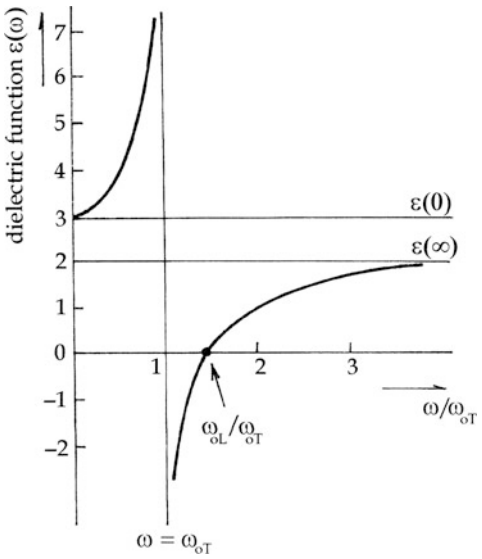

Fig. 9.1 Dispersion curve for a dielectric function $\varepsilon(\omega)$. A forbidden gap between $\varepsilon(0)$ and $\varepsilon(\infty)$; $\varepsilon(\omega_{\mathrm{L}}) = 0$.

Assuming that both $\chi_<$ and $\chi_>$ obey Curie–Weiss' laws (6.6ab) in the vicinity of T_{o}, we can write

$$\omega_{\mathrm{oT}}^2(T > T_{\mathrm{o}}) \propto T - T_{\mathrm{o}} \quad \text{and} \quad \omega_{\mathrm{oT}}^2(T < T_{\mathrm{o}}) \propto T_{\mathrm{o}} - T, \tag{9.5}$$

suggesting that frequencies of the transverse modes diminish or *soften*, if T_{o} is approached from both sides. Thus, soft modes can be predicted from the LST formula, if combined with Curie–Weiss laws.

9.2 Soft Lattice Modes in Condensates

In the above theory, amplitudes $\boldsymbol{P}_{\mathrm{o}}$ and $\boldsymbol{u}_{\mathrm{o}}$ proportional to $\exp i\, \boldsymbol{k} \cdot \boldsymbol{r}$ are related to an arbitrary lattice point $\boldsymbol{r}$, signifying a mesoscopic distribution. However, if this exponential factor is just equal to 1, we have a maximum response from $\boldsymbol{P}_{\mathrm{o}}$ and $\boldsymbol{u}_{\mathrm{o}}$. This applies at the lattice point $\boldsymbol{r} = R = 0$ if $\boldsymbol{k} = 0$, and at $\boldsymbol{r} = 2R$ if $\boldsymbol{k} = \boldsymbol{G}/2$, since we have $\exp i\, \boldsymbol{G} \cdot \boldsymbol{R} = 1$ in both cases. Here, $\boldsymbol{G}$ is a translation vector in the reciprocal lattice and these two cases represent the center and boundary points of the first Brillouin zone, respectively. In Sect. 9.1, a response of the dielectric polarization to an applied field was discussed at the zone center $\boldsymbol{k} = 0$, whereas similar soft modes were also studied at the zone boundary $\boldsymbol{k} = \boldsymbol{G}/2$ by neutron inelastic scattering experiments. Dielectric properties of crystals originate from displaced charges at the lattice sites $\boldsymbol{R}$. On the other hand, neutron inelastic scatterings can take place with mass displacements associated with two unit cells in size of $2\boldsymbol{R}$. In any case, soft modes are observed from condensates in crystals in

thermodynamic environment, for which the above theory is only approximate, because we assumed harmonic displacements $\boldsymbol{u}_{\rm o}$ in (9.2).

In the presence of correlations, pseudospins are in collective motion, which is driven by the internal adiabatic potential in modulated lattice, shifting frequency and damping energy via phonon scatterings. Soft modes are significant objectives to study, subjecting to symmetry and anharmonicity of the adiabatic potential.

9.2.1 The Lattice Response to Collective Pseudospins

Considering longitudinal and transverse displacements $\boldsymbol{u}_{\rm L} \parallel \boldsymbol{k}$ and $\boldsymbol{u}_{\rm T} \perp \boldsymbol{k}$ from equilibrium positions, the adiabatic lattice potential in a condensate can generally be expressed as

$$\begin{aligned}\Delta U = V^{(1)}\left(u_{\rm L} + \sum_{\rm T} u_{\rm T}\right) + V^{(2)}\left(u_{\rm L}^2 + \sum_{\rm T} u_{\rm T}^2\right) + V^{(3)}\left(u_{\rm L}^3 + u_{\rm T}^3\right) \\ + V^{(3)}\left\{u_{\rm L}\left(\sum_{\rm T} u_{\rm T}^2\right) + u_{\rm L}^2\left(\sum_{\rm T} u_{\rm T}\right)\right\} + V^{(4)}\left\{u_{\rm L}^4 + u_{\rm L}^2\left(\sum_{\rm T} u_{\rm T}^2\right)\right\} + \cdots,\end{aligned} \tag{9.6}$$

where $\sum_{\rm T}\cdots$ is the summation for independent transverse directions along the y- and z-axes and $V^{(1)}, V^{(2)}, V^{(3)}, V^{(4)}, \ldots$ are expansion coefficients of the corresponding powers 1, 2, 3, 4,.... Here $u_{\rm L}$ and $u_{\rm T}$ are finite displacements but small in amplitude in the vicinity of $T_{\rm c}$. This ΔU expressed by (9.6) can then be truncated at the fourth order, and composed of component terms of $V^{(1)}, \ldots, V^{(4)}$.

Expressing the phonon wave function by $|\boldsymbol{q}, \omega\rangle$, we can calculate the matrix elements $\langle \boldsymbol{q}', \omega' | \Delta U | \boldsymbol{q}, \omega\rangle$ for the isothermal average $(\Delta U)_T$ at T. Time-dependent $(\Delta U)_{\rm T}$ can arise from the matrix element $\langle \boldsymbol{q}', \omega' | u_{\rm T} | \boldsymbol{q}, \omega\rangle$ for $\boldsymbol{q}' \neq \boldsymbol{q}$. These parts expressed by $\Delta U_{\rm t}$ are subjected to *inelastic phonon scatterings* in a crystal. On the other hand, the secular potential $\Delta U_{\rm s}$ can be expressed as

$$\Delta U_{\rm s} = \Delta U_{\rm sL} + \Delta U_{\rm sT}.$$

The longitudinal component is given by

$$\Delta U_{\rm sL} = (V^{(2)} + V^{(4)} u_{\rm oL}^2) u_{\rm L}^2 + V^{(4)} u_{\rm L}^4; \tag{9.7a}$$

by writing $\sum_{\rm T} u_{\rm T}^2 = u_+^2 + u_-^2$, the transverse potential can be decomposed as

$$\Delta U_{\rm sT} = \Delta U_{\rm s+} + \Delta U_{\rm s-},$$

where

$$\Delta U_{s+} = (V^{(2)} + V^{(4)} u_{oL}^2) u_+^2 \quad \text{and} \quad \Delta U_{s-} = (V^{(2)} + V^{(4)} u_{oL}^2) u_-^2. \tag{9.7b}$$

In contrast, time-dependent components ΔU_t contain nonzero elements $\langle \boldsymbol{q}', \omega' | u_T | \boldsymbol{q}, \omega \rangle \neq 0$ and $\langle \boldsymbol{q}', \omega' | u_T^3 | \boldsymbol{q}, \omega \rangle \neq 0$ for $q' - q = k$ and $\omega' - \omega = \Delta\omega$, which are responsible for *inelastic phonon scatterings*. Taking a time-dependent element, for example, $V^{(1)}$, we have

$$\langle \boldsymbol{q}', \omega' | \Delta U^{(1)} | \boldsymbol{q}, \omega \rangle = V^{(1)} \langle \boldsymbol{q}' | u_{L,T} | \boldsymbol{q} \rangle \exp \mathrm{i}(t\Delta\omega);$$

the scattering probability can thereby be expressed as the time average of

$$P = 2\left|V^{(1)}\right|^2 \langle \boldsymbol{q}' | u_{L,T} | \boldsymbol{q} \rangle^2 \frac{1 - \cos(t\Delta\omega)}{\Delta\omega^2}$$

integrated over phonon collision time t_o. Therefore, calculating $\langle P \rangle_t = \frac{1}{2t_o} \int_{-t_o}^{+t_o} P \mathrm{d}t$, we obtain

$$\langle P \rangle_t = 2\left|V^{(1)}\right|^2 \langle \boldsymbol{q}' | u_{L,T} | \boldsymbol{q} \rangle^2 \frac{\sin(t_o\Delta\omega)}{t_o\Delta\omega}, \tag{9.8}$$

where the factor $\sin(t_o\Delta\omega)/t_o\Delta\omega$ is nearly equal to 1, if $t_o > 1/\Delta\omega$.

For lattice modes $u_L = u_{oL} \exp(-\mathrm{i}\omega t)$ and $u_T = u_{oT} \exp(-\mathrm{i}\omega t)$, the probability (9.8) at temperature T can be calculated for phonon scatterings between $\boldsymbol{q}$ and $\boldsymbol{q}'$, while $\hbar\Delta\omega$ represents the energy transfer to the surroundings, which is equal to $k_B T$. Considering u_T for thermal perturbation, the factor $\left|V^{(1)}\right|^2$ in (9.8) represents energy damping from the u_L mode. Noting from (9.6) that the damping is also contributed by $V^{(3)} u_T^3$ and higher time-dependent terms, the overall damping can be expressed by an empirical constant γ as in the following analysis. Setting u_L aside, the equations of motion for the transverse mode u_T can be written as

$$m\left(\frac{\mathrm{d}^2 u_T}{\mathrm{d}t^2} + \gamma \frac{\mathrm{d}u_T}{\mathrm{d}t} + \omega_o^2 u_T\right) = -\frac{\partial U_{s\pm}}{\partial x} = F_{s\pm} \exp(-\mathrm{i}\omega t), \tag{9.9}$$

where $F_{s\pm} = -(V^{(2)} + V^{(4)} u_{oL}^2)(\partial u_\pm^2 / \partial x)$ from (9.7b), which is the driving force; ω_o is the characteristic frequency and γ the damping constant of the unforced mode.

Equation (9.9) represents a harmonic oscillator forced by an external force, which can be used for a zone-center transition at $\boldsymbol{G} = 0$ as perturbed by an applied electric field, and also for a structural transition at zone-boundaries at $(1/2)\boldsymbol{G}$. In the latter experiment, the momentum loss of neutrons is equal to $\hbar\boldsymbol{G}/2$.

Using $u_T = u_{o\pm} \exp(-\mathrm{i}\omega t)$ in (9.9), we obtain the steady solution of (9.9)

$$m(-\omega^2 - i\omega\gamma + \omega_o^2) u_{o\pm} = F_{s\pm},$$

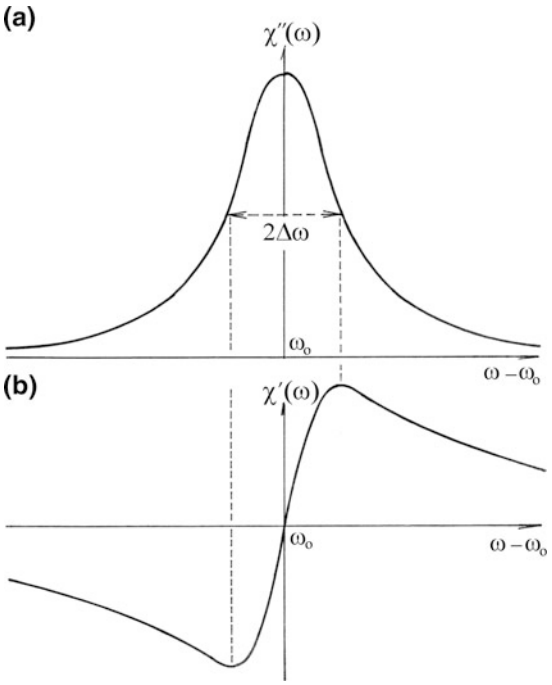

Fig. 9.2 A complex susceptibility $\chi(\omega) = \chi'(\omega) - \mathrm{i}\chi(\omega)$: (**a**) imaginary part $\chi(\omega)$. (**b**) real part $\chi'(\omega)$.

from which we can define the *complex susceptibility* as

$$\chi(\omega) = \frac{mu_{\mathrm{o}\pm}}{F_{\mathrm{s}\pm}} = \frac{1}{\omega_{\mathrm{o}}^2 - \omega^2 - \mathrm{i}\omega\gamma}. \tag{9.10}$$

Expressing in a complex form as $\chi(\omega) = \chi'(\omega) - \mathrm{i}\chi''(\omega)$, the real and imaginary parts of (8.10) can be expressed as

$$\chi'(\omega) = \frac{\omega_{\mathrm{o}}^2 - \omega^2}{\left(\omega_{\mathrm{o}}^2 - \omega^2\right)^2 + \omega^2\gamma^2} \quad \text{and} \quad \chi''(\omega) = \frac{\omega\gamma}{\left(\omega_{\mathrm{o}}^2 - \omega^2\right)^2 + \omega^2\gamma^2}, \tag{9.11}$$

respectively. These two parts of a complex susceptibility are plotted against ω in Fig. 9.2, where $\chi''(\omega)$ is a dumbbell-shaped symmetric curve, if $\gamma > \left|\omega_{\mathrm{o}}^2 - \omega^2\right|/\omega^2 \approx 2\Delta\omega$ where $\Delta\omega = \omega - \omega_{\mathrm{o}}$. Otherwise, $\chi(\omega) \sim 1/\omega\gamma$ for $\gamma < \Delta\omega$, showing no peak at $\omega = \omega_{\mathrm{o}}$, and is called *overdamped*; the otherwise case for $\gamma > \Delta\omega$ is *underdamped*. For a complex susceptibility (9.10), the neutron experiment can reveal the energy loss expressed as proportional to $\hbar\omega \propto \chi(\omega)$.

Experimentally, the characteristic frequency ω_{o} of soft modes becomes close to zero in the vicinity of T_{c}, where (9.9) is dominated by the damping term. Therefore, we write

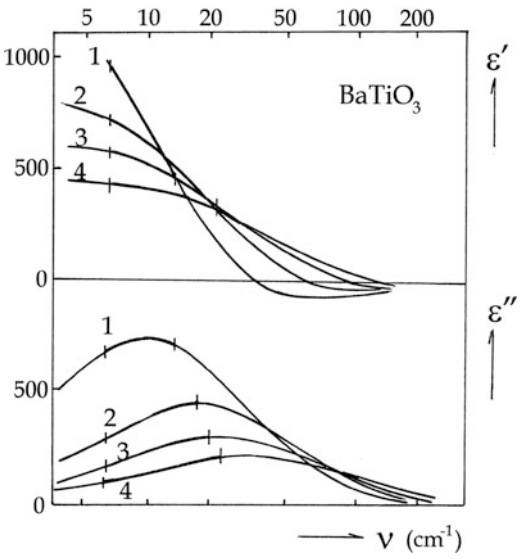

Fig. 9.3 Dielectric soft-mode spectra $\varepsilon(\omega)$ observed from $BaTiO_3$ crystals by backward-wave techniques. Curves for 1, 2, 3, 4 were obtained at temperatures 474, 535, 582, and 667 K, respectively (from [20]).

$$\gamma \frac{\mathrm{d}u_T}{\mathrm{d}t} + \omega_\mathrm{o}^2 u_\mathrm{T} = \frac{F_{\mathrm{o}\pm}}{m} \exp(-\mathrm{i}\omega t).$$

Abbreviating as $\omega_\mathrm{o}^2/\gamma = 1/\tau$ and $F_{\mathrm{o}\pm}/m\gamma = F'$, this equation is expressed as

$$\frac{\mathrm{d}u_\mathrm{T}}{\mathrm{d}t} + \frac{u_\mathrm{T}}{\tau} = F' \exp(-\mathrm{i}\omega t), \tag{9.12}$$

where τ is a *relaxation time*. Equation (9.12) is known as *Debye's relaxation*. Setting $u_\mathrm{T} = A\exp(-\mathrm{i}\omega t)$, we obtain the susceptibility for such a *relaxator*, that is,

$$\chi_\mathrm{D}(\omega) = \frac{1}{-i\omega + (1/\tau)} = \frac{\tau}{1+\omega^2\tau^2} + \frac{\mathrm{i}\omega\tau^2}{1+\omega^2\tau^2}. \tag{9.13}$$

It is noted that (9.12) and (9.13) are of the same Debye's type in an overdamped soft mode where τ and F' are related to γ and $F_{\mathrm{s}\pm}$. In practical crystals with lattice imperfections, such a relaxation as described by (9.13) was found near $\omega = 0$ independently, but showing a sharp peak distinct from the overdamped soft mode. The parameters γ and F' for the soft mode are related to the lattice periodicity, and the sharp line can be attributed to lattice imperfections and independent of the lattice.

Figure 9.3 shows an example of dielectric functions from ferroelectric crystals of $BaTiO_3$ obtained by Petzelt and his coworkers [16], showing the presence of soft modes in the paraelectric phase, as characterized by dispersive $\varepsilon'(\omega)$ of the Debye's type and absorptive $\varepsilon''(\omega)$ of dumbbell shape. Some results from neutron scattering

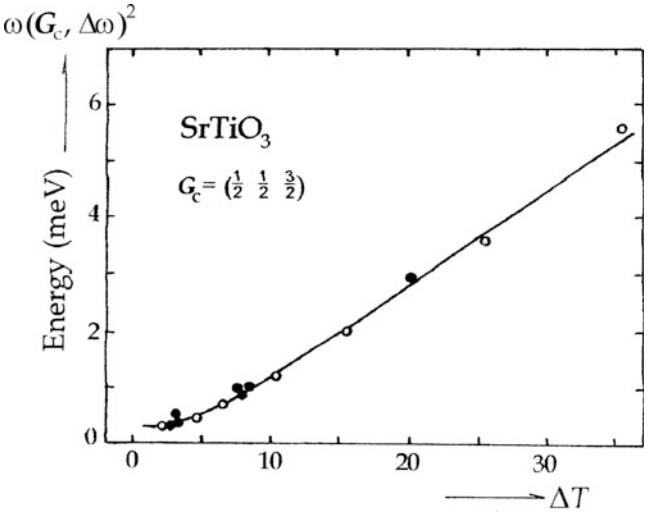

Fig. 9.4 A plot of squared soft-mode frequencies versus $T - T_c$ obtained by neutron scatterings from $SrTiO_3$ (from [21]).

experiments are discussed in Chap. 10. In observed squared frequencies ω_o^2 versus $T_c - T$ shown in Fig. 9.4, there is a noticeable deviation from the straight line predicted by the mean-field theory.

9.2.2 Temperature Dependence

Equation (9.9) represents a dynamical oscillator in thermodynamic environment. The damping constant γ and characteristic frequency ω_o are temperature dependent. Temperature dependences of γ and ω_o are attributed to the adiabatic potential subjected to phonon scatterings, and we already discussed damping γ in the previous section. On the other hand, the temperature-dependent frequency ω_o arising from ΔU should be confirmed separately.

Under a constant pressure, the crystal structure is strained by ΔU, resulting in a small volume change. In this context, we need to verify if such an adiabatic potential can cause a frequency change in phonon spectra. Assuming that a strained lattice is an isotropic and continuous medium, the Gibbs potential of the lattice can be written as

$$\boldsymbol{G}(\boldsymbol{k}) = k_B T \ln \frac{\hbar\omega(\boldsymbol{k})}{k_B T} + \frac{(\Delta V)^2}{2\kappa V},$$

where κ is the compressibility, and here $\Delta V/V$ represents *volume strains* that may be temperature dependent. From the equilibrium condition, we set $(\partial G/\partial V)_T = 0$ to

obtain the relation $\Delta V/V = -\kappa[k_B T/\omega(\boldsymbol{k})][\partial\omega(\boldsymbol{k})/\partial V]$ in the first order. On the other hand, from (2.32) and (2.33), combining with the equipartition theorem $U_{\text{vib}} = k_B T$, we can write

$$\frac{\Delta V}{V} = -\kappa\Delta p = -\frac{\kappa\gamma}{V}U_{\text{vib}} = -\frac{\kappa\gamma k_B T}{V},$$

where $\gamma = -\mathrm{d}\ln\omega(\boldsymbol{k})/\mathrm{d}\ln V$ is Grüneisen's constant, which is normally considered as temperature independent. If so, the frequency $\omega(\mathbf{k})$ may vary adiabatically with V. This result implies that no thermal shift of $\omega(\mathbf{k})$ is expected in isotropic crystals; hence, a thermal frequency shift should be attributed to time-dependent ΔU_s.

Paying no attention to the volume change, we consider ΔU_s that can be expressed as

$$\Delta U_s = V^{(3)}u_L^2(u_y \pm \mathrm{i}u_z) + V^{(4)}u_L^2(u_y^2 + u_z^2),$$

where $\sum_T u_T$ in (9.9) is replaced by a complex displacement $u_y \pm \mathrm{i}u_z$ in a y–z plane, for calculating convenience. Cowley [19] showed that inelastic phonon scatterings by the term of $V^{(3)}$ occur via $u_y \pm \mathrm{i}u_z$; whereas the second term of $V^{(4)}$ is responsible for elastic scatterings via $u_y^2 + u_z^2$. In (9.9), the damping terms $(V^{(1)} + V^{(3)}u_L^2)\sum_T u_T$ are also complex, so the damping factor can be expressed in a complex form as $\gamma = \Gamma - \mathrm{i}\Phi$. In his theory, the secular frequency is written as $\omega(\boldsymbol{k}, \Delta\omega)$, where $\Delta\omega$ represents energy changes $\pm\hbar\Delta\omega$ during the inelastic phonon process; Γ and Φ are also functions of $\boldsymbol{k}$ and $\Delta\omega$.

In Cowley's theory, the steady-state solution of (9.9) can be written as

$$u_{o\pm}(\boldsymbol{k}, \Delta\omega) = \frac{F_{s\pm}/m}{-\omega(\boldsymbol{k})^2 + \omega_o^2 - i\omega(\boldsymbol{k})(\Gamma - \mathrm{i}\Phi)},$$

for which the squared characteristic frequency can be expressed effectively as

$$\omega(\boldsymbol{k}, \Delta\omega)^2 = \omega_o^2 + \omega(\boldsymbol{k})\Phi(\boldsymbol{k}, \Delta\omega). \tag{9.14}$$

Here, the factor $\Phi(k, \Delta\omega)$ is contributed by three parts, that is,

$$\Phi(\boldsymbol{k}, \Delta\omega) = \Phi_o + \Phi_1(\boldsymbol{k}) + \Phi_2(\boldsymbol{k}, \Delta\omega),$$

where

$$\Phi_o = \frac{\partial\omega(\boldsymbol{k})}{\partial V}\Delta V$$

is negligible for $\Delta V = 0$ as discussed earlier. The second term is expressed as

$$\Phi_1(\boldsymbol{k}) = \frac{\hbar}{N\omega(\boldsymbol{k})} \frac{\left(n+\frac{1}{2}\right)V^{(4)}u_{\mathrm{L}}^2}{\omega'} \langle -\boldsymbol{K}, \boldsymbol{K}|u_{\mathrm{T}}^2|\boldsymbol{K}', -\boldsymbol{K}'\rangle,$$

where n is the number of scattered phonons $(\boldsymbol{K}', \omega')$, giving rise to a temperature-dependent frequency shift with $\Phi_1(\boldsymbol{k}) \propto T$, if combining with the equipartition theorem $\hbar\omega'\left(n+\frac{1}{2}\right) = k_{\mathrm{B}}T$.

The expressions for $\Phi_2(k, \Delta\omega)$ and for $\Gamma(\boldsymbol{k}, \Delta\omega)$ are similar, thereby the effective damping parameter becomes

$$\begin{aligned} 2\Gamma(k, \Delta\omega) = \frac{\pi\hbar}{16N\omega(k)} \sum_{1,2} \frac{\left|V^{(3)}u_{\mathrm{L}}^2\langle k|u_{\mathrm{T}}|K_1, K_2\rangle\right|^2}{\omega_1\omega_2} \\ \times[(n_1+n_2+1)\{-\delta(\omega+\omega_1+\omega_2)+\delta(\omega-\omega_1-\omega_2)\}] \\ -[(n_1-n_2)\{-\delta(\omega-\omega_1+\omega_2)+\delta(\omega+\omega_1-\omega_2)\}] \end{aligned}.$$

Considering two temperatures $T_1 = (\hbar\omega(k)/k_{\mathrm{B}})(n_1+n_2+1)$ and $T_2 = (\hbar\omega(\boldsymbol{k})/k_{\mathrm{B}})(n_1-n_2)$, this damping term indicates that the phonon energy $\hbar\omega(2n_2+1)$ is transferred to the heat reservoir, which is equal to $k_{\mathrm{B}}(T_1 - T_2)$.

It was controversial, if the soft-mode frequency converges to zero. Experimentally, it is a matter of timescale of observation; however, no answer can be given to this question, because the transition threshold is always obscured by unavoidable fluctuations. Considering that $\omega(k)$ is determined at $\boldsymbol{k} = 0$ and signified by $\Delta\omega$ for a soft mode, that is, $\omega(0) = \omega_{\mathrm{o}} \pm \Delta\omega$, we can write (9.14) for the effective characteristic frequency $\omega(0, \Delta\omega)$ as

$$\omega(0, \Delta\omega)^2 = \omega_{\mathrm{o}}^2 + \Phi_1(0)(\omega_{\mathrm{o}} \pm \Delta\omega).$$

This can be made equal to zero, if we choose $\Delta\omega = \pm\Phi_1(0)/4$, in which case we obtain $\omega_{\mathrm{o}} = \pm\Delta\omega/2$. Assuming that $\Delta\omega$ emerges at T_{o}, we may write $\omega_{\mathrm{o}}^2 = A'T_{\mathrm{o}}$. Further writing the second term in the above as $\Phi_1(0)(\omega_{\mathrm{o}} \pm \Delta\omega) = \pm A'T$, we obtain $\omega(0, \Delta\omega)^2 = A'(T_{\mathrm{o}} \pm T)$, which agree with Landau's hypothesis (9.5).

For a zone-boundary transition, a soft mode can be studied with intensities of inelastically scattered neutrons in the scattering geometry $\boldsymbol{K} + \boldsymbol{k} \to \boldsymbol{K}'$, where $\boldsymbol{K}$ and $\boldsymbol{K}'$ are wave vectors of neutrons. The timescale of neutron collision is significantly short, so that the critical anomalies can be studied by scanning scattering angles with varying temperature of the sample crystal. In this case, (9.14) can be expanded for small $|\boldsymbol{k}|$ as

$$\omega(\boldsymbol{k}, \Delta\omega)^2 = \omega(0, \Delta\omega)^2 + \kappa\boldsymbol{k}^2 + \cdots,$$

with a small constant κ, so that we can write approximate relations

$$\begin{aligned} \omega(\boldsymbol{k}, \Delta\omega)^2 &= A_>{}'(T - T_\mathrm{o}) + \kappa_> \boldsymbol{k}^2 \quad \text{for} \quad T > T_\mathrm{o}, \\ \omega(\boldsymbol{k}, \Delta\omega)^2 &= A_<{}'(T_\mathrm{o} - T) + \kappa_< \boldsymbol{k}^2 \quad \text{for} \quad T < T_\mathrm{o}, \end{aligned} \tag{9.15}$$

which are useful formula for the intensity analysis of scattered neutrons in a fixed geometry, as shown by Fig. 5.4.

9.2.3 Cochran's Model

Temperature-dependent lattice modes were observed in early spectroscopic studies on structural transitions, but it was after Cochran's theory (1690) [36] that such modes are called *soft modes*. Based on a simplified model of an ionic crystal, he showed that the frequency softening can occur as a consequence of counteracting short- and long-range interactions. In this section, we review Cochran's theory, but modifying ionic displacements for a condensate in a crystal, assuming displaceable charges with effective masses that are considerably lighter than ions.

If a particle of mass m and charge $+e$ is displaced by u from its site, a *hole* of mass m' and charge $-e$ is left behind, creating a dipole moment $\sigma = eu$ that is regarded as the order variable. Dynamically, such a dipole σ is in motion with respect to the center of mass, characterized by the reduced mass $\mu = mM/(m + M)$, where m and M are masses of the charge and the ion with a hole, respectively. Nevertheless, as $\mu \approx m$ if $m < M$, we can disregard the lattice structure in Cochran's model.

In his model, one-dimensional chain of mass particles m and m' is considered in an applied field $E = E_\mathrm{o} \exp \mathrm{i}\omega t$. We assume that these dipoles $\sigma_i = eu_i$ are correlated between neighboring sites, so that the crystal as a whole is polarized as expressed by the polarization P along the direction of the chain. Accordingly, we consider a depolarizing field as expressed by $-P/\varepsilon_\mathrm{o}$ along the direction of the chain. Further, taking dipolar interactions from all other chains into account, Cochran included the Lorentz field $-P/3\varepsilon_\mathrm{o}$, assuming an uniform crystal. Acceptable in the mean-field accuracy, his theory can bring a temperature dependence into dynamic equations through the temperature-dependent polarization P.

Denoting the transverse displacements of charges $+e$ and $-e$ by u_T^+ and u_T^-, respectively, we can write equations of motion as

$$m \frac{\mathrm{d}^2 u_T^+}{\mathrm{d}t^2} = -C(u_\mathrm{T}^+ - u_\mathrm{T}^-) + e\left(E + \frac{P}{3\varepsilon_\mathrm{o}}\right) \quad \text{and}$$

$$m' \frac{\mathrm{d}^2 u_\mathrm{T}^-}{\mathrm{d}t^2} = -C(u_\mathrm{T}^- - u_\mathrm{T}^+) - e\left(E + \frac{P}{3\varepsilon_\mathrm{o}}\right),$$

where C is a restoring constant that represents a short-range interaction. Assuming $P = e(u_\mathrm{T}^+ - u_\mathrm{T}^-)/v$, where v is the specific volume of a crystal, these equations can be combined as

$$\mu \frac{\mathrm{d}^2 P}{\mathrm{d}t^2} = \frac{e^2}{v}\left(E + \frac{P}{3\varepsilon_\mathrm{o}}\right) - CP. \tag{9.16a}$$

For a given field $E = E_\mathrm{o} \exp \mathrm{i}\omega_\mathrm{T} t$, we set $P = P_\mathrm{o} \exp \mathrm{i}\omega_\mathrm{T} t$ in (9.16a) and obtain the expression for the susceptibility

$$\chi(\omega_\mathrm{T}) = \frac{P_\mathrm{o}}{\varepsilon_\mathrm{o} E_\mathrm{o}} = \frac{e^2/\varepsilon_\mathrm{o} v}{C - (e^2/3\varepsilon_\mathrm{o} v) - \mu\omega_\mathrm{T}^2},$$

which shows a singularity if $\mu\omega_\mathrm{T}^2 = C - (e^2/3\varepsilon_\mathrm{o} v)$. Therefore, if the condition $C = e^2/3\varepsilon_\mathrm{o} v$ is met, ω_T can be zero, for which $\chi(\omega_\mathrm{T})$ or $P(\omega_\mathrm{T})$ can be regarded to represent a soft mode.

On the other hand, if charges e and $-e$ are signified by longitudinal displacements u_L^+ and u_L^-, respectively, by defining $P = e(u_\mathrm{L}^+ - u_\mathrm{L}^-)/v$ we have the equation

$$\mu \frac{\mathrm{d}^2 P}{\mathrm{d}t^2} = \frac{e^2}{v}\left(E - \frac{P}{\varepsilon_\mathrm{o}} + \frac{P}{3\varepsilon_\mathrm{o}}\right) - CP, \tag{9.16b}$$

from which the longitudinal susceptibility can be written as

$$\chi(\omega_\mathrm{L}) = \frac{e^2/\varepsilon_\mathrm{o} v}{C + (2e^2/3\varepsilon_\mathrm{o} v) - \mu\omega_\mathrm{L}^2}.$$

Since C is a positive constant, the frequency determined by $\mu\omega_\mathrm{L}^2 = C + (2e^2/3\varepsilon_\mathrm{o} v)$ cannot vanish. In Cochran's theory, the soft mode should be a transverse mode, and both ω_T and ω_L can be temperature dependent.

9.3 Central Peaks

For a binary displacive structural change, we consider that pseudospins emerged at T_c^* and then clustered in periodic lattice at T_c. In the process of condensate formation, the corresponding lattice displacement u_T of clustered pseudospins should be different from unclustered ones dynamically. Therefore, in the following, we specify these displacements by u_T and v_T, respectively, which are pinned and observed in practical experiments.

We can assume that these two modes are coupled in such a way as $v_\mathrm{T} = cu_\mathrm{T}$, where c is temperature dependent. For the coupled system, the equations of motion can be written as

$$\frac{\mathrm{d}^2 u_\mathrm{T}}{\mathrm{d}t^2} + \gamma \frac{\mathrm{d}u_\mathrm{T}}{\mathrm{d}t} + \gamma' \frac{\mathrm{d}v_\mathrm{T}}{\mathrm{d}t} + \omega_\mathrm{o}^2 u_\mathrm{T} = \frac{F_{\mathrm{s}\pm}}{m} \exp(-\mathrm{i}\omega t)$$

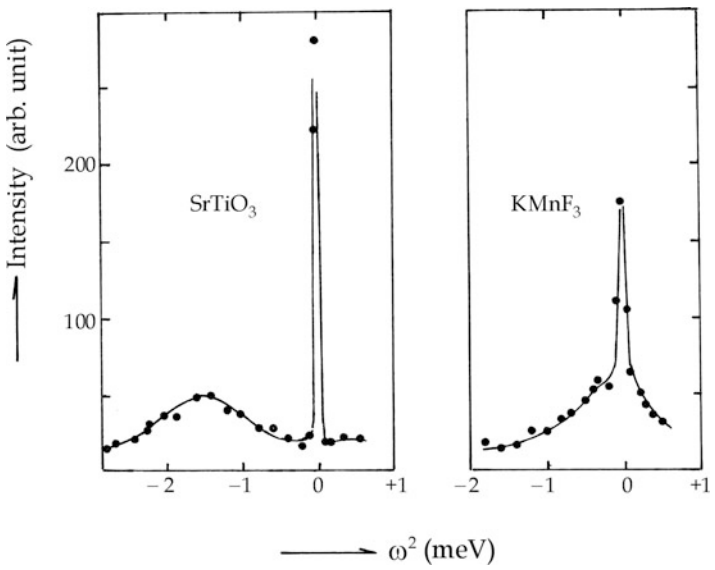

Fig. 9.5 Soft-mode spectra from $SrTiO_3$ and $KMnF_3$, consisting of a soft-mode and a central peak (from [22]).

and

$$\frac{\mathrm{d}v_\mathrm{T}}{\mathrm{d}t}+\frac{v_\mathrm{T}}{\tau}=F'\exp(-\mathrm{i}\omega t).$$

The steady-state solutions can be expressed as

$$u_{\mathrm{o}\pm}(-\omega^2-i\omega\gamma+\omega_\mathrm{o}^2)-i\omega\gamma' v_{\mathrm{o}\pm}=\frac{F_{\mathrm{s}\pm}}{m}\quad\text{and}\quad v_{\mathrm{o}\pm}\left(-i\omega+\frac{1}{\tau}\right)=F',$$

from which we can derive the susceptibility function for the coupled oscillator:

$$\chi(\omega)=\frac{mu_{\mathrm{o}\pm}}{F_{\mathrm{s}\pm}}=\frac{1}{\omega_\mathrm{o}^2-\omega^2-\mathrm{i}\omega\gamma-\mathrm{i}c\gamma' F'(\omega\tau/1-\mathrm{i}\omega\tau)}.$$

Setting $\delta^2=c\gamma' F'$, this susceptibility formula is simplified as

$$\chi(\omega)=\frac{1}{\omega_\mathrm{o}^2-\omega^2-\mathrm{i}\omega\gamma-(\delta^2\omega\tau/1-\mathrm{i}\omega\tau)}. \tag{9.17}$$

If these two modes u and v are independent, that is, $\delta=0$ or $c=0$, (9.17) is characterized by a simple oscillator formula for the u-mode. If the observed susceptibility contains such an additional independent response as given by (9.13) in the vicinity of $\omega=0$, we have

$$\chi(\omega) = \frac{1}{\omega_o^2 - \omega^2 - i\omega\gamma} + \frac{\tau}{1 - i\omega\tau}. \tag{9.18}$$

Nevertheless at $\omega_o \approx 0$, these two terms at a very low frequency become overlapped, and indistinguishable unless $\gamma < 1/\tau$. Experimentally however, such a response of Debye's type happens to be a distinctively sharp peak, and observed distinctively in zone-boundary transitions at near-zero frequency, which is called a *central peak*, as shown in Fig. 9.5.

9.4 A Change in Lattice Symmetry

Macroscopically, a structural transformation is characterized by a symmetry change in a crystal. It is considered as arising from an adiabatic potential emerging at the critical temperature. We assume that the potential ΔU_s given by (9.7a) and (9.7b) is significant at the outset of pseudospin ordering along the x-axis, and for $T < T_c$ the potential expressed by

$$\Delta U_{tr} = V^{(3)}(u_y^2 + u_z^2) + V^{(4)}u_x^2(u_y^2 + u_z^2) \tag{9.19}$$

can be responsible for lowering symmetry via phonon scatterings by transverse displacements u_y and u_z. Noted that (9.7a), (9.7b), and (9.19) are characterized by the same class of a cubic symmetry group; the transition may take place with minimal energy for deforming lattice structure. Fig. 9.6a, b illustrate examples for symmetry changes at transition temperatures T_c, as observed from soft-mode spectra.

Soft modes observed by optical experiments on TSCC crystals, and identified as B_{2u} modes for $T > T_c$ and A_1 modes for $T < T_c$, and propagating along x and z directions, respectively. Except for the critical region, the adiabatic potentials are written as

$$\Delta U_{B_u} = \frac{1}{2}Au_x^2 + \frac{1}{4}Bu_x^4 \quad \text{and} \quad \Delta U_{A_1} = \frac{1}{2}Au_z'^2 + \frac{1}{4}Bu_z'^4.$$

For the symmetry change between B_{2u} and A_1, we postulate the coordinate transformation from $\pm u_x$ to $\pm u_y' \mp u_z'$, corresponding to phonon scatterings $K_x \leftrightarrow -K_x$ and $K_y, -K_z \leftrightarrow -K_y, K_z$, respectively. Therefore, the process can be determined by a linear combination

$$u' = c_x u_x' + c_y u_y' \quad \text{where} \quad c_x^2 + c_y^2 = 1,$$

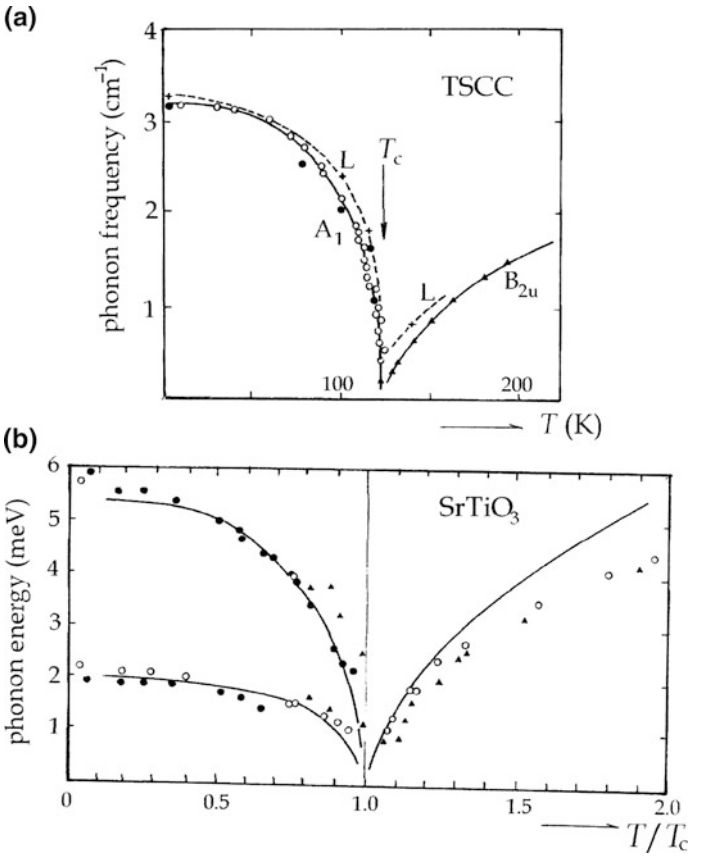

Fig. 9.6 Soft-mode spectra as a function of temperature: (**a**) from TSCC, (**b**) $SrTiO_3$ (from [23, 24]).

with which the potential in the critical region is expressed by

$$\Delta U_{\rm cr} = \frac{1}{2}Au'^2 + \frac{1}{4}Bu'^2u_x^2, \tag{9.14}$$

where the second quartic term represents a coupling between $\Delta U_{B_{2u}}$ and ΔU_{A_1}. Therefore, we re-express (9.14) as

$$\Delta U_{\rm cr} = c_x^2\left(\frac{A}{2}u_x'^2 + \frac{B}{4}u_x'^4\right) + c_y^2\left(\frac{A}{2}u_y'^2 + \frac{B}{4}u_x'^2u_y'^2\right).$$

We assume that the critical state can change by $c_x^2 \to 0$ and $c_y^2 \to 1$ to establish the normal state, where we should have $u_x'^2 = -A/B$ in thermal equilibrium. Therefore,

$$\lim_{c_y \to 1} \Delta U_{cr} \to +\frac{A}{4} u_y^2. \tag{9.15}$$

This indicates that the A_1 mode below T_c is characterized by $\omega(0)^2 = 2A(T_o - T)$, which appears to be substantiated by the curves in Fig. 9.6.

For phonon-energy curves for $SrTiO_3$ below 105°K in Fig. 9.6b, the quadratic potential should also be related effectively to anisotropic quartic potentials, depending on $\boldsymbol{k}$. These curves are determined by $\omega_<(0,\boldsymbol{k})^2 = A(\boldsymbol{k})(T_o - T) + \kappa \boldsymbol{k}^2$, where the coefficient $A(\boldsymbol{k})$ depends on the direction of $\boldsymbol{k}$. Experimentally, near-linear relations between $\omega_<(0,0)^2$ and $T_o - T$ as shown in Fig. 9.4, were obtained for many structural transitions. Consistent with the mean-field theory however, we have no significant reason to support this linear relation. Hence, we usually write $\omega_<(0,0) \propto (T_o - T)^\beta$, where β is called a *critical exponent* that is determined empirically; $\beta = 1/2$ in mean-field approximation.

Exercises 9

1. In Cochran's theory, the polarization $\boldsymbol{P}$ is a macroscopic variable. How his theory can be modified for a mesoscopic polarization?
2. In Landau's theory, he postulated that $A = A'(T - T_o)$ where A' is a positive constant; hence, A is positive for $T > T_o$ but negative for $T < T_o$. In practical crystals, A' is not necessarily a constant, depending on the wave vector $\boldsymbol{k}$ of the order parameter. Why? Discuss the mechanism for variable A'. Representing primarily a harmonic potential, but often including a quartic potential effectively, so that the soft-mode frequency exhibits often a different temperature dependence, as shown in Fig. 9.6a, b.

Chapter 10
Experimental Studies of Mesoscopic States

Mesoscopic states in crystals can be characterized by the phase variable, which is observable from condensates pinned by intrinsic and extrinsic potentials. Condensates in crystals are primarily longitudinal in one dimension, although showing transversal features as well in practical crystals. Except for thermal and mechanical measurements, such mesoscopic condensates can generally be studied by *sampling* experiments. Experiments are therefore focused on their frequency dispersion and pseudospin arrangement that vary with temperature for $T<T_c$. Samplings can be performed by using photons, neutrons, nuclear and paramagnetic probes, constituting basic techniques in contemporary physics of solid materials. These probes can sample specific parts of constituents selectively; photons are generally sensitive to order variables, neutrons are useful for studying displacements of heavy constituents, and magnetic resonance probes yield information about local structural changes, which are all complementary. In this chapter, such experiments as X-ray diffraction, dielectric measurements, light and neutron inelastic scatterings, and magnetic resonance spectroscopy are outlined for condensate studies with relevant results to substantiate theoretical arguments.

10.1 Diffuse X-Ray Diffraction

The crystal structure is usually determined by X-ray diffraction. A collimated X-ray beam is scattered from a crystal, forming a diffraction pattern on a photographic plate, depending on the orientation with respect to the beam. Such a diffraction pattern is basically due to elastic scattering of X-ray photons by distributed electron densities. Soft X-ray photons in keV energies are scattered by electrons distributed in crystal planes, while keeping heavy nuclei intact under normal circumstances. On the other hand, in the critical region, the lattice is modulated along symmetry directions, so that X-ray diffraction patterns exhibit anomalous broadenings, called *diffuse diffraction*.

M. Fujimoto, *Thermodynamics of Crystalline States*,
DOI 10.1007/978-1-4419-6688-9_10,

In early crystallographic studies, Bragg established the concept of *crystal planes* of constituents that signifies the periodic lattice structure in normal crystals. A collimated X-ray beam reflects like optical light from a large number of parallel crystal planes, showing an interference pattern on a photographic plate placed nearby. Figure 10.1 illustrates an experimental arrangement for analyzing such diffraction patterns.

In light of Born-Huang's principle, we postulate for binary transitions that condensates are formed for minimal structural strains, in such a way that the lattice modulation occurs along a specific symmetry axis. Denoting such an axis by a, Fig. 10.1 shows schematically how the diffraction is modified along the a-axis. Assuming that a collimated beam of monochromatic X-ray of a wave vector $\boldsymbol{K}_{\mathrm{o}}$ is incident perpendicularly on the a-axis, Bragg's diffraction law can be written as

$$\boldsymbol{K}_{\mathrm{o}} - \boldsymbol{K} = \pm \boldsymbol{G}. \tag{10.1}$$

Here, $\boldsymbol{K}$ is the wave vector of diffracted X-ray and $\boldsymbol{G} = n\boldsymbol{a}$ is the translation vector along the a-axis, where n is an integer, representing a group of parallel crystal planes perpendicular to the axis. On the other hand, only the magnitude $|\boldsymbol{G}|$ is significant for the beam of $\boldsymbol{K}$ to diffract in all directions in three dimensions; all of these satisfy (10.1). Namely, these diffracted beams $\boldsymbol{K}$ are lying on *conical* surfaces with respect to the a-axis as shown in Fig. 10.1; such conically diffracted beams constitute Laue's law for constructing diffraction patterns. We show in the figure how the lattice modulation can occur along the a-axis for a given wave vector k.

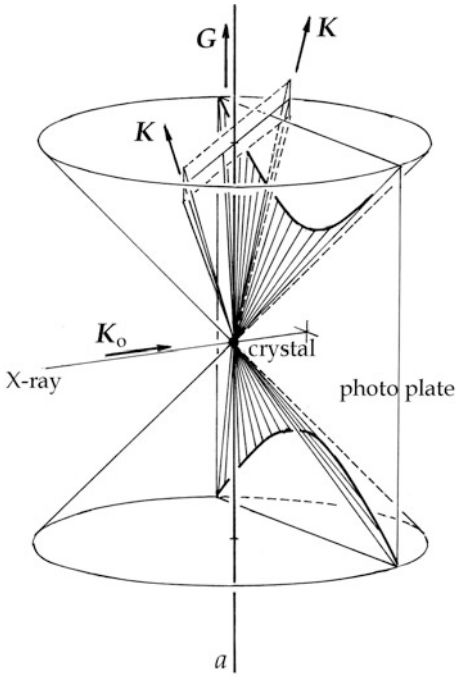

Fig. 10.1 X-ray diffraction setup. Incident X-ray beam $\boldsymbol{K}_{\mathrm{o}}$, diffracted beam $\boldsymbol{K}$ on a conical surface. The modulated axis is indicated by $\boldsymbol{G} \parallel \boldsymbol{a}$.

Considering a charge element $\rho(\boldsymbol{r}_\mathrm{o})\mathrm{d}^3\boldsymbol{r}$ that scatters an incident X-ray photon field $E_\mathrm{o}\exp\mathrm{i}(\boldsymbol{K}_\mathrm{o}\cdot\boldsymbol{r}_\mathrm{o}-\omega t_\mathrm{o})$ at a point $\boldsymbol{r}_\mathrm{o}$ and time t_o, the scattered field is spherical and expressed by the classical theory of radiation as

$$\boldsymbol{A}(\boldsymbol{r},t)\propto\int_{V(\boldsymbol{r}_\mathrm{o})}\mathrm{d}^3\boldsymbol{r}_\mathrm{o}\rho(\boldsymbol{r}_\mathrm{o})E_\mathrm{o}\exp\mathrm{i}(\boldsymbol{K}_\mathrm{o}\cdot\boldsymbol{r}_\mathrm{o}-\omega t)\frac{\exp\mathrm{i}\{\boldsymbol{K}\cdot(\boldsymbol{r}-\boldsymbol{r}_\mathrm{o})-\omega(t-t_\mathrm{o})\}}{|\boldsymbol{r}-\boldsymbol{r}_\mathrm{o}|}.$$

Hence, the scattered amplitude at a distance $r\gg r_\mathrm{o}$ is given by an approximate form $\boldsymbol{A}(\boldsymbol{r},t)\propto\exp\mathrm{i}(\boldsymbol{K}\cdot\boldsymbol{r}-\omega t)/r=A_\mathrm{o}$, which can be re-expressed by

$$\frac{A_\mathrm{o}}{E_\mathrm{o}}\propto\int_{V(\boldsymbol{r}_\mathrm{o})}\mathrm{d}^3\boldsymbol{r}_\mathrm{o}\{\rho(\boldsymbol{r}_\mathrm{o})\exp\mathrm{i}(\boldsymbol{K}_\mathrm{o}-\boldsymbol{K})\cdot\boldsymbol{r}_\mathrm{o}\}. \tag{10.2}$$

For elastic scatterings from a rigid crystal, by the relation $\exp\mathrm{i}(\pm\boldsymbol{G}\cdot\boldsymbol{r}_\mathrm{o})=1$, the intensity ratio (10.2) gives maximum scattered amplitude, which is proportional to the net charge at the lattice point $\boldsymbol{r}_\mathrm{o}$.

In practice however, a collimated X-ray beam strikes a finite area on a crystal plane, so that the reflected beam arises from all scatterers in the impact area. Letting positions of scatterers as $\boldsymbol{r}_{om}$, where $m=1,2,\ldots$ in the impact area, (10.2) can be re-expressed as

$$\frac{A_\mathrm{o}}{E_\mathrm{o}}=\sum_m f_m(G)\exp(-\mathrm{i}\boldsymbol{G}\cdot\boldsymbol{r}_{om}), \tag{10.3}$$

where

$$f_m(\boldsymbol{G})=\int_{V(\boldsymbol{r}_{om})}\rho(\boldsymbol{r}_{om})\mathrm{d}^3\boldsymbol{r}_{om}.$$

This is called the *atomic form factor*. However, electronic densities overlap significantly between neighboring atoms, and (10.3) overestimates individual contributions. In this context, we need to redefine independent factors for these constituents. Replacing $\boldsymbol{r}_{om}$ by a continuous variable $\boldsymbol{s}-\boldsymbol{r}_{om}$, we can write

$$\begin{aligned}\int_{V(\boldsymbol{s})}\rho(\boldsymbol{s})\exp(-\mathrm{i}\boldsymbol{G}\cdot\boldsymbol{s})\mathrm{d}^3\boldsymbol{s}&=\int_{V(\boldsymbol{s})}\rho(\boldsymbol{s}-r_{om})\exp\{-\mathrm{i}\boldsymbol{G}\cdot(\boldsymbol{s}-\boldsymbol{r}_{om})\}\mathrm{d}^3(\boldsymbol{s}-\boldsymbol{r}_{om})\\&\quad\times\exp(-\mathrm{i}\boldsymbol{G}\cdot\boldsymbol{r}_{om})\\&=f_m(\boldsymbol{G})\exp(-\mathrm{i}\boldsymbol{G}\cdot\boldsymbol{r}_{om}),\end{aligned}$$

where

$$f_m(\boldsymbol{G})=\int_{V(\boldsymbol{s})}\rho(\boldsymbol{s}-\boldsymbol{r}_{om})\exp\{-\mathrm{i}(\boldsymbol{s}-\boldsymbol{r}_{om})\}\mathrm{d}^3(\boldsymbol{s}-\boldsymbol{r}_{om}). \tag{10.4}$$

With (10.4), (10.3) can be expressed as

$$S(\boldsymbol{G}) = \sum_m f_m(\boldsymbol{G}) \exp(-\mathrm{i}\boldsymbol{G}\cdot\boldsymbol{r}_{om}) = \sum_m f_m(\boldsymbol{G}) \exp\left\{\frac{2\pi\mathrm{i}}{\Omega}(x_m h + y_m k + z_m l)\right\}.$$

This is called the *structural form factor*, with which the field of a scattered beam at a distant position r can be expressed as

$$\frac{E_G(\boldsymbol{r})}{E_\mathrm{o}} = \frac{S(\boldsymbol{G})}{r} \exp \mathrm{i}(\boldsymbol{K}\cdot\boldsymbol{r} - \omega t).$$

Using the structural factor, the intensity of the scattered beam is given by

$$\frac{I(\boldsymbol{G})}{I_\mathrm{o}} = \frac{1}{r^2} S^*(\boldsymbol{G}) S(\boldsymbol{G}). \tag{10.5}$$

If a crystal is modulated in a direction of the a-axis, the periodicity of pseudospins is modified by the wave vectors $\boldsymbol{G} \pm \boldsymbol{k}$ and the energies $\mp\Delta\varepsilon = \hbar(\omega - \omega_\mathrm{o}) = \mp\hbar\Delta\omega$, so that the scatterings should be inelastic. We therefore consider conservation laws

$$\boldsymbol{K}_\mathrm{o} - \boldsymbol{K} = \boldsymbol{G} \pm \boldsymbol{k} \quad \text{and} \quad \varepsilon(\boldsymbol{K}_\mathrm{o}) - \varepsilon(\boldsymbol{K}) = \mp\Delta\varepsilon(\boldsymbol{k}), \tag{10.6}$$

by which (10.2) can be revised for inelastic scatterings as

$$\begin{aligned}\frac{A_\mathrm{o}}{E_\mathrm{o}} &\propto \int \mathrm{d}^3\boldsymbol{r}_\mathrm{o}\rho(\boldsymbol{r}_\mathrm{o}) \exp \mathrm{i}(\boldsymbol{K}_\mathrm{o}\cdot\boldsymbol{r}_\mathrm{o} - \omega_\mathrm{o} t_\mathrm{o}) \frac{\exp \mathrm{i}\{\boldsymbol{K}\cdot(\boldsymbol{r}-\boldsymbol{r}_\mathrm{o}) - \omega(t-t_\mathrm{o})\}}{|\boldsymbol{r}-\boldsymbol{r}_\mathrm{o}|} \\ &\approx \int \mathrm{d}^3\boldsymbol{r}_\mathrm{o} \frac{\rho(\boldsymbol{r}_\mathrm{o}) \exp \mathrm{i}(\boldsymbol{K}\cdot\boldsymbol{r} - \omega t)}{r} \exp \mathrm{i}\{(\boldsymbol{K}_\mathrm{o} - \boldsymbol{K})\cdot\boldsymbol{r} - (\omega_\mathrm{o} - \omega)t_\mathrm{o}\}.\end{aligned}$$

Using (10.6) in this expression, we obtain

$$\begin{aligned}\frac{E_G(\boldsymbol{r})}{E_\mathrm{o}} &\propto \frac{\exp \mathrm{i}(\boldsymbol{K}\cdot\boldsymbol{r} - \omega t)}{r} \\ &\quad \times \sum_m \{f(\boldsymbol{G}+\boldsymbol{k}) \exp \mathrm{i}(\boldsymbol{k}\cdot\boldsymbol{r}_m - \Delta\omega t_\mathrm{o}) + f(\boldsymbol{G}-\boldsymbol{k}) \exp \mathrm{i}(-\boldsymbol{k}\cdot\boldsymbol{r}_m + \Delta\omega t_\mathrm{o})\},\end{aligned}$$

where

$$f(\boldsymbol{G}\pm\boldsymbol{k}) = \int_{V(\boldsymbol{r}_\mathrm{o})} \mathrm{d}^3\boldsymbol{r}_\mathrm{o}\rho(\boldsymbol{r}_\mathrm{o}) \exp \mathrm{i}(\boldsymbol{G}\pm\boldsymbol{k})\cdot\boldsymbol{r}_\mathrm{o}.$$

We consider $|\boldsymbol{k}|<|\boldsymbol{G}|$ for a weak modulation, in which case $f(\boldsymbol{G}\pm\boldsymbol{k})\approx f(\boldsymbol{G})$, and phase fluctuations $\exp \mathrm{i}(\boldsymbol{G}\pm\boldsymbol{k})\cdot\boldsymbol{r}_\mathrm{o}$ can be separated to amplitude and phase modes, similar to the critical condition discussed in Chap. 6. Taking these symmetric and antisymmetric modes into account, we can derive the corresponding intensity at r, that is,

$$\frac{I(\boldsymbol{G}\pm\boldsymbol{k})}{I_\mathrm{o}}=\frac{I(\boldsymbol{G})}{I_\mathrm{o}}+\frac{2|f(\boldsymbol{G})|^2}{r^2}\sum[\cos\{\boldsymbol{k}\cdot(\boldsymbol{r}_m-\boldsymbol{r}_n)-\Delta\omega(t_m-t_n)\}+\sin\{\boldsymbol{k}\cdot(\boldsymbol{r}_m-\boldsymbol{r}_n)-\Delta\omega(\boldsymbol{t}_m-\boldsymbol{t}_n)\}].$$

Here, the first term on the right-hand side represents elastic scatterings, while phase fluctuations in the impact area S are explicit in the second inelastic term. Considering timescale of observation t_o, the latter represents the intensity anomaly due to diffuse diffraction, that is,

$$\frac{\langle I(\boldsymbol{G}\pm\boldsymbol{k})\rangle_t-\langle I(\boldsymbol{G})\rangle_t}{I_\mathrm{o}}=\frac{2|f(\boldsymbol{G})|^2}{r^2}\frac{1}{S}\int_S\{\langle\cos\phi\rangle_t+\langle\sin\phi\rangle_t\}\mathrm{d}S, \tag{10.7b}$$

where $\phi=\boldsymbol{k}\cdot(\boldsymbol{r}_m-\boldsymbol{r}_n)-\Delta\omega(t_m-t_n)$ represents fluctuating phases. Here, it is convenient to consider that $\boldsymbol{r}_m-\boldsymbol{r}_n=\boldsymbol{r}$ and $t_m-t_n=\tau$ are continuous space-time, that is, $\phi=\boldsymbol{k}\cdot\boldsymbol{r}-\Delta\omega\cdot\tau$; (10.7b) expresses that time averages $\langle\cos\phi\rangle_t$ and $\langle\sin\phi\rangle_t$ are integrated over the area S.

Assuming a rectangular area $S=L_xL_y$ and continuous $\phi=kx-\Delta\omega\cdot\tau$, the symmetric spatial fluctuations can be calculated as

$$\frac{1}{S}\int_S\langle\cos\phi\rangle_t\mathrm{d}S=\left(\frac{1}{L_x}\int_0^{L_x}\langle\cos\phi\rangle_t\mathrm{d}x\right)\left(\frac{1}{L_y}\int_0^{L_y}\mathrm{d}y\right)=\left\langle\frac{1}{kL_x}\int_{\phi_1}^{\phi_2}\cos\phi\,\mathrm{d}\phi\right\rangle_t=\left\langle\frac{2}{\phi_2-\phi_1}\sin\frac{\phi_2-\phi_1}{2}\cos\frac{\phi_2+\phi_1}{2}\right\rangle_t,$$

Here, ϕ_1 and ϕ_2 indicate limits of the space integration at x_1 and x_2; hence, $\phi_2-\phi_1=\Delta\phi=kL_x$ and $(\phi_2+\phi_1)/2=kx-\Delta\omega\cdot\tau$. After a similar calculation for $\frac{1}{S}\int_S\langle\sin\phi\rangle_t\mathrm{d}S$, we obtain the formula for the net intensity anomaly:

$$\frac{\langle\Delta I(\boldsymbol{G})\rangle_t}{I_\mathrm{o}}=\frac{\sin kL_x}{kL_x}\frac{\sin(t_\mathrm{o}\Delta\omega)}{t_\mathrm{o}\Delta\omega}\{\langle\cos kx\rangle_t+\langle\sin kx\rangle_t\}. \tag{10.7c}$$

This formula should explain diffused intensities of X-ray diffraction; however, broadened diffraction spots and lines are hardly resolvable in X-ray experiments. In contrast, in neutron inelastic scatterings and magnetic resonance studies, such anomalies are resolved and analyzed as expressed by (10.7c).

10.2 Neutron Inelastic Scatterings

By X-ray diffraction studies, it is possible to detect transition anomalies, but failed to see their detail because of insufficient resolution. The difficulty was also related to detected patterns that are generally obscured by strong elastic scatterings masking inelastic scatterings. On the other hand, the symmetric and antisymmetric contributions were resolved in neutron experiments.

For one-dimensional modulation, we notice that if collimated X-ray beam is parallel to the modulated axis, that is, if $\boldsymbol{K}_{\mathrm{o}} \parallel \boldsymbol{G}$, from (10.1) we have $\boldsymbol{K} = 0$. In contrast, inelastic scatterings occur in neutron experiments at the zone boundaries $\pm \boldsymbol{G}/2$. If $\boldsymbol{K} = 0$, no diffraction of the beam from $\boldsymbol{G}$-planes is expected, while in the direction perpendicular to $\boldsymbol{K}_{\mathrm{o}}$ only inelastically scattered neutrons can be detected. Figure 10.2 illustrates such an arrangement that inelastic scatterings can be studied in the perpendicular direction, avoiding elastic scatterings; this is a practical arrangement, provided that the incident beam $\boldsymbol{K}_{\mathrm{o}}$ has a sufficiently high intensity. In this figure, we notice that the incident beam is almost in parallel to the a-axis, where some amount of elastic reflection is unavoidable at a small $\boldsymbol{K}$. Thermal neutrons from a nuclear reactor are characterized by de Broglie's wavelengths comparable with lattice spacing, so that inelastic scatterings can be observed in higher resolution than X-ray.

It is fortunate that an intense thermal neutron source is made available for such experiments, which were indeed performed at leading laboratories in the world. In this section, we discuss the principle for the experiment and representative results. In Fig. 10.3 shown is a sketch of a *triple-axis spectrometer*, consisting of

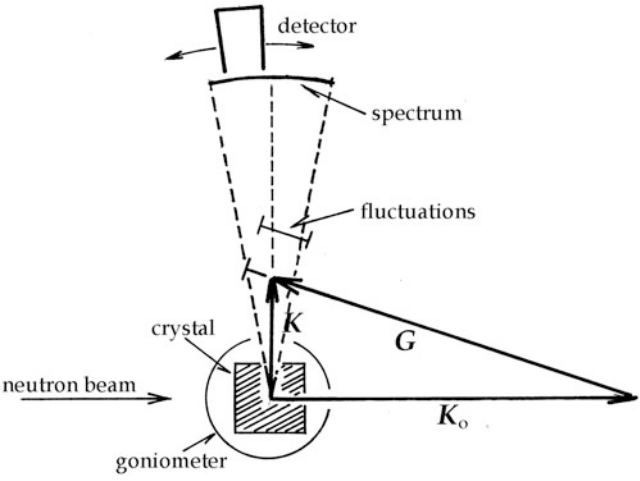

Fig. 10.2 Experimental arrangement for neutron inelastic scatterings. Incident beam $\boldsymbol{K}_{\mathrm{o}}$. In perpendicular directions $\boldsymbol{K}$, only inelastic scatterings can be observed with no diffraction. The fluctuation spectrum can be recorded by scanning the scattering angle.

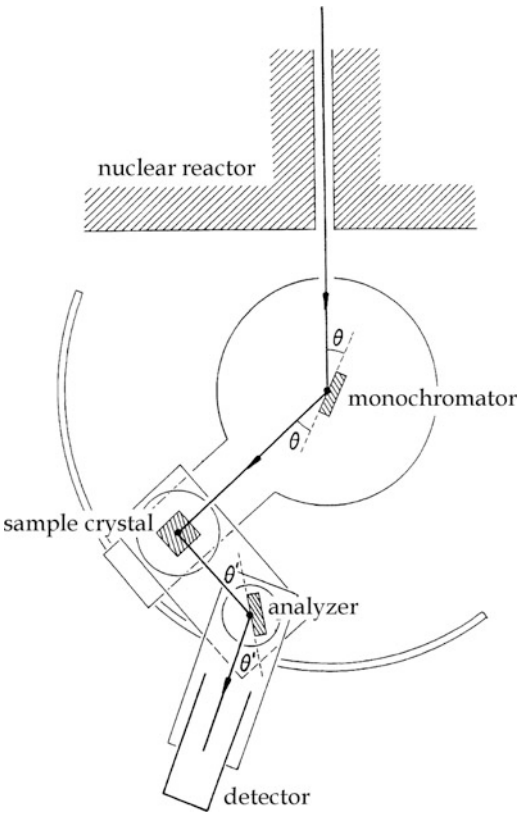

Fig. 10.3 Triple-axis spectrometer for neutron scattering experiments. The monochrometer, goniometer, and analyzer are all rotatable around their axes in parallel.

monochrometer, goniometer, and analyzer which are all rotatable individually around their parallel axes. The monochrometer and analyzer are diffraction devices utilizing crystals of known lattice spacing; thereby, the wavelength can be selected and measured by adjusting angles θ and θ', respectively, as indicated in the figure. A sample crystal is mounted on the goniometer, which can be rotated around a symmetry axis to scan scatterings in the vicinity of $\boldsymbol{K}_\mathrm{o} \parallel \boldsymbol{G}$, as shown in Fig. 10.2.

Similar to X-ray, momentum and energy conservation laws can be applied to neutron impact on a scatterer, that is,

$$\boldsymbol{K}_\mathrm{o} - \boldsymbol{K} = \boldsymbol{G}_i \pm \boldsymbol{k} \quad \text{and} \quad \varepsilon(\boldsymbol{K}_\mathrm{o}) - \varepsilon(\boldsymbol{K}) = \mp\Delta\varepsilon(\boldsymbol{k}) = \mp\hbar\Delta\omega, \tag{10.8}$$

where $\Delta\varepsilon(\boldsymbol{k})$ represents a transferred energy between the neutron and scatterer. Here, we have written specifically the lattice vector $\boldsymbol{G}_i$, because the neutron experiments indicated that the transition occurred near the Brillouin zone boundaries $\pm\boldsymbol{G}/2$. The zone-boundary transition is signified by scatterers combining two unit cells, and hence called the *cell-doubling transition*. Experimentally, the translation vector $\boldsymbol{G}_i$ was not exactly $\boldsymbol{G}/2$, but some shift from the boundary was detected, arising from a perturbation.

Expressing an incident neutron by the wave function $\psi \approx \exp \mathrm{i}(\boldsymbol{K}_\mathrm{o} \cdot \boldsymbol{r}_\mathrm{o} - \omega_\mathrm{o} t_\mathrm{o})$, the scattered neutron from a scatterer at a lattice point $\boldsymbol{r}_\mathrm{o}$ can be described by the wave function

$$\psi(\boldsymbol{r}, t) \approx \int_{V(\boldsymbol{r}_\mathrm{o})} \mathrm{d}^3 \boldsymbol{r}_\mathrm{o} \rho(\boldsymbol{r}_\mathrm{o}) \frac{\exp \mathrm{i}\{\boldsymbol{K} \cdot (\boldsymbol{r} - \boldsymbol{r}_\mathrm{o}) - \omega(t - t_\mathrm{o})\}}{|\boldsymbol{r} - \boldsymbol{r}_\mathrm{o}|} \times \exp \mathrm{i}\{(\boldsymbol{K} - \boldsymbol{K}_\mathrm{o}) \cdot \boldsymbol{r}_\mathrm{o} - (\omega - \omega_\mathrm{o}) t_\mathrm{o}\},$$

where $\boldsymbol{r}_\mathrm{o}$ and t_o represent the space-time of the impact. In the direction perpendicular to $\boldsymbol{K}_\mathrm{o}$, we require the condition for no elastic scatterings, that is, $\boldsymbol{K} = \mp \boldsymbol{k}$ and $\boldsymbol{K}_\mathrm{o} = -\boldsymbol{G}_i$, for which case $\psi(\boldsymbol{r}, t)$ can be modified as

$$\psi(\boldsymbol{r},t) \approx \int_{V(\boldsymbol{r}_\mathrm{o})} \mathrm{d}^3 \boldsymbol{r}_\mathrm{o} \rho(\boldsymbol{r}_\mathrm{o}) \frac{\exp \mathrm{i}\{\mp \boldsymbol{k} \cdot (\boldsymbol{r} - \boldsymbol{r}_\mathrm{o}) - \omega(t - t_\mathrm{o})\}}{|\boldsymbol{r} - \boldsymbol{r}_\mathrm{o}|} \exp \mathrm{i}\{(\boldsymbol{G}_i \pm \boldsymbol{k}) \cdot \boldsymbol{r}_\mathrm{o} \mp \Delta\omega \cdot t_\mathrm{o}\}.$$

We can define the structural factor for a finite area that include many scatterers at $\boldsymbol{r}_{\mathrm{o}m}$ as

$$f(\boldsymbol{G}_i \pm \boldsymbol{k}) = \int_{V(\boldsymbol{r}_\mathrm{o})} \mathrm{d}^3 \boldsymbol{r}_\mathrm{o} \rho(\boldsymbol{r}_\mathrm{o}) \exp \mathrm{i}(\boldsymbol{G}_i \pm \boldsymbol{k}) \cdot \boldsymbol{r}_\mathrm{o},$$

and express the wave function, by assuming $|\boldsymbol{r} - \boldsymbol{r}_{\mathrm{o}m}| \approx \boldsymbol{r}$ and $t_{\mathrm{o}m} \approx t_\mathrm{o}$, as

$$\Psi(\boldsymbol{G}_i \pm \boldsymbol{k}) \propto \frac{\exp \mathrm{i}\{\mp \boldsymbol{k} \cdot \boldsymbol{r} \pm \omega(t - t_\mathrm{o})\}}{r} \times \sum_m \{f(\boldsymbol{G}_i + \boldsymbol{k}) \exp \mathrm{i}(\boldsymbol{k} \cdot \boldsymbol{r}_{\mathrm{o}m} - \Delta\omega \cdot t_{\mathrm{o}m}) + f(\boldsymbol{G}_i - \boldsymbol{k}) \exp \mathrm{i}(-\boldsymbol{k} \cdot \boldsymbol{r}_{\mathrm{o}m} + \Delta\omega \cdot t_{\mathrm{o}m})\}.$$

Writing $n_m(\boldsymbol{G}_i \pm \boldsymbol{k}) = f(\boldsymbol{G}_i \pm \boldsymbol{k}) \exp \mathrm{i}(\pm \boldsymbol{k} \cdot \boldsymbol{r}_{\mathrm{o}m} \mp \Delta\omega \cdot t_{\mathrm{o}m})$, the intensity of scattered neutrons can be given by

$$I(\boldsymbol{G}_i \pm \boldsymbol{k}) = \langle |\Psi(\boldsymbol{G}_i \pm \boldsymbol{k})|^2 \rangle_t \propto \left\langle \sum_{m,n} \{n_m^*(\boldsymbol{G}_i + \boldsymbol{k}) n_n(\boldsymbol{G}_i + \boldsymbol{k}) + n_m^*(\boldsymbol{G}_i - \boldsymbol{k}) n_n(\boldsymbol{G}_i - \boldsymbol{k})\} \right\rangle_t$$
$$= \left\langle \sum_m |n_m(\boldsymbol{G}_i \pm \boldsymbol{k})|^2 \right\rangle_t + \left\langle \sum_{m \neq n} \{n_m^*(\boldsymbol{G}_i + \boldsymbol{k}) n_n(\boldsymbol{G}_i + \boldsymbol{k}) + n_m^*(\boldsymbol{G}_i - \boldsymbol{k}) n_n(\boldsymbol{G}_i - \boldsymbol{k})\} \right\rangle_t.$$

The first term represents elastic scatterings at $\pm \boldsymbol{k}$, whereas the second one indicates inelastic contributions. The latter can be expressed as

$$\langle \Delta I(\boldsymbol{G}_i \pm \boldsymbol{k})\rangle_t \propto \Bigg\langle \sum_{m\neq n} \exp \mathrm{i}\boldsymbol{G}_i \cdot (\boldsymbol{r}_{om} - \boldsymbol{r}_{on}) \times \Big[|f(\boldsymbol{G}_i + \boldsymbol{k})|^2 \exp \mathrm{i}\{\boldsymbol{k} \cdot (\boldsymbol{r}_{om} - \boldsymbol{r}_{on}) - \Delta\omega(t_{om} - t_{on})\} + |f(\boldsymbol{G}_i - \boldsymbol{k})|^2 \exp \mathrm{i}\{-\boldsymbol{k} \cdot (\boldsymbol{r}_{om} - \boldsymbol{r}_{on}) + \Delta\omega(t_{om} - t_{on})\} \Big] \Bigg\rangle_t .$$

Considering that $\boldsymbol{r}_{om} - \boldsymbol{r}_{on} = \boldsymbol{r}$ and $t_{om} - t_{on} = t$ are continuous space-time, the intensity anomaly $\langle \Delta I(\boldsymbol{G}_i \pm \boldsymbol{k})\rangle_t$ is signified by phase fluctuations $\phi = \boldsymbol{k} \cdot \boldsymbol{r} - \Delta\omega \cdot t$ and $-\phi = -\boldsymbol{k} \cdot \boldsymbol{r} + \Delta\omega \cdot t$.

If these scattering factors $f(\boldsymbol{G}_i \pm \boldsymbol{k})$ can be approximated for a small $\boldsymbol{k}$ as

$$|f(\boldsymbol{G}_i \pm \boldsymbol{k})|^2 = |f(\boldsymbol{G}_i)|^2 \pm 2\mathrm{i}\boldsymbol{k} \cdot \nabla_k |f(\boldsymbol{G}_i)|^2,$$

we can express the intensity anomaly as

$$(\Delta I(\boldsymbol{G}_i \pm \boldsymbol{k}))_t = A\langle \cos\phi\rangle_t + P\langle \sin\phi\rangle_t, \tag{10.9}$$

where

$$A \propto \int_{V(\boldsymbol{r})} |f(\boldsymbol{G}_i)|^2 \cos(\boldsymbol{G}_i \cdot \boldsymbol{r}) \mathrm{d}^3\boldsymbol{r} \quad \text{and} \quad P \propto \int_{V(\boldsymbol{r})} 2\boldsymbol{k} \cdot \nabla_k |f(\boldsymbol{G}_i)|^2 \cos(\boldsymbol{G}_i \cdot r) \mathrm{d}^3\boldsymbol{r}.$$

Here, we considered that the fluctuations are pinned symmetrically at the zone boundary. It is noted that the scattering anomalies given by (10.9) are identical to (10.7c) for X-ray diffraction.

Expression (10.9) indicates that the intensity anomaly is contributed by two modes of phase fluctuations $\langle \cos\phi\rangle_t$ and $\langle \sin\phi\rangle_t$ at intensities A and P. In Chap. 6, we have discussed such distributed intensities with respect to the phase $\phi = \boldsymbol{k} \cdot \boldsymbol{r} + \phi_o(t_o)$, where $\phi_o(t_o)$ is an arbitrary phase depending on t_o, as shown in Fig. 3.6. Figure 10.4 shows examples of anomalous intensities of scattered neutrons, which were observed from magnetic MnF_2 crystals near the critical Neél temperature T_N. These anomalies observed in different scattering geometries show clearly anisotropic intensities composed by A and P, showing phase fluctuations in these two modes. For observing such fluctuations, it is noted that the timescale t_o in the scattering process should be comparable to $\Delta\omega^{-1}$ for the energy transfer, otherwise the scattering anomalies vanish for $t_o > \Delta\omega^{-1}$.

10.3 Light Scattering Experiments

Insulating crystals are optically transparent, where light waves are refracting as normally characterized by the refractive index. However, intense coherent light waves from a *laser* oscillator can be used to detect generally feeble scattered light

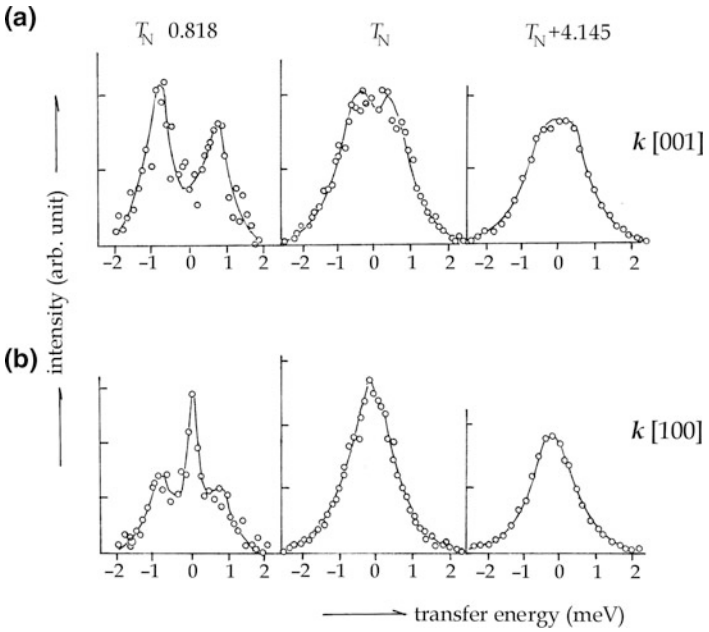

Fig. 10.4 Typical intensity distributions observed from a magnetic MnF_2 crystal at the Neél temperature T_N (from [28]).

in sizable intensity, permitting studies of phonon spectra. Incident light induces dielectric fluctuations among constituent atoms, producing *Rayleigh radiation* that are attributed to elastic impact of photons, while inelastic scatterings of laser light also occur in a substantial intensity, yielding information about phonons in a crystal.

10.3.1 Brillouin Scatterings

When sound waves are set up as standing waves in liquid, an incident monochromatic light beam exhibits a diffraction pattern that characterizes the periodically modulated densities. In this case, induced dielectric fluctuations are responsible for scatterings of light. This phenomenon is known as the *Brillouin scatterings*. The principle can be applied to sound waves in an insulating crystal, if there is a *photoelastic* mechanism for constituents to interact with the light. Such scatterings are basically inelastic collision processes between photons and constituents in a crystal, where the crystal symmetry affects minimal strains in the lattice in consequence of Born-Huang's principle.

In Fig. 10.5a, we consider that an intense monochromatic light of wave vector $\boldsymbol{K}_o$ polarized along the y-direction is incident upon the (101) plane of a sample crystal,

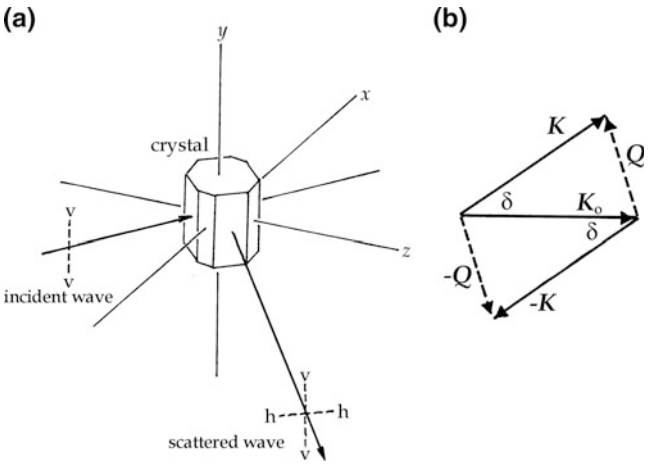

Fig. 10.5 (**a**) A light scattering arrangement for Brillouin scatterings. Incident light is polarized in the *y*-direction as marked v. . .v, while scattered light is depolarized to v. . .v and h. . .h directions. (**b**)A general Brillouin scattering geometry with phonon excitations $\pm \boldsymbol{Q}$.

and that the scattered light of $\boldsymbol{K}$ is detected in the perpendicular direction $[\bar{1}01]$. In this case, phonons of wave vectors $\pm \boldsymbol{Q}$ should participate in the scattering process as shown in Fig. 10.5b, illustrating a scattering geometry for $\boldsymbol{K}$, $\boldsymbol{K}_o$, and $\pm \boldsymbol{Q}$. It is noted that owing to photoelastic properties determined by symmetry of the crystal, the phonon waves are not necessarily longitudinal but transversal as well; consequently the scattered light $\boldsymbol{K}$ can be polarized in two directions v-v and h-h, as indicated in Fig. 10.5a. The symmetry relation between incident and scattered lights should be expressed exactly in terms of the group operations; however, we simply consider the scattered components fluctuating in vertical and horizontal directions. Namely, $\Delta p_v = \alpha_v E$ and $\Delta p_h = \alpha_h E$, where α_v and α_h are polarizabilities, if the amplitude of light is E.

Denoting the polarized laser light by the electric field $\boldsymbol{E}_o \exp i(\boldsymbol{K}_o \cdot \boldsymbol{r}_o - \omega_o t_o)$ at the impact position and time $(\boldsymbol{r}_o, t_o)$, the induced polarization is $\Delta \boldsymbol{p}(\boldsymbol{r}_o, t_o) = (\alpha)\boldsymbol{E}_o \exp i(\boldsymbol{K}_o \cdot \boldsymbol{r}_o - \omega_o t_o)$, where (α) represents a tensor with components α_v and α_h. As given in Sect. 10.1, the scattered field can be expressed for a distant point $|\boldsymbol{r} - \boldsymbol{r}_o| \approx r$ as

$$\boldsymbol{E}(\boldsymbol{r}, t) \approx \frac{\exp i(\boldsymbol{K} \cdot \boldsymbol{r} - \omega t)}{r} \iint \Delta \boldsymbol{p}(\boldsymbol{r}_o, t_o) \cdot \boldsymbol{E}_o \times \exp i\{(\boldsymbol{K}_o - \boldsymbol{K}) \cdot \boldsymbol{r}_o - (\omega_o - \omega)t_o\} d^3\boldsymbol{r}_o dt_o. \tag{10.10}$$

If $\omega = \omega_o$, (10.10) is maximum at all $|\boldsymbol{K}| = |\boldsymbol{K}_o|$, representing elastic collisions known as the *Rayleigh scatterings*. Defining the scattering angle ϕ by $\boldsymbol{K}_o \cdot \boldsymbol{r}_o = (2\pi r_o/\lambda)\cos\varphi$, where λ is the wavelength, the Rayleigh intensity $I_R(\boldsymbol{K})$ can be expressed for $r_o \ll \lambda$ as

$$\frac{I_{\mathrm{R}}(\boldsymbol{K})}{I(\boldsymbol{K}_{\mathrm{o}})} \propto \frac{2\pi^2 v^2}{r^2 \lambda^4}(1+\cos^2\varphi),$$

where the two terms on the right-hand side represent intensities for $\boldsymbol{E}_{\mathrm{v}}$ and $\boldsymbol{E}_{\mathrm{h}}$, respectively.

For inelastic Brillouin scatterings, the conservation rules are

$$\boldsymbol{K}_{\mathrm{o}} - \boldsymbol{K} = \pm\boldsymbol{Q} \quad \text{and} \quad \omega_{\mathrm{o}} - \omega = \mp\Delta\omega,$$

where $\pm\boldsymbol{Q}$ and $\mp\Delta\omega$ are the wave vectors and frequencies of scattering phonons, as illustrated in Fig. 10.5b. The angle δ between $\boldsymbol{K}_{\mathrm{o}}$ and $\boldsymbol{K}$ is called the *scattering angle*, with which the magnitude of $\boldsymbol{Q}$ is expressed as

$$|\boldsymbol{Q}| = 2|\boldsymbol{K}_{\mathrm{o}}| \sin\frac{\delta}{2}. \tag{10.11a}$$

Experimentally, to keep incident photons away from the detecting photon counter, we normally select $\delta = 90^\circ$, but the Rayleigh scatterings cannot be avoided, obscuring Brillouin spectra. In isotropic media characterized by the optical index n, for laser light of wavelengths λ, we have $|\boldsymbol{K}_{\mathrm{o}}| = 2\pi n/\lambda$ and Brillouin scatterings show frequency shifts given by

$$\Delta\nu_{\mathrm{B}} = \pm\frac{2\pi v}{\lambda}\sin\frac{\delta}{2}. \tag{10.11b}$$

The speed of phonon propagation can be evaluated from the Brillouin shift $\Delta\nu_{\mathrm{B}}$ using (10.11b).

Brillouin intensities can be expressed as

$$I_{\mathrm{B}}(\boldsymbol{K}_{\prime} \pm \boldsymbol{Q}) \propto \frac{1}{r^2}\iint (\Delta p_i \Delta p_j)\exp\mathrm{i}\{\pm\boldsymbol{Q}\cdot(\boldsymbol{r}'_{\mathrm{o}} - \boldsymbol{r}_{\mathrm{o}}) \mp \Delta\omega(t'_{\mathrm{o}} - t_{\mathrm{o}})\}\mathrm{d}^3(\boldsymbol{r}'_{\mathrm{o}} - \boldsymbol{r}_{\mathrm{o}})\mathrm{d}(t'_{\mathrm{o}} - t_{\mathrm{o}}), \tag{10.11c}$$

where $(\Delta p_i \Delta p_j)$ is a *dyadic tensor* with elements, for example, $\Delta p_{\mathrm{v}}\Delta p_{\mathrm{h}}$, for which the time average over fluctuations should be performed with respect to the time-scale of measurement.

While Brillouin scatterings are always found in crystals, we are interested in soft modes that are signified by temperature-dependent frequencies and their fluctuations. Therefore, the experimental task is to find the direction of a sound wave $\boldsymbol{Q}$ where $\Delta\nu_{\mathrm{B}}$ is temperature dependent. On the other hand, the critical fluctuations exhibited by Brillouin intensities $I_{\mathrm{B}}(\boldsymbol{K}, \pm\boldsymbol{Q})$ are difficult to isolate from the Rayleigh line, if $\Delta\nu_{\mathrm{B}}$ is too close to zero.

For a typical dielectric crystal, if assuming $n \approx 1.5$, $v \approx 2 \times 10^3\,\mathrm{m\,s^{-1}}$, and $\lambda = 514.5\,\mathrm{nm}$, the Brillouin shift can be estimated to be of the order of $\Delta\nu_{\mathrm{B}} \simeq 6\times 10^9\,\mathrm{Hz} = 0.2\,\mathrm{cm^{-1}}$. A Fabry-Pérot interferometer as sketched in Fig. 10.6 is

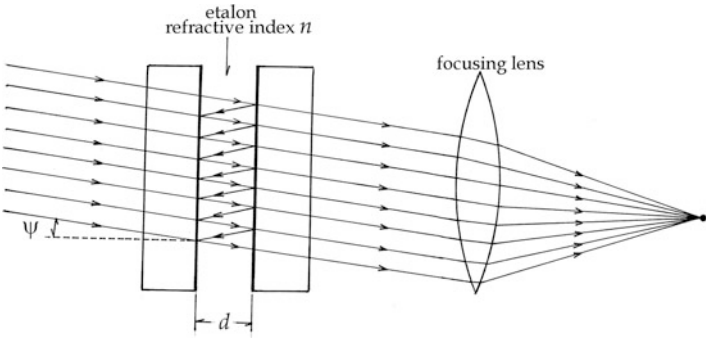

Fig. 10.6 Fabry-Pérot interferometer.

commonly used for analyzing Brillouin spectra, where a device of parallel semi-transparent planes with a narrow gap d enhances interference after multiple reflections. Denoting the index of refraction of air by n, we can write the interference condition for an incident angle ψ as

$$2nd\cos\psi = m\lambda \quad (m : \text{integers}).$$

In this device, the wavelength λ can be scanned by varying the index n with controlled air pressure.

Normally, $\psi = 0^\circ$ is chosen for normal incidence for such an interferometer, in which case $1/\lambda = m/2d$. Assuming that a wave of $\lambda - \Delta\lambda$ gives positive interference at $m + 1$, we have $1/(\lambda - \Delta\lambda) = (m + 1)/2d$; hence, the resolvable frequency range of spectra is determined by

$$\frac{1}{\lambda - \Delta\lambda} - \frac{1}{\lambda} = \frac{1}{2d}.$$

This is called the *free spectral range* (FSR) of the interferometer.

Light scattering experiments are generally performed with a fixed geometry of wave vectors as shown in Fig. 10.5b, for which the Brillouin intensities can be evaluated with (10.11c) averaged with respect to $t'_{\rm o} - t_{\rm o}$ over the timescale of observation. For the scattering geometry where $\boldsymbol{K}_{\rm o} = \boldsymbol{G}$, where $\boldsymbol{G}$ represents the unique axis of modulation, (10.11c) gives rise to intensity anomalies similar to (10.9) for neutron inelastic scatterings. For such light scatterings, the equation of motion can be written for induced dipole displacements as

$$m(\ddot{u}_i + \gamma\dot{u}_i + \omega_{\rm o}^2 u_i) = eE_{\rm v}\exp(-{\rm i}t\Delta\omega),$$

where e and m are the charge and mass of the dipole moment $\Delta p_i = eu_i$. The steady-state solution is derived as

$$\Delta p_i = \frac{e^2}{m}\frac{E_\mathrm{v}}{-\Delta\omega^2 + \omega^2 \mp \mathrm{i}\gamma\Delta\omega} = (\alpha_i' \mp \mathrm{i}\alpha_i'')E_\mathrm{v},$$

where

$$\alpha_i' \mp \mathrm{i}\alpha_i'' = \frac{e^2\varepsilon_\mathrm{o}/m}{-\Delta\omega^2 + \omega^2 \mp \mathrm{i}\gamma\Delta\omega}$$

are complex polarizabilities due to E_v. Therefore, (10.11c) can be expressed as

$$\Delta I_i(\boldsymbol{K} \pm \boldsymbol{k}) \propto \frac{E_\mathrm{v}^2}{r^2}\{(\alpha_i''\alpha_\mathrm{v})\langle\cos\phi\rangle_t + (\alpha_i'\alpha_\mathrm{v})\langle\sin\phi\rangle_t\},$$

where $\phi = \boldsymbol{k}\cdot\boldsymbol{r} - \Delta\omega\cdot t$ is the fluctuating phase in the range $0 \le \phi \le 2\pi$. We already discussed in Chap. 6 such anomalies.

Figure 10.7a, b shows a typical result of Brillouin spectra that were obtained from KDP crystals [25, 26]. The frequency shifts of Brillouin lines in Fig. 10.7a are different, depending on polarized components of scattered light, while exhibiting clearly temperature dependences as shown in Fig. 10.7b. The temperature-dependent frequency shift $\Delta\nu_\mathrm{B}$ represents clearly soft modes of $\pm\boldsymbol{k}$ and $\mp\Delta\omega$, while sinusoidal fluctuations turn theoretically to elliptical ones with increasing E_v^2. However, small Brillouin shifts near the critical temperature are masked by the intense Rayleigh line near the center, making the detail unknown. Line shapes of Brillouin lines are theoretically asymmetrical, appearing however as practically symmetrical in observed spectra.

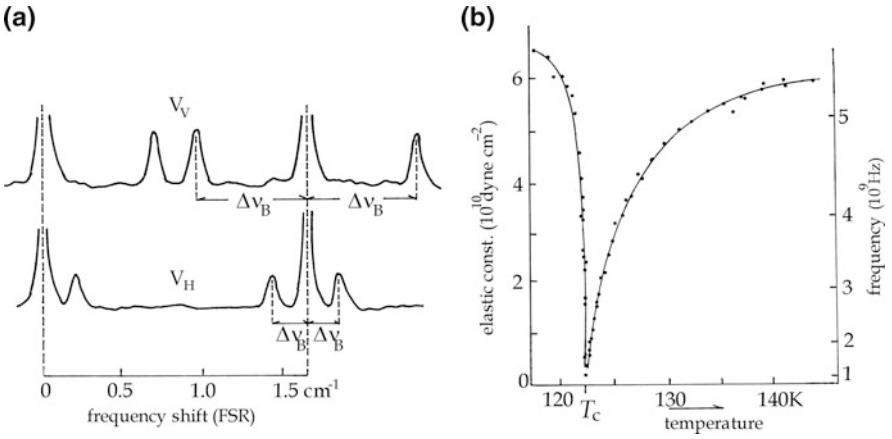

Fig. 10.7 (**a**) Examples of Brillouin spectra from KDP at room temperature. Observed in v...v and h...h directions. (**b**) Soft-mode frequency versus temperature (from [26]).

10.3.2 Raman Scatterings

Light scatterings in crystals also observed from constituent molecules that are also vibrating independently from the lattice. However, such a scattered light from constituents themselves shows a frequency shift arising from their interactions with the lattice, as first discovered by Raman. Such a frequency shift can also be analyzed for the lattice properties; this is known as the *Raman scattering*.

Following Placzek [2], assuming the lattice vibrations are characterized by a single frequency ω, Raman scatterings of a polarized monochromatic light are sketched in this section. For a constituent molecule, we consider wave equations

$$\mathcal{H}\varphi_{\mathrm{o}} = \varepsilon_{\mathrm{o}}\varphi_{\mathrm{o}} \quad \text{and} \quad \mathcal{H}\varphi_1 = \varepsilon_1\varphi_1$$

for the ground and excited energies ε_{o} and ε_1, respectively. For such a molecule embedded in a lattice, the net wave function can be written as $\varphi_{\mathrm{o}}\chi$ and $\varphi_1\chi$ in adiabatic approximation, where χ represents the wave function of vibrating lattice specified by the phonon number n.

Linearly polarized light can be decomposed into two circularly polarized components in opposite directions, namely

$$\boldsymbol{E}\cos\Omega t = \frac{1}{2}\boldsymbol{E}_+ \exp \mathrm{i}\Omega t + \frac{1}{2}\boldsymbol{E}_- \exp(-\mathrm{i}\Omega t).$$

Therefore, the Schrödinger equation for the perturbed system can be written as

$$\left\{\mathcal{H} - \frac{1}{2}\boldsymbol{p}\cdot\boldsymbol{E}_+ \exp \mathrm{i}\Omega t - \frac{1}{2}\boldsymbol{p}\cdot\boldsymbol{E}_- \exp(-\mathrm{i}\Omega t)\right\}\Psi = \mathrm{i}\hbar\frac{\partial\Psi}{\partial t},$$

where $\boldsymbol{p}$ is a dipole moment induced in the molecule. The wave function representing the ground state perturbed by $\boldsymbol{E}$ can be written as

$$\Psi_{\mathrm{o}} = \{\psi_{\mathrm{o}} + \psi_{\mathrm{o}+} \exp \mathrm{i}\Omega t + \psi_{\mathrm{o}-} \exp(-\mathrm{i}\Omega t)\} \exp\left\{-\mathrm{i}t\frac{\varepsilon_{\mathrm{o}} + n\hbar\omega}{\hbar}\right\}.$$

Hence, in the first-order approximation, we have

$$\{\mathcal{H} - (\varepsilon_{\mathrm{o}} + n\hbar\omega \pm \hbar\Omega)\}\psi_{\mathrm{o}\pm} = \boldsymbol{p}\cdot\boldsymbol{E}_\pm\psi_{\mathrm{o}},$$

which relate the unperturbed ground state ψ_{o} and polarized ground states $\psi_{\mathrm{o}\pm}$. We therefore write

$$\psi_{\mathrm{o}} = \varphi_{\mathrm{o}}\chi_{\mathrm{o}} \quad \text{and} \quad \psi_{\mathrm{o}\pm} = \varphi_{\mathrm{o}}(c_+\chi_+ + c_-\chi_-) + c_{\mathrm{o}}\psi_{\mathrm{o}},$$

where

$$c_{\pm} = \frac{\langle \pm|\boldsymbol{p}|0\rangle \cdot \boldsymbol{E}_{\pm}}{\hbar(\pm\omega \pm \Omega)}.$$

The dipole moment in the ground state can then be expressed with components

$$p_i(t) = \langle 0|p_i|0\rangle + \sum_j \{\alpha_{ij}(\Omega)E_{+j}\exp \mathrm{i}\Omega t + \alpha_{ij}(-\Omega)E_{-j}\exp(-\mathrm{i}\Omega t)\},$$

where

$$\alpha_{ij}(\Omega) = \frac{\langle 0|p_i|+\rangle\langle +|p_j|0\rangle}{\hbar(\omega+\Omega)} + \frac{\langle 0|p_j|+\rangle\langle +|p_i|0\rangle}{\hbar(\omega-\Omega)} + \frac{\langle 0|p_i|-\rangle\langle -|p_j|0\rangle}{\hbar(-\omega+\Omega)} + \frac{\langle 0|p_j|-\rangle\langle -|p_i|0\rangle}{\hbar(-\omega-\Omega)}$$

constitute the *polarizability tensor* with respect to $i, j = x, y$ in the plane of $\boldsymbol{E}_{\pm}$. For this tensor, we can verify the relations $\alpha_{ij} = \alpha_{ij}^*$ and $\alpha_{ij} = \alpha_{ji}^*$, indicating that (α_{ij}) is a *real* and *hermitic* tensor.

We can write similar expressions for the excited molecular state, that is,

$$\Psi_1 = \{\psi_{1+}\exp \mathrm{i}\Omega t + \psi_{1-}\exp(-\mathrm{i}\Omega t)\}\exp\left(-\mathrm{i}t\frac{\varepsilon_1 + n\hbar\omega}{\hbar}\right)$$

where

$$\psi_{1\pm} = \frac{\langle \pm|\boldsymbol{p}|0\rangle \cdot \boldsymbol{E}_{\pm}}{\hbar(\pm\omega \pm \Omega)}.$$

Using this Ψ_1, the induced transition probability for emission processes can be calculated with the matrix elements

$$\begin{aligned}\langle \Psi_{\mathrm{o}}^*|\boldsymbol{p}|\psi_{1\pm}\rangle &= \exp\frac{\mathrm{i}\varepsilon_{1\mathrm{o}}t}{\hbar}\int \{c_{\mathrm{o}}^*\langle\psi_{\mathrm{o}}^*|\boldsymbol{p}|\psi_1\rangle + c_+^*\langle\psi_+^*|\boldsymbol{p}|\psi_1\rangle + c_-^*\langle\psi_-^*|\boldsymbol{p}|\psi_1\rangle\}\mathrm{d}v \\ &= c_{\mathrm{o}}^*\langle\psi_{\mathrm{o}}^*|\boldsymbol{p}|\psi_1\rangle\exp\frac{\mathrm{i}\varepsilon_{1\mathrm{o}}t}{\hbar} + \frac{\langle 0|\boldsymbol{p}^*|\pm\rangle\langle\pm|\boldsymbol{p}|0\rangle}{\hbar(\pm\omega+\Omega)}\exp \mathrm{i}t\left(\Omega \pm \frac{\varepsilon_{1\mathrm{o}}}{\hbar}\right) \\ &\quad + \frac{\langle 0|\boldsymbol{p}^*|\pm\rangle\langle\pm|\boldsymbol{p}|0\rangle}{\hbar(\pm\omega-\Omega)}\exp \mathrm{i}t\left(-\Omega \pm \frac{\varepsilon_{1\mathrm{o}}}{\hbar}\right),\end{aligned}$$

where $\varepsilon_{1\mathrm{o}} = \varepsilon_1 - \varepsilon_{\mathrm{o}}$. The first term on the right-hand side is independent of the phonon energy $\hbar\omega$, whereas the second and third terms indicate Raman emission processes at $\Omega = \omega_{1\mathrm{o}} \pm \omega$ that are signified by $\Delta n = \pm 1$. The emission spectrum consists therefore of two satellite lines, as illustrated by Fig. 10.8a, traditionally called Stokes and anti-Stokes lines for plus and minus phonon, respectively. Since the phonon frequency ω is represented by frequency shifts of Raman satellites, it should exhibit softening at temperatures close to T_{c}. Figure 10.8b shows an example of Raman results of soft modes. Masked by Rayleigh radiation, the critical

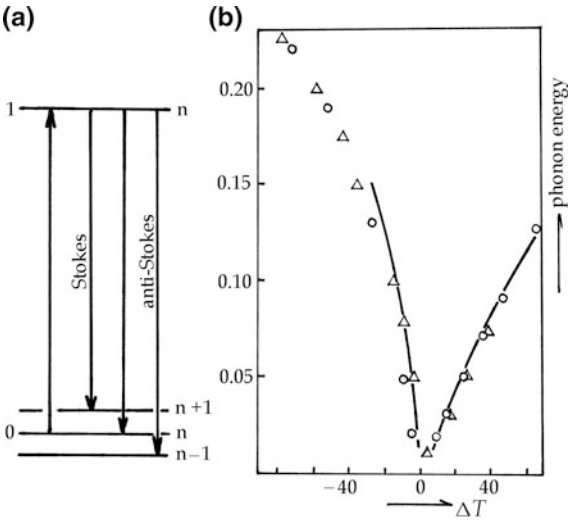

Fig. 10.8 (**a**) Raman transitions with Stokes and anti-Stokes lines. (**b**) An example of Raman studies. Soft modes from ferroelastic LaP_5O_{14} and $La_{0.5}Nd_{0.5}P_5O_{14}$ (from [29]).

anomalies are not resolved in Raman studies, which is a common difficulty in all light scattering experiments.

It should be noted, however, that the Raman satellites do not always occur, since their probabilities depend on the polarizability tensor. For example, if $\boldsymbol{p}$ is a permanent dipole and not directly associated with lattice strains, Raman emission is restricted to the selection $\Delta n = 0$, and no satellites. In general, the so-called *Raman activity* must be examined exactly prior to the experimental work.

10.4 Magnetic Resonance

The magnetic resonance technique utilizes either nuclear spins or paramagnetic ions, probing local changes in a crystal undergoing a structural transition. Normally, naturally abundant isotopic spins can be used as nuclear probes; in contrast, paramagnetic probes need to be implanted as impurities in normal crystals. In such chemically *doped* crystals, we have to be careful if the physical properties are not much modified. Nevertheless, if the process remains close to practically unchanged from undoped crystals, impurity ions provides very significant information sensitive to the transition mechanism. On the other hand, nuclear probes can be used with no such worry about structural modification; but in practice, usable isotopes may not be abundant in nature.

10.4.1 Principles of Magnetic Resonance and Relaxation

Although well known in molecular beam experiments, the equation of motion of magnetic moments in condensed matter was established by Bloch [27] for nuclear

spins, which is applicable to paramagnetic moments as well. The magnetic moments are normally independent of the hosting lattice; however, their energy transfer to the lattice is described as a relaxation process.

Microscopically, the elemental magnetic moment $\boldsymbol{\mu}$ is in Larmor precession in an applied uniform magnet field $\boldsymbol{B}_\mathrm{o} \parallel z$ at a constant frequency $\omega_\mathrm{L} = \gamma B_\mathrm{o}$, where γ is the gyromagnetic ratio, as shown in Fig. 10.9a. Its z-component μ_z is kept constant while in precession around the z-direction; the perpendicular component $\mu_\perp$ is driven by an oscillating magnetic field $\boldsymbol{B}_1$ that is applied perpendicular to $\boldsymbol{B}_\mathrm{o}$. The linearly oscillating field $\boldsymbol{B}_1$ is composed of two circularly rotating components as

$$B_1 \propto \cos\omega t = \frac{1}{2}(\exp \mathrm{i}\omega t + \exp(-\mathrm{i}\omega t)),$$

hence exerting a torque $-\mu_\perp B_1$ on $\boldsymbol{\mu}$ by the circular field in the first term, if $\omega = \omega_\mathrm{L}$, to increase the angle θ of precession. This phenomenon is the magnetic resonance. Considering such $\boldsymbol{\mu}$ in a crystal, the motion of macroscopic magnetization $\boldsymbol{M} = \sum \boldsymbol{\mu}$ should be discussed, for which Bloch wrote the equations for M_z and $M_\perp$ separately as

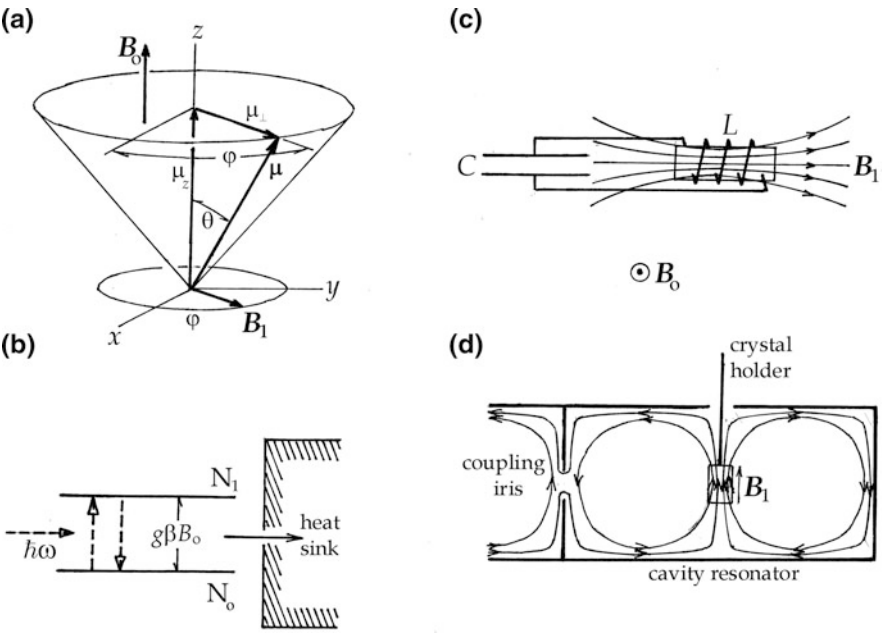

Fig. 10.9 (**a**) Larmor precession. (**b**) Magnetic resonance in thermal environment. (**c**) A *LC* resonator for magnetic resonance at radio frequencies. (**d**) A microwave resonator for a paramagnetic resonance experiment.

$$\frac{\mathrm{d}M_z}{\mathrm{d}t} = -\frac{M_z - M_\mathrm{o}}{T_1} \quad \text{and} \quad \frac{\mathrm{d}M_\perp}{\mathrm{d}t} = -\frac{M_\perp}{T_2}. \tag{10.12}$$

The first equation signifies a relaxation to thermal equilibrium with the lattice, and T_1 is called the *spin-lattice relaxation time*. The second one describes that the synchronization of microscopic $\mu_\perp$ becomes in phase to exhibit the net precession of $M_\perp = \sum \mu_\perp$; the phasing time is indicated by T_2. Bloch considered that spin-spin interactions of magnitude ΔB among microscopic $\mu_\perp$ are responsible for diverse precessions of $\boldsymbol{\mu}$, becoming in phase after T_2 that is called the *spin-spin relaxation time*. For random precessions of $\boldsymbol{\mu}$ in the presence of ΔB, it is necessary to meet the condition

$$\frac{1}{T_2} = \gamma \Delta B \ll \gamma B_1. \tag{10.13}$$

Equation (10.13) is referred to as the condition for *slow passage*.

In these two magnetic fields $\boldsymbol{B}_\mathrm{o}$ and $\boldsymbol{B}_1$, the Bloch equations are written as

$$\begin{aligned} \frac{\mathrm{d}M_\pm}{\mathrm{d}t} \pm \gamma B_\mathrm{o} M_\pm + \frac{M_\pm}{T_2} &= -\mathrm{i}\gamma B_1 M_z \exp(\mp \mathrm{i}\omega t), \\ \frac{\mathrm{d}M_z}{\mathrm{d}t} + \frac{M_z - M_\mathrm{o}}{T_1} &= \frac{\mathrm{i}}{2}\gamma B_\mathrm{o}\{M_+ \exp(-\mathrm{i}\omega t) + M_- \exp(\mathrm{i}\omega t)\}. \end{aligned} \tag{10.14}$$

In (10.14) known also as the *Bloch equations*, $M_\pm$ are the transverse components of $\boldsymbol{M}$ synchronized with the rotating fields $B_1 \exp(\mp \mathrm{i}\omega t)$.

A steady-state solution under the slow passage condition is given by $M_z =$ constant; hence from the first equation, we obtain

$$M_\pm = \frac{\gamma B_1 M_z \exp(\mp \mathrm{i}\omega t)}{\mp\omega + \gamma B_\mathrm{o} + (\mathrm{i}/T_2)}.$$

Using this result into (10.12), we can derive

$$\frac{M_z}{M_\mathrm{o}} = \frac{1 + (\omega - \omega_\mathrm{L})^2 T_2^2}{1 + (\omega - \omega_\mathrm{L})^2 + \gamma^2 T_1 T_2} \quad \text{and} \quad \frac{M_\pm}{M_\mathrm{o}} = \frac{\{(\omega - \omega_\mathrm{L})T_2 + \mathrm{i}\}\gamma B_1 \exp(\mp \mathrm{i}\omega t)}{1 + (\omega - \omega_\mathrm{L})^2 T_2^2 + \gamma^2 B_1^2 T_1 T_2}.$$

If $(\gamma B_1 T_1 T_2)^2 \ll 1$, from the first relation we have $M_z \approx M_\mathrm{o}$, for which the angle θ can be expressed as

$$\tan\theta = \frac{M_\pm}{M_\mathrm{o}} \approx \frac{\gamma B_1 T_2}{1 + (\omega - \omega_\mathrm{L})^2 T_2^2}.$$

Defining the high-frequency susceptibility by $M_\pm = \chi(\omega) B_1 \exp(\mp \mathrm{i}\omega t)$, and writing $M_\mathrm{o} = \chi_\mathrm{o} B_\mathrm{o}$, we obtain the susceptibility in complex form $\chi(\omega) = \chi'(\omega) - \mathrm{i}\chi''(\omega)$, where the real and imaginary parts are

$$\frac{\chi'(\omega)}{\chi_o} = \frac{\omega_L(\omega - \omega_L)}{(\omega - \omega_L)^2 + \delta\omega^2 + \gamma^2 B_1^2 T_1 \delta\omega}$$

and

$$\frac{\chi''(\omega)}{\chi_o} = \frac{\omega_L \delta\omega}{(\omega - \omega_L)^2 + \delta\omega^2 + \gamma^2 B_1^2 T_1 \delta\omega}. \tag{10.15}$$

Here, we have set $\delta\omega = 1/T_2$ for convenience. Magnetic resonance specified by $\omega = \omega_L$ can be detected from either $\chi'(\omega_L)$ or $\chi''(\omega_L)$; the former shows frequency dispersion in the vicinity of ω_L, whereas the latter is related to the loss of high-frequency energy, as illustrated by the curves in Fig. 9.2. These expressions in (10.15) are normally called *dispersion* and *absorption* of magnetic resonance, which can be measured as changes in resonant circuits when scanning the oscillator frequency ω or applied magnetic field B_o across the resonance condition $\omega_L = \gamma B_o$. Nevertheless, in practice, most experiments are using the field-scan method at a fixed oscillator frequency ω.

The paramagnetic moment $\boldsymbol{\mu}$ is associated with the angular momentum of electrons, that is, $\boldsymbol{\mu} = \gamma \boldsymbol{J} = \gamma\hbar(\boldsymbol{L} + \boldsymbol{S})$, where $\boldsymbol{L}$ and $\boldsymbol{S}$ are total orbital and spin angular momenta, respectively. The energy levels in a field $\boldsymbol{B}_o$ are given by $\varepsilon_m = -\gamma\hbar J_m B_o$, where $J_m = J, J-1, \ldots, -J$, for which the selection rule is $\Delta J_{m,m-1} = \pm 1$. Hence, the magnetic resonance takes place when the radiation quantum $\hbar\omega$ is equal to the energy gap between adjacent levels, that is,

$$\hbar\omega = \varepsilon_m - \varepsilon_{m-1} = \hbar\gamma B_o \Delta J_{m,m-1} = \hbar\gamma B_o \quad \text{and} \quad \omega = \gamma B_o.$$

The latter is exactly the same as the Larmor frequency ω_L. Figure 10.9b shows the quantum view of magnetic resonance. For an electron, the Larmor frequency is expressed as $\omega_L = g\beta B_o$, where $\beta = \gamma/2\hbar$ and g are Bohr's *magneton* and Landé's factor, respectively; $g = 2$ for an electron in particular.

In quantum theory, the magnetic resonance can be described as absorption and emission of a photon $\hbar\omega$ with probabilities

$$w_{m-1,m} = \frac{\pi B_1^2}{2\hbar^2} |\langle m|\mu_\perp|m-1\rangle|^2 f(\omega),$$

where $f(\omega) = 1/T_2$ is a shape function normalized as $\int f(\omega)\mathrm{d}\omega = 1$. Under practical experimental conditions where ω is a radio or microwave frequency, *induced transitions* are predominant and the *spontaneous emission* is negligible. Further, for these magnetic moments in a crystal at a normal temperature T, the population N_m at an energy level ε_m is determined by the Boltzmann statistics, that is, $N_m \propto \exp(-\varepsilon_m/k_B T)$. Therefore, at resonance $\omega = \omega_L$, the energy transfer rate to the magnetic system can be written as

$$\begin{aligned} w_{m,m-1}(\hbar\omega_L)(N_m - N_{m-1}) &= w_{m,m-1}(\hbar\omega_L) N_m \left(1 - \exp\left(-\frac{\hbar\omega_L}{k_B T}\right)\right) \\ &\approx w_{m.m-1}(\hbar\omega_L) N_m \frac{\hbar\omega_L}{k_B T} = N_m \frac{\pi\omega_L^2 B_1^2}{k_B T} |\langle m|\mu_\perp|m-1\rangle|^2 f(\omega_L). \end{aligned}$$

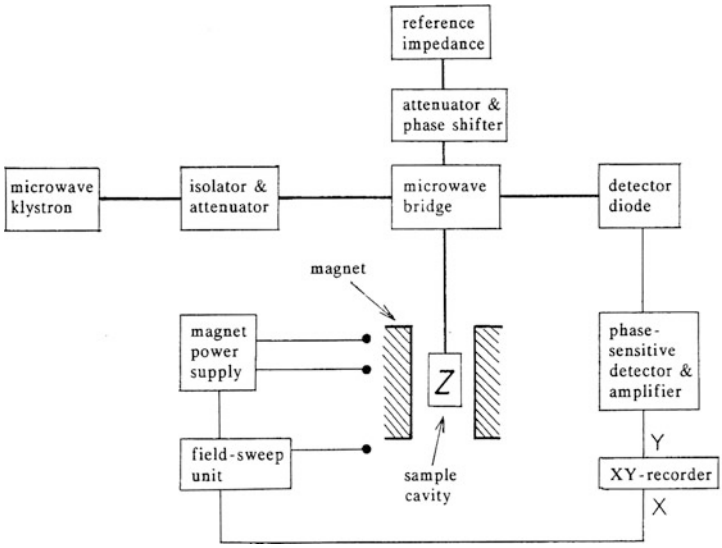

Fig. 10.10 A microwave bridge spectrometer for a paramagnetic resonance.

This should be equivalent to the macroscopic energy loss $\frac{1}{2}\omega_{\mathrm{L}}\chi''(\omega_{\mathrm{L}})B_1^2$ in a resonator, and therefore we can write

$$\chi''(\omega_{\mathrm{L}}) = N_m \frac{\pi\omega_{\mathrm{L}}}{k_{\mathrm{B}}T} |\langle m|\mu_{\perp}|m-1\rangle|^2 f(\omega_{\mathrm{L}}),$$

indicating that magnetic resonance intensity is appreciable at low temperatures.

The magnetic resonance signified by a complex susceptibility can be measured from a sample crystal placed in an inductor $L = \chi(\omega)L_{\mathrm{o}}$, where L_{o} is the *inductance* of the empty coil, producing a field B_1 by an oscillating current on L_{o}. With a conventional laboratory magnet of $B_{\mathrm{o}} \sim 10^4$ gauss, the Larmor frequency ω_{L} is of the order of 1–10 MHz for nuclear resonance, whereas it is a microwave frequency of 9–35 GHz for paramagnetic resonance. Accordingly, for these measurements, we use a *LC* resonator or a *cavity resonator*, as illustrated by Fig. 10.9c and d, respectively, in which sample crystals are placed at a location of B_1 in a maximum strength. Such a loaded inductor combined with a *capacitor C* for a radio wave measurement, and a resonant cavity for microwaves, can be expressed by an *impedance Z*, that is,

$$Z = R + \mathrm{i}\omega L + \frac{1}{\mathrm{i}\omega C} = R + \omega\chi'' L_{\mathrm{o}} + \mathrm{i}\left(\omega\chi' L_{\mathrm{o}} - \frac{1}{\omega C}\right),$$

where R is the resistance in the resonator. Figure 10.10 shows a block diagram of a microwave bridge, which is basically an impedance bridge, commonly used for paramagnetic resonance experiments. In balancing such a bridge, the real and

imaginary parts of Z can be measured independently. Although these parts are related mathematically, it is convenient in practice for $\chi'(\omega)$ and $\chi''(\omega)$ to be measured separately.

10.4.2 The Spin Hamiltonian

Although a magnetic impurity ion in a nonmagnetic crystal is primarily independent of the lattice, its electronic density is deformed by the *spin-orbit coupling* that can then modify the local symmetry. The impurity site is considered as signified by a static potential, called *crystalline potential*, representing such modified local symmetry. We postulate that such a potential can be orthorhombic with respect to impurity center, and expressed by the coordinates x, y, and z in a quadratic form

$$V(x, y, z) = Ax^2 + By^2 + Cz^2. \tag{10.16}$$

Here, for these coefficients, we have the relation $A + B + C = 0$, because such a static potential should satisfy the Laplace equation $\boldsymbol{\nabla}^2 V = 0$. Further, such a local symmetry axes are generally not the same as the symmetry axes of the lattice, since the unit cell contains usually even numbers of equivalent constituent ions. In this case, the coordinates x, y, z and the symmetry axes a, b, c of a crystal are related by a coordinate transformation, which can be determined experimentally.

Most paramagnetic impurities for typical probing are ions in the groups of *transition elements*. Considering ions of the iron groups, electrons are characterized by their net orbital and spin angular momenta, $\boldsymbol{L}$ and $\boldsymbol{S}$, which are coupled as $\lambda \boldsymbol{L} \cdot \boldsymbol{S}$, where the spin-orbit coupling constant λ is of the order of 300 cm^{-1}. On the other hand, the crystalline field energy is typically of the order of thousands cm^{-1}. Therefore, in the first approximation, we can consider that $\boldsymbol{L}$ is quantized in precession around the crystalline field, while the spin $\boldsymbol{S}$ is left as free from the lattice, which is usually described as *orbital quenching*. In this approximation, the spin-orbit coupling energy can be expressed as the first-order perturbation

$$E_{\mathrm{LS}}^{(1)} = \lambda(L_x S_x + L_y S_y + L_z S_z), \tag{10.17}$$

assuming λ as constant. The second-order perturbation energy can be calculated as

$$E_{\mathrm{LS}}^{(2)} = \frac{\lambda^2}{\Delta\varepsilon} \sum_{i,j} S_i S_j \left(\int_v \psi_{\mathrm{o}}^* L_i \psi_\varepsilon \mathrm{d}v \right) \left(\int_v \psi_\varepsilon^* L_j \psi_{\mathrm{o}} \mathrm{d}v \right),$$

which is determined by nonvanishing off-diagonal elements of $L_i L_j$ between states with an energy gap $\Delta\varepsilon$. Hence, this can be expressed in a convenient form as

$$E_{\mathrm{LS}}^{(2)} = \sum_{i,j} S_i D_{ij} S_j = \langle \boldsymbol{S} | \boldsymbol{D} | \boldsymbol{S} \rangle, \tag{10.18}$$

where $\boldsymbol{D}$ is a tensor

$$(D_{ij}) = \frac{\lambda^2}{\Delta\varepsilon}\left(\int_v \psi_o^* L_i \psi_\varepsilon \mathrm{d}v\right)\left(\int_v \psi_\varepsilon^* L_j \psi_o \mathrm{d}v\right)$$

that is called the *fine-structure tensor*, for which we can verify the relation

$$\text{trace}\,\boldsymbol{D} = \sum_i D_{ii} = 0 \quad \text{or} \quad D_{xx} + D_{yy} + D_{zz} = 0. \tag{10.19}$$

The tensor $\boldsymbol{D}$ represents the ionic charge cloud ellipsoidally deformed in the crystalline field, as illustrated in Fig. 10.11a. In this case, the spin $\boldsymbol{S}$ modified by the spin-orbit coupling interacts with the crystalline potential as describe by (10.18).

In an applied magnetic field $\boldsymbol{B}_o$, the spin can interact with $\boldsymbol{B}_o$ as expressed by the *Zeeman energy* $\mathcal{H}_Z = -\beta(\boldsymbol{L} + 2\boldsymbol{S}) \cdot \boldsymbol{B}_o$, where the orbital angular momentum $\boldsymbol{L}$ is quenched by the crystalline field; therefore, $\mathcal{H}_Z$ must be expressed to the second-order accuracy. In the first-order approximation, $\mathcal{H}_Z$ is determined by the effective magnetic moment of $\boldsymbol{S}$ only; $E_Z^{(1)} = -2\beta \boldsymbol{S} \cdot \boldsymbol{B}_o$ where $g_o = 2$. Assuming that $\boldsymbol{B}_o \parallel z$, the second-order energy is expressed as $E_Z^{(2)} = (2\lambda/\Delta\varepsilon) S_z B_o$, so that the Zeeman energy determined by $E_Z^{(1)} + E_Z^{(2)}$ is given by

$$E_z = -g_z \beta S_z B_o \quad \text{where} \quad g_z = 2\left(1 + \frac{2\lambda}{\Delta\varepsilon}\right).$$

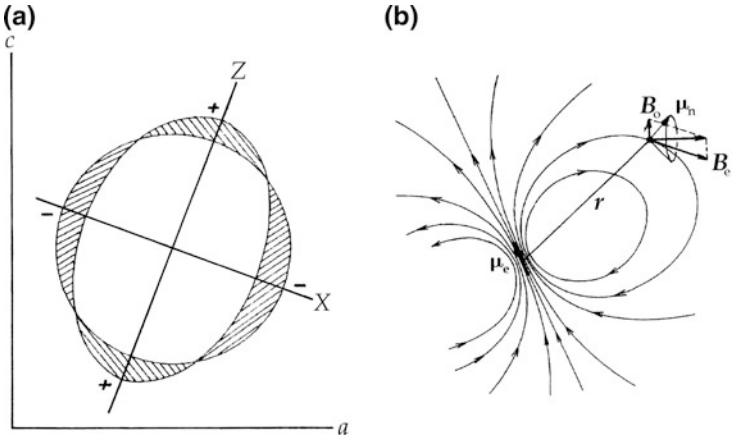

Fig. 10.11 (**a**) A symmetric distortion of a quadratic tensor of zero trace. Here, it is shown in two dimension. (**b**) The magnetic hyperfine field $\boldsymbol{B}_e$ is shown at the position of a nuclear spin μ_n in precession around the net field $\boldsymbol{B}_e + \boldsymbol{B}_o$.

If assuming $\boldsymbol{B}_\mathrm{o} \parallel x$, or y, by a similar calculation we can derive different $g_{x,y}$ expressed by

$$E_{x,y} = -g_{x,y}\beta S_{x,y}B_\mathrm{o} \quad \text{where} \quad g_x = g_y = 2\left(1 - \frac{\lambda}{\Delta\varepsilon}\right).$$

Here, we considered for simplicity that the crystalline potential is uniaxial along the z-direction. These g-factors depend on the direction of applied field, so that the Zeeman energy can generally be expressed as a tensor product by defining a tensor quantity $\boldsymbol{g} = (g_{ij})$, that is,

$$\mathcal{H}_Z = -\beta\langle \boldsymbol{S}|\boldsymbol{g}|\boldsymbol{B}_\mathrm{o}\rangle. \tag{10.20a}$$

For experimental convenience, we usually specify the applied field as $\boldsymbol{B}_\mathrm{o} = B_\mathrm{o}\boldsymbol{n}$ with the unit vector $\boldsymbol{u}$along the direction. It is therefore convenient to express (10.20a) as

$$\mathcal{H}_Z = -g_n\beta\boldsymbol{S}\cdot\boldsymbol{B}_\mathrm{o} \quad \text{where} \quad g_n^2 = \langle \boldsymbol{n}|\boldsymbol{g}^2|\boldsymbol{n}\rangle. \tag{10.20b}$$

In paramagnetic resonance, we consider the Hamiltonian consisting of (10.18) and (10.20b), that is,

$$\mathcal{H} = -g_n\beta\boldsymbol{S}\cdot\boldsymbol{B}_\mathrm{o} + \langle \boldsymbol{S}|\boldsymbol{D}|\boldsymbol{S}\rangle, \tag{10.21}$$

which is called the *spin Hamiltonian*.

For experimental convenience, the spin is considered as quantized with respect to the applied field $\boldsymbol{B}_\mathrm{o}$, and so we express $S_n = M\hbar$, where the quantum number M are $\pm$ half-integers. From (10.20a) and (10.20b), we have $g_n\boldsymbol{S} = \langle \boldsymbol{S}|\boldsymbol{g}$; hence, the second term in (10.21) can be modified as $\langle \boldsymbol{S}|\boldsymbol{g}\boldsymbol{D}\boldsymbol{g}^\dagger|\boldsymbol{S}\rangle/g_n^2$. However, since $\boldsymbol{g}$ and $\boldsymbol{D}$ are coaxial tensors, the tensor $\boldsymbol{D}' = \boldsymbol{g}\boldsymbol{D}\boldsymbol{g}^\dagger/g_n^2$ is usually written as $\boldsymbol{D}$, replacing what was originally defined as the fine-structure tensor. Accordingly, (10.21) is written for $\boldsymbol{S}$ quantized with $\boldsymbol{B}_\mathrm{o}$ as

$$\mathcal{H} = -g_n\beta S_n B_\mathrm{o} + \langle \boldsymbol{n}|\boldsymbol{D}|\boldsymbol{n}\rangle S_n^2.$$

The quantities $g_n^2 = \langle \boldsymbol{n}|\boldsymbol{g}^2|\boldsymbol{n}\rangle$ and $\langle \boldsymbol{n}|\boldsymbol{D}|\boldsymbol{n}\rangle S_n^2$ can be determined from magnetic resonance spectra recorded for all directions of $\boldsymbol{B}_\mathrm{o}$, which can be numerically diagonalized for the *principal axes* x, y, and z.

10.4.3 Hyperfine Interactions

In paramagnetic resonance spectra, the interaction between the paramagnetic moment $\boldsymbol{\mu}_\mathrm{e}$ and nuclear magnetic moment $\boldsymbol{\mu}_\mathrm{n}$ located within the orbital yields often significant structural information. As illustrated in Fig. 10.11b, such an interaction, known as the *hyperfine interaction*, can be a classical dipole-dipole

interaction, but quantum theoretically contributed by the charge density at the position of $\boldsymbol{\mu}_\mathrm{n}$ that is called a *contact* interaction. The hyperfine interaction is thus characterized by their orientation and expressed as $\langle\boldsymbol{\mu}_\mathrm{e}|\boldsymbol{A}|\boldsymbol{\mu}_\mathrm{n}\rangle$, but trace $\boldsymbol{A} \neq 0$ because of the contact contribution. Writing $\langle\boldsymbol{\mu}_\mathrm{e}| = \beta\langle\boldsymbol{S}|\boldsymbol{g}$ and $\langle\boldsymbol{\mu}_\mathrm{n}| = \gamma\langle\boldsymbol{I}|$, where $\boldsymbol{I}$ is the nuclear spin, the hyperfine interaction can be expressed as

$$\mathcal{H}_\mathrm{HF} = \beta\gamma\langle\boldsymbol{S}|\boldsymbol{g}\boldsymbol{A}|\boldsymbol{I}\rangle. \tag{10.22}$$

As $\boldsymbol{S}$ is quantized along $\boldsymbol{B}_\mathrm{o}$, (10.22) can be expressed as

$$E^{(1)}_\mathrm{HF} = -\gamma\boldsymbol{B}_\mathrm{e}\cdot\boldsymbol{I},$$

where $\boldsymbol{B}_\mathrm{e} = \beta M\sqrt{\langle\boldsymbol{n}|\boldsymbol{g}\boldsymbol{A}\boldsymbol{A}^\dagger\boldsymbol{g}^\dagger|\boldsymbol{n}\rangle}$ is the effective magnetic field due to μ_e, as shown in Fig. 10.11b; the nuclear moment $\gamma\boldsymbol{I}$ can be considered to be in precession around $\boldsymbol{B}_\mathrm{e}$, if $B_\mathrm{e} \gg B_\mathrm{o}$. In this case, the first-order hyperfine energy is given by

$$E^{(1)}_\mathrm{HF} = -g_n\beta K_n M m' \quad \text{where} \quad g_n^2K_n^2 = \langle\boldsymbol{n}|\boldsymbol{g}\boldsymbol{A}\boldsymbol{A}^\dagger\boldsymbol{g}^\dagger|\boldsymbol{n}\rangle. \tag{10.23}$$

In fact, the quantity K_n defined here is in energy unit, while in magnetic resonance practice more convenient to express it in magnetic field unit. In the field unit, we note that the hyperfine energy can simply be written as $E^{(1)}_\mathrm{HF} = -K_nMm'$. In any case, for practical convenience, we may define the hyperfine tensor $\boldsymbol{K} = \boldsymbol{g}\boldsymbol{A}/g_n$, so that (10.22) is expressed as $\mathcal{H}_\mathrm{HF} = \langle\boldsymbol{S}|\boldsymbol{K}|\boldsymbol{I}\rangle$. Further noted is that the quadratic form of K_n^2 can be diagonalized, but the principal axes do not coincide with those for the crystalline potential.

10.4.4 Magnetic Resonance in Modulated Crystals

Paramagnetic resonance spectra of transition ions are generally complicated to analyze, due to the fact that the applied magnetic field is not sufficiently strong enough to avoid complexity due to forbidden transitions. Nevertheless, the transition anomalies can be detected in anomalous g-factors, fine and hyperfine structures in selected directions of $\boldsymbol{B}_\mathrm{o}$, although complete analysis is not always possible.

We assume that a probe spin $\boldsymbol{S}$ can be modulated in a mesoscopic phase by the order variable $\sigma(\phi)$ in such a way that

$$\boldsymbol{S}' = \boldsymbol{a}\cdot\boldsymbol{S} \quad \text{where} \quad \boldsymbol{a} = \boldsymbol{1} + \langle\sigma|\boldsymbol{e}. \tag{10.24}$$

Here $\boldsymbol{1}$ and $\boldsymbol{e}$ are the tensors for identity and strains in the crystal; the latter deforms local symmetry, restricted by trace $\boldsymbol{e} = 0$. The spin Hamiltonian can therefore be modified as

$$\mathcal{H}' = -\beta\langle\boldsymbol{S}'|\boldsymbol{g}|\boldsymbol{B}_\mathrm{o}\rangle + \langle\boldsymbol{S}'|\boldsymbol{D}|\boldsymbol{S}'\rangle + \langle\boldsymbol{S}'|\boldsymbol{K}|\boldsymbol{I}\rangle.$$

Using (10.24), this can be expressed as

$$\mathcal{H}' = \mathcal{H} + \mathcal{H}_1,$$

where

$$\mathcal{H} = -\beta\langle \boldsymbol{S}|\boldsymbol{g}|\boldsymbol{B}_{\rm o}\rangle + \langle \boldsymbol{S}|\boldsymbol{D}|\boldsymbol{S}\rangle + \langle \boldsymbol{S}|\boldsymbol{K}|\boldsymbol{I}\rangle$$

and

$$\mathcal{H}_1 = -\sigma\beta\langle \boldsymbol{S}|\boldsymbol{e}^\dagger\boldsymbol{g}|\boldsymbol{B}_{\rm o}\rangle + \sigma\langle \boldsymbol{S}|\boldsymbol{e}^\dagger\boldsymbol{D} + \boldsymbol{D}\boldsymbol{e}|\boldsymbol{S}\rangle + \sigma^2\langle \boldsymbol{S}|\boldsymbol{e}^\dagger\boldsymbol{D}\boldsymbol{e}|\boldsymbol{S}\rangle + \sigma\langle \boldsymbol{S}|\boldsymbol{e}^\dagger\boldsymbol{K}|\boldsymbol{I}\rangle. \quad (10.25)$$

These terms in (10.25) are basic formula for anomalies in paramagnetic spectra in modulated phases.

In practice, we analyze such anomalies in terms of quantum numbers M and m' for $\boldsymbol{S}$ and $\boldsymbol{I}$. The Zeeman and hyperfine anomalies expressed by the first and last terms are given by $-g_n\beta MB_{\rm o}$ and $K_{\rm n}Mm'$, respectively, where the spin is linearly modulated by σ at a binary transition, hence exhibiting symmetrical and antisymmetrical fluctuations. On the other hand, the fine-structure term of $\boldsymbol{D}$ is quadratic with respect to σM, being characterized by σ and σ^2.

For the hyperfine term in (10.25), we obtain the expression

$$K_n'^2 = \langle n|\boldsymbol{a}^\dagger\boldsymbol{K}^\dagger\boldsymbol{K}\boldsymbol{a}|n\rangle = \langle n|\boldsymbol{K}^2|n\rangle + \sigma\langle n|\boldsymbol{e}^\dagger\boldsymbol{K}^2 + \boldsymbol{K}^2\boldsymbol{e}|n\rangle + \sigma^2\langle n|\boldsymbol{e}^\dagger\boldsymbol{K}\boldsymbol{e}|n\rangle;$$

therefore for a binary splitting characterized by $\pm\sigma$, we can write

$$K_n'(+)^2 - K_n'(-)^2 = 2\sigma\langle n|\boldsymbol{e}^\dagger\boldsymbol{K}^2 + \boldsymbol{K}^2\boldsymbol{e}|n\rangle.$$

The hyperfine splitting can then be expressed as

$$\Delta K_n' = K_n'(+) - K_n'(-) = \frac{2\sigma}{\bar{K}_n'}\langle n|\boldsymbol{e}^\dagger\boldsymbol{K}^2 + \boldsymbol{K}^2\boldsymbol{e}|n\rangle,$$

where $\bar{K}_n' = \frac{1}{2}(K_n'(+) + K_n'(-))$, signifying the anomaly as proportional to σ, similar to the g_n anomaly.

On the other hand, the fine-structure anomaly derived from (10.25) is

$$\mathcal{H}_{\rm 1F} = \sigma\langle S_n|\boldsymbol{e}^\dagger\boldsymbol{D} + \boldsymbol{D}\boldsymbol{e}|S_n\rangle + \sigma^2\langle S_n|\boldsymbol{e}^\dagger\boldsymbol{D}\boldsymbol{e}|S_n\rangle,$$

yielding a modulated energy

$$\Delta E_{\rm F}^{(1)} = (a_n\sigma + b_n\sigma^2)M^2,$$

where

$$a_n = \langle n|\boldsymbol{e}^\dagger\boldsymbol{D} + \boldsymbol{D}\boldsymbol{e}|n\rangle \quad \text{and} \quad b_n = \langle n|\boldsymbol{e}^\dagger\boldsymbol{D}\boldsymbol{e}|n\rangle.$$

Hence, the magnetic resonance condition for the selection rules $\Delta M = \pm 1$ is given by

$$\hbar\omega = g_n \beta B_n + (D_n + \Delta D_n)(2M + 1),$$

where

$$\Delta D_n = a_n \sigma + b_n \sigma^2. \tag{10.27a}$$

It is noted that a binary structural change is signified by a *mirror plane* characterized by $\sigma \rightarrow \pm\sigma$. Therefore, the critical region is signified by symmetric and antisymmetric fluctuations between $+ a_n\sigma + b_n\sigma^2$ and $- a_n\sigma + b_n\sigma^2$, so that the binary fluctuations are given specially by

$$\Delta D_n(A) = 2a_n\sigma_{\mathrm{A}} \quad \text{and} \quad \Delta D_n(P) = 2a_n\sigma_{\mathrm{P}} \tag{10.27b}$$

in all directions of $\boldsymbol{B}_{\mathrm{o}}$. For fluctuations in amplitude and phase modes, we have $\sigma_{\mathrm{A}} = \sigma_{\mathrm{o}} \cos\phi$ and $\sigma_{\mathrm{P}} = \sigma_{\mathrm{o}} \sin\phi$. In Fig. 10.12, $\Delta D_n(P)$ in (10.27b) and ΔD_n in (10.27a) are sketched according to magnetic resonance practice. These drawings are made on derivatives of distributed intensities with respect to the microwave frequency v, representing $\Delta v = v_1 \cos\phi$ and $\Delta v = v_1 \cos\phi + v_2 \cos^2\phi$. It is only a matter of technical convenience that magnetic resonance spectra are displayed as the first derivative.

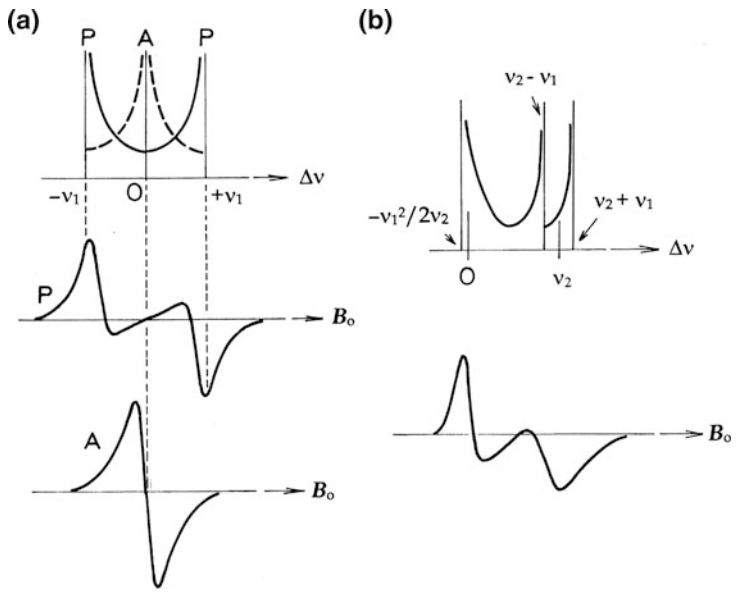

Fig. 10.12 Magnetic resonance anomalies displayed by first derivatives of the absorption $\chi''(\boldsymbol{B}_{\mathrm{o}})$. (**a**) Line shape given by (10.27b). (**b**) Line shape given by (10.27a).

10.4.5 Examples of Transition Anomalies

10.4.5.1 Mn^{2+} Spectra in TSCC

The ferroelectric phase transition in TSCC crystals at $T_c = 130\,K$ was thoroughly investigated with paramagnetic impurities, Mn^{2+}, Cr^{3+}, Fe^{3+}, VO^{2+}, etc. Although trivalent impurities show complex spectra as associated with unavoidable charge defects, there should be no problem with divalent ions. Mn^{2+} ions are particularly useful, among others, because of the simple spectral analysis in TSCC. In Fig. 10.13a shown is a Mn^{2+} spectrum when B_o applied in the *bc*-plane, where two lattice sites in a unit cell give identical spectra at temperatures above T_c. The *g*-tensor and the hyperfine tensor with a ^{55}Mn nucleus ($I = 5/2$) were found as isotropic, while the spectra in all directions of B_o were dominated by the fine structure. In Fig. 10.14a, the observed D plotted in the solid curves are for $T > T_c$, where these lines split into two broken lines at temperatures $T < T_c$,

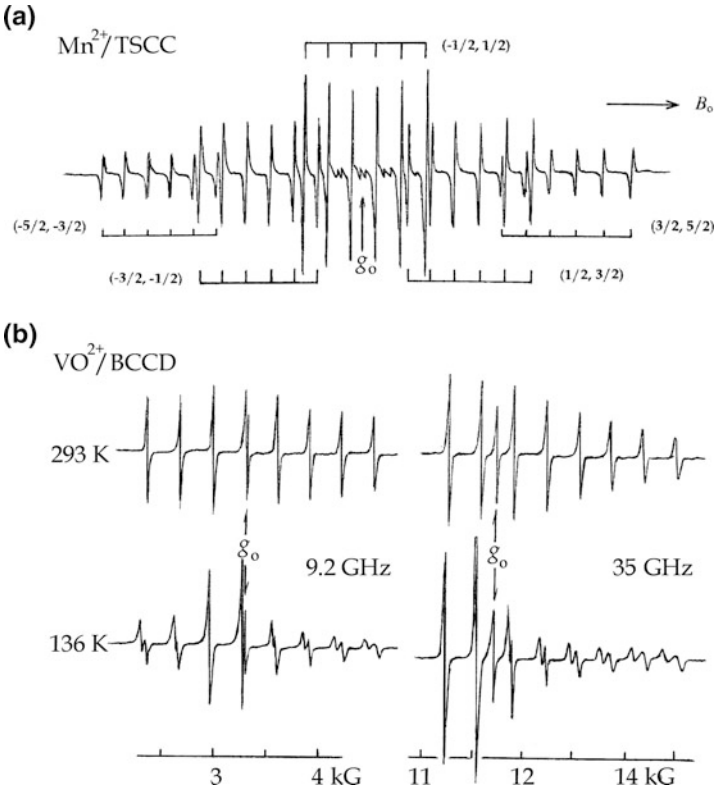

Fig. 10.13 (**a**) A representative resonance spectrum of Mn^{2+} ions in TSCC (from [30]). (**b**) Representative VO^{2+} spectra in BCCD. Spectra observed at different microwave frequencies are compared at temperatures above and below $T_c = 164\,K$ (from [31]).

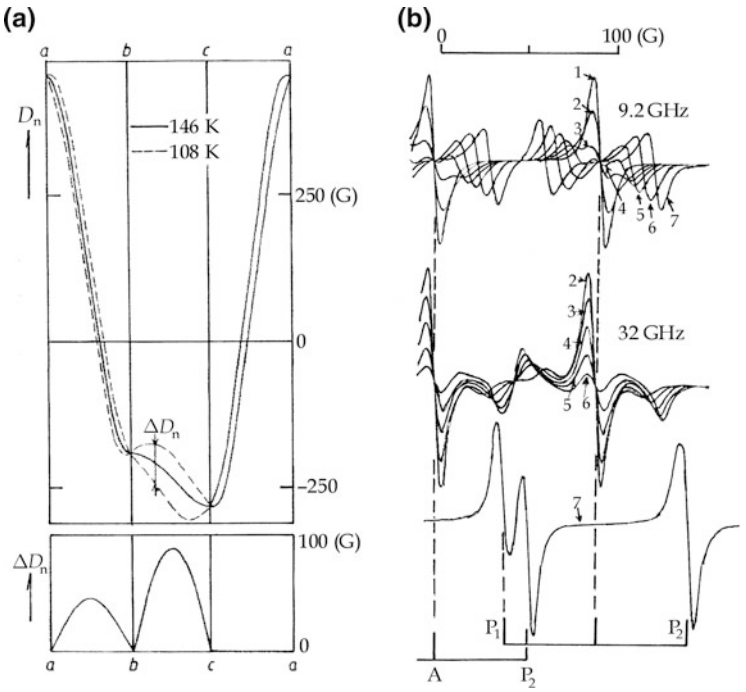

Fig. 10.14 (**a**) Angular dependence of the fine-structure splitting D_n and anomaly ΔD_n in Mn^{2+} spectra in TSCC. (**b**) Representative change of a Mn^{2+} hyperfine line with temperature. The temperature was lowered from T_c downward as $1 \rightarrow 2 \rightarrow 3 \rightarrow \cdots \rightarrow 7$. No anomaly was observed 7 (from [30]).

showing anomalous line shape with decreasing temperature. Figure 10.14b shows changing line shapes for the transition $\Delta M = 1$ and $\Delta m' = 0$ at 9.2 and 35 GHz with decreasing temperature. It is noted that the shape and splitting are explained by (10.27b) with different timescales in these resonance experiments. Also noticeable is that the central line A is more temperature dependent than the stable domain lines P.

10.4.5.2 Mn^{2+} Spectra in BCCD

BCCD crystals exhibit a sequential phase changes, as in Fig. 10.15c, showing commensurate and incommensurate phases that are indicated by C and I, where soft modes were found at thresholds in some of these transitions. Mn^{2+} impurities substituted for Ca^{2+} ions exhibited spectra distinguishing these phases, however too complex for complete analysis. Nevertheless, Mn^{2+} spectra are characterized by larger fine-structure splitting than in TSCC. Due to the large crystalline potential, the spectra exhibit both allowed and forbidden lines in comparable $\boldsymbol{B}_o$ parallel to the principal axes x, y, and z, where only allowed transitions are observed. In some other directions $\boldsymbol{n}$, transition anomalies were revealed in resonance lines for

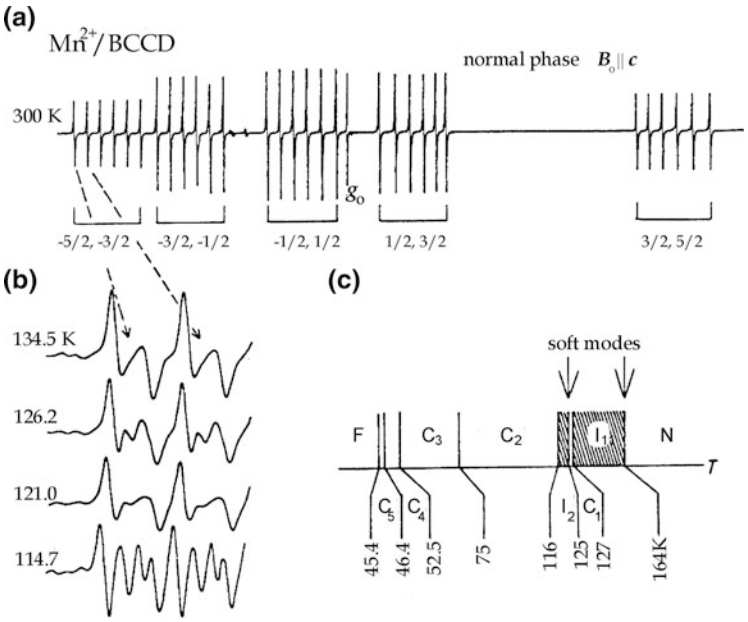

Fig. 10.15 (**a**) A Mn^{2+} spectrum from the normal phase of BCCD for $B_o \parallel c$. (**b**) A change in anomalous lines with decreasing temperature. (**c**) Sequential transitions in BCCD. *N* normal phase, *I* incommensurate phase, *C* commensurate phase, *F* ferroelectric phase (from [32]).

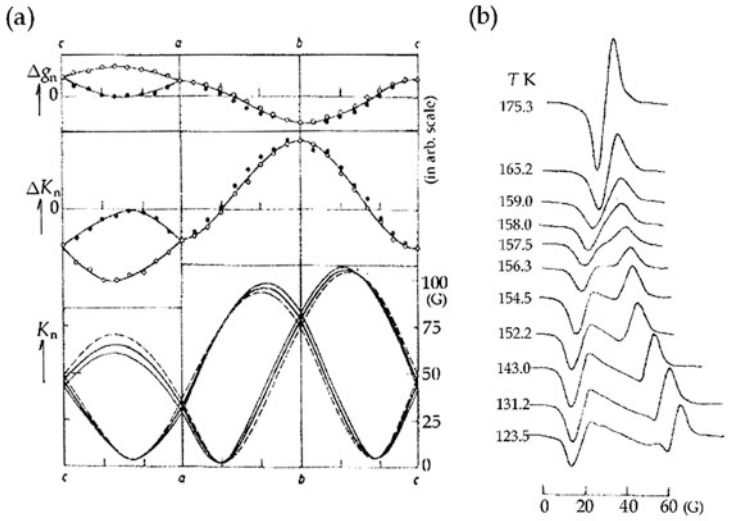

Fig. 10.16 (**a**) Angular dependences of Δg_n, ΔK_n, and K_n obtained from VO^{2+} spectra in BCCD at 130 K. (**b**) Change in line shape of a VO^{2+} hyperfine line with decreasing temperature (from [32]).

$M = \pm 5/2$, as shown in Fig. 10.15b. Here six components of ^{55}Mn hyperfine lines are in anomalous shape as illustrated by Fig. 10.12b, which is characterized by fluctuations of $a_n\sigma + b_n\sigma^2$, indicating that such resonance lines do not represent domain splitting.

10.4.5.3 VO^{2+} Spectra in BCCD

VO^{2+} ions substituted for Ca^{2+} in a BCCD crystal show simple spectra as in Fig. 10.13b, which are dominated by the hyperfine structure of ^{51}V nucleus ($I = 7/2$). Eight hyperfine component lines observed at 9.2 and 35 GHz are in different shapes, which are similar but with different separations, as can be explained by (10.26). The g_n-factor and hyperfine splitting K_n are both anisotropic, as shown in Fig. 10.16a, and the anomalies ΔK_n are of type (10.26) in all directions of $\boldsymbol{B}_{\mathrm{o}\prime}$ m' in best resolution. Observed temperature dependence of a hyperfine line is shown in Fig. 10.16b.

Part III
Superconducting States in Metals

Chapter 11
Electrons in Metals

Identical constituent molecules in a crystal are attractively correlated in the lattice structure. In a binary system below a critical temperature T_c, such correlations can be expressed as $J_{ij}\boldsymbol{\sigma}_i \cdot \boldsymbol{\sigma}_j$, where J_{ij} is undetermined by the first principle. On the other hand, in Chap. 9, we discussed that such correlations in a whole crystal can be represented by a soliton potential arising from the structure deformed by a collective mode of $\boldsymbol{\sigma}_k$. The pseudospin $\boldsymbol{\sigma}_i$ or its Fourier transform $\boldsymbol{\sigma}_k$ can be regarded as a classical field, consisting of *Fermion* particles if quantized. In metallic crystals, electrons are quantum mechanically correlated as described by Pauli's principle; such electron correlations are related with their spin directions, which are notably similar to $\boldsymbol{\sigma}_i\,\boldsymbol{\sigma}_j$ for classical molecular correlations. In this context, we may expect a similar relation between binary and electron systems, leading to analogous phase transitions.

Superconductivity was a peculiar phenomenon when discovered by Kamerlingh Onnes in 1911, but is now known as arising from a phase transition between normal and superconducting states at a very low temperature. This transition is essentially due to interplay between lattice excitations and electron correlations, which are fundamental in a multi-electron system in a crystal, as described by the quantum field theory. In this chapter, the field theory is outlined as a prerequisite for superconducting transitions in metals, where quantum correlations among electrons play an essential role, in addition to electron-phonon condensates in crystalline metals.

11.1 Phonon Statistics 2

In Chap. 2, we discussed phonons as *particles* characterized by the energy $\hbar\omega_k$ and momentum $\hbar\boldsymbol{k}$, when the lattice vibration field is quantized. The quantized vibrations can thus be equivalent to a large number of phonons that behave like independent particles. In classical language, such particles are described as

M. Fujimoto, *Thermodynamics of Crystalline States*,
DOI 10.1007/978-1-4419-6688-9_11,

independent and collision-free, whereas in the quantum field theory we consider many correlated phonons that are subjected to the uncertainty principle.

We discussed a normal mode of lattice vibrations, which are indexed by the wave vector k for the Hamiltonian $\mathcal{H}_k$, and obtained (2.14) to define operators b_k and $b_k^\dagger$. The total Hamiltonian and total number of phonons are then expressed by

$$\mathcal{H} = \sum_k \mathcal{H}_k = \sum_k \hbar\omega_k \left(b_k^\dagger b_k + \frac{1}{2} \right) \quad \text{and} \quad N = \sum_k b_k^\dagger b_k, \tag{11.1}$$

respectively. Thermodynamic properties of a phonon gas can therefore be determined by normal modes with energies $\varepsilon_k = n_k \hbar\omega_k$ composed of $n_k = b_k^\dagger b_k$ phonons at a given temperature T, moving freely in all directions of $\boldsymbol{k}$ in this approximation. Noted that ω_k are characteristic frequencies of the lattice, for which n_k can take an arbitrary value, while the total $N = \sum_k n_k$ is left undetermined.

As defined in Sect. 2.2, the operators $b_k^\dagger$ and b_k signify the energy ε_k plus and minus one phonon energy $\hbar\omega_k$, being referred to as the creation and annihilation operators, respectively. From one of the commutation relations $[b_{k'}, b_k^\dagger] = \delta_{k',k}$, we notice that these operators commute as $b_{k'} b_k^\dagger = b_k^\dagger b_{k'}$ at different k' and k, signifying that the lattice is invariant by exchanging phonons $\hbar\omega_k$ and $\hbar\omega_{k'}$ between the states k and k'. In terms of energy and momentum, two phonons $(\hbar\omega_k, \hbar k)$ and $(\hbar\omega_{k'}, \hbar k')$ are not identifiable in the crystal space, while each phonon is characterized by the rest energy $\hbar\omega_\mathrm{o}$ at $|\boldsymbol{k}| = 0$. Consisting of a large number of identical particles of $\hbar\omega_\mathrm{o}$, the vibration field can be regarded as a gas described by the Bose-Einstein statistics, as already discussed in Sect. 2.7.

For a small $|\boldsymbol{k}|$ compared with reciprocal lattice spacing, the lattice is considered as if a continuous medium. In the field theory, classical displacements q_i and the conjugate momenta p_i can be replaced by continuous variables, $q(\boldsymbol{r}, t)$ and $p(\boldsymbol{r}, t)$, propagating along an arbitrary direction. Expressed by Fourier series in one dimension, these variables can be a function of the phase of propagation, that is, $\phi = \boldsymbol{k} \cdot \boldsymbol{r} - \omega_k t$, where $\boldsymbol{r}$ and t are arbitrary position and time in a crystal, respectively. Correspondingly, the quantized field can be expressed by the field $\psi(\boldsymbol{r}, t)$ and its conjugate momentum $\pi(\boldsymbol{r}, t) = \rho[\partial\psi(\boldsymbol{r}, t)/\partial t]$, where ρ is the effective mass density. Normalizing to the volume Ω in the periodic structure, these field variables can be expressed as

$$\begin{aligned}
\psi(\boldsymbol{r}, t) &= \frac{1}{\sqrt{\Omega}} \sum_k \sqrt{\frac{\hbar}{2\rho\omega_k}} \{ b_k \exp \mathrm{i}(\boldsymbol{k} \cdot \boldsymbol{r} - \omega_k t) + b_k^\dagger \exp \mathrm{i}(-\boldsymbol{k} \cdot \boldsymbol{r} - \omega_k t) \}, \\
\pi(\boldsymbol{r}, t) &= \frac{\mathrm{i}}{\sqrt{\Omega}} \sum_k \sqrt{\frac{\hbar\rho\omega_k}{2}} \{ -b_k \exp \mathrm{i}(\boldsymbol{k} \cdot \boldsymbol{r} - \omega_k t) + b_k^\dagger \exp \mathrm{i}(-\boldsymbol{k} \cdot \boldsymbol{r} - \omega_k t) \},
\end{aligned} \tag{11.2}$$

where $b_k^\dagger = b_{-k}$. Imposing the relation

$$\int_\Omega \psi(\boldsymbol{r},t)\delta(\boldsymbol{r}-\boldsymbol{r}')\mathrm{d}\Omega = \psi(\boldsymbol{r}',t)$$

for the field $\psi(\boldsymbol{r},t)$, we can show the following commutation relations for these field variables, that is,

$$\pi(\boldsymbol{r},t)\psi(\boldsymbol{r}',t) - \psi(\boldsymbol{r}',t)\pi(\boldsymbol{r},t) = \frac{\hbar}{\mathrm{i}}\delta(\boldsymbol{r}-\boldsymbol{r}'),$$

$$\psi(\boldsymbol{r},t)\psi(\boldsymbol{r}',t) - \psi(\boldsymbol{r}',t)\psi(\boldsymbol{r},t) = 0,$$

and

$$\pi(\boldsymbol{r},t)\pi(\boldsymbol{r}',t) - \pi(\boldsymbol{r}',t)\pi(\boldsymbol{r},t) = 0.$$

Writing the Hamiltonian density as $\mathcal{H} = (\pi^2/2\rho) + (\kappa/2)(\boldsymbol{\nabla}\psi)^2$, where κ is a restoring factor per volume, we can show that (11.2) are solutions of the Heisenberg equation $-\mathrm{i}\hbar[\partial\psi(\boldsymbol{r},t)/\partial t] = \mathcal{H}\psi(\boldsymbol{r},t)$, as verified with the *Lagrangian formalism*. Nevertheless, we shall not discuss the formal theory in this book; interested readers are referred to a standard book, for example, *Quantenfeldtheorie des Festkörpers* by Haken [33].

In thermodynamics of a phonon gas, we consider that energy levels $n_k\hbar\omega_k, \ldots$ are like excitation levels that are occupied by n_k phonons at a given temperature T. Assuming the presence of correlations among unidentifiable phonons, we must put a statistical weight λ^{n_k} on the isothermal probability $\exp\left(-n_k\hbar\omega_k/k_\mathrm{B}T\right)$, where λ represents an adiabatic chance to add one phonon to this level [37]. If *phonon-phonon correlations* exist, phonon numbers n_k can be changed as if driven by a potential, which is expressed by a probability λ. In fact, λ is equivalent to the *chemical potential* μ, that is, $\lambda = \exp(\mu/k_\mathrm{B}T)$, for an *open thermodynamic system*. Using λ, the partition function of $\mathcal{H}_k$ can be written as

$$\mathrm{Z_k} = \sum_{n_k} \lambda^{n_k} \exp\left(-\frac{n_k\hbar\omega_k}{\mathrm{k_B}T}\right) = \sum_{n_k}\left\{\lambda\exp\left(-\frac{\hbar\omega_k}{\mathrm{k_B}T}\right)\right\}^{n_k}.$$

This is an infinite power series of a small quantity $x = \lambda\exp\left(-\hbar\omega_k/k_\mathrm{B}T\right) < 1$, so that Z_k can be expressed simply as $1/(1-x)$ for $n_k = 0, 1, 2, \ldots, \infty$; hence, we obtain $\mathrm{Z_k} = 1/[1-\lambda\exp(\hbar\omega_k/k_\mathrm{B}T)]$. The partition function for the whole crystal is given by the product $\mathrm{Z} = \prod_\mathrm{k}\mathrm{Z_k}$, with which the thermal average of the number of phonons can be calculated as

$$\langle n\rangle = \frac{1}{Z}\sum_k n_k\lambda^{n_k}\exp\left(-\frac{n_k\hbar\omega_k}{k_\mathrm{B}T}\right) = \lambda\frac{\partial}{\partial\lambda}\ln Z = \lambda\frac{\partial}{\partial\lambda}\sum_k \ln Z_k.$$

Therefore, we have $\langle n \rangle = \sum_k \langle n_k \rangle$, where

$$\langle n_k \rangle = \lambda \frac{\partial}{\partial \lambda} \ln \mathrm{Z_k} = -x \frac{\mathrm{d}}{\mathrm{d}x} \ln(1-x) = \frac{x}{1-x} = \frac{1}{\frac{1}{\lambda} \exp\,(\hbar\omega_k / k_\mathrm{B} T) - 1}.$$

Using μ instead of λ, the average number of phonons $\langle n_k \rangle$ at the k-state is therefore expressed by

$$\langle n_k \rangle = \frac{1}{\exp\,\{(\hbar\omega_k - \mu)/k_\mathrm{B} T\} - 1}. \tag{11.3}$$

In the limit of $T \to (\hbar\omega_k - \mu)/k_\mathrm{B} \doteq 0$, we have $\langle n_k \rangle \to \infty$, meaning that if $\mu = \varepsilon_k$, almost all phonons are thermally at the first level $\varepsilon_k = \hbar\omega_k$; this is called the *Bose-Einstein condensation*. Clearly, such a condensation can occur only at very low temperatures; however if $\mu = 0$, there is no phonon condensation.

11.2 Conduction Electrons in Metals

11.2.1 The Pauli Principle

Electrons are familiar particles in nature, known *as basic constituents of matter*. If characterized by the mass and charge, the electron is a classical particle; however, it should be treated as a quantum particle in a multielectron system, as signified by their mutual correlations. Electrons in atomic orbital states are governed by Pauli's principle that permits for two electrons with antiparallel spins to occupy each state. An electron is therefore characterized by an additional degree of freedom that is expressed by intrinsic spin variables $\pm 1/2$. Two electrons coupled with antiparallel spins are not distinguishable from each other, interacting with a force different from the electrostatic Coulomb force. The spin interaction between $+1/2$ and $-1/2$ plays a significant additional role in a multielectron system. Of course, the Coulomb interaction cannot be ignored between electrons; however, spin correlations are essential in close distance particularly.

A state of two electrons can be expressed by the wave function $\psi(\boldsymbol{r}_1, \sigma_1; \boldsymbol{r}_2, \sigma_2)$, where $\boldsymbol{r}_1$ and $\boldsymbol{r}_2$ are their positions, and σ_1 and σ_2 express spin directions of these electrons. An operator P can be defined for exchanging these electrons 1 and 2 in such a state of two electrons, that is,

$$P\,\psi(\boldsymbol{r}_1, \sigma_1; \boldsymbol{r}_2, \sigma_2) = \psi(\boldsymbol{r}_2, \sigma_2; \boldsymbol{r}_1, \sigma_1).$$

Applying P once again on both sides, the state should return to the original one, therefore

$$P^2 \psi(\boldsymbol{r}_1, \sigma_1; \boldsymbol{r}_2, \sigma_2) = P\,\psi(\boldsymbol{r}_2, \sigma_2; \boldsymbol{r}_1, \sigma_1) = \psi(\boldsymbol{r}_1, \sigma_1; \boldsymbol{r}_2, \sigma_2),$$

from which we obtain

$$P^2 = 1 \quad \text{or} \quad P = \pm 1. \tag{11.4}$$

Therefore, the wave function is given by either *symmetric* or *antisymmetric* combination of wave functions in exchanging their positions, which can be expressed by $P = +1$ or $P = -1$, respectively; the operator P is called the *parity*. Since the parity P and the Hamiltonian H are commutable, that is, $[H, P] = 0$, the eigenfunction of two electrons is given by a linear combination of $\psi(\boldsymbol{r}_1, \sigma_1; \boldsymbol{r}_2, \sigma_2)$ and $\psi(\boldsymbol{r}_2, \sigma_2; \boldsymbol{r}_1, \sigma_1)$, that is,

$$\frac{1}{\sqrt{2}}\{\psi(\boldsymbol{r}_1, \sigma_1; \boldsymbol{r}_2, \sigma_2) \pm \psi(\boldsymbol{r}_2, \sigma_2; \boldsymbol{r}_1, \sigma_1)\}.$$

Phonons and electrons are known as examples of particles in different categories that are expressed by $P = +1$ and $P = -1$, respectively; the parity and spin are therefore *intrinsic* properties of these particles. Phonons in crystals and electromagnetic *photons* are both characterized by zero spins and $P = +1$, whereas electrons and protons are particles of spin $\pm\frac{1}{2}$ and $P = -1$. In general, elementary particles have spins $1/2n$, where n is either even or odd integers, corresponding to the parity $+1$ or -1, respectively. In the theory of elementary particles, the parity and spin are intrinsic properties of particles, although disregarded in the classical theory. In the following, a large number of conduction electrons in metals are discussed, which are nearly free but can be correlated significantly at very low temperatures.

Conduction electrons in normal metal are in nearly free motion, for which we can apply the Sommerfeld's model (1928). Considering, for simplicity, a metallic crystal of cubic volume $V = L^3$ with periodic boundary conditions, one-particle state of an electron is expressed by a plane wave

$$\psi_{k,\sigma} = \exp \mathrm{i}\boldsymbol{k} \cdot \boldsymbol{r}\ \chi(\sigma) \tag{11.5}$$

with energy eigenvalues $\varepsilon(\boldsymbol{k}) = \hbar^2\boldsymbol{k}^2/2m$, where $\boldsymbol{k}$ is the wave vector, and $\chi(\sigma)$ is the spin function. Due to the Pauli's principle, each of these energy states specified by $\boldsymbol{k}$ and σ can be occupied by two electrons with antiparallel spins; all energy levels are filled with such pairs up to the level $\boldsymbol{k} = \boldsymbol{k}_\mathrm{F}$, called the *Fermi level*. If there are odd number of electrons in crystals, only the top level $\varepsilon(\boldsymbol{k}_\mathrm{F})$ is occupied by one electron with arbitrary spin, while all other levels $\varepsilon(\boldsymbol{k})$ for $k < k_\mathrm{F}$ are filled with two electrons each with antiparallel spins at $T = 0\,\mathrm{K}$. In any case, electrons near the Fermi level $\varepsilon(\boldsymbol{k}_\mathrm{F})$ can be excited by an applied electric field $\boldsymbol{E}$, causing electrical conduction, while all others can stay intact at levels $\varepsilon(\boldsymbol{k})$ below $\varepsilon(\boldsymbol{k}_\mathrm{F})$. In this model, total number of states is determined by the spherical volume of radius k_F in the reciprocal space times two, that is, $(4\pi k_\mathrm{F}^3/3) \times 2$. On the other hand, a small cube of volume $(2\pi/L)^3$ in the reciprocal space can be occupied by one state only.

Denoting the total number of electron per volume by N, we have the relation $N = 2 \times 4\pi k_{\mathrm{F}}^3/3/(2\pi/L)^3$. On the other hand, letting $L^3 = V$ the volume of a crystal, $\rho_{\mathrm{o}} = N/V$ is the number density of electrons; hence, the Fermi energy can be expressed as

$$\varepsilon_{\mathrm{F}} = \varepsilon(k_{\mathrm{F}}) = \frac{\hbar^2}{2m}(3\pi^2\rho_{\mathrm{o}})^{2/3}. \tag{11.6}$$

11.2.2 The Coulomb Interaction

In the Sommerfeld model, Coulomb's interactions among electrons are disregarded, although justifiable only in approximate manner; besides, normal crystals are electrically neutralized with ionic charges. The insignificance of Coulomb's interactions in a multielectron system was verified by Thomas and Fermi [34] in their theory of the screening effect. Placing a charge -e at the origin of coordinates in a metal, they have proved that there is no significant electrostatic effect due to other charges. Considering the static potential energy $V_{\mathrm{o}} = (1/4\pi\varepsilon_{\mathrm{o}})(e^2/r)$ and the kinetic energy $\varepsilon(\boldsymbol{k}_{\mathrm{F}})$ of an electron is perturbed by V_o, that is, $\varepsilon(\boldsymbol{k}'_{\mathrm{F}}) = \varepsilon(\boldsymbol{k}_{\mathrm{F}}) + V_{\mathrm{o}}$, resulting in the effective density $\rho' = (1/3\pi^2\hbar^3)(2mV_{\mathrm{o}} + p_{\mathrm{F}}^2)^{3/2}$, where $p_{\mathrm{F}} = \hbar k_{\mathrm{F}}$ is the Fermi-level momentum. With this density ρ', we can write the Poisson equation $\nabla^2 V' = -(\rho' - \rho_{\mathrm{o}})/\varepsilon_{\mathrm{o}}$, where ε_o is the dielectric constant of vacuum, whereas the Coulomb potential V_o should satisfy the Laplace equation $\nabla^2 V_{\mathrm{o}} = 0$. We can calculate the density difference approximately as

$$\begin{aligned}\rho' - \rho_{\mathrm{o}} &= \frac{(2m)^{3/2}}{3\pi^2\hbar^3\varepsilon_{\mathrm{o}}}\left\{\left(V_{\mathrm{o}} + \frac{p_{\mathrm{F}}^2}{2m}\right)^{3/2} - \left(\frac{p_{\mathrm{F}}^2}{2m}\right)^{3/2}\right\} \\ &= \frac{p_{\mathrm{F}}^3}{3\pi^2\hbar^3\varepsilon_{\mathrm{o}}}\left\{\left(1 + \frac{V_{\mathrm{o}}}{p_{\mathrm{F}}^2/2m}\right)^{3/2} - 1\right\} + \frac{4mp_{\mathrm{F}}}{\pi\hbar^3}V_{\mathrm{o}}\left\{1 + O\left(\frac{V_o}{p_{\mathrm{F}}^2/2m}\right)\right\}.\end{aligned}$$

Assuming that $V' = V_{\mathrm{o}}\{1 + O(V_{\mathrm{o}}/p_{\mathrm{F}}^2/2m)\}$ for a small ratio $V_{\mathrm{o}}/p_{\mathrm{F}}^2/2m = V_{\mathrm{o}}/\varepsilon_{\mathrm{F}}$, the Poisson equation can be reduced to

$$\frac{1}{r^2}\frac{\mathrm{d}}{\mathrm{d}r}\left(r^2\frac{V'}{\mathrm{d}r}\right) = -\kappa V',$$

where $\kappa = 4mp_{\mathrm{F}}/\pi\hbar^3\varepsilon_{\mathrm{o}}$. This equation gives a solution expressed by $V' \sim \exp(-\kappa r^2)$, implying that the charge $-e$ at $r = 0$ is *screened* within an effective

length $\kappa^{-\frac{1}{2}}$. Such a screening length, depending on the value of $\kappa \geq k_F$, is shorter than the nearest-neighbor distance in a typical metal. Thus, in spite of the crude assumption $V_o < \varepsilon_F$, we can postulate that Coulomb's interactions are screened and hence ignored, supporting Sommerfeld's *free electron* model.

11.2.3 The Lattice Potential

In a periodic crystal, conduction electrons cannot be free from the lattice potential

$$V(\boldsymbol{r}) = V(\boldsymbol{r} + n_1\boldsymbol{a}_1 + n_2\boldsymbol{a}_2 + n_3\boldsymbol{a}_3),$$

where (n_1,n_2,n_3) are integers along the symmetry axes. The Fourier transform of $V_{(\mathbf{r})}$ can be expressed as

$$V(\boldsymbol{r}) = \sum_G \mathrm{V_G} \exp \mathrm{i}\, \boldsymbol{G} \cdot \boldsymbol{r}, \tag{11.7a}$$

where $G = h\boldsymbol{a}_1^* + k\boldsymbol{a}_2^* + l\boldsymbol{a}_3^*$ is a translation vector in the reciprocal lattice, corresponding to the lattice translation $(\boldsymbol{a_1},\boldsymbol{a_2},\boldsymbol{a_3})$, as defined by (3.10).

In adiabatic approximation, the electronic motion is perturbed by the lattice potential, resulting in a modulated wave function

$$\psi_k(\boldsymbol{r},\sigma) = u_k(\boldsymbol{r}) \exp \mathrm{i}\boldsymbol{k} \cdot \boldsymbol{r}\ \chi(\sigma), \tag{11.7b}$$

where the amplitude $u_k(\boldsymbol{r})$ is a periodic function in the lattice. However, such a function as called Bloch's function is not uniquely determined, as seen from the relation

$$\psi_{k,\sigma}(\boldsymbol{r}) = \{u_k(\boldsymbol{r}) \exp \mathrm{i}(\pm\boldsymbol{G} \cdot \boldsymbol{r})\} \exp \mathrm{i}\{(\boldsymbol{k} \mp \boldsymbol{G}) \cdot \boldsymbol{r}\}\chi(\sigma), \tag{11.7c}$$

which is held at any lattice point $\boldsymbol{r} = \boldsymbol{R}_n$ for any k satisfying the relation

$$\boldsymbol{k} \mp \boldsymbol{G} = \boldsymbol{k}; \tag{11.8}$$

thereby, (11.7c) is another Bloch's function. Along the normal direction of a *crystal plane* (h,k,l), (11.8) represents a Bragg diffraction of the plane wave $\exp \mathrm{i}\boldsymbol{k} \cdot \boldsymbol{r}$ by such planes of $\pm\boldsymbol{G}$, reflecting and interfering in phase for a constructive diffraction pattern. Such diffraction is originated from *elastic* collisions of electrons and lattice. Therefore, the Bloch wave in the lattice behaves like a free wave modified

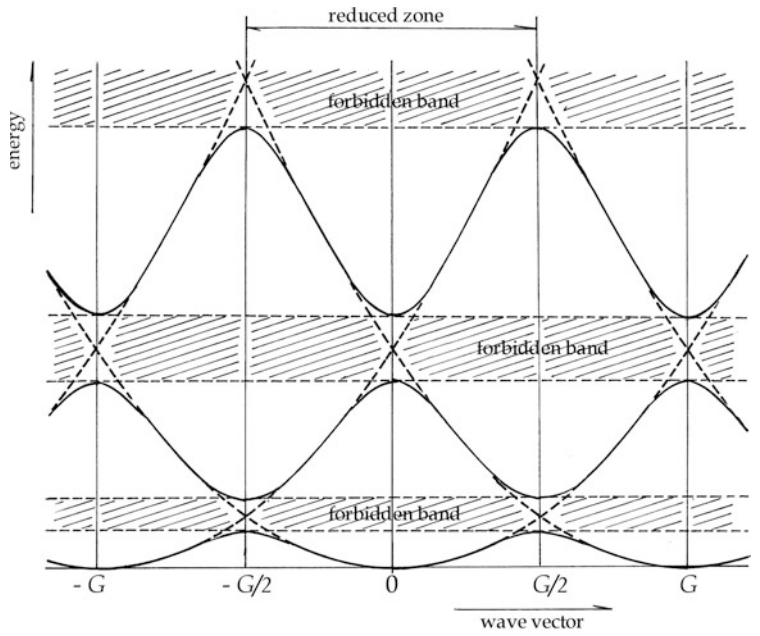

Fig. 11.1 Energy band structure of a Bloch electron in one-dimensional crystal.

by such elastic reflections at Brillouin zone boundaries. From (11.8), we note that $\varepsilon(\boldsymbol{k} \mp \boldsymbol{G}) = \varepsilon(\boldsymbol{k})$. Squaring (11.8), we have $\pm 2\boldsymbol{k} \cdot \boldsymbol{G} + \boldsymbol{G}^2 = 0$, indicating that diffractions of electron wave take place at $k = \frac{1}{2}|\boldsymbol{G}|$. Therefore, for the Bloch wave, we can reduce the reciprocal space to the first zone determined by the lowest value of $\frac{1}{2}|\boldsymbol{G}|$, that is, the first Brillouin zone. Figure 11.1 shows schematically the effect of a periodic lattice in one dimension.

In fact, at the zone boundaries, two waves $\exp \mathrm{i}(\pm \frac{\boldsymbol{G}}{2} \cdot \boldsymbol{r})$ are no longer independent, as the degenerate energy is split into $\varepsilon(\boldsymbol{G}/2) \pm V_{G/2}$, forming a band structure with forbidden energy gap $2V_{G/2}$, as shown in the figure. In addition, the energy band theory shows that the mass for a Bloch electron should be expressed by a modified effective mass m^* as given by

$$\varepsilon(\boldsymbol{k}) = \sum_{i,j} \frac{\hbar^2}{m^*} k_i k_j + \text{constant}.$$

Electrons in a metal can be described basically as free particles, although modulated by the periodic lattice, disregarding Coulomb's interactions. Since the Bloch wave is sinusoidal, electrons can interact significantly with sinusoidal lattice modes in respect to their phase relation.

11.3 Many-Electron System

Although described as nearly free particles, at very low temperature we should consider spin-spin correlations among electrons play a significant role in metals, as determined by the Pauli's principle. Due to their correlations, thermal properties of conduction electrons cannot be described by the Boltzmann statistics.

We consider a system of N electrons that are primarily independent free particles. The wave function Ψ of the system can be constructed by one-electron wave function $\psi_{k,\sigma}$ expressed by (11.5) with energies $\varepsilon(k) = \frac{\hbar^2 k^2}{2m^*}$, where m^* is the effective mass. Denoting electrons by $1, 2, \ldots, N$, such a function Ψ can be constructed with a linear combination of products of $\psi_{k,\sigma}$ in the form of Slater's determinant, that is,

$$\Psi(1,2,\ldots,N) = \begin{vmatrix} \psi_{k_1,\sigma}(1) & \psi_{k_2,\sigma}(2) & \psi_{k_3,\sigma}(3) & \ldots & \psi_{k_N,\sigma}(N) \\ \psi_{k_1,\sigma}(2) & \psi_{k_2,\sigma}(3) & \psi_{k_3,\sigma}(4) & \ldots & \psi_{k_N,\sigma}(N-1) \\ \psi_{k_1,\sigma}(3) & \psi_{k_2,\sigma}(4) & \psi_{k_3,\sigma}(5) & \ldots & \psi_{k_N,\sigma}(N-2) \\ \ldots & \ldots & \ldots & \ldots & \ldots \\ \psi_{k_1,\sigma}(N) & \psi_{k_2,\sigma}(N-1) & \psi_{k_3,\sigma}(N-2) & \ldots & \psi_{k_N,\sigma}(1) \end{vmatrix},$$

in order to satisfy Pauli's principle.

In the presence of a perturbing lattice potential *V(n)*, the eigenstate of one electron is determined by Schrödinger equation:

$$-\frac{\hbar^2}{2m}\Delta\psi_{k',\sigma} + V\psi_{k',\sigma} = \varepsilon(k').$$

In this approximation, $\Psi(1,2,\ldots,N)$ is not the eigenfunction of the whole system, but a similar Slater's determinant of the perturbed wave functions $\psi_{k',\sigma}(n)$ can represent the perturbed state of N electrons.

Electrons are indistinguishable particles, and hence each label in the wave function $\Psi(1,2,\ldots,N)$ should indicate the presence or absence of an electron in each *one-electron state*. In this sense, labels $1, 2, \ldots, N$ can be replaced, for example, by $\Psi(0_k, 1_k, \ldots, 1_k)$, etc., where 1_k and 0_k express the presence and absence of an electron in these k-states, respectively.

Creation and annihilation operators $a_k^\dagger$ and a_k can be defined for electrons, to express the following properties:

$$a_k^\dagger \psi_{k,\sigma}(0_k) = \psi_{k,\sigma}(1_k), \tag{11.9a}$$

$$a_k^\dagger \psi_{k,\sigma}(1_k) = 0, \tag{11.9b}$$

$$a_k \psi_{k,\sigma}(0_k) = 0, \tag{11.9c}$$

and

$$a_k \psi_{k,\sigma}(1_k) = \psi_{k,\sigma}(0_k). \tag{11.9d}$$

Among these, particularly (11.9b) manifests Pauli's principle; namely, no more than one particle can be in any state specified by k and σ It follows from (11.9b) and (11.9c) that

$$(a_k^\dagger)^2 = (a_k)^2 = 0.$$

To exchange two electrons in the system, we can use two creation operators $a_k^\dagger$ and $a_{k'}^\dagger$, and write

$$\begin{aligned} &a_k^\dagger a_{k'}^\dagger \{\psi_1(0_1)\psi_2(0_2)\cdots\psi_{k,\sigma}(0_k)\cdots\psi_{k',\sigma'}(0_{k'})\cdots\} \\ &\quad = \psi_1(0)\psi_2(0)\cdots\psi_{k,\sigma}(1_k)\cdots\psi_{k',\sigma'}(1_{k'})\cdots. \end{aligned}$$

Then, the antisymmetric nature for two electrons can be expressed as

$$a_k^\dagger a_{k'}^\dagger \Psi(\ldots,0_k,\ldots,0_{k'},\ldots) = -a_{k'}^\dagger a_k^\dagger \psi(\ldots,0_{k'},\ldots,0_k,\ldots). \tag{11.10}$$

Therefore, exchanging two creation operators is equivalent to exchanging $\psi_{k,\sigma}$ and $\psi_{k',\sigma'}$ in the Slater's determinant. It is noted that (11.9) and (11.10) are satisfied, if these operators obey the commutation rules

$$\begin{aligned} &[a_k, a_{k'}^\dagger]_+ = a_k a_{k'}^\dagger + a_{k'}^\dagger a_k = \delta_{k,k'}, \\ &[a_k^\dagger, a_{k'}^\dagger]_+ = 0, \quad [a_k, a_{k'}]_+ = 0. \end{aligned} \tag{11.11}$$

As in the phonon case, the number operator in the state $\psi_{k,\sigma}$ can be defined by

$$n_k = a_k^\dagger a_k, \tag{11.12}$$

so that the total number of electrons is expressed as $N_\mathrm{e} = \sum_k n_k$. We can confirm from the commutating relations in (11.11) that

$$n_k \psi_{k,\sigma}(0_k) = a_k^\dagger a_k \psi_{k,\sigma}(0_k) = 0$$

and

$$n_k \psi_{k,\sigma}(1_k) = a_k^\dagger \{a_k \psi_{k,\sigma}(1_k)\} = a_k^\dagger \psi_{k,\sigma}(0_k) = \psi_{k,\sigma}(1_k),$$

indicating that eigenvalues of the number operator n_k are 0 and 1, respectively.

The Hamiltonian for noninteracting electrons can be expressed as

$$\mathcal{H} = \sum_k \varepsilon(\boldsymbol{k}) n_k = \sum_k \varepsilon(\boldsymbol{k}) a_k^\dagger a_k, \tag{11.13}$$

where k in the foregoing one-dimensional theory can be replaced by a vector k, for which $\varepsilon(\mathbf{k})$ is the eigenvalue of one-electron Hamiltonian in three dimensions. Despite the perturbation, (11.13) can also be used for the perturbed many-electron system, if specified by eigenvalues $\varepsilon(\boldsymbol{k}')$, where $\boldsymbol{k}'$ is the perturbed wave vector. We are thus allowed to use operators $a^{\dagger}_{k'}$ and $a_{k'}$ for perturbed one-electron states $\varepsilon(\boldsymbol{k}')$.

The parity of electrons $P = -1$ is scalar and the correlation energy between electrons at $\boldsymbol{r}_i$ and $\boldsymbol{r}_j$ can be described by a scalar potential $V(\boldsymbol{r}_i - \boldsymbol{r}_j)$, representing spatial correlations. Total correlations are expressed as

$$\mathcal{H}_{\text{int}} = \frac{1}{2}\sum_{i\neq j} V(|\boldsymbol{r}_i - \boldsymbol{r}_j|). \tag{11.14}$$

Such interaction energy is determined by matrix elements between one-electron states in Slater's determinants. For almost free electrons, $\mathcal{H}_{\text{int}}$ may have nonzero matrix elements, if the potential $V(|\boldsymbol{r}_i - \boldsymbol{r}_j|)$ is a periodic function associated with lattice excitations. Assuming that

$$V(|\boldsymbol{r}_i - \boldsymbol{r}_j|) = \sum_{\pm Q} V_Q \exp\{-\mathrm{i}\boldsymbol{Q}\cdot|\boldsymbol{r}_i - \boldsymbol{r}_j|\} \quad \text{or}$$
$$V_Q = \frac{1}{\Omega}\int_{\Omega} \mathrm{d}^3|\boldsymbol{r}_i - \boldsymbol{r}_j| \exp \mathrm{i}Q\cdot|\boldsymbol{r}_i - \boldsymbol{r}_j|, \tag{11.15}$$

such matrix elements can be written as

$$\langle \boldsymbol{k}, \boldsymbol{k}'|\mathcal{H}_{\text{int}}|\boldsymbol{k}'', \boldsymbol{k}'\rangle = \frac{1}{2\Omega}\int\!\!\int_{\Omega} \mathrm{d}^3\boldsymbol{r}_i \mathrm{d}^3\boldsymbol{r}_j V(|\boldsymbol{r}_i - \boldsymbol{r}_j|) \exp \mathrm{i}\{(k - k'')\cdot\boldsymbol{r}_i + (k' - k')\cdot\boldsymbol{r}_j\}.$$

Therefore, such $\mathcal{H}_{\text{int}}$ as related to (10.15) can give rise to a secular perturbation, if we have the relations

$$\boldsymbol{k} - \boldsymbol{k}' = \boldsymbol{Q} \quad \text{and} \quad \boldsymbol{k}'' - \boldsymbol{k}''' = -\boldsymbol{Q} \tag{11.16}$$

or

$$\boldsymbol{k} - \boldsymbol{k}' = \boldsymbol{k}''' - \boldsymbol{k}'',$$

where $\pm\boldsymbol{Q}$ are phonon vectors. This implies that an electron emits a phonon $\hbar\boldsymbol{Q}$ on collision with the lattice, which is subsequently absorbed by the lattice, so that the two-electron process (11.16) appears as if elastic scatterings. Hence, for this process, the matrix element can be expressed as

$$\langle \boldsymbol{k}, \boldsymbol{Q} | \mathcal{H}_{\text{int}} | \boldsymbol{k}'', -\boldsymbol{Q} \rangle = \frac{1}{2\Omega} \sum_{k,k'',Q} V_Q a^\dagger_{k+Q} a_k a^\dagger_{k''-Q} a_{k''}. \tag{11.17}$$

In a *static* periodic lattice potential, we noticed that electrons can be *scattered* as in the Bragg diffraction; however, such scatterings, in contrast, may occur dynamically in a modulated lattice structure. As discussed later, Fröhlich considered phonon-electron interactions as described in the above argument.

11.4 Fermi–Dirac Statistics for Conduction Electrons

In a metallic crystal, energy levels $\varepsilon(\boldsymbol{k})$ of one conduction electron are practically continuous, which are thermally accessible in thermodynamic environment. Obeying the Pauli's principle, such one-electron state ψ_k is either vacant or occupied by one electron in specified spin state, that is, $\psi_k(0)$ or $\psi_k(1)$ with thermal probabilities 1 or $\exp\left(-\varepsilon(\boldsymbol{k})/k_{\text{B}}T\right)$, corresponding to excitation energy zero or ε, respectively. Considering correlations among these electrons, the latter should be modified by multiplying the factor λ as in the case of phonons; we can write the Gibbs sum

$$Z_k = 1 + \lambda \exp\left(-\frac{\varepsilon(\boldsymbol{k})}{k_{\text{B}}T}\right).$$

For electrons, the energy ε**(k)** can be occupied by only one electron in a specific spin state, so that n_k=1. Therefore, the thermodynamic probability for a one-particle state ε to be occupied by one electron is given by

$$P(\varepsilon, 1) = \frac{1}{\exp\frac{(\varepsilon-\mu)}{k_{\text{B}}T} + 1}. \tag{11.18}$$

Electrons are particles obeying (11.8) at temperature T, which is called the Fermi-Dirac distribution.

Exercises 11

1. The Bose-Einstein distribution is determined by the probability for an energy level $\varepsilon = n\varepsilon_{\text{o}}$ to be occupied by n particles of energy $\varepsilon_{\text{o}} = \hbar\omega$, which is expressed by

$$P_{\text{BE}}(\varepsilon, n) = \frac{1}{\exp\frac{(\varepsilon-\mu)}{k_{\text{B}}T} - 1}.$$

On the other hand, the Fermi-Dirac distribution is given by

$$P_{\mathrm{FD}}(\varepsilon, 1) = \frac{1}{\exp\frac{(\varepsilon-\mu)}{k_{\mathrm{B}}T} + 1}.$$

Show that these distributions become identical, if $\exp\frac{(\varepsilon-\mu)}{k_{\mathrm{B}}T} = 1$, that is,

$$P_{\mathrm{BE}}(\varepsilon, n) \approx P_{\mathrm{FD}}(\varepsilon, 1) \approx \exp\frac{\mu - \varepsilon}{k_{\mathrm{B}}T}.$$

This is the Gibbs factor in Boltzmann–Gibbs statistics. Discuss these results in terms of the criterion for quantum and classical particles.

2. Show that a pressure of a Fermi electron gas in the ground state is given by

$$p = \frac{(3\pi^2)^{\frac{2}{3}}}{5}\frac{\hbar^2}{m}\left(\frac{N}{V}\right)^{\frac{5}{3}}.$$

Find an expression for the entropy of a Fermi electron gas, assuming $k_{\mathrm{B}}T << \varepsilon_{\mathrm{F}}$.

Chapter 12
Superconducting Phases

In 1911, Kamerlingh Onnes discovered superconducting mercury, which however remained as puzzling for some time with no significant applications. It is now recognized as a fundamental problem in the many-electron system superconductivity occurs in many conductors below critical temperatures T_c of phase transitions. In this chapter, the superconducting phenomenon and related theories are summarized, prior to discussing the Bardeen-Cooper-Schrieffer theory in Chap. 13. The superconducting state is characterized not only by zero electrical resistance, but also as *perfect diamagnetism*, making the thermodynamic description more complex than structural phase transitions.

12.1 Superconducting States

12.1.1 Zero Electrical Resistance

The electric conduction in metals originates from drifting electrons as described by the Ohm's law. The energy loss of electrons can be attributed to inelastic collisions between electrons and the lattice; the electrical resistance obeys normally Matthiessen's rule expressed by

$$R = R_{\text{ideal}} + R_{\text{res}}.$$

Here, R_{ideal} is due to scatterings by the lattice, whereas the residual resistance R_{res} is caused by impurities and imperfections in the lattice. The resistance R_{ideal} exhibits temperature dependence proportional to T^5 at temperatures below the Debye's temperature Θ_D, whereas R_{res} is virtually temperature independent. Figure 12.1a, b compares a typical normal resistance of platinum with superconducting mercury. The Matthiessen's rule is clearly seen from Fig. 12.1a, while the electric resistance of Hg shows an abrupt drop down to near zero at a specific temperature T_c. This was

M. Fujimoto, *Thermodynamics of Crystalline States*,
DOI 10.1007/978-1-4419-6688-9_12, © Springer Science+Business Media, LLC 2010

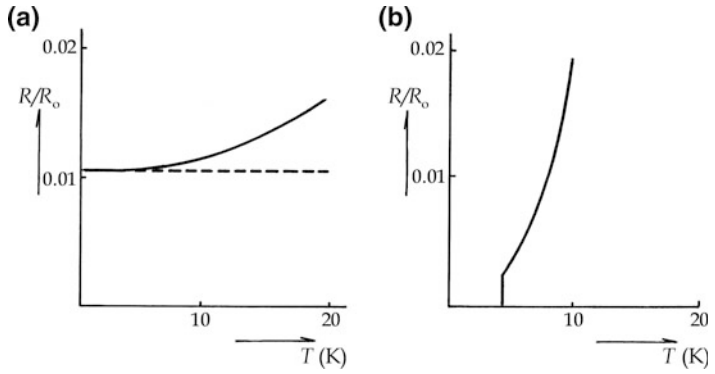

Fig. 12.1 (**a**) Electrical resistance in normal metals. (**b**) Electrical resistance of superconducting mercury.

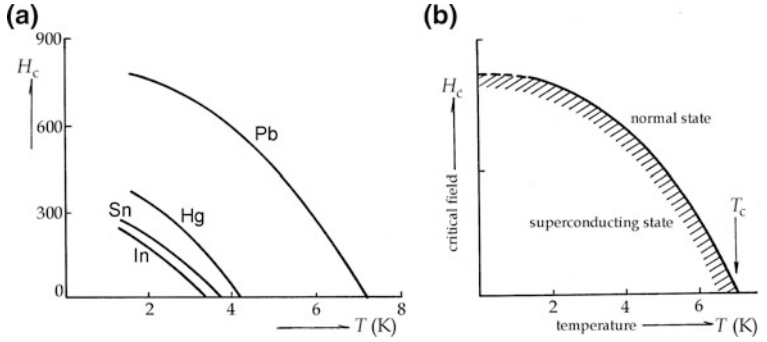

Fig. 12.2 H_c - T phase diagram of superconducting metals. (**a**) Observed results. (**b**) Idealized phase diagram.

a peculiar phenomenon, judging from a normal conductivity shown in Fig. 12.1a. The nearly zero resistance of Hg below T_c implies that the corresponding current becomes infinite, according to the Ohm's law; the metal can thereby be characterized by infinite conductivity. In this case, the current in a superconducting coil should be persistent, which was in fact demonstrated by Collins, who estimated that the resistance is near zero, that is, $R_{\text{super}} < R_{\text{normal}} \times 10^{-15}$.

Nevertheless, early attempts to obtain a high magnetic field using a superconducting solenoid were a failure. It was learned that the superconductivity was destroyed by own magnetic field of the coil. It became clear experimentally that at temperatures below T_c there is a *critical magnetic field* H_c to destroy superconductivity. The field H_c was found to be a function of T that appeared to be parabolic as shown in Fig. 12.2a. The lowest temperature in these measurements was limited to about 1.7 K, the H_c versus T relation was extended close to 0 K on a parabolic curve

$$H_c = H_o\left(1 - \frac{T^2}{T_c^2}\right). \tag{12.1}$$

Here H_o is the extrapolated value of H_c to 0 K, which is relatively weak as shown in Fig. 12.2 for these superconducting metals. Inspired by such a $H_c - T$ curve, Fig. 12.2b looks like a phase diagram between normal and superconducting states, although the origin of a critical magnetic field is not immediately clear.

12.1.2 The Meissner Effect

Meissner and Ochsenfeld (1933) discovered the effect of a magnetic field applied to a superconductor. If a conductor in near-ellipsoidal shape is cooled down below the transition temperature in the presence of a magnetic field of sufficient strength, all magnetic field lines are found to be all pushed outside, as illustrated by Fig. 12.3. Such a magnetic effect, known as the *Meissner's effect*, idealizes the superconducting state by zero flux density inside the conductor, that is,

$$\boldsymbol{B} = 0. \tag{12.2}$$

For a magnetizable material, ellipsoidal shapes can be employed for simplicity, in which case we can write $\boldsymbol{B} = \mu_0\boldsymbol{H} + \boldsymbol{M}$, where $\boldsymbol{M}$ is the magnetization; thereby, the Meissner effect (12.2) can be expressed by the susceptibility $\chi_m = M/H = -\mu_o$ in MKS unit. In this context, the superconducting state can be referred to as *perfect diamagnetism*. Figure 12.4a shows the magnetization curve for an *idealized superconductor*, where the magnetization rises as proportional to the applied field strength, however diminishing suddenly to zero at the critical field H_c. Thus, an ideal superconductor is characterized by perfect diamagnetism in addition to infinite conductivity, although their relation is unknown.

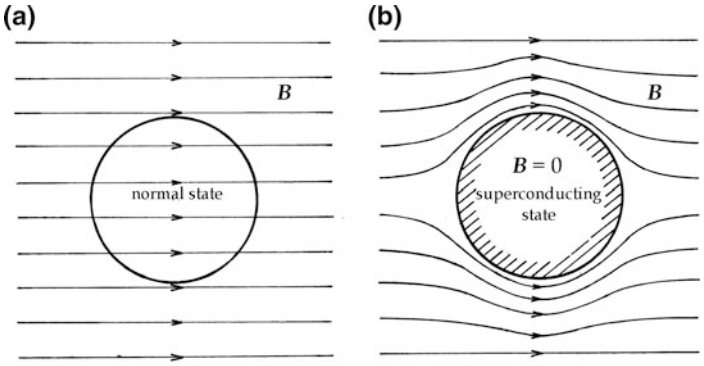

Fig. 12.3 The Meissner's effect in an idealized superconducting sphere. (**a**) Normal state. (**b**) Superconducting state.

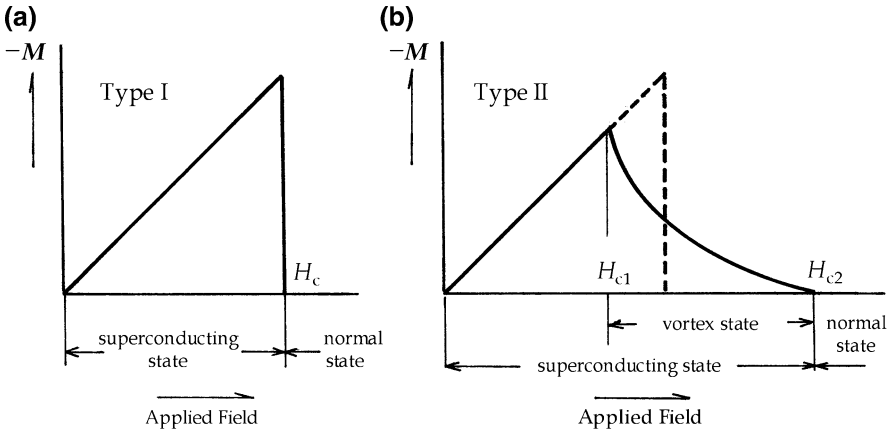

Fig. 12.4 Magnetization curves for Meissner's effect in superconductors. (**a**) Type I. (**b**) Type II.

Using Ohm's law, the superconducting current density can be expressed as $\boldsymbol{j} = \sigma \boldsymbol{E}$, where $\boldsymbol{E}$ is an applied electric field. Such an electric field $\boldsymbol{E}$ must, however, be zero if $\sigma = \infty$, in which case from the Maxwell's equations, we obtain $\partial \boldsymbol{B}/\partial t = 0$, implying that $\boldsymbol{B}$ must be constant of time. This suggests that the magnetic flux density $\boldsymbol{B}$ penetrated into a conductor at temperatures above T_c should be *frozen* in the superconducting state, when the temperature is lowered below T_c. In contrast, the Meissner effect characterizes a superconductor by $\boldsymbol{B} = 0$, and moreover we cannot determine the superconducting current $\boldsymbol{j}$ by the Maxwell theory. We must therefore consider that Meissner's effect is independent from the supercurrent $\boldsymbol{j}$.

On the other hand, the magnetization $\boldsymbol{M}$ due to Meissner's effect is distributed generally in practical samples depending on its shape, and hence the critical field cannot be uniform. Pure metals were studied with samples in long cylindrical shape that are regarded as approximately ellipsoidal, where H_c can take a well-defined single value. Such an idealized superconductor as characterized by a magnetization curve in Fig. 12.4a is referred to as *Type I*. However, there are some superconductors of alloy compounds, which are characterized by intrinsically distributed H_c, and called *Type II*. In Fig. 12.4 shown is a typical magnetization curve of a Type II superconductor, which is signified by two critical fields H_{c1} and H_{c2}, as indicated in the figure. The region between H_{c1} and H_{c2} is generally called the *vortex region*. Type II superconductors can be considered for important applications, if H_{c2} is sufficiently high, for the superconductivity is extended to a vortex region in relatively high magnetic fields.

12.1.3 Normal and Superconducting Phases in Equilibrium

We consider a superconducting state of a Type I metal specified by magnetization $\boldsymbol{M}$ due to the Meissner effect. As inferred from Fig. 12.2b, the superconducting

state can be in mixed normal and superconducting phases in equilibrium. In contrast to the normal phase that is nonmagnetic, the superconducting phase is characterized by a magnetization $\boldsymbol{M}$ that can be considered as induced by a magnetic field $\boldsymbol{H} = -\boldsymbol{M}/\mu_0$, so that the Meissner effect can be represented by an external work $-\boldsymbol{H}\cdot\mathrm{d}\boldsymbol{M}$ per unit superconducting volume. Therefore, under a constant volume condition, the first law of thermodynamics can be written for the superconducting phase as

$$\mathrm{d}U = \boldsymbol{H}\cdot\mathrm{d}\boldsymbol{M} + T\mathrm{d}S. \tag{12.1}$$

Defining the Gibbs function as

$$G(H,T) = U - TS - HM, \tag{12.3}$$

the thermal equilibrium can be specified by $\mathrm{d}G \leq 0$ against variations of T and H.

The condition for the two phases to coexist at a temperature T at the critical field H_c is that the densities of Gibbs functions g_s and g_n – which are defined by the relations $g_\mathrm{s}V_\mathrm{s} = G_\mathrm{s}$, $g_\mathrm{n}V_\mathrm{n} = G_\mathrm{n}$, and $V_\mathrm{s} + V_\mathrm{n} = V$ – can take the same value if the two phases are in thermal contact. We therefore write

$$g_\mathrm{s}(H_\mathrm{c},T) = g_\mathrm{n}(H_\mathrm{c},T), \tag{12.4}$$

on the equilibrium line in Fig. 12.2b. In the normal phase, g_n has nothing to do with the magnetic field H_c; hence, $g_\mathrm{n}(H_\mathrm{c},T)$ can be replaced by $g_\mathrm{n}(0,T)$.

At T_c, in the absence of an external field, we have

$$g_\mathrm{n}(0,T_\mathrm{c}) = g_\mathrm{s}(0,T_\mathrm{c}), \tag{12.5}$$

implying that the transition is continuous. On the other hand, in the presence of an applied field H for $T<T_\mathrm{c}$, the Gibbs function $G_\mathrm{s}(H_\mathrm{c},T)$ should be calculated as

$$G_\mathrm{s}(H_\mathrm{c},T) = G_\mathrm{s}(0,T) - V\int_0^{H_\mathrm{c}} M(H)\mathrm{d}H = G_\mathrm{s}(0,T) + V\left(\frac{1}{2}\mu_\mathrm{o}H_\mathrm{c}^2\right).$$

This superconducting phase is in equilibrium with the normal $G_\mathrm{n}(0,T)$ in H_c. Hence, the transition is discontinuous at T, as expressed by

$$g_\mathrm{n}(0,T) - g_\mathrm{s}(0,T) = \frac{1}{2}\mu_\mathrm{o}H_\mathrm{c}^2. \tag{12.6}$$

Using the thermodynamic relation

$$S_\mathrm{n} - S_\mathrm{s} = -\left\{\frac{\partial}{\partial T}(G_\mathrm{n} - G_\mathrm{s})\right\}_V,$$

the latent heat L per volume can then be expressed as

$$L = -\mu_o T H_c \frac{dH_c}{dT}. \tag{12.7}$$

In Ehrenfest's classification, such a transition below T_c is first order, changing between normal and superconducting phases with applied field in the range $0 \leq H \leq H_c$ in mixed volumes of these phases. The transition at T_c is second order, for which $L = 0$; hence, we obtain $H_c = 0$ from (12.7).

On the other hand, the specific heat exhibits a discontinuity at T_c because of a sudden change in the magnetization, which can be calculated at a constant volume V as

$$c_s - c_n = T\left\{\frac{\partial(s_s - s_n)}{\partial T}\right\}_V = \mu_o T\left\{H_c \frac{d^2 H_c}{dT^2} + \left(\frac{dH_c}{dT}\right)^2\right\}. \tag{12.8a}$$

Since $H_c = 0$ at T_c, the discontinuity at T_c is given by

$$(c_s - c_n)_{T_c} = \mu_o T_c \left(\frac{dH_c}{dT}\right)^2, \tag{12.8b}$$

which is known as *Rutger's formula*.

The temperature dependence of H_c is significant in the above argument, particularly when the absolute zero is approached. According to the third law of thermodynamics, we should expect $s_n - s_s \to 0$ in the limit of $T \to 0$. In (12.8b), this condition is fulfilled if

$$\lim_{T \to 0} \frac{dH_c}{dT} = 0. \tag{12.9}$$

Therefore, the tangent at $T = 0$ is horizontal, so that the equilibrium curve is not exactly parabolic.

12.2 Long-Range Order in Superconducting States

The superconducting state below T_c is composed of two volumes of normal and superconducting states, whose ratio depends on the magnitude of applied magnetic field. The transition at T_c is second order with no latent heat, accompanying a discontinuous specific heat. On the other hand, below T_c, the superconducting state consists of normal and superconducting phases, whose volumes vary adiabatically with an external magnetic field; hence, the transition is first order. In this case, it is logical to define an order parameter with Landau's theory to describe such an

adiabatic process in a superconducting state. With such an order parameter, we can sketch the *mesoscopic* process in terms of temperature and applied magnetic field, although Landau's theory is limited only to the mean-field accuracy.

In a superconducting state, the order parameter can be defined as $\eta = 0$ at T_c and $\eta = 1$ for complete order at $T = 0$K. Disregarding structural details of the lattice, we can consider the density of Gibbs function as $g(\eta, T)$ and write

$$g(0, T_c) = -\frac{1}{2}\gamma T_c^2, \tag{i}$$

where γT_c represents the specific heat of conduction electrons at T_c, as derived from Sommerfeld's formula $c_{el} = \gamma T$ for a electron gas. On the other hand, $g(1,0)$ should represent the order energy of condensed electrons per unit volume at $T = 0$, which is given by

$$g(1, 0) = -\frac{1}{2}\mu_o H_o^2. \tag{ii}$$

Unlike binary systems, no inversion symmetry exists in multielectron system, so that the Gibbs function can be expressed in a series expansion with even and odd power terms. That is,

$$g(\eta, T) = g_o + \alpha(H, T)\eta + \frac{1}{2}\beta(H, T)\eta^2 + \cdots. \tag{iii}$$

Gorter and Casimir wrote $g(\eta,T)$ in an alternative form

$$g(\eta, T) = g_o - \frac{\mu_o H_c^2}{2}\eta - \frac{\gamma T^2}{2}\sqrt{1-\eta}. \tag{12.10}$$

Here, the factor $\sqrt{1-\eta}$ of the third term in (12.10) is somewhat ambiguous; however, their $g(\eta,T)$ is appropriate to meet requirements (i) and (ii). In Landau's function (iii), these coefficients α, β,. . . are left arbitrary, so that (iii) and (12.10) are not conflicting. Nevertheless, Gorter-Casimir's formula is a useful approximation to deal with observed specific heat and $H_c(T)$ for $T<T_c$.

Using (12.10), thermal equilibrium can be determined from $(\frac{\partial g}{\partial \eta})_{H,T} = 0$, that is,

$$\frac{\gamma T^2}{4\sqrt{1-\eta}} = \frac{\mu_o H_o^2}{2}.$$

At $T = T_c$, we should have $\eta = 0$ and hence $\gamma {T_c}^2/4 = \mu_o {H_o}^2/2$. Therefore, the order parameter can be expressed as

$$\eta = 1 - \left(\frac{T}{T_c}\right)^4. \tag{12.11}$$

Substituting η into (12.10), and differentiating two times with respect to temperature, we can derive the specific heat:

$$c_s = \frac{3\gamma T^3}{T_c^2}. \tag{12.12}$$

In this model, $c_s \propto T^3$, giving the same temperature dependence as c_{Debye} for lattice vibrations, but these two can be distinguished by different proportionality factors.

Using (12.12) and Sommerfeld's formula for a normal conductor $c_n = \gamma T$ in (12.8a), we can derive the expression $H_c = H_o\{1 - (T^2/T_c^2)\}$, which is parabolic, representing temperature dependence of H_c in mean-field approximation. Thus, the empirical formula (12.1) is consistent with Gorter-Casimir's theory. Nonetheless, it is significant to realize that such assumptions as (iii) and (12.10) agree conceptually with an internal adiabatic potential in condensates that drives ordering processes.

Fig. 12.5a shows experimental data of specific heat of gallium metal. Experimentally, normal and superconducting phases are separated in the presence of a magnetic field with strength lower than H_c in mixed volumes like domains in binary magnets. To analyze the temperature-dependence of the specific heat of the superconducting phase, $c_s/\gamma T_c$ versus T_c/T were plotted against the applied magnetic field in the range between 0 and 300 gauss. Deviating slightly from the linear relation, the mean-field approximation does not fully support the experimental result, while normal phase can be considered primarily as a free-electron gas. Nevertheless, such

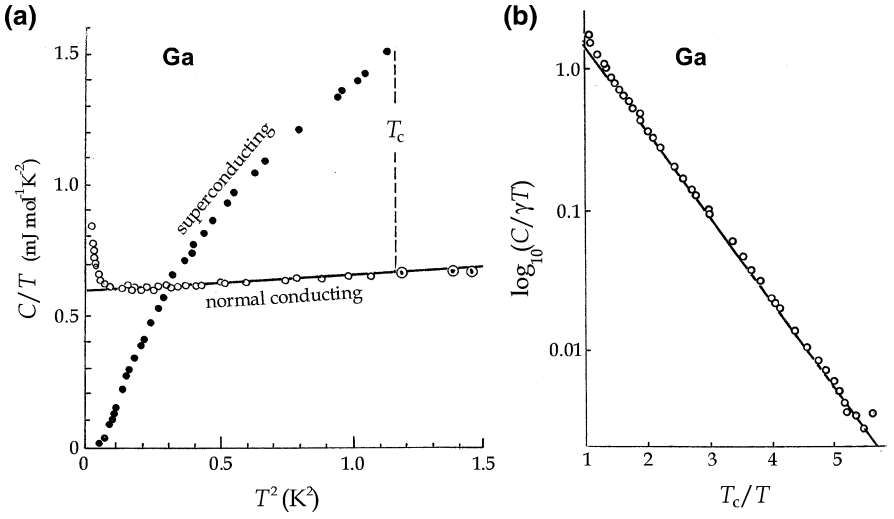

Fig. 12.5 Specific heat measured in superconducting gallium. (**a**) C/T versus T^2. (**b**) A semi-log plot of $C/\gamma T$ versus T_c/T (from [35]).

Table 12.1 Superconducting metals

Δ(0) (in eV) extrapolated to 0 K (T_c in K) [H_o (in Gauss) extrapolated to 0 K]											
								Al	3.4 (1.140) [105]		
		V	16 (5.38) [1,420]			Zn	2.4 (0.875) [53]	Ga	3.3 (1.091) [51]		
		Nb	30.5 (9.50) [1,980]	Mo	2.7 (0.92) [95]	Cd	1.5 (0.56) [30]	In	10.5 (3.0435) [293]	Sn	11.5 (3.722) [309]
La	19 (6.00) [1,100]	Ta	14 (4.438) [830]			Hg	16.5 (4.153) [412]	Tl	7.35 (2.39) [171]	Pb	27.3 (7.193) [803]

Data compiled from Kittel [35]

anomalies are significant at extremely low temperatures. Figure 12.5b in semi-log plot shows clearly an anomaly in logarithmic character, that is,

$$c_s \sim \exp\left(-\frac{b}{T}\right) \tag{12.13}$$

with a constant b, which is known as a *logarithmic anomaly*.

Exponential c_s expressed by (12.13) allows the temperature dependence to be interpreted in terms of a Boltzmann factor $\exp(-E_g/k_BT)$. Assuming this $E_g = k_Bb$ to represent an *energy gap* in the superconducting spectrum, the exponential c_s suggests the presence of an energy gap E_g proportional to b between normal electrons and unidentified superconducting charge carriers. Writing as $E_g = \Delta/2$, the parameter Δ is the *electron-electron* coupling in the theory of superconducting transition, as will be discussed in Chap. 13. The logarithmic anomaly can therefore be important evidence for the gap Δ that is essential in the theory of superconducting states.

The gap Δ is a function of temperature T, while the theoretical $\Delta(T)$ was later derived by Bardeen, Cooper, and Schrieffer. With their formula, values of $\Delta(0)$ were estimated by extrapolating measured plots to $T = 0$ K for various superconductors, which are listed in Table 12.1. The table also includes observed values of T_c and $H_c(0)$, where the latter was previously denoted by H_o.

12.3 Electromagnetic Properties of Superconductors

Superconductivity was first characterized by infinite electrical conductivity and later revised with additional perfect diamagnetism. These two phenomena were considered as consistent with Maxwell's theory of electromagnetism, but not quite as such at temperatures below T_c because of unknown charge carriers. Besides,

normal and superconducting phases can be studied separately with an applied magnetic field. Consequently, it is now realized that the superconducting phase is characterized by the Meissner effect, whereas the normal phase exhibits a usual conduction described by Ohm's law. For the former, we consider that superconducting charge carriers are particles of charge e' and mass m', which are different from electrons of e and m.

With different charge carriers, the normal and superconducting current densities, $\boldsymbol{J}_\mathrm{n}$ and $\boldsymbol{J}_\mathrm{s}$, are considered as determined by an applied electric field as

$$\boldsymbol{J}_\mathrm{n} = \sigma \boldsymbol{E} \tag{12.14a}$$

and

$$\Lambda \frac{\partial \boldsymbol{J}_\mathrm{s}}{\partial t} = \boldsymbol{E}, \tag{12.14b}$$

respectively. Equation (12.14a) is the Ohm's law, whereas (12.14b) is equivalent to the current density $\boldsymbol{J}_\mathrm{s} = n_\mathrm{s} e' \upsilon_\mathrm{s}$ in accelerating motion of n_s superconducting particles, that is,

$$m' \frac{\mathrm{d}\upsilon_\mathrm{s}}{\mathrm{d}t} = e' \boldsymbol{E}.$$

Hence, from (12.14b), we have

$$\Lambda = \frac{m'}{n_\mathrm{s} e'^2}. \tag{12.15}$$

Expressing the superconducting state by the *supercurrent* density $\boldsymbol{J}_\mathrm{s}$, we can write the Maxwell equations

$$\mathrm{curl}\, \boldsymbol{E} = -\frac{\partial \boldsymbol{B}}{\partial t} \quad \text{and} \quad \mathrm{curl}\, \boldsymbol{B} = \mu_\mathrm{o} \left(\boldsymbol{J}_\mathrm{s} + \varepsilon_\mathrm{o} \frac{\partial \boldsymbol{E}}{\partial t} \right).$$

Combining the first equation with (12.14b), we obtain

$$\mathrm{curl} \left(\Lambda \frac{\partial \boldsymbol{J}_\mathrm{s}}{\partial t} \right) = -\frac{\partial \boldsymbol{B}}{\partial t}. \tag{12.16}$$

Assuming $\partial \boldsymbol{E}/\partial t = 0$ in the second Maxwell equation, we have $\mathrm{curl}\, \boldsymbol{B} = \mu_\mathrm{o} \boldsymbol{J}_\mathrm{s}$, which expresses spatially distributed $\boldsymbol{B}$. Combining this and (12.16), we can write

$$\frac{\partial \boldsymbol{B}}{\partial t} = -\mathrm{curl} \left(\frac{\Lambda}{\mu_\mathrm{o}} \mathrm{curl} \frac{\partial \boldsymbol{B}}{\partial t} \right) = -\lambda^2 \mathrm{curl}\, \mathrm{curl} \frac{\partial \boldsymbol{B}}{\partial t} = \lambda^2 \nabla^2 \frac{\partial \boldsymbol{B}}{\partial t},$$

where the parameter λ is a constant defined as

$$\lambda^2 = \frac{\Lambda}{\mu_o}.$$

It is realized that these differential equations deal with local properties of a superconductor, so that Meissner's effect in a bulk body cannot be decribed. Nevertheless, we notice that (12.16) is for $\dot{\boldsymbol{J}}_s$, and the corresponding $\dot{\boldsymbol{E}}_s$ should be obtained to determine the magnetic field $\boldsymbol{B}$ that penetrates to a depth λ from the superconducting surface. For simplicity, writing the equation for $\dot{B}_z$ in the z-direction perpendicular to the surface as

$$\lambda^2 \nabla^2 \dot{B}_z - \dot{B}_z = 0, \tag{12.17}$$

the solution can be expressed as $\dot{B}_z = \dot{B}_o \exp(-z/\lambda)$; $z = \lambda$ gives the effective penetration depth of $\dot{B}_z$, and $\dot{B}_z = 0$ for $z > \lambda$. However, notice that this result is not the same as $B_z = 0$, so the Meissner effect does not arise from Maxwell's theory.

To obtain the Meissner effect in the region $0 < z < \lambda$, London proposed to revise (12.16) and (12.17) as

$$\text{curl}(\Lambda \boldsymbol{J}_s) = -\boldsymbol{B} \tag{12.18}$$

and

$$\boldsymbol{B} = \lambda^2 \nabla^2 \boldsymbol{B}. \tag{12.19}$$

Equation (12.18) gives the relation between $\boldsymbol{J}_s$ and $\boldsymbol{B}$, while the constant λ in (12.19) describes the penetration depth. In the layer of thickness λ, the Meissner effect is said as *incomplete*, and beyond $z = \lambda$ we have complete Meissner's effect $\boldsymbol{B} = 0$. Equation (12.19) may be oversimplified in practical cases, giving however a correct order magnitude of λ, which is estimated as 10^{-5} cm.

The London equation (12.18) can be modified by using the vector potential $\boldsymbol{A}$ defined by $\boldsymbol{B}$= curl $\boldsymbol{A}$ that satisfies the relation div $\boldsymbol{B} = 0$. Using $\boldsymbol{A}$, (12.17) can be expressed as

$$\text{curl}(\Lambda \boldsymbol{J}_s + \boldsymbol{A}) = 0. \tag{12.20a}$$

If the superconducting body is *simply connected*, as illustrated by the curve C_1 in Fig. 12.6, we can write

$$\Lambda \boldsymbol{J}_s + \boldsymbol{A} = \boldsymbol{\nabla} \chi', \tag{12.20b}$$

where χ' is an arbitrary scalar function that satisfies $\boldsymbol{\nabla}^2 \chi' = 0$, hence giving unique values of $\boldsymbol{J}_s$ and $\boldsymbol{A}$ at any point inside C_1. On the other hand, if the body is *multiply*

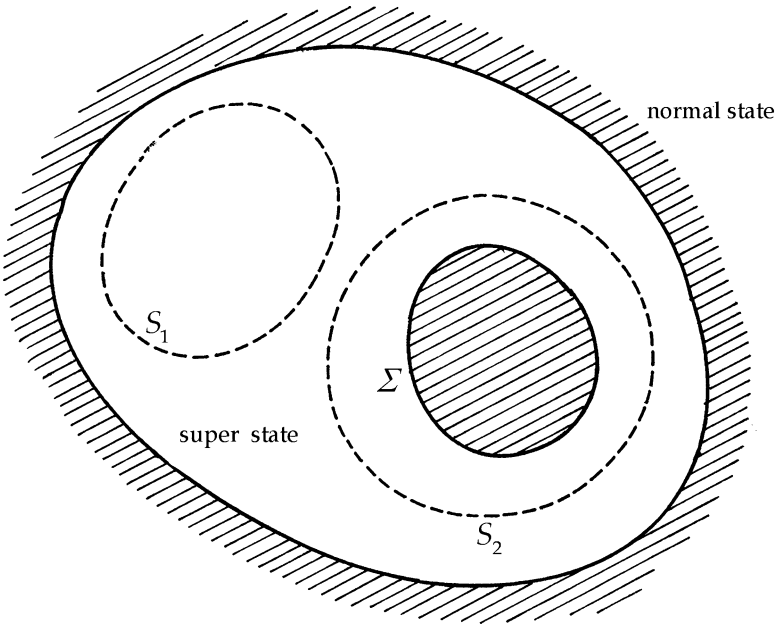

Fig. 12.6 A superconducting body surrounded by a normal conductor. A closed surface S_1 is filled by superconducting state completely, whereas the surface S_2 enclosing a void or normal state Σ. These spaces in S_1 and S_2 are singly and multiply connected.

connected, (12.20a) should be written in integral form to obtain a relation between the *persistent surface supercurrent* and the vector potential $\boldsymbol{A}$**.** Leaving the latter case aside, in a simply connected body, we can choose the gauge with div $\boldsymbol{A} = 0$ for a time-independent case, to write another vector potential as $\boldsymbol{A} + \boldsymbol{\nabla}\chi$ with an arbitrary χ. This allows choosing $\chi = -\chi'$. Using such a new gauge χ', called the *London gauge*, (12.20b) can be simplified as

$$\boldsymbol{J}_\mathrm{s} = -\frac{1}{\Lambda}\boldsymbol{A} = -\frac{1}{\mu_\mathrm{o}\lambda^2}\boldsymbol{A}. \tag{12.21}$$

Equation (12.21), called also *London's equation*, we can deal with Meissner's effect in a simply connected metal.

Equation (12.21) indicates that each of n_s superconducting carriers produce a current $(m'/e')\boldsymbol{j}_\mathrm{s}$, where $n_\mathrm{s}\boldsymbol{j}_\mathrm{s} = \boldsymbol{J}_\mathrm{s}$ represents the total supercurrent density. Therefore, for a system of independent superconducting particles, we can write the Hamiltonian

$$\mathcal{H}_\mathrm{system} = \sum_i \frac{1}{2m'}\{\boldsymbol{p}_\mathrm{s}(\boldsymbol{r}_i) - e'\boldsymbol{A}(\boldsymbol{r}_i)\}^2, \tag{12.22}$$

in which the momentum $\boldsymbol{p}_s(\boldsymbol{r}_i)$ and position $\boldsymbol{r}_i$ constitute a field that can interact with the electromagnetic field. In this case, assuming a continuous field of $(\boldsymbol{p}_s(\boldsymbol{r}_i), \boldsymbol{r}_i)$, we can define the Hamiltonian density $\mathcal{H}$ from $\mathcal{H}_{\text{system}} = \int_{\text{volume}} \mathcal{H} \mathrm{d}^3\boldsymbol{r}$, that is,

$$\mathcal{H} = \frac{1}{2m'} \{\boldsymbol{p}_s(\boldsymbol{r}) - e'\boldsymbol{A}(\boldsymbol{r})\}^2,$$

which is called *one-particle Hamiltonian*.

The potential $\boldsymbol{A}(\boldsymbol{r})$ is invariant under a gauge transformation, that is, $\boldsymbol{A}(\boldsymbol{r}') = \boldsymbol{A}(\boldsymbol{r}) + \boldsymbol{\nabla}\chi(\boldsymbol{r})$, where the scalar function $\chi(\boldsymbol{r})$ can be arbitrarily selected with $\boldsymbol{\nabla}^2\chi\,(\boldsymbol{r}) = 0$. However, the gauge invariance of the Hamiltonian $\mathcal{H}$ must be fabricated to be consistent with the electromagnetic field. In quantum theory, considering $\boldsymbol{p}_s(\boldsymbol{r})$ as a differential operator $-\mathrm{i}\hbar\boldsymbol{\nabla}$, the Schrödinger equation $\mathcal{H}\psi(\boldsymbol{r}) = E\psi(\boldsymbol{r})$ with the energy eigenvalue E can be made as invariant under the gauge transformation. We postulate that a transformed equation

$$\frac{1}{2m'} \{-\mathrm{i}\hbar\boldsymbol{\nabla}_{\boldsymbol{r}'} - e'\boldsymbol{A}(\boldsymbol{r}')\}^2 \psi(\boldsymbol{r}') = E\psi(\boldsymbol{r}')$$

can be written as

$$\frac{1}{2m'} \{-\mathrm{i}\hbar\boldsymbol{\nabla}_{\boldsymbol{r}} - e'\boldsymbol{A}(\boldsymbol{r}) - e'\nabla_r\chi(\boldsymbol{r})\}^2 \psi(\boldsymbol{r}') = E\psi(\boldsymbol{r}').$$

We notice that this equation can be satisfied by a transformed function

$$\psi(\boldsymbol{r}') = \exp\frac{\mathrm{i}e'\chi(\boldsymbol{r})}{\hbar}\psi(\boldsymbol{r}).$$

This function $\psi\ (\boldsymbol{r}')$ can therefore be characterized by a phase shift $e'\chi(\boldsymbol{r})/\hbar$ from $\psi\ (\boldsymbol{r})$, which is assumed as due to a transformation by $\chi\ (\boldsymbol{r})$.

On the other hand, the momentum $\boldsymbol{p}(\boldsymbol{r}) = -\mathrm{i}\hbar\boldsymbol{\nabla}_{\boldsymbol{r}}$ is a field operator related to the speed of a superconducting carrier particle at a position $\boldsymbol{r}$, and hence we can express it as $m'\boldsymbol{v}(\boldsymbol{r}) = p_s(\boldsymbol{r}) - e'\boldsymbol{A}(\boldsymbol{r})$. Therefore, for the total momentum $\boldsymbol{P}_s(\boldsymbol{r}) = n_s\boldsymbol{p}_s(\boldsymbol{r})$, we can write

$$\boldsymbol{P}_s(\boldsymbol{r}) = e'\Lambda\boldsymbol{J}_s(\boldsymbol{r}) + e'\boldsymbol{A}(\boldsymbol{r}). \tag{12.23}$$

Accordingly, (12.20a) and (12.20b) can be expressed as

$$\operatorname{curl}\boldsymbol{P}_s(\boldsymbol{r}) = 0 \quad \text{and} \quad \boldsymbol{P}_s(\boldsymbol{r}) = n_s\boldsymbol{\nabla}\chi'(\boldsymbol{r}),$$

where $\chi'(\boldsymbol{r})$ is a scalar function in a simply connected conductor. Nevertheless, considering $-n_s\chi'$ as the transformation gauge, the London's equation (12.21) is equivalent to

$$\boldsymbol{P}_s(\boldsymbol{r}) = 0. \tag{12.24}$$

Equations (12.23) and (12.24) indicate that zero momentum $\boldsymbol{P}_s = 0$ is established with the London gauge in a simply connected superconductor, exhibiting the Meissner effect. This can be interpreted for the *long-range order of momenta* $\boldsymbol{p}_i$ to show the value zero in the superconducting state. It is noted that *inversion symmetry* does exist in these momentum variables $\boldsymbol{p}(\boldsymbol{r})$, and the corresponding wave function represents a significant feature of the correlated charge carriers in a superconducting state.

In multiply connected conductor, $\chi'(\boldsymbol{r})$ cannot be a unique function of $\boldsymbol{r}$, so we must discuss it separately. Figure 12.6 sketches a superconducting domain surrounded by a normal phase that is shaded in the figure. In a practical metal, the body may be porous, where the inside shaded part bordered by Σ can be in normal phase or an empty space. Inside the closed curve C_1 the metal is superconducting, whereas C_2 has a different phase inside as shown, representing simply connected and multiply connected cases, respectively. Equation (12.23) is a formula for an arbitrary local point $\boldsymbol{r}$; hence in integral form, we have

$$\int_{S_{1+}} \boldsymbol{p}_s \cdot \mathrm{d}\boldsymbol{S}_{1+} = -\int_{S_{1-}} \boldsymbol{p}_s \cdot \mathrm{d}\boldsymbol{S}_{1-}$$

for C_1, where $\boldsymbol{S}_{1+}$ and $\boldsymbol{S}_{1-}$ are surfaces above and below the page, respectively, both subtending the curve C_1 in common. For such a simply connected medium, fluxes of $\boldsymbol{p}_s$ threading in and out of C_1 are equal and opposite, leading to (12.24).

It was an important experimental finding that a persisting current flows along a superconducting coil for considerably long time of about a year or so. Based on such findings, the Meissner's effect in a simply connected body can be revised for a multiconnected body by trapping the flux of magnetic field lines threading Σ. Choosing the curve C_2 including Σ as a doubly connected space, two integrals $\oint_{S_2} \boldsymbol{p}_s \cdot \mathrm{d}\boldsymbol{S}_2$ and $\oint_{\Sigma} \boldsymbol{p}_s \cdot \mathrm{d}\Sigma$ can be calculated, but the former vanishes because of (12.24), so that only the latter contributes the total integral. In this case, it is convenient to use the magnetic induction vector $\boldsymbol{B}$, and for the trapped flux inside Σ we write the induction law as

$$-\frac{\partial}{\partial t}\oint_{\Sigma} \boldsymbol{B} \cdot \mathrm{d}\boldsymbol{S}_{\Sigma} = \oint_{\Sigma} (\mathrm{curl}\, \boldsymbol{E}) \cdot \mathrm{d}\boldsymbol{S}_{\Sigma} = \oint_{\Sigma} \boldsymbol{E} \cdot \mathrm{d}\boldsymbol{l}_{\Sigma},$$

ignoring the surface penetration for simplicity. Here, the Stokes theorem is used for deriving the last equation, $\boldsymbol{S}_{\Sigma}$ represents a closed surface subtending the curve Σ, and $\mathrm{d}\boldsymbol{l}_{\Sigma}$ is the line element along Σ. Also, using (12.14b) to replace $\boldsymbol{E}$, we obtain

$$\frac{\partial}{\partial t}\left(\oint_{\Sigma} \boldsymbol{B} \cdot \mathrm{d}\boldsymbol{S}_{\Sigma} + \Lambda \oint_{\Sigma} \boldsymbol{J}_s \cdot \mathrm{d}\boldsymbol{l}_{\Sigma}\right) = 0. \tag{12.25a}$$

Defining the total flux $\Phi = \oint_{\Sigma} \boldsymbol{B} \cdot \mathrm{d}\boldsymbol{S}_{\Sigma} + \Lambda \oint_{\Sigma} \boldsymbol{J}_s \cdot \mathrm{d}\boldsymbol{l}_{\Sigma}$ through the curve Σ, we have the formula

$$\frac{\partial \Phi}{\partial t} = 0 \quad \text{or} \quad F = \text{constant}. \tag{12.25b}$$

The surface integral in (11.26a) can be replaced by $\int_\Sigma (\mathrm{curl}\boldsymbol{A}) \cdot \mathrm{d}\boldsymbol{S}_\Sigma = \int_\Sigma \boldsymbol{A} \cdot \mathrm{d}\boldsymbol{l}_\Sigma$, and hence

$$\Phi = \oint_\Sigma (\boldsymbol{A} + \Lambda \boldsymbol{J}_\mathrm{s}) \cdot \mathrm{d}\boldsymbol{l}_\Sigma. \tag{12.26}$$

For a simply connected body, we have shown in (12.20a) and (12.20b) that the vector $\boldsymbol{A} + \Lambda \boldsymbol{J}_\mathrm{s}$ can be expressed as $\boldsymbol{\nabla}\chi'$, and the London's equation (12.21) was obtained by choosing the London gauge, resulting in $\Phi = 0$. In a multiply connected body, on the contrary $\Phi =$ constant because of a trapped magnetic flux in Σ, for which the function χ' cannot be uniquely determined, indicating that a supercurrent returns to any point on its passage repeatedly. Mathematically, the line integral in (12.25a) can be limited to one circulation along the path Σ, where $\Phi(\boldsymbol{r}') = \Phi(\boldsymbol{r})$ on returning to $\boldsymbol{r}' = \boldsymbol{r}$, accompanying a phase shift $e'\chi/\hbar = 2\pi$. Therefore, the London gauge can be selected as $\chi' = n_\mathrm{s}(2\pi\hbar/e')$, and in such a superconductor the trapped flux in a hole Σ can be expressed as

$$\Phi = \oint_\Sigma \nabla\chi'(\boldsymbol{r}) \cdot \mathrm{d}\boldsymbol{l}_\Sigma = n_\mathrm{s}\frac{2\pi\hbar}{e'}. \tag{12.27}$$

Experimentally, it was found that Φ is determined by $e' = 2e$, indicating that the superconducting charge carriers consist of two electrons. Therefore, the quantized flux Φ is an integral multiple of $\Phi_\mathrm{o} = h/2e = 2.0678 \times 10^{-15}$ tesla m^2. This unit flux Φ_o is usually called a *fluxoid*. Owing to the trapped flux in voids in practical conductors, supercurrents can exist on their surfaces, even after removing the applied magnetic field. This explains a persisting current observed in a superconducting coil. Practical superconductors are thus signified by such trapped magnetic flux, in addition to resistance-free conduction.

12.4 The Ginzburg–Landau Equation and the Coherence Length

In the forgoing, we learned that the superconducting phase is characterized by an ordered momentum $\boldsymbol{P}_\mathrm{s}(\boldsymbol{r})$ in (12.23), while in a multiply connected conductor the flux Φ of an applied field is trapped in a void as in (12.27). However, the differential relations in Sect. 12.3 are local, referring to an arbitrary point in the surface layer of depth λ. Inside the layer, for distributed $\boldsymbol{J}_\mathrm{s}(\boldsymbol{r})$ and $\boldsymbol{A}(\boldsymbol{r})$, their spatial correlations should be taken into account to determine the thermodynamic properties. It is logical to consider the wave function $\psi\boldsymbol{r}$ to represent distributed order variables in terms of the distributed density as

$$n_\mathrm{s} = \psi^*(\boldsymbol{r})\psi(\boldsymbol{r}). \tag{12.28}$$

Considering (12.28) for the order parameter η expressed by (iii) of Sect. 12.2, Ginzburg and Landau wrote Gibbs free energy density for the superconducting state as

$$g_s = g_n + \frac{1}{2m'}|(\boldsymbol{p}_s - e'\boldsymbol{A})\psi|^2 + \alpha|\psi|^2 + \frac{1}{2}\beta(|\psi|^2)^2 + \frac{1}{2}\boldsymbol{B}^2. \tag{12.29}$$

Here on the right-hand side, the second term represents the *kinetic energy* of the order parameter, the third and fourth are the adiabatic potential as in Landau's theory of a binary system, and the last is the magnetic field energy density. The adiabatic potential associated with lattice deformation should also be related to the applied magnetic field. In contrast to (iii) in Sect. 12.2, the Ginzburg-Landau function (12.29) describes a superconducting transition in more detail, because the kinetic energy is included. It is particularly important to determine the role of long-range order for superconducting domains that coexist with normal conducting domains. The Ginzburg-Landau theory shows a straightforward approach to the superconducting transition.

In equilibrium, the total Gibbs function $G_s = \int_V g_s \mathrm{d}V$ must be minimized against arbitrary variations of ψ and $\boldsymbol{A}$. From the condition $\delta G_s = 0$, we obtain

$$\delta g_s = \left(\frac{\partial g_s}{\partial \psi}\right)_A \delta\psi + \left(\frac{\partial g_s}{\partial \boldsymbol{A}}\right)_\psi \cdot \delta\boldsymbol{A} = 0.$$

Hence from $(\frac{\partial g_s}{\partial \psi})_A = 0$ and $(\frac{\partial g_s}{\partial \boldsymbol{A}})_\psi = 0$, we can derive the equations

$$\frac{1}{2m'}(-\mathrm{i}\hbar\boldsymbol{\nabla} - e'\boldsymbol{A})^2\psi + (\alpha + \beta|\psi|^2)\psi = 0 \tag{12.30}$$

and

$$\boldsymbol{J}_s(\boldsymbol{r}) = -\frac{\mathrm{i}\hbar e'}{2m'}(\psi^*\boldsymbol{\nabla}\psi - \psi\boldsymbol{\nabla}\psi^*) - \frac{e'^2}{m'}\psi^*\psi\boldsymbol{A}, \tag{12.31}$$

respectively. Equation (12.30) is called the *Ginzburg-Landau equation* and (12.31) represents the superconducting current density.

In the absence of an applied field, that is, $\boldsymbol{A} = 0$, (12.30) is identical to (7.1a) that is a nonlinear equation of propagation in an adiabatic potential $\Delta U = \alpha\psi + \beta|\psi|^2\psi$ in classical analogy. For simplicity, we consider one-dimension wave function $\psi(x)$ at a given time t, for which (12.30) can be expressed as

$$\frac{\hbar^2}{2m'}\frac{\mathrm{d}^2\psi}{\mathrm{d}x^2} + \alpha\psi + \beta|\psi|^2\psi = 0, \tag{12.32}$$

where we consider $\alpha < 0$ and $\beta > 0$ for $T < T_c$. In fact, the differential equation of this type was already discussed in Sect. 7.1, and hence we use the results directly in the present argument. We are interested in a solution that can be derived in the form of $\psi = \psi_o f(\phi)$ with $\phi = kx$ that represents the phase of propagation.

We set the boundary conditions $\psi = 0$ at $x = 0$ and $\psi =$ constant at $x = \infty$, signifying the threshold and complete superconducting order, respectively. Near at $x = 0$, we can assume that ψ is very small, so that (12.32) for the threshold is approximately expressed as

$$\frac{\hbar^2}{2m'}\frac{\mathrm{d}^2\psi}{\mathrm{d}x^2} + \alpha\psi = 0.$$

This is a harmonic oscillator equation, whose solution is simply given as

$$\psi = \psi_\mathrm{o} \exp\frac{\mathrm{i}x}{\xi} \quad \text{where} \quad \xi = \sqrt{\frac{\hbar^2}{2m'|\alpha|}} \tag{12.33}$$

and ψ_o can be infinitesimal. We note that $(\frac{\mathrm{d}\psi}{\mathrm{d}x})_{x=0} = \psi_\mathrm{o}$; therefore, we have $\lambda = \mu = 1$ or $\kappa = 1$, which will be required later.

For the ordered state determined near at $x = \infty$, we have $\psi_\mathrm{o} \doteq$ constant; hence (12.31), can be written as $\alpha + \beta|\psi_\mathrm{o} f(\phi)|^2 = 0$, and consequently $|\psi_\mathrm{o} f(\phi)|^2 = |\alpha|/\beta$ regardless of ϕ. Using this result into (12.31), we can obtain the solution

$$\psi(x) = \sqrt{\frac{|\alpha|}{\beta}} \tanh\frac{x}{\sqrt{2}\xi}.$$

Here, the parameter ξ signifies an approximate distance for the density $n_\mathrm{s} = |\psi|^2$ to reach a plateau in the direction x, which is a significant measure for the supercurrent to exist, and called the *coherence length*. By definition, ξ depends on $m'|\alpha|$ that is an intrinsic constant of the superconductor, different from the penetration depth λ of an applied field.

Using $|\psi|^2 = |\alpha|/\beta$ in (12.29), we obtain the relation

$$g_\mathrm{s} - g_\mathrm{n} = -\frac{\alpha^2}{2\beta},$$

representing an ordered state of the superconductor. This should be identical to (12.6), from which we obtain the relation

$$H_\mathrm{c} = \sqrt{\frac{\alpha^2}{\mu_\mathrm{o}\beta}}. \tag{12.34}$$

The corresponding supercurrent density (12.30) can be expressed as

$$\boldsymbol{J}_\mathrm{s}(\boldsymbol{r}) = -\frac{e'^2}{m'}|\psi|^2\boldsymbol{A},$$

which is London's equation (12.20), and therefore the penetration depth λ can be expressed as

$$\lambda = \sqrt{\frac{m'\beta}{\mu_o e'^2 \alpha}}. \tag{12.35}$$

On the other hand, at the threshold (12.30) can be written as

$$\frac{1}{2m'}(-i\hbar\boldsymbol{\nabla} - e'\boldsymbol{A})^2\psi = \alpha\psi.$$

For the magnetic field B applied parallel to the y-axis, this equation is expressed as

$$-\frac{\hbar}{2m'}\left(\frac{\partial^2}{\partial x^2} + \frac{\partial^2}{\partial z^2}\right)\psi + \frac{1}{2m'}\left(i\hbar\frac{\partial}{\partial y} + e'B\right)^2\psi = \alpha\psi.$$

Setting $\psi = \psi_o(x)\exp i(k_y y + k_z z)$, we obtain

$$\frac{1}{2m'}\left\{-\hbar^2\frac{d^2}{dx^2} + \hbar^2 k_z^2 + (\hbar k_y - e'Bx)^2\right\}\psi_o = \sigma\psi_o.$$

This can be modified as

$$\frac{1}{2m'}\left\{-\hbar^2\frac{d^2}{dx^2} + e'^2B^2x^2 - 2\hbar k_y e'Bx\right\}\psi_o = \left(\alpha - \frac{\hbar^2(k_y^2 + k_z^2)}{2m'}\right)\psi_o.$$

Using a coordinate transformation $x - \dfrac{\hbar k_y e'B}{2m'} \to x'$, this equation can be expressed as a harmonic oscillator equation, that is,

$$\left(-\frac{\hbar^2}{2m'}\frac{d^2}{dx'^2} - \frac{1}{2}m'\omega_L^2 x'^2\right)\psi_o = \left(\alpha - \frac{\hbar^2 k_z^2}{2m'}\right)\psi_o,$$

where $\omega_L = e'B/m'$. Therefore, the threshold H_{c2} of a superconductor of Type 2 is determined by the lowest eigenvalue of the above equation, that is, α, if $k_z = 0$. That is, from the relation $\frac{1}{2}\hbar\omega_L = \alpha$, we can solve the equation for $B = \mu_o H_{c2}$. Combining (12.33), (12.36), and (12.34) for ξ, λ, and α versus H_c, respectively, we can derive the equation

$$H_{c2} = \sqrt{2}\kappa H_c \quad \text{where} \quad \kappa = \frac{\lambda}{\xi}. \tag{12.36}$$

When $\kappa > 1/\sqrt{2}$, we have $H_{c2} > H_c$, which characterizes Type II superconductor. The ratio κ is a significant parameter to determine the type of superconductors; Type I or II depending on the value of κ, either $\kappa < 1/\sqrt{2}$ or $\kappa > 1/\sqrt{2}$, respectively.

It is interesting that we can write H_{c2} in terms of the quantized flux $\Phi = n_s\Phi_o$, where $\Phi_o = 2\pi\hbar/e'$. Combining (12.34) and (12.36) with the unit flux Φ_o, we can state that

$$H_{c2} = \frac{2m'\alpha}{e'\hbar} \cdot \frac{e'\Phi_o}{2\pi\hbar} \cdot \frac{\hbar^2}{2m'\xi^2} = \frac{\Phi_o}{2\pi\xi^2}. \tag{12.37}$$

We note that H_{c2} is equal to the unit flux per area $2\Pi\xi^2$ that signifies the ordered area at the superconducting threshold.

Exercises 12

1. Consider a superconducting plate of large area and thickness δ, where the penetration of a magnetic field can be along the normal direction x. Show that

$$B(x) = B_o \cosh \frac{x/\lambda}{\delta/2\lambda}.$$

   The effective magnetization $M(x)$ in the plate is given by $B(x) - B_o = M(x)$. Derive the equation $M(x) = -B_o[(\delta^2 - 4x^2)/8\lambda^2]$.

2. In a superconductor at temperatures for $0 < T < T_c$, we consider the normal and supercurrents, $\boldsymbol{j}_n$ and $\boldsymbol{j}_s$, obeying the Ohm's law and the London's equation, respectively. Consider a plane electromagnetic wave $(\boldsymbol{E},\boldsymbol{B}) \propto \exp\, \mathrm{i}(\boldsymbol{k}\cdot\boldsymbol{r}-\omega t)$ propagating through the superconductor. Using the Maxwell's equations, derive the dispersion relation between k and ω that can be expressed as

$$c^2k^2 = \frac{\sigma\omega}{\varepsilon_o}\mathrm{i} - \frac{c^2}{\lambda^2} + \omega^2.$$

   Here, σ and λ are the normal conductivity and superconducting penetration depth, respectively.

3. Consider an infinitely long cylindrical superconductor, where the magnetic induction B has a cylindrical symmetry. Write the penetration equation $\boldsymbol{B} - \lambda^2\nabla^2\boldsymbol{B} = 0$ with cylindrical coordinates (ρ,θ,z), and show

$$B(\rho) = \frac{\Phi_o}{2\pi\lambda^2} \ln\frac{\lambda}{\rho} \quad \text{for } \xi<\rho<\lambda,$$

$$B(\rho) = \frac{\Phi_o}{2\pi\lambda^2}\sqrt{\frac{\pi\lambda}{2\rho}}\exp\frac{-\rho}{\lambda} \quad \text{for } \lambda < \rho.$$

Here

$$\Phi_o = 2\pi\int_0^\infty B(\rho)\rho\,\mathrm{d}\rho$$

is the total flux.

Chapter 13
Theories of Superconducting Transitions

Nearly free independent electrons in metals become correlated on lowering temperatures, causing a superconducting transition. Observed anomalies at the transition threshold are informative about the correlations, but not quite revealing. On the other hand, the critical temperature T_c varies with isotopic mass M composing the lattice, providing evidence for the lattice to be involved in the superconducting mechanism. Nevertheless, electron–electron correlations are essential in such a multielectron system in a superconducting crystal. Following Fröhlich's proposal for electron–phonon interactions, Cooper proposed an electron-pair model for superconducting charge carriers. Based on this model, Bardeen, Cooper, and Schrieffer presented the theory of superconducting transitions, which is the objective for discussions in this chapter. The superconducting transition can thereby be described in terms of electron-pair carriers, in analogy of pseudospin clusters for structural phase changes.

13.1 The Fröhlich Condensate

Electron scatterings are essential for the electron–lattice interaction in a crystal. It is noted that electron scatterings in a harmonic lattice are elastic, with which the energy exchange occurs according to conservation laws. In this case, electrons behave like *free particles* in the lattice, but colliding with the crystal surface. However, phonon excitations strain the lattice, where the modulated structure can be interpreted in term of electron-phonon interactions. At low temperatures, the lattice vibrations are slow in timescale of observation, so that the strained lattice can be described by classical displacements in finite magnitude.

M. Fujimoto, *Thermodynamics of Crystalline States*,
DOI 10.1007/978-1-4419-6688-9_13,

Denoting by $\boldsymbol{u}$ the displacement from a regular lattice point $\boldsymbol{r}_\mathrm{o}$, the displaced lattice coordinate is expressed as $\boldsymbol{r} = \boldsymbol{r}_\mathrm{o} + \boldsymbol{u}$; the lattice potential is thereby modified in the first order as

$$V(\boldsymbol{r}) = V(\boldsymbol{r}_\mathrm{o}) + \boldsymbol{u} \cdot \boldsymbol{\nabla} V(\boldsymbol{r}), \tag{13.1a}$$

where $V(\boldsymbol{r}_\mathrm{o})$ represents the rigid lattice specified by the space group. On the other hand, $\boldsymbol{u}$ is a function of $\boldsymbol{r}$, as expressed in Fourier series

$$\boldsymbol{u}(\boldsymbol{r}) = \sum_q \boldsymbol{u}_q \exp \mathrm{i}(\boldsymbol{q} \cdot \boldsymbol{r} - \omega t), \tag{13.1b}$$

where $\boldsymbol{q}$ is the wave vector of lattice translation. In Chap. 2, such a lattice vibration at a small $\boldsymbol{q}$ was discussed as a vibration *field*, which is expressed in terms of phonons $(\hbar\omega, \hbar\boldsymbol{q})$, if quantized. Assuming that the lattice is constructed with mass points M, the Fourier transform $\boldsymbol{u}_q$ is expressed with phonon creation and annihilation operators, $b_q^\dagger$ and b_q, as

$$\boldsymbol{u}_q = \frac{\boldsymbol{q}}{q} \sqrt{\frac{2M\omega}{\hbar}} (b_q^\dagger - b_q). \tag{13.1c}$$

The Hamiltonian of a system of electrons and the hosting lattice can be written as

$$\mathcal{H} = \mathcal{H}_\mathrm{el} + \mathcal{H}_\mathrm{L} + \mathcal{H}_\mathrm{int} + \mathcal{H}_\mathrm{coul}. \tag{13.2}$$

Here, the electronic term is assumed to be given by (10.11), that is,

$$\mathcal{H}_\mathrm{el} = \sum_k \varepsilon(\boldsymbol{k}) a_k^\dagger a_k, \tag{13.3a}$$

composed of many *one-electron modes* specified by wave vectors $\boldsymbol{k}$ and energies $\hbar^2\boldsymbol{k}^2/2m$, where m is the effective mass. The lattice term is given by

$$\mathcal{H}_\mathrm{L} = \sum_q (\hbar\omega_q) b_q^\dagger b_q. \tag{13.3b}$$

The Coulomb's interaction term $\mathcal{H}_\mathrm{coul}$ is added to (13.2) to make $\mathcal{H}$ complete, which can however be ignored, as justified by the shielding effect in a system of closely packed charges. We assume the Bloch's approximation for electrons, allowing each one to behave like a free particle in the lattice. Accordingly, the *one-electron wave function* is expressed as $\psi_k(\boldsymbol{r}) = \psi_\mathrm{o} \exp \mathrm{i}(\boldsymbol{k} \cdot \boldsymbol{r} + \varphi_k)$, where the phase constant φ_k can be arbitrary and randomly distributed in the crystal.

The interaction term $\mathcal{H}_{\rm int}$ arises from the term $\boldsymbol{u}\cdot\boldsymbol{\nabla}V(\boldsymbol{r}_{\rm o})$ in (12.1a) that is signified by such a matrix element as

$$\int_{\Omega}\langle u'_q|\psi'_k(\boldsymbol{r})\boldsymbol{u}\cdot\boldsymbol{\nabla}V(\boldsymbol{r}_{\rm o})\psi_k(\boldsymbol{r})|u_q\rangle{\rm d}^3\boldsymbol{r} \tag{13.4}$$

Here, $\langle u'_q|$ and $\langle u_q|$ are phonon wave functions before and after scatterings. Because of the sinusoidal nature of the wave function of electrons, the integral $\int_{\Omega}\psi^*_{k'}(\boldsymbol{r})\boldsymbol{u}\cdot\boldsymbol{\nabla}V(\boldsymbol{r}_{\rm o})\psi_k(\boldsymbol{r}){\rm d}^3\boldsymbol{r}$ does not vanish if $\boldsymbol{k}'-\boldsymbol{k}=\boldsymbol{q}$, which is detectable at low frequencies if observed at $\boldsymbol{r}_{\rm o}$ in sufficiently long timescale. In this case, $\mathcal{H}_{\rm int}$ can be expressed by a delta function $\delta(\boldsymbol{k}'-\boldsymbol{k}-\boldsymbol{q}+\boldsymbol{G})$, where $\boldsymbol{G}$ is any reciprocal vector of the lattice. Here, we consider $\boldsymbol{G}=0$ for the present discussion, ignoring $\boldsymbol{G}\neq 0$ for simplicity.

Matrix elements (13.4) have always undetermined phase factors $\exp{\rm i}\Delta\varphi_k$ due to phase differences $\Delta\varphi_k$ in these scattering processes in a crystal; however, the element can take a maximum value for $\Delta\boldsymbol{k}=\boldsymbol{q}$, if there is a process for $\Delta\varphi_k\to 0$. As proposed by Born and Huang, we consider such a phasing process for minimizing lattice strains; thus, $\mathcal{H}_{\rm int}$ can represent *condensates* at $\Delta\boldsymbol{k}=\boldsymbol{q}$ and $\Delta\varphi_k=0$, as in the case of binary transitions. With respect to phonon states, if (13.4) can be off diagonal, that is, $\langle u'_q|\cdots|u_q\rangle\neq 0$, such a time-dependent $\mathcal{H}_{\rm int}$ can be thermally unstable, but stabilized by adiabatic phasing, constituting condensates in the modified lattice. Abrupt rise of the specific heat before reaching the superconducting state can be attributed to such a phasing mechanism in short time.

At a given time, $\mathcal{H}_{\rm int}$ can be expressed as

$$\mathcal{H}_{\rm int}=-\int_{\Omega}{\rm d}^3\boldsymbol{r}\{\rho(\boldsymbol{r})\boldsymbol{u}(\boldsymbol{r})\cdot\boldsymbol{\nabla}V(\boldsymbol{r})\}, \tag{13.5}$$

where $\rho=\sum_i\rho_q\exp(-{\rm i}\boldsymbol{q}\cdot\boldsymbol{r}_i)$ is the modulated electron density to interact with $\boldsymbol{u}(\boldsymbol{r})$. For the Fourier transform $\rho_q=\sum_i\rho(\boldsymbol{r}_i)\exp({\rm i}\boldsymbol{q}\cdot\boldsymbol{r}_i)/\Omega$expressed as $\rho(\boldsymbol{r})\exp({\rm i}\boldsymbol{q}\cdot\boldsymbol{r})/\Omega$ for a small $|\boldsymbol{q}|$, we can write

$$\rho_q=\sum_k a^{\dagger}_{k+q}a_k \tag{13.6}$$

in the second-quantization scheme. The interaction $\mathcal{H}_{\rm int}$ can therefore be expressed in terms of ρ_q as

$$\mathcal{H}_{\rm int}={\rm i}\sum_q D_q(\rho_q b^{\dagger}_q-\rho^{\dagger}_q b_q), \tag{13.7a}$$

where the constant D_q is determined by phonon spectra as

$$D_q^2=\frac{4}{9}\frac{C^2\hbar\omega_q}{NM\Omega v_{\rm o}^2}, \tag{13.7b}$$

under isothermal conditions. In this case,

$$C = \frac{\hbar^2}{2m} \int_\Omega |\nabla \psi_o|^2 d^3 \boldsymbol{r}$$

is a constant for the Bloch's function ψ_o; v_o is the sound velocity of the phonon mode of $\boldsymbol{q}$. Considering $\mathcal{H}_{int}$ as an adiabatic perturbation, we can leave D_q as a temperature-independent constant.

In the second-quantization scheme, the Hamiltonian $\mathcal{H}$ represents the total ordering energy, in which $\mathcal{H}_{int}$ represents a propagating condensate of an electron coupled with a phonon in phase. Such a phasing can be interpreted as synchronized electron scatterings that are driven by the lattice displacement $\boldsymbol{u}(\boldsymbol{r})$.

13.2 The Cooper Pair

Noting that a condensate is involved in *off-diagonal* elements of displacements, we can consider electron–electron interactions, if two condensates can interact coherently. We consider such coupled condensates can carry two electronic charges in a superconducting state. For such a coupling, we have to consider another thermodynamic situation where an adiabatic process occurs for two condensates to bound in inversion symmetry $\boldsymbol{q} \leftrightarrows -\boldsymbol{q}$, accompanying a phase difference with respect to the displacement $\boldsymbol{u}(\boldsymbol{r})$. For such pairs to be considered as *identical* charge carriers, these phases should be forced to synchronize with $\boldsymbol{u}$ in a slow passage on decreasing temperature. While the factor D_q in (13.7a) is considered as temperature independent, we need to assume an additional phasing process, which is analogous to pseudospin clusters in binary systems. We write the Hamiltonian for identical pairs as $\tilde{\mathcal{H}}$, which should be different from $\mathcal{H}$ for Fröhlich's condensates, but derived by a canonical transformation with an action variable that can represent such a thermal process.

We write the Hamiltonian (13.2) of single carriers as

$$\mathcal{H} = \mathcal{H}_o + \lambda \mathcal{H}', \tag{i}$$

where $\lambda \mathcal{H}'$ replaces $\mathcal{H}_{int}$ for convenience. Performing a canonical transformation on $\mathcal{H}$ with an action variable S, we can obtain the Hamiltonian $\tilde{\mathcal{H}}$ for electron–electron interactions. The canonical transformation

$$\tilde{\mathcal{H}} = \exp(-S)\mathcal{H} \exp S \tag{ii}$$

converts $\mathcal{H}$ to $\tilde{\mathcal{H}}$, for which the action S is attributed to an adiabatic potential for minimal lattice strains.

Expanding $\tilde{\mathcal{H}}$ into a power series, we have

$$\tilde{\mathcal{H}} = \mathcal{H} + [\mathcal{H}, S] + \frac{1}{2}[[\mathcal{H}, S], S] + \cdots .$$

With (i), this expression can be written as

$$\tilde{\mathcal{H}} = \mathcal{H}_\mathrm{o} + \lambda\mathcal{H}' + [\mathcal{H}_\mathrm{o}, S] + [\lambda\mathcal{H}', S].$$

Here, if S is chosen in such a way that

$$\lambda\mathcal{H}' + [\mathcal{H}_\mathrm{o}, S] = 0, \tag{iii}$$

we have

$$\tilde{\mathcal{H}} = \mathcal{H}_\mathrm{o} + [\lambda\mathcal{H}', S]. \tag{iv}$$

Since $\mathcal{H}_\mathrm{o}$ is diagonal, from (iii) we obtain matrix elements of S, that is,

$$\begin{aligned} \langle 1_q|S|0_q\rangle &= -\mathrm{i}D_q \sum_k \frac{a^\dagger_{k-q}a_k}{\varepsilon_k - \varepsilon_{k-q} - \hbar\omega_q} \quad \text{and} \\ \langle 0_q|S|1_q\rangle &= \mathrm{i}D_q \sum_{k'} \frac{a^\dagger_{k'+q}a_{k'}}{\varepsilon_{k'} - \varepsilon_{k'+q} + \hbar\omega_q}. \end{aligned} \tag{v}$$

With these results, (iv) can be expressed

$$\tilde{\mathcal{H}} = \mathcal{H}_\mathrm{o} + \frac{D_q^2}{2} \sum_{k,k'} a^\dagger_{k'+q}a_{k'}a^\dagger_{k-q}a_k \left(\frac{1}{\varepsilon_k - \varepsilon_{k-q} - \hbar\omega_q} - \frac{1}{\varepsilon_{k'} - \varepsilon_{k'+q} + \hbar\omega_q} \right). \tag{vi}$$

In (v), scatterings with $\boldsymbol{q}$ and $-\boldsymbol{q}$ signify *emission* and *absorption* of a phonon $\hbar\omega_q$ from and to the displacement $\boldsymbol{u}_q$, respectively, which occur in the processes $\boldsymbol{k} \to \boldsymbol{k} - \boldsymbol{q}$ and $\boldsymbol{k}' + \boldsymbol{q} \to \boldsymbol{k}'$. These terms in (vi) can take a large value, if $|\Delta\boldsymbol{k}| = |\boldsymbol{q}|$ and $-\Delta\boldsymbol{k} \approx \Delta\boldsymbol{k}'$, which can be achieved after phasing. Such a scattering process is illustrated by a vector diagram in Fig. 13.1a.

Considering that the off-diagonal elements $a^\dagger_{k-q}a_k$ and $a^\dagger_{k'+q}a_{k'}$ of the electron density matrix associated with the coupling process, $\tilde{\mathcal{H}}$ expresses for two electrons to be a bound object, if the momentum conservation rule restricts the interaction to a specific scattering $\boldsymbol{k}' = -\boldsymbol{k}$. In this case, illustrated in Fig. 13.1b, the binding energy of two electrons can be determined from (vi) as

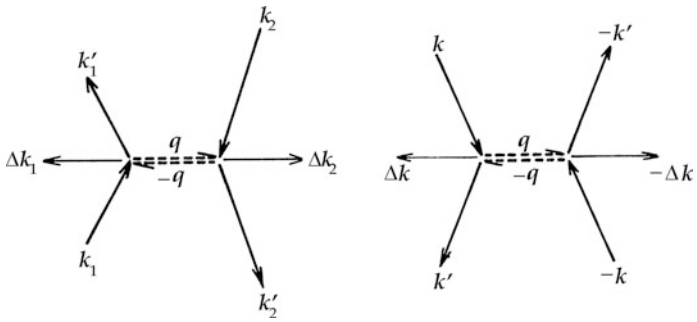

Fig. 13.1 (**a**) A coupled Fröhlich's condensates. (**b**) A Cooper's pair.

$$\tilde{\mathcal{H}} = D_q^2 \sum_{q,k} \frac{\hbar\omega_q}{(\varepsilon_{k-q} - \varepsilon_k)^2 - (\hbar\omega_q)^2} a_{k-q}^\dagger a_k a_{-k+q}^\dagger a_{-k}. \tag{13.8a}$$

Or for a lattice of many q, we can write

$$\tilde{\mathcal{H}} = -\sum_{k,q} V(\boldsymbol{k}, \boldsymbol{q}) a_{k-q}^\dagger a_k a_{-k+q}^\dagger a_{-k}, \tag{13.8b}$$

where

$$-V(\boldsymbol{k}, \boldsymbol{q}) = D_q^2 \frac{\hbar\omega_q}{(\varepsilon_{k-q} - \varepsilon_k)^2 - (\hbar\omega_q)^2}. \tag{13.8c}$$

The interaction $\tilde{\mathcal{H}}$ is attractive, if $V(\boldsymbol{k}, \boldsymbol{q})>0$, suggesting that such a pair of electrons can be a superconducting charge carrier of $2e$. If this is the case, from (13.8c), we should have

$$|\varepsilon_{k\pm q} - \varepsilon_k| < \hbar\omega_q; \tag{13.8d}$$

otherwise, $\tilde{\mathcal{H}}$ is repulsive. By definition, the constant D_q is proportional to $\hbar\omega_q$ and (13.8d) implies that one-electron energies ε_k should be modulated by an amount $\Delta\varepsilon_k$ smaller than $\hbar\omega_q$, in order for $\tilde{\mathcal{H}}$ to be attractive. In the limit of $\Delta\varepsilon_k \to \hbar\omega_q$, we obtain an intense coupling of two electrons (13.8c).

However, $\boldsymbol{k}'$ and $\boldsymbol{k}$ are distributed with the scattering geometry $\boldsymbol{k}' = \boldsymbol{k} \pm \boldsymbol{q}$ for a given $\boldsymbol{q}$, thereby modulating the spherical Fermi surface ε_F by $\pm\hbar\omega_q$. Therefore, $\tilde{\mathcal{H}}$ generates thermal instability of the surface for the particular scatterings $\Delta\boldsymbol{k} = -\Delta\boldsymbol{k}'$. Figure 13.2 shows schematically a Fermi sphere in the $\boldsymbol{k}$-space modulated by $\pm\hbar\omega_q$, leading to a *singularity* when $\Delta\varepsilon_k = \hbar\omega_q$. With singular scatterings in Fig.13.1b, Cooper proposed that this specific interaction yields a *pseudoparticle* of two electrons, called *Cooper's pairs*, playing the essential role in

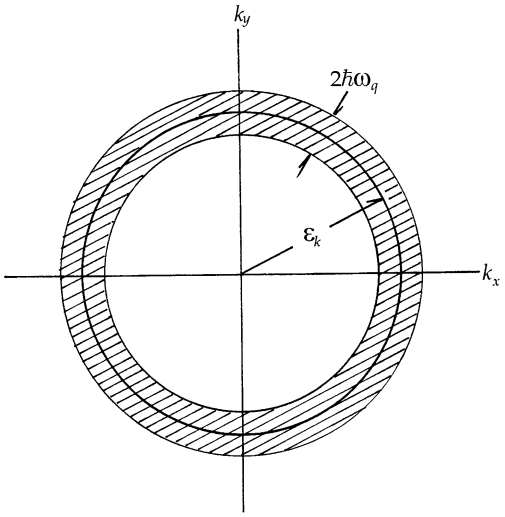

Fig. 13.2 A one-electron energy surface ε_k modulated by Debye's phonons in $k_x k_y$-space.

superconducting states. Supported by experimental evidence, Cooper's pairs are identical pseudoparticles, whose number is considerable for the superconducting phase. In fact, Bardeen, Cooper, and Schrieffer elaborated the theory of superconducting transitions, assuming Cooper's pairs as charge carriers.

It is realized that a Cooper pair can be treated as a single particle of charge $e' = 2e$ and mass $m' = 2m$, whose motion can be discussed relative to the lattice. With the fixed center of mass, a Cooper's pair is a single particle in free space; however with respect to the fixed lattice, an adiabatic potential must be considered for the motion.

It is noted that the Cooper pair can be characterized by inversion $\boldsymbol{q} \leftrightarrows -\boldsymbol{q}$, for which a binary order variable can be defined. In this case, a superconducting transition can be described like a binary transition with Fröhlich's condensates. In fact, Anderson showed that such an order variable can be defined from the Bardeen–Cooper–Schrieffer theory.

13.3 Critical Anomalies and the Superconducting Ground State

13.3.1 Critical Anomalies and Energy Gap in a Superconducting State

As characterized by $\Delta \boldsymbol{k}' = -\Delta \boldsymbol{k}$, the Cooper pair was described with respect to the center-of-mass coordinate system, where $\boldsymbol{k}' + \boldsymbol{k} = 0$. However, with respect to the lattice, $\boldsymbol{k}' + \boldsymbol{k}$ cannot be equal to zero, for which an adiabatic potential is responsible. Considering such pairs to emerge at T_c, signifying the threshold of a

superconducting phase, the transition can be characterized by a process to establish inversion symmetry $\boldsymbol{q} \leftrightarrows -\boldsymbol{q}$.

The transition is initiated by the potential $-\boldsymbol{\nabla} V(\boldsymbol{r}_\mathrm{o})$ that emerges at T_c, where critical anomalies appear as related to fluctuations, as discussed in Sect. 6.3. It is noted that the Cooper pair is associated with the symmetric mode of fluctuations $\frac{1}{\sqrt{2}}(u_q + u_{-q})$; hence, we have to consider the antisymmetric mode $\frac{1}{\sqrt{2}}(u_q - u_{-q})$ for uncoupled electrons. The wave function of the Cooper pair is symmetrically modulated by the lattice wave $u_{\pm q} \sim \exp(\pm \mathrm{i}\boldsymbol{q} \cdot \boldsymbol{r})$, so that the modulated wave function of an electron pair is given by $\psi_k(u_q + u_{-q})$. Therefore, the corresponding kinetic energy is modulated between ε_{k+q} and ε_{k-q}, and

$$\varepsilon_{k\pm q} - \varepsilon_k = \pm \frac{\hbar^2 kq}{m}.$$

In this context, the Fermi level for $k = k_\mathrm{F}$ shows an *energy gap* E_g at T_c, that is,

$$2\frac{\hbar^2 k_\mathrm{F} q_\mathrm{o}}{m} = E_\mathrm{g},$$

where q_o is the critical phonon wave vector. We can define the coherence length by $\xi_\mathrm{o} = 1/2q_\mathrm{o}$ at T_c, which is therefore expressed by

$$\xi_\mathrm{o} = \frac{\hbar^2 k_\mathrm{F}}{m E_\mathrm{g}}. \tag{13.9}$$

Clearly, the lattice modulation is responsible for the coherence length ξ_o, which was not defined as related to the lattice in Ginzburg–Landau's theory. The critical singularity is due to the discontinuity in forming Cooper's pairs, similar to clusters in structural transitions.

For a Cooper's pair, we consider scattering processes signified by $\boldsymbol{k} \to \boldsymbol{k}' = \boldsymbol{k} + \boldsymbol{q}$ and $-\boldsymbol{k} \to -\boldsymbol{k}' = -\boldsymbol{k} - \boldsymbol{q}$, with respect to the center-of-mass coordinates. Therefore, in the relative coordinate frame of reference, the wave functions $\psi_k(\boldsymbol{r})$ and $\psi_{k'}(\boldsymbol{r})$ must be functions of $\boldsymbol{r} = \boldsymbol{r}_1 - \boldsymbol{r}_2$ with respect to the fixed center of mass, that is, $\boldsymbol{r}_\mathrm{o} = 0$, where we can write Schrödinger equation

$$\left\{\frac{\hbar^2}{2m}\left(\boldsymbol{k}^2 + \sum_{k'} \boldsymbol{k}'^2\right) + \tilde{\mathcal{H}}\right\}\psi_{k,k'}(\boldsymbol{r}) = \lambda \psi_{k,k'}(\boldsymbol{r}),$$

where λ is the eigenvalue and $\psi_{k,k'}(\boldsymbol{r}) = \sum_k \alpha_k \exp \mathrm{i}\boldsymbol{k} \cdot \boldsymbol{r}$. Denoting the unperturbed energy by E_k, we can write the secular equation

$$(E_k - \lambda)\alpha_k + \sum_{k'} \alpha_{k'} \langle \boldsymbol{k}, -\boldsymbol{k} | \tilde{\mathcal{H}} | \boldsymbol{k}', -\boldsymbol{k}' \rangle = 0,$$

where $\boldsymbol{k} = \boldsymbol{k}' - \boldsymbol{q}$ and $-\boldsymbol{k} = -\boldsymbol{k}' + \boldsymbol{q}$. The perturbation $\tilde{\mathcal{H}}$ in (13.8b) is related with distributed $\boldsymbol{k}'$ deviated from $\boldsymbol{k}_\mathrm{F}$ in a small range that is limited by the Debye's cutoff frequency ω_D. In this case, the second term in the above is assumed as a constant C in the first approximation, so that we obtain $\alpha_k = C/(E_k - \lambda)$. As the second approximation, the summation is replaced by an integral over the corresponding energy $E_{k'}$, that is,

$$(E_k - \lambda)\alpha_k = -V \int_{E_\mathrm{F}}^{E_k} \alpha_{k'} \rho_{k'} \mathrm{d}E_{k'},$$

where $E_{k'} - E_\mathrm{F} = \Delta < \hbar\omega_\mathrm{D}$. Assuming $\rho_{k'} \approx \rho_\mathrm{F}$, we obtain

$$\frac{1}{\rho_\mathrm{F} V} = \int_{E_\mathrm{F}}^{E_{k'}} \frac{\mathrm{d}E_{k'}}{E_{k'} - \lambda} = \ln \frac{E_{k'} - \lambda}{E_\mathrm{F} - \lambda} = \ln \frac{E_{k'} - E_\mathrm{F} + \Delta}{\Delta}.$$

Letting $E_{k'} - E_\mathrm{F} = \hbar\omega_\mathrm{D}$, we have the expression

$$\Delta = \frac{2\hbar\omega_\mathrm{D}}{\exp(1/\rho_\mathrm{F} V) - 1}, \tag{13.10}$$

which is the binding energy of the Cooper's pair with respect to the Fermi level.

13.3.2 Order Variables in Superconducting States

Bardeen, Cooper, and Schrieffer published the theory of superconducting transitions in 1957, assuming that Cooper's pairs are dominant charge carriers in the superconducting phase. Hereafter, their theory is called the *BCS theory*.

We write the Hamiltonian for interacting electrons as expressed by

$$\mathcal{H} = \sum_k (\varepsilon_k a_k^\dagger a_k + \varepsilon_{-k} a_{-k}^\dagger a_{-k}) - \sum_{k',k} V(\boldsymbol{k}, -\boldsymbol{k}) a_{k'}^\dagger a_{-k'}^\dagger a_{-k'} a_k,$$

where $\varepsilon_k = \varepsilon_{-k}$ is the energy of a single electron at $\boldsymbol{k}$ and $-\boldsymbol{k}$ on the Fermi surface. Here, one-electron energy is ε_k, referring to the Fermi energy as zero. The above Hamiltonian can be re-expressed by

$$\mathcal{H} = \sum_{k,k'} \varepsilon_k a_k^\dagger a_k - \sum_{k',k;q} V(\boldsymbol{k}', \boldsymbol{k}; \boldsymbol{q}) a_{k'+q}^\dagger a_{k-q}^\dagger a_{k'} a_k. \tag{i}$$

The wave function can usually be expressed as $\psi(\ldots, n_k, \ldots, n_{k'}, \ldots)$, where n_k and $n_{k'}$ take values either 1 or 0, depending on one-particle states $\boldsymbol{k}$ and $\boldsymbol{k}'$ either occupied or unoccupied, respectively. In contrast, in BCS theory the Cooper's pair is expressed by a two-particle wave function $\psi(n_k, n_{k'})$, and therefore using

number operators $n_k = a_k^\dagger a_k$ and $n_{-k}^\dagger = a_{-k}^\dagger a_{-k}$, we rewrite (i) for the BCS Hamiltonian $\mathcal{H}_{\rm BCS}$ as

$$\mathcal{H}_{\rm BCS} = -\sum_k (1 - n_k - n_{-k})\varepsilon_k - V\sum_{k',k} a_{k'}^\dagger a_{-k'}^\dagger a_{-k} a_k, \tag{ii}$$

where V is assumed as a constant. Applying (ii) to $\psi(n_k, n_{-k})$ of the two-particle subspace, we have paired states for $n_k = n_{-k}$ of $\boldsymbol{k}$ and $-\boldsymbol{k}$, which are either both occupied or both unoccupied, and hence

$$(1 - n_k - n_{-k})\psi(1_k, 1_{-k}) = -\psi(1_k, 1_{-k})$$

and

$$(1 - n_k - n_{-k})\psi(0_k, 0_{-k}) = \psi(0_k, 0_{-k}).$$

Therefore, expressing these paired states by column matrices $\begin{pmatrix} 0 \\ 1 \end{pmatrix}$ and $\begin{pmatrix} 1 \\ 0 \end{pmatrix}$, respectively, the operator $1 - n_k - n_{-k}$ can be expressed by a matrix

$$1 - n_k - n_{-k} = \begin{pmatrix} 1 & 0 \\ 0 & -1 \end{pmatrix} = \sigma_{k,z}.$$

This is the z-component of Pauli's matrix σ. Further noting that

$$a_k^\dagger a_{-k}^\dagger \psi(1_k 1_{-k}) = 0 \quad \text{and} \quad a_k^\dagger a_{-k}^\dagger \psi(0_k 0_{-k}) = \psi(1_k 1_{-k}),$$

the operator $a_k^\dagger a_{-k}^\dagger$ can be related to x- and y-components of Pauli's σ. Considering that

$$\sigma_{k,x} = \begin{pmatrix} 0 & 1 \\ 1 & 0 \end{pmatrix} \quad \text{and} \quad \sigma_{k,y} = \begin{pmatrix} 0 & -\mathrm{i} \\ \mathrm{i} & 0 \end{pmatrix},$$

we can define

$$\sigma_k^+ = \sigma_{k,x} + \mathrm{i}\sigma_{k,y} = \begin{pmatrix} 0 & 2 \\ 0 & 0 \end{pmatrix}$$

and

$$\sigma_k^- = \sigma_{k,x} - \mathrm{i}\sigma_{k,y} = \begin{pmatrix} 0 & 0 \\ 2 & 0 \end{pmatrix}.$$

Then, we can obtain the relations

$$a_k^\dagger a_{-k}^\dagger = \frac{1}{2}\sigma_k^- \quad \text{and} \quad a_{-k} a_k = \frac{1}{2}\sigma_k^+.$$

Using these results,

$$\mathcal{H}_{\mathrm{BCS}} = -\sum_k \varepsilon_k \sigma_{k,z} - \frac{V}{4}\sum_{k',k} \sigma_{k'}^{-}\sigma_k^{+}$$
$$= -\sum_k \varepsilon_k \sigma_{k,z} - \frac{V}{4}\sum_{k',k} (\sigma_{k',x}\sigma_{k,x} + \sigma_{k',y}\sigma_{k,y}). \tag{iii}$$

In this argument, $\sigma_{k,z}$ is an operator for creating or destroying the paired states $\pm \boldsymbol{k}$. However, writing (iii) as a scalar product of vectors $\boldsymbol{\sigma}_k$ and a field $\boldsymbol{F}_k$ defined by

$$\left(-\frac{V}{2}\sum_{k'} \sigma_{k',x}, -\frac{V}{2}\sum_{k'} \sigma_{k',y}, \varepsilon_k\right),$$

that is,

$$\mathcal{H}_{\mathrm{BCS}} = -\sum_k \boldsymbol{\sigma}_k \cdot \boldsymbol{F}_k. \tag{iv}$$

This can be interpreted as the interaction energy of classical vectors $\boldsymbol{\sigma}_k$ in the field $\boldsymbol{F}_k$ that represents a Weiss field due to the other $\boldsymbol{\sigma}_{k'}$ in the system. In this classical interpretation, in order for (iv) to be minimum, $\boldsymbol{\sigma}_k$ should be parallel to $\boldsymbol{F}_k$, characterizing for these quantities to be in phase.

In (iv), the direction of such classical vectors may be expressed in terms of an angle θ_k with respect to the z-axis, representing the effective sinusoidal phase. Assuming $\boldsymbol{\sigma}_k$ confined to the xz-plane for simplicity, we can write the relation $\boldsymbol{\sigma}_k \parallel \boldsymbol{F}_k$ as

$$\frac{F_{k,x}}{F_{k,z}} = \frac{\sigma_{k,x}}{\sigma_{k,z}} = \frac{\frac{V}{2}\sum_{k'} \sigma_{k',x}}{\varepsilon_k} = \tan\theta_k. \tag{v}$$

In fact, V is a function of $\boldsymbol{k}'$ and $\boldsymbol{k}$, depending also on distances, but it can be assumed as constant in the critical region, if characterized by smaller $|\boldsymbol{k}|$ and ε_k. Further, judging from (13.8c), $V(\boldsymbol{k}', \boldsymbol{k})$ has a well-defined singularity. Assuming for the singularity to occur at $\theta_k = 0$, we can write $\sigma_{k',x} = \sigma_{k'\mathrm{o}} \sin\theta_{k'}$. Noticing that the amplitude $\sigma_{k'\mathrm{o}}$ depends only on $|\boldsymbol{k}'|$, we can write $V'_k = \sum_{k'} V(\boldsymbol{k}', \boldsymbol{k})\sigma_{|k'|\mathrm{o}}$ and obtain

$$\tan\theta_k = \frac{V'_k}{2\varepsilon_k}\sum_{k'} \sin\theta_{k'}. \tag{vi}$$

Such a phase angle θ_k as determined by (vi) expresses the mesoscopic feature of superconducting condensate clusters conveniently, which is however not directly observable in conducting materials. Nevertheless, we pay attention to the singular behavior of $\tan\theta_k$ at $\theta_k = 0$, which represents a boundary wall, like domain walls in magnetic ordering processes. Writing $\tan\theta_k = \Delta_k/\varepsilon_k$, the singularity of θ_k can be attributed to the parameter Δ_k, which satisfies the relation

$$\Delta_k = \frac{V'_k}{2}\sum_{k'}\frac{\Delta_k}{\sqrt{\Delta_k^2+\varepsilon_{k'}^2}} \quad \text{or} \quad 1 = \frac{V'_k}{2}\sum_{k'}\frac{1}{\sqrt{\Delta_k^2+\varepsilon_{k'}^2}}. \tag{vii}$$

The summation $\sum_{k'}\cdots$ can be replaced by integration with respect to distributed region of $\varepsilon_{k'}$, if $|\boldsymbol{k}'|$ is small. Assuming energies $\varepsilon_{k'}$ are distributed between $-\hbar\omega_\mathrm{D}$ and $+\hbar\omega_\mathrm{D}$, where ω_D is the Debye's frequency, (vii) can be calculated by integration

$$1 = \frac{V'\rho_\mathrm{F}}{2}\int_{-\hbar\omega_\mathrm{D}}^{+\hbar\omega_\mathrm{D}}\frac{\mathrm{d}\varepsilon}{\sqrt{\Delta^2+\varepsilon^2}} = V'\rho_\mathrm{F}\sinh^{-1}\frac{\hbar\omega_\mathrm{D}}{\Delta},$$

where indexes k and k' are omitted for simplicity, and ρ_F is the density of states at the Fermi level. Therefore, for $V'\rho_\mathrm{F} = 1$, we can derive the expression

$$\Delta = \frac{\hbar\omega_\mathrm{D}}{\sinh(1/V'\rho_\mathrm{F})} \cong 2\hbar\omega_\mathrm{D}\exp\left(-\frac{1}{V'\rho_\mathrm{F}}\right). \tag{viii}$$

This is the BCS formula for the energy gap Δ, which is positive, if $V' > 0$. It is noted that the field $\boldsymbol{F}$ is by no means static, but interpreted for inverting the quasispin $\boldsymbol{\sigma}_k$ between $\sigma_{kz} = \pm 1$, for which a work $2|\boldsymbol{F}| = 2\sqrt{\varepsilon_k^2+\Delta_k^2}$ is required. The minimum work is 2Δ at the Fermi level that is obtained by $\varepsilon_k \to 0$, which is the energy gap in a superconductor at $T \le T_\mathrm{c}$.

The BCS Hamiltonian $\mathcal{H}_\mathrm{BCS}$ is responsible for exciting Cooper's pairs at the Fermi level, so that the ground state in a superconductor can be specified by (iv) plus the energy for creating paired electrons. Assuming $\sigma_{ky} = 0$, the ground state can be characterized by

$$\begin{aligned} E_\mathrm{o} &= -\sum_k \varepsilon_k\sigma_{k\mathrm{o}}\cos\theta_k - \frac{V}{4}\sum_{k',k}\sigma_{k'x}\sigma_{kx} + \sum_{\text{pair}} 2\varepsilon_k \\ &= -\sum_k \varepsilon_k\sigma_{k\mathrm{o}}\left(\cos\theta_k + \frac{1}{2}\sin\theta_k\tan\theta_k\right) + \sum_{\text{pair}} 2\varepsilon_k. \end{aligned}$$

Simplifying the second term with (vii) as

$$\sum_k \varepsilon_k\sin\theta_k\tan\theta_k = \sum_k \frac{\Delta^2}{\sqrt{\varepsilon_k^2+\Delta^2}} = \frac{2\Delta^2}{V'},$$

and replacing $\sum_k\cdots$ by integration, we have

$$E_{\mathrm{o}} = 2\rho_{\mathrm{F}} \int_0^{\hbar\omega_{\mathrm{D}}} \left(\varepsilon - \frac{\varepsilon^2}{\sqrt{\varepsilon^2 + \Delta^2}} \right) \mathrm{d}\varepsilon - \frac{\Delta^2}{V'}.$$

Assuming $\Delta = \hbar\omega_{\mathrm{D}}$, this can be evaluated as

$$E_{\mathrm{o}} = \rho_{\mathrm{F}} (\hbar\omega_{\mathrm{D}})^2 \left(1 - \sqrt{1 + \left(\frac{\Delta}{\hbar\omega_{\mathrm{D}}} \right)^2} \right) \approx -\frac{1}{2} \rho_{\mathrm{F}} \Delta^2.$$

For thermodynamics, we have to deal with the energy gap Δ given by (viii) as a function of temperature. Near the critical temperature T_{c}, the interaction potential $V'_k = \sum_{k'} V(\boldsymbol{k}', \boldsymbol{k}) \sigma_{|k'|\mathrm{o}}$ or $V \sum_{k'} \sigma_{k'z}$ in (v) may be assumed to be determined by the statistical average

$$\langle \sigma_{k'z} \rangle = \frac{\exp \frac{(+1)F_{k'z}}{k_{\mathrm{B}}T} - \exp \frac{(-1)F_{k'z}}{k_{\mathrm{B}}T}}{\exp \frac{(+1)F_{k'z}}{k_{\mathrm{B}}T} + \exp \frac{(-1)F_{k'z}}{k_{\mathrm{B}}T}} = \tanh \frac{F_{k'z}}{k_{\mathrm{B}}T}.$$

Hence, (v) can be written as

$$\tan \theta_k = \frac{V}{2\varepsilon_k} \sum_{k'} \tanh \frac{F_{k'z}}{k_{\mathrm{B}}T} \sin \theta_{k'} = \frac{\Delta}{\varepsilon_k},$$

where $F_{k'z}$ is in energy unit, so that we can replace it by $\sqrt{\varepsilon_{k'}^2 + \Delta_{k'}^2}$. If the transition is characterized by $\Delta = 0$, this equation can specify the critical temperature T_{c} as

$$1 = V \sum_{k'} \frac{1}{2\varepsilon_{k'}} \tanh \frac{\varepsilon_{k'}}{k_{\mathrm{B}}T}.$$

Replacing $\sum_{k'} \cdots$ by integration, we obtain

$$\frac{2}{V\rho_{\mathrm{F}}} = \int_{-\hbar\omega_{\mathrm{D}}}^{+\hbar\omega_{\mathrm{D}}} \frac{\mathrm{d}\varepsilon}{\varepsilon} \tanh \frac{\varepsilon}{2k_{\mathrm{B}}T} = 2 \int_0^{\hbar\omega_{\mathrm{D}}/2k_{\mathrm{B}}T_{\mathrm{c}}} \frac{\tanh \xi}{\xi} \mathrm{d}\xi, \tag{ix}$$

which is the BCS formula for T_{c}. By graphical integration, these authors showed that T_{c} is given as

$$k_{\mathrm{B}}T_{\mathrm{c}} = 1{,}14\hbar\omega_{\mathrm{D}} \exp\left(-\frac{1}{V\rho_{\mathrm{F}}} \right). \tag{x}$$

Combined with (viii), the energy gap is related with T_{c} as $2\Delta = 3.5T_{\mathrm{c}}$. Experimentally, the values of $2\Delta/T_{\mathrm{c}}$ obtained from Sn, Al, Pb, and Cd are 3.5, 3.4, 4.1 and 3.3, respectively. In fact, Δ is a function of temperature T. Figure 13.3 shows the

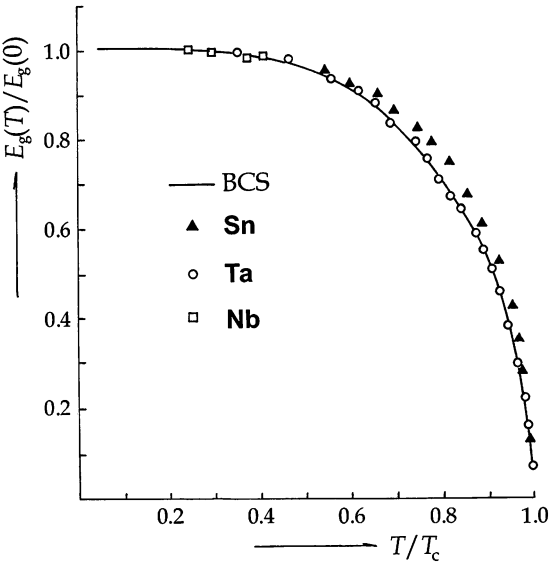

Fig. 13.3 The energy gap E_g as a function of temperature T. The BCS formula compared with experimental results (from [35]).

theoretical curve of $\Delta/k_B T_c$ versus T/T_c, where experimental results are compared with the BCS calculation. The agreement is quite reasonable, supporting the assumption for the interaction potential V'_k. The isotope effect expressed by $M^{0.5}T_c = \text{constant}$ follows directly from (x), since the Debye's frequency ω_D is proportional to $M^{-0.5}$.

13.3.3 BCS Ground States

Supported by the isotope effect, the BCS Hamiltonian describes the interacting electron–lattice system in a metal. We need next to formulate the equation of motion for thermodynamics of superconducting transition.

Writing the BCS Hamiltonian (i) as $\mathcal{H}_{BCS} = \sum_k \mathcal{H}_k$, where

$$H_k = \varepsilon_k(a_k^\dagger a_k + a_{-k}^\dagger a_{-k}) - V\sum_{k'} a_{k'}^\dagger a_{-k'}^\dagger a_{-k} a_k,$$

the operators $a_k^\dagger$ and a_k are dynamical variables whose time variation is determined by the Heisenberg equation;. Therefore from

$$i\hbar\frac{\partial a_k^\dagger}{\partial t} = [a_k^\dagger, H_k] \quad \text{and} \quad i\hbar\frac{\partial a_k}{\partial t} = [a_k, H_k]$$

with the identity relations $a_k a_k = 0$ and $a_k^\dagger a_k^\dagger = 0$, we obtain

$$\mathrm{i}\hbar\dot{a}_k = \varepsilon_k a_k - a^{\dagger}_{-k}\left(V\sum_{k'} a_{-k'}a_{k'}\right)$$

and

$$\mathrm{i}\hbar\dot{a}^{\dagger}_{-k} = -\varepsilon_k a^{\dagger}_{-k} - a_k\left(V\sum_{k'} a^{\dagger}_{k'}a^{\dagger}_{-k'}\right).$$

We can define the quantity $\Delta_k = V\sum_{k'} a_{-k'}a_{k'}$ and its complex conjugate $\Delta^*_k = V\sum_{k'} a^{\dagger}_{k'}a^{\dagger}_{-k'}$, expressing interactions between condensates for $|\varepsilon_k| < \hbar\omega_{\mathrm{D}}$. If $|\varepsilon_k| > \hbar\omega_{\mathrm{D}}$, we have to take $\Delta_k = \Delta^*_k = 0$, signifying for no electron pairs to be formed.

Using Δ_k, the equations of motion are linearized, that is,

$$\mathrm{i}\hbar\dot{a}_k = \varepsilon_k a_k - \Delta_k a^{\dagger}_{-k} \quad \text{and} \quad \mathrm{i}\hbar\dot{a}_{-k} = -\varepsilon_k a^{\dagger}_{-k} - \Delta^*_k a_k. \tag{i}$$

These equations have a solution proportional to $\exp\{-\mathrm{i}(\lambda_k/\hbar)t\}$, if we can set a determinant equation

$$\begin{vmatrix} \lambda_k - \varepsilon_k & \Delta_k \\ \Delta_k & \lambda_k + \varepsilon_k \end{vmatrix} = 0 \quad \text{or} \quad \lambda_k^2 = \varepsilon_k^2 + \Delta_k\Delta^*_k. \tag{ii}$$

Equations (i) represent an eigenvalue problem, where a real λ_k expresses the binding energy of a Cooper's pair. The operators for (i) and (ii) can be determined by linear combinations of these one-electron operators

$$\begin{aligned} \alpha_k &= u_k a_k - v_k a^{\dagger}_{-k}, \quad \alpha_{-k} = u_k a_{-k} + v_k a^{\dagger}_k, \\ \alpha^{\dagger}_k &= u_k a^{\dagger}_k - v_k a_{-k}, \quad \alpha^{\dagger}_{-k} = u_k a^{\dagger}_{-k} + v_k a_k. \end{aligned} \tag{iii}$$

Relations (iii) are known as the *Bogoliubov transformation*. The coefficients u_k and v_k are real and symmetric and antisymmetric, respectively, with regard to inversion $\boldsymbol{k} \to -\boldsymbol{k}$, that is, $u_k = u_{-k}$ and $v_k = -v_{-k}$, normalized as $u_k^2 + v_k^2 = 1$. And, for the operators $\alpha^{\dagger}_k$ and α_k,we have the following anticommutator relations:

$$[\alpha_k, \alpha^{\dagger}_{k'}]_+ = u_k u_{k'}[a_k, a^{\dagger}_{k'}]_+ + v_k v_{k'}[a^{\dagger}_{-k}, a_{-k'}]_+ = \delta_{kk'}(u_k^2 + v_k^2) = \delta_{kk'}$$

and

$$[\alpha_k, \alpha_{-k}]_+ = u_k v_k[a_k, a^{\dagger}_k]_+ - v_k u_k[a^{\dagger}_{-k}, a_{-k}]_+ = u_k v_k - v_k u_k = 0.$$

Differentiating (i), we obtain $\lambda_k u_k = \varepsilon_k u_k + \Delta_k v_k$. Combining this result with (ii), we derive the relation

$$\Delta_k (u_k^2 - v_k^2) = 2\varepsilon_k u_k v_k.$$

It is noted that this expression is identical to $\tan\theta_k = \Delta_k/\varepsilon_k$, which was previously discussed in Sect. 12.3.2, if we write

$$u_k = \cos\frac{\theta_k}{2} \quad \text{and} \quad v_k = \sin\frac{\theta_k}{2}. \tag{iv}$$

Using the operator α_k, the ground state of the system may be represented by a wave function

$$\alpha_{-k}\alpha_k \Phi_{\text{vac}} = (-v_k)(u_k + v_k a_k^\dagger a_{-k}^\dagger)\Phi_{\text{vac}}.$$

This is not normalized, however omitting the factor $-v_k$, we can confirm that

$$\langle \Phi_{\text{vac}} | (u_k^* + v_k^* a_{-k} a_k)(u_k + v_k a_k^\dagger a_{-k}^\dagger) | \Phi_{\text{vac}} \rangle = (u_k^2 + v_k^2)\langle \Phi_{\text{vac}} | | \Phi_{\text{vac}} \rangle;$$

hence, the function

$$\Phi_{\text{o}} = \prod_k (u_k + v_k a_k^\dagger a_{-k}^\dagger)\Phi_{\text{vac}} \tag{13.11}$$

is considered for the normalized wave function for the ground state. This wave function (13.11) was originally postulated in the BCS theory, proposing that Cooper's pairs and unpaired condensates are determined by probabilities v_k^2 and u_k^2, respectively. With Bogoliubov's operators' creation and annihilation of a Cooper's pair can be described conveniently. In fact, the normalization $u_k^2 + v_k^2 = 1$ assumed in the BCS theory is confirmed by Bogoliubov's theory.

We can further verify that

$$\alpha_{k'}\Phi_{\text{o}} \propto \alpha_{k'}(\alpha_{-k'}\alpha_{k'}) \prod_{k \neq k'} \alpha_{-k}\alpha_k \Phi_{\text{vac}} = 0 \quad \text{for} \quad \alpha_{k'}\alpha_{k'} = 0,$$

signifying annihilation of a pseudoparticle. Also, from

$$\alpha_{k'}^{\dagger}\Phi_{\rm o} = (u_{k'}a_{k'}^{\dagger} - v_{k'}a_{-k'})(u_{k'} + v_{k'}a_{k'}^{\dagger}a_{-k'}^{\dagger})\prod_{k\neq k'}(u_k + v_k a_k^{\dagger}a_{-k}^{\dagger})\Phi_{\rm vac}$$
$$= a_{k'}^{\dagger}\prod_{k\neq k'}(u_k + v_k a_k^{\dagger}a_{-k}^{\dagger})\Phi_{\rm vac},$$

we see that the operator $\alpha_k^{\dagger}$ creates a single particle; $\alpha_k^{\dagger}\alpha_{-k'}^{\dagger}$ is for the pair creation.

The number operator in the $\boldsymbol{k}$-state can be expressed in terms of Bogoliubov operators as

$$n_k = a_k^{\dagger}a_k = (u_k\alpha_k^{\dagger} + v_k\alpha_{-k})(u_k\alpha_k + v_k\alpha_{-k}^{\dagger}).$$

Using θ_k given by (iv), u_k and v_k in (12.9) are related to

$$u_k^2 = \cos^2\frac{\theta_k}{2} = \frac{1}{2}\left(1 + \frac{\varepsilon_k}{\lambda_k}\right) \quad \text{and} \quad v_k^2 = \sin^2\frac{\theta_k}{2} = \frac{1}{2}\left(1 - \frac{\varepsilon_k}{\lambda_k}\right), \tag{13.12}$$

indicating that these probabilities depend on the ratio ε_k/λ_k.

Finally, the previous result of the energy gap $E_{\rm g}$ can be verified with $\Phi_{\rm o}$ in (13.11). Namely, the expectation value of the kinetic energy is expressed as

$$\langle\Phi_{\rm o}|a_{k'}^{\dagger}a_{k'}|\Phi_{\rm o}\rangle = \langle\Phi_{\rm o}|v_{k'}^2\alpha_{-k'}\alpha_{-k'}^{\dagger}|\Phi_{\rm o}\rangle = v_{k'}^2$$

and the potential energy term is

$$-\langle\Phi_{\rm o}|a_{k'}^{\dagger}a_{-k'}^{\dagger}a_{-k''}a_{k''}|\Phi_{\rm o}\rangle = \langle\Phi_{\rm o}|u_{k'}v_{k'}u_{k''}v_{k''}\alpha_{-k'}\alpha_{-k'}^{\dagger}\alpha_{-k''}\alpha_{-k''}^{\dagger}|\Phi_{\rm o}\rangle = u_{k'}v_{k'}u_{k''}v_{k''}.$$

Hence,

$$\langle\Phi_{\rm o}|\mathcal{H}_{\rm BCS}|\Phi_{\rm o}\rangle = 2\sum_k \varepsilon_k v_k^2 - V\sum_{k,k'} u_k v_k u_{k'} v_{k'}$$
$$= \sum_k \varepsilon_k(1 - \cos\theta_k) - \frac{V}{4}\sum_{k,k'}\sin\theta_k\sin\theta_{k'}$$
$$= -\sum_k \varepsilon_k\cos\theta_k - \frac{\Delta^2}{V}.$$

The energy gap is then given as $E_{\rm g} = \langle\Phi_{\rm o}|\mathcal{H}_{\rm BCS}|\Phi_{\rm o}\rangle + \sum_k|\varepsilon_k|$.

13.3.4 Superconducting States at Finite Temperatures

The BCS result in Sect. 13.3.3 is applicable to absolute zero of temperature. However, at a finite temperature, the ground state Φ_o should be modified by adiabatic excitations of condensates, as described by Ginzburg–Landau's theory. In the following, we discuss the BCS theory modified in thermodynamic environment.

The number of quasiparticles of Cooper's pairs can be assumed to be temperature dependent, for which we consider the complete set of temperature-dependent states

$$|\Phi_o\rangle,\ \alpha_k^\dagger|\Phi_o\rangle,\ \alpha_k^\dagger\alpha_{k'}^\dagger|\Phi_o\rangle,\ldots,$$

forming the basis. Here, $|\cdots\rangle$ expresses temperature-dependent ket-states.

To study thermodynamic properties of a superconductor, we need to introduce the statistical average number of quasiparticles as given by the function

$$f_k = \langle\alpha_k^\dagger\alpha_k\rangle.$$

Assuming statistical independence of excitations, the entropy of the system can be given by

$$S = k_B\sum_k\{f_k\ln f_k + (1-f_k)\ln(1-f_k)\}.$$

We re-express the Hamiltonian of interacting pairs $H_k = \varepsilon_k(a_k^\dagger a_k + a_{-k}^\dagger a_{-k}) - V(a_k^\dagger a_{-k}^\dagger a_{-k}a_k)$ by the Bogoliubov transformation. The kinetic energy term can be converted to

$$\sum_k\langle\varepsilon_k(u_k\alpha_k^\dagger + v_k\alpha_{-k})(u_k\alpha_k + v_k\alpha_{-k}^\dagger)\rangle = \sum_k\varepsilon_k\{v_k^2(1-f_k) + u_k^2 f_k\}, \qquad \text{(i)}$$

in which we noted that $\alpha_k^\dagger\alpha_{-k}^\dagger = 0$. The first term on the right-hand side of (i) can be interpreted as representing the condensate system that has no quasiparticle at the state of wave vector $\boldsymbol{k}$, with thermal probability v_k^2. The second term, on the other hand, u_k^{22} is the probability for the state to be occupied by quasiparticles. The factors $1-f_k$ and f_k in these terms are the statistical weights due to average numbers of quasiparticles.

Similarly, the interaction term can be calculated as

$$\sum_{k,k'}V(\boldsymbol{k},\boldsymbol{k}';q)(1-2f_k)(1-2f_{k'}).$$

It is noted from (13.8c) that $V(\boldsymbol{k},\boldsymbol{k}';q)$ can be factorized as $V_k(\boldsymbol{q})V_{-k}(-\boldsymbol{q})$. Therefore, the thermodynamic potential can be expressed as

$$\begin{aligned} g(T,p) = \langle \mathcal{H}_{\mathrm{BCS}} \rangle - TS = &\sum_k \varepsilon_k \{u_k^2 f_k + v_k^2(1-f_k)\} \\ &- \sum_{k,k'} V_k V_{k'} u_k u_{k'} v_k v_{k'} (1-2f_k)(1-2f_{k'}) \\ &- k_{\mathrm{B}} T \sum_k \{f_k \ln f_k + (1-f_k)\ln(1-f_k)\}. \end{aligned} \tag{ii}$$

We first minimize this Gibbs function with respect to v_k. This procedure is the same as in the zero-temperature case of Sect. 13.3.3, so that we can arrive at (13.12) without repeating calculation, that is,

$$u_k^2 = \frac{1}{2}\left(1 + \frac{\varepsilon_k}{\sqrt{\varepsilon_k^2 + \Delta_k(T)^2}}\right) \quad \text{and} \quad v_k^2 = \frac{1}{2}\left(1 - \frac{\varepsilon_k}{\sqrt{\varepsilon_k^2 + \Delta_k(T)^2}}\right),$$

where $\Delta_k(T) = \sum_k V_k u_k v_k (1-2f_k)$, representing one-half of the gap at the superconducting transition, which is now verified as temperature dependent.

Minimizing the Gibbs function (ii) with respect to f_k, we obtain

$$k_{\mathrm{B}} T\{\ln f_k + \ln(1-f_k)\} + \sqrt{\varepsilon_k^2 + \Delta_k(T)^2} = 0,$$

that is,

$$f_k = \frac{1}{1 + \exp(E_k/k_{\mathrm{B}}T)} \quad \text{where} \quad E_k = \sqrt{\varepsilon_k^2 + \Delta_k(T)^2}.$$

This is the Fermi–Dirac distribution function for temperature-dependent E_k.

In fact, as seen from Fig.12.2, the Gibbs potential is a function of temperature T as well as an applied magnetic field H, that is, $G(H,T)$. In the absence of H, the superconducting transition at T_{c} is second order characterized by no latent heat, signifying that $E_k(T_{\mathrm{c}}) = 0$. On the other hand, in the presence of H, the transition is discontinuous, as signified by a finite energy gap $E_k(T)$ that is temperature dependent. With the BCS theory, the value of E_k is thus calculable, as shown in Fig. 13.3, where the calculated result is compared with experimental values from some superconducting metals, showing a reasonable agreement.

Exercises 13

1. We can define creation and annihilation operators for Cooper's pairs by

$$a_k^\dagger = a_k^\dagger a_{-k}^\dagger \quad \text{and} \quad a_k = a_k a_{-k},$$

respectively, where a_k, $a_{-k}^\dagger$, etc., are one-particle Fermion operators. Show that the pair operators satisfy the commutation relations

$$[a_k, a_{k'}^\dagger] = (1 - n_k - n_{-k})\delta_{k,k'},$$

$$[a_k, a_{k'}] = 0,$$

and

$$[a_k, a_{k'}]_+ = 2a_k a_{k'}(1 - \delta_{k,k'}).$$

2. Show that the total number of particles is conserved with the equations of motion (i) in Sect. 13.3.3.

3. In this chapter, we defined the coherence length ξ with respect to the critical wave vector of modulation q_o. Justify the reason why it is referred to as *coherence* length.

Appendix

1. *Elliptic Integrals*

   Elliptic integrals of the first kind:

$$F(\kappa,\varphi)=\int_0^{\varphi}\frac{\mathrm{d}\varphi}{\sqrt{1-\kappa^2\sin^2\varphi}}=\int_0^{\sin\varphi}\frac{\mathrm{d}z}{\sqrt{(1-z^2)(1-\kappa^2z^2)}},$$

   and the complete elliptic integral is

$$F\Big(\kappa,\frac{\pi}{2}\Big)=\int_0^{\pi/2}\frac{\mathrm{d}\varphi}{\sqrt{1-\kappa^2\sin^2\varphi}}=\int_0^{1}\frac{\mathrm{d}z}{\sqrt{(1-z^2)(1-\kappa^2z^2)}}=K(\kappa).$$

   Elliptic integral of the second kind:

$$E(\kappa,\varphi)=\int_0^{\varphi}\sqrt{1-\kappa^2\sin^2\varphi}\,\mathrm{d}\varphi=\int_0^{\sin\varphi}\sqrt{\frac{1-\kappa^2z^2}{1-z^2}}\mathrm{d}z,$$

   and the complete elliptic integral is

$$\begin{aligned}E\Big(\kappa,\frac{\pi}{2}\Big)&=\int_0^{\pi/2}\sqrt{1-\kappa^2\sin^2\varphi}\,\mathrm{d}\varphi=\int_0^{1}\sqrt{\frac{1-\kappa^2z^2}{1-z^2}}\mathrm{d}z=E(\kappa)\\&=\int_0^{K(\kappa)}\mathrm{dn}^2(u,\kappa)\mathrm{d}u.\end{aligned}$$

   where $\mathrm{dn}(u,\kappa)$ is the Jacobi's dn-function.
   Defining $\kappa'=\sqrt{1-\kappa^2}$, $K(\kappa')=K'$, and $E(\kappa')=E'$, we have the relation

$$EK'+E'K-KK'=\frac{\pi}{2}.\quad\text{(Legendre's relation.)}$$

2. *Jacobi's Elliptic Function*

From the elliptic integral

$$u(x) = \int_0^x \frac{\mathrm{d}z}{\sqrt{(1-z^2)(1-\kappa^2 z^2)}},$$

we write the reverse function as

$$z = \mathrm{sn}\, u = \mathrm{sn}(u, \kappa),$$

which is Jacobi's sn-function. Considering the relations with trigonometric and hyperbolic functions, we also define the corresponding cn- and dn-functions by

$$\mathrm{cn}^2 u = 1 - \mathrm{sn}^2 u \quad \text{and} \quad \mathrm{dn}^2 u = 1 - \kappa^2 \mathrm{sn}^2 u.$$

In the limit of $\kappa \to 0$,

$$\mathrm{sn}\, u \to \sin u, \quad \mathrm{cn}\, u \to \cos u, \quad \text{and} \quad \mathrm{dn}\, u \to 1.$$

On the other hand, if $\kappa \to 1$, we have

$$\mathrm{sn}\, u \to \tanh u, \quad \mathrm{cn}\, u \to \mathrm{sech}\, u, \quad \text{and} \quad \mathrm{dn}\, u \to \mathrm{sech}\, u.$$

Differential formula:

$$\frac{\mathrm{d}\,\mathrm{sn}\, u}{\mathrm{d}u} = \mathrm{cn}\, u\, \mathrm{dn}\, u, \quad \frac{\mathrm{d}\,\mathrm{cn}\, u}{\mathrm{d}u} = -\mathrm{sn}\, u\, \mathrm{dn}\, u, \quad \frac{\mathrm{d}\,\mathrm{dn}\, u}{\mathrm{d}u} = -\kappa^2 \mathrm{sn}\, u\, \mathrm{cn}\, u.$$

Expansion formula:

$$\mathrm{sn}\, u = u - \frac{1+\kappa^2}{3!}u^3 + \frac{1+14\kappa+\kappa^4}{5!}u^5 + \cdots,$$

$$\mathrm{cn}\, u = 1 - \frac{1}{2}u^2 + \frac{1+4\kappa^2}{4!}u^4 - \frac{1+44\kappa^2+16\kappa^4}{6!}u^6 + \cdots,$$

$$\mathrm{dn}\, u = 1 - \frac{\kappa^2}{2}u^2 + \frac{(4+\kappa^2)\kappa^2}{4!}u^4 - \frac{(16+44\kappa^2+\kappa^4)\kappa^2}{6!}u^6 + \cdots.$$

References

[1] J. G. Kirkwood and I. Oppenheim, *Chemical Thermodynamics* (McGraw-Hill, New York, 1961)
[2] M. Born and K. Huang, *Dynamical Theory of Crystal Lattices* (Oxford University Press, Oxford, 1968)
[3] R. Becker, *Theory of Heat*, 2nd ed. (Springer, New York, 1967) (revised by G. Leibfried)
[4] T. Ashida, S. Bando and M. Kakudo, Acta Crystallogr. B **28**, 1131 (1972)
[5] M. Tinkham, *Group Theory and Quantum Mechanics* (McGraw-Hill, New York, 1964)
[6] L. D. Landau and E. M. Lifshitz, *Statistical Physics* (Pergamon, London, 1958)
[7] R. Blinc and B. Zeks, *Soft Modes in Ferroelectrics and Antiferroelectrics* (North-Holland, Amsterdam, 1974)
[8] T. Nagamiya, *Solid State Physics*, Vol. 20 (Academic, New York, 1963); L. R. Walker, *Magnetism I* (Academic, New York, 1963)
[9] Th. Von Waldkirch, K. A. Müller and W. Berlinger, Phys. Rev. B **5**, 4324 (1972); Th. Von Waldkirch, K. A. Müller and W. Berlinger, Phys. Rev. B **7**, 1052 (1973)
[10] C. Kittel, *Quantum Theory of Solids* (Wiley, New York, 1963)
[11] M. J. Rice, *Charge Density Wave Systems* in *Solitons and Condensed Matter Physics*, ed. A. R. Bishop and T. Schneider (Springer, Berlin, 1978)
[12] R. Comes, R. Courrat, F. Desnoyer, M. Lambert and A. M. Quittet, Ferroelectrics **12**, 3 (1976)
[13] F. C. Nix and W. Shockley, Rev. Mod. Phys. **10**, 1 (1938)
[14] M. Iizumi, J. D. Axe, G. Shirane and K. Shimaoka, Phys. Rev. B **15**, 4392 (1977)
[15] J. A. Krumshansl and J. R. Schrieffer, Phys. Rev. B **11**, 3535 (1975); S. Aubry, J. Chem. Phys. **64**, 3392 (1976)
[16] X. Pan and H.-G. Unruh, J. Phys. Condens. Matter **2**, 323 (1990)
[17] P. M. Morse and H. Feshbach, *Methods of Theoretical Physics*, p. 1651 (McGraw-Hill, New York, 1953)
[18] M. Abramovitz and I. A. Stegun, *Handbook of Mathematical Functions*. National Bureau of Standards Applied Mathematics Series, p. 253 (Government Printing Office, Washington, DC, 1964)
[19] J. Petzelt, G. V. Kozlov and V. V. Volkov, Ferroelectrics **73**, 101 (1987)
[20] A. Cowley, Prog. Phys. **31**, 123 (1968)
[21] R. Currat, K. A. Müller, W. Berlinger and F. Desnoyer, Phys. Rev. B **17**, 2937 (1978)
[22] S. M. Shapiro, J. D. Axe, G. Shirane and T. Riste, Phys. Rev. B **6**, 4332 (1972)
[23] J. F. Scott, Raman spectroscopy of structural phase transitions in *Light Scattering Near Phase Transitions*, ed. H. Z. Cummins and A. P. Levanyuk (North-Holland, Amsterdam, 1983)
[24] J. Feder and E. Pytte, Phys. Rev. B **1**, 4803 (1970)
[25] E. M. Brody and H. Z. Cummins, Phys. Rev. Lett. **21**, 1263 (1968)

[26] E. M. Brody and H. Z. Cummins, Phys. Rev. **9**, 179 (1974)
[27] F. Bloch, Phys. Rev. **70**, 460 (1946)
[28] M. P. Schulhof, P. Heller, R. Nathans and A. Linz, Phys. Rev. B **1**, 2403 (1970)
[29] J. C. Toledano, E. Errandonea and I. P. Jaguin, Solid State Commun. **20**, 905 (1976)
[30] M. Fujimoto, S. Jerzak and W. Windsch, Phys. Rev. B **34**, 1668 (1986)
[31] M. Fujimoto and Y. Kotake, J. Chem. Phys. **90**, 532 (1989)
[32] M. Fujimoto and Y. Kotake, J. Chem. Phys. **91**, 6671 (1989)
[33] H. Haken, *Quantenfeldtheorie des Festkörpers*, Chap. 3 (B. G. Teubner, Stuttgart, 1973)
[34] N. F. Mott and H. Jones, *The Theory of the Properties of Metals and Alloys* (Clarendon, Oxford, 1936)
[35] C. Kittel, *Introduction to Solid State Physics*, 6th ed. (Wiley, New York, 1986)
[36] W. Cochran, *The Dynamics of Atoms in Crystals*, Chap. 8 (Edward Arnold, London, 1973)
[37] C. Kittel and H. Kroemer, *Thermal Physics* (Freeman, San Francisco, CA, 1980)

Index